UNIVERSITÉ DU LUXEMBOURG

PhD-FSTM-2021-075
The Faculty of Science, Technology and Medicine

DISSERTATION

Defence held on 11/10/2021 in Esch-sur-Alzette

to obtain the degree of

DOCTEUR DE L'UNIVERSITÉ DU LUXEMBOURG EN BIOLOGIE

by

Christophe CAPELLE
Born on 25 November 1989 in Luxembourg (Luxembourg)

INVESTIGATING T CELLS IN THE CONTEXT OF NEUROIMMUNOLOGY: MOLECULAR AND CELLULAR MECHANISMS DURING A STRESS RESPONSE AND A PATIENT-BASED STUDY IN PARKINSON'S DISEASE

Dissertation defence committee

Dr Feng He, Dissertation Supervisor
Principal investigator, Luxembourg Institute of Health

Dr Paul Heuschling, Chairman
Professor, Université du Luxembourg

Dr Markus Ollert, Vice Chairman
Director of the Department of Infection and Immunity of the Luxembourg Institute of Health
Professor, Odense University Hospital, University of Southern Denmark

Dr Klaus Schughart
Professor, Helmholtz Center for Infection Research

Dr Astrid Westendorf
Professor, Essen University Hospital

Affidavit

I herby confirm that the PhD thesis entitled “Investigating T cells in the context of neuroimmunology: Molecular and cellular mechanisms during a stress response and a patient-based study in Parkinson's disease” has been written indipendently and without any other sources than cited.

Luxembourg, 15th of December 2021,

Christophe Capelle

Table of content

Acknowledgements 1
Summary 3
General introduction 7
Overview on the immune system (IS) 7
T cells 8
T cell receptor (TCR) signalling 10
Mechanisms of T cell regulation 12
The nervous system in a nutshell 15
Anatomical and functional connection of the nervous system and the immune system 16
Immune-to-neuro communication 17
Neuro-to-immune communication 18
Neuroimmunology during a stress response 20
Clinical relevance of the neuro-immune axis 21
Scope and Aims 25
Chapter 1: Identification of VIMP as a gene inhibiting cytokine production in human CD4+ effector T cells. 31
Abstract 31
Graphical Abstract 31
Keywords 32
Introduction 33
Results 34
Discussion 39
Limitations of the study 42
Resource availability 43
Methods 43
Acknowledgements 50
Author contributions 51
Declaration of Interests 51
Figures 52
Chapter 2: Stress hormone signalling intrinsically inhibits Th1 polarization in naïve CD4 cells via the clock gene Period1 and mTORC1. 65
Abstract 65
Keywords 66
Introduction 66
Results 68
Discussion 76

Materials and Methods 79
Acknowledgements 85
Author contributions 85
Conflict of Interest 86
Figures 87
Chapter 3: Systems immunology reveals a cytotoxic immune cell profile in Parkinson's disease patients. 107
Abstract 108
Keywords 108
Introduction 109
Results 111
Discussion 119
Limitations of the study 122
Materials & Methods 123
Acknowledgements 127
Author contributions 127
Conflict of Interest 127
Figures 128
Supplementary Tables 145
General discussion and Perspectives 157
List of Abbreviations 165
List of scientific outcomes 171

Acknowledgements

First and foremost, I would like to express my gratitude to my research supervisor Dr. Feng He. Thank you for giving me the opportunity to carry out my PhD under your guidance. I am grateful for the trust that I have been receiving for the past 5 years and the freedom to explore any hypothesis, independently. I also highly appreciate the additional support during the COVID19 pandemic. We will always be bound by the bond of student and supervisor and by the difficult times we came up against together.

I would like to extend my sincere thanks to Prof. Dr. Markus Ollert, Director of the Department of Infection and Immunity of the Luxembourg Institute of Health, as well as, Prof. Dr. Jorge Goncalves and Associate Prof. Dr. Alexander Skupin from the Luxembourg Center of Systems Biomedicine (LCSB) and coordinators of the CRITCIS doctoral teaching unit (DTU) for their assistance and insightful comments at every stage of the research projects. My gratitude also goes to the NEXTIMMUNE DTU for providing additional training opportunities.

I am also deeply grateful to my CET and defence committee members: Ass. Prof. Dr. Alexander Skupin, Prof. Dr. Paul Heuschling, Dean of the Faculty of Science, Technology and Communication of the University of Luxembourg, Prof. Dr. Markus Ollert, Prof. Dr. Astrid Westendorf of the Essen University Hospital and Prof. Dr. Klaus Schughart from the Helmholtz Center for Infection Research for the guidance during the years of my PhD and for taking the time to evaluate the thesis.

A very special thanks goes to the members of the group of Immune Systems Biology (GISB) for the laughs and the joyful moments, as well as for the support in the lab and in life: Alexandre Baron, Ni Zeng, Dmitrii Pogorelov, Séverine Ciré, Egle Danileviciute, Sebastian Bode, Anna Chen, and Nils Scheib. Many thanks also go to all the research teams in the Department of Infection and Immunity in the LIH.

I also offer my thanks to the Integrated Biobank Luxembourg (IBBL), the National Cytometry Platform (NCP), the Clinical and Epidemiological Investigation Centre (CIEC) and the Parkinson Research Clinic (PCR) for the overwhelming support in the different research projects.

I would like to express my heartfelt appreciation to my fellow PhD students for the scientific input, the shared beers, the nights out and generally all the good and bad times we shared. A special thanks to those that found a place in my heart as friends, rather than colleagues. Thank you for making the rough path of a PhD more enjoyable.

None of this would have been possible without the everlasting support of my family and friends. First, I would like to thank my parents and sister for the unconditional support, the love and the understanding, which I felt throughout my life. Irreplaceable thanks go to my grandparents, in particular Bobo, for spoiling me ever since I was born and for always being proud of me. Many thanks go to my close friends for always being there and cheering me up when everything else feels too heavy.

Last, but not least, thank you Fond National de la Recherche (FNR) for funding my PhD training via the PRIDE program and the research projects.

Summary

For a long time, the nervous system and the immune system have been studied as isolated entities, but a growing body of evidence shows that there is an extensive crosstalk between both systems. In fact, neurons and immune cells share certain functional features and reside in close proximity within the tissues, enabling them to effectively communicate. T cells are crucial for mounting and controlling almost any kind of immune response. However, when dysregulated, T cells fail to protect the host from invading pathogens or can cause damage to surrounding tissues, leading to autoimmunity-related pathology. In the first part of this cumulative thesis, we aimed at identifying novel genes regulating CD4 T cell responses and identified VIMP, one of the 25 human proteins containing the 21st amino acid selenocysteine, as a gene having anti-inflammatory functions. Furthermore, T cells express various neurotransmitter receptors allowing the integration of neuronal signal for an appropriate response. In the second part, we showed a CD4-T-cell-intrinsic mechanism through which stress hormones mediate their control over the immune system. We identified a previously unrecognized pathway regulating CD4 T cell differentiation that involves the circadian clock gene Per1 and mTORC1 signalling. Finaly, T cells involvement in different neuropathologies has been reported in the past few decades. Emerging evidence indicates the involvement of the immune system and in particular T cells in the pathogenesis of Parkinson's disease (PD), the 2nd most common neurodegenerative disease. In the 3rd part of the thesis we systematically characterized the immunological status of early-to-mid stage PD patients and matched healthy controls, and identified a distinct peripheral immunological fingerprint in PD patients, especially in the CD8 T-cell compartment. The findings of the studies described in this cumulative thesis advance our understanding of the regulatory nodes of CD4 T cells during a stress response and fill the knowledge gap on the early involvement of CD8 T cells and other immune subsets in neurodegenerative diseases in the case of PD.

General Introduction

General introduction

Overview on the immune system (IS)

Immunology is the study of a host's defence systems against certain threats. These threats can be external, such as bacteria, viruses and parasites, but also arise within the own body, as in the context of cancer. During the course of evolution, the human body was equipped with a plethora of protection strategies to clear any signs of potential hazards. The immune system can broadly be subdivided into the innate and the adaptive immune system [1]. The innate immune system is, after the barrier tissues, such as the skin, the gut and the airways, the 1st line of defence of the body. A myriad of different immune cells, including dendritic cells (DCs), monocytes/macrophages, natural killer (NK) cells, innate lymphoid cells (ILCs), mast cells and granulocytes constitute the innate immune compartment. Although some cells types are more specialized in certain functions, their role is to recognize foreign antigens (Ag), degrade them via phagocytosis and/or eliminate them through cytotoxic molecules. They then present the captured Ag to the adaptive immune system, while producing cytokines that activate specific functions of surrounding cells. Innate immune cells recognize broad structures of foreign antigens, termed pattern-associated molecular pattern (PAMPs) through intra- and extra-cellular pattern recognition receptors (PRR), including Toll-like receptors (TLRs) and NOD-like receptors (NLRs). Upon recognition, the Ag is taken up via phagocytosis, processed into different smaller peptides and loaded onto a major histocompatibility complex (MHC) for antigen-presentation. At the same time, molecular signalling pathways downstream of the PRRs induce the expression of different cytokines and antimicrobial peptides, which initiate an immune response. The MHC-Ag complexes are presented to T and B lymphocytes, the major cell types of the adaptive immune system. Whereas the innate immune cells broadly recognize conserved molecular patterns, different T and B cell clones recognize specific MHC-Ag complexes via the T-cell receptor (TCR) and B-cell receptor (BCR), respectively. Upon TCR/BCR binding, those specific clones undergo clonal proliferation, activate effector functions and establish immune memory for the specific target. B cells' key function lies in the humoral immunity and the production of different types of immunoglobulins, also knowns as antibodies, which have the ability to bind and neutralize the invading pathogens. On the other hand, T cells mediate the cellular immunity, killing virus-infected or malignant cells by secreting cytotoxic molecules and regulate the immune responses by expressing different cytokines. As this work focuses on T cells, their generation, maturation and functions are described in more detail in the next section.

T cells

T cells can be categorized into CD4 helper T cells and CD8 cytotoxic T cells. Whereas CD8 T cell's main functions lie in the cytotoxic killing of infected or malignant cells [2, 3], CD4 T helper cells are the main regulators of immune responses [4]. As most immune cells, T cell generation starts in the bone marrow from hematopoietic stem cells (HSC) [5]. Common lymphoid progenitors arising from the HSCs migrate to the thymus where the T cell maturation begins. Sequential rearrangement of the TCR gene segments (VDJ recombination) gives rise to a highly divers repertoire of T cells that are able to recognize a huge variety of different epitopes. Those immature, CD4 and CD8 double-negative (DN) T cells undergo a first thymic selection process to give rise to αβ TCR expressing cells able to recognize self-MHC receptors (positive selection). After this pre-maturation step, the T cells develop into CD4/CD8 double-positive (DP) T cells, followed by a differentiation into CD4 or CD8 single-positive (SP) T cell cells. The final maturation step is the negative selection process during which T cells with a high avidity against MHC-presented self Ags undergo apoptosis to ensure immune tolerance and to avoid the generation of "self"-reactive T cells. The two-step selection process ensures that the generated T cells are able to recognize MHC-Ag complexes presented by innate immune cells and avoid that self-Ag activate an immune response, which could lead to tissue damage.

This maturation process results in the 2 major T cell populations: CD4 T helper (Th) cells and CD8 cytotoxic T cells (Tc). As the name indicates, cytotoxic CD8 T cells are able to kill virus-infected and tumorigenic cells via cytotoxic molecules, such as granzymes and perforins. CD8 T cells also produce different cytokines, including interferon γ (IFNγ) and tumor necrosis factor α (TNFα), to promote the activation of phagocytic cells, such as macrophages. Upon activation, naïve CD8 T cells undergo clonal proliferation and differentiate into cytotoxic effector cells and memory cells. Memory cells can be broadly categorized into central memory (CM), expressing lymph node (LN) homing receptors, and effector memory (EM) (and terminally-differentiated effector memory T cells (TEMRA) in humans), patrolling the periphery [6, 7]. CM T cells retain a high proliferative capacity, whereas EM T cells, in particular TEMRA, continuously retain effector functions [8]. Unlike the cytotoxic function of CD8 T cells, the main function of CD4 T helper cells lies in the production of specific cytokines in order to regulate context-specific immune responses. As such, CD4 T cells are able to differentiate into different subsets that secrete different sets of cytokines depending on the nature of the immune response. Those subsets are termed Th1, Th2 and Th17 [9], the less-characterized Th9 [10] and Th22 [11], and the regulatory T cells (Treg) [12] (**Illustration 1: CD4 T helper differentiation**). The differentiation into each subset requires specific cytokines to be secreted by surrounding immune cells upon

recognition of a foreign Ag [13]. The differentiation into the Th1 subset requires the presence of Interleukin 12 (IL-12) secreted by innate immune cells (e.g. DCs). On the other hand, Th2 cells require IL-4, whereas Th17 require Transforming growth factor beta (TGFβ) and IL-6 for their differentiation. The signalling downstream of the TCR and the respective cytokine receptors induce the expression of lineage-specific transcription factors (TFs) that enable the expression of Th signature cytokines: Th1 rely on Tbet for the expression of IFNγ and TNFα; Th2 are characterized by GATA3 expression and produce IL-5, IL-4 and IL-13; Th17 express RORγT and secrete mainly IL-17 and IL21. This compartmentalisation enables the CD4 T cells to mount a tailored and context-specific immune response, depending on the nature of the Ag and the signals provides by innate immune cells [4]. Th1 cells, promote cellular immunity and the clearance of infected or malignant cells by activating phagocytes (e.g. macrophages) and cytotoxic cells (e.g. NK and CD8). Under different conditions, Th2 cells and their set of cytokines contribute to humoral immunity. By inducing B cell maturation, antibody class-switching and affinity maturation, Th2 cells play a major role in allergy and the elimination of extracellular parasites. The function of Th17 cells lies in antifungal immunity and tissue inflammation, but is also associated with several autoimmune or inflammatory diseases, affecting different organs. Last but not least, the aforementioned Treg have particular functions in regulating/suppressing the different immune responses. They develop either directly in the thymus or can be induced from naïve CD4 T cells in the tissues by TGFβ and IL-2 signalling [14]. Treg are characterized by the transcription factor FOXP3 and have the ability to supress effector immune responses via the expression of anti-inflammatory cytokines and/or cell contact-dependent mechanisms to restore homeostasis and avoid tissue damage by an overactive immune system. Overall, T cells are able to differentiate into different subsets with specific functions, depending on the nature of the pathogen and the immune response that is required for its clearance. After discussing the main requirements and functions of different T cell subsets, we will further dissect the molecular signalling pathways that trigger the differentiation in the following sections.

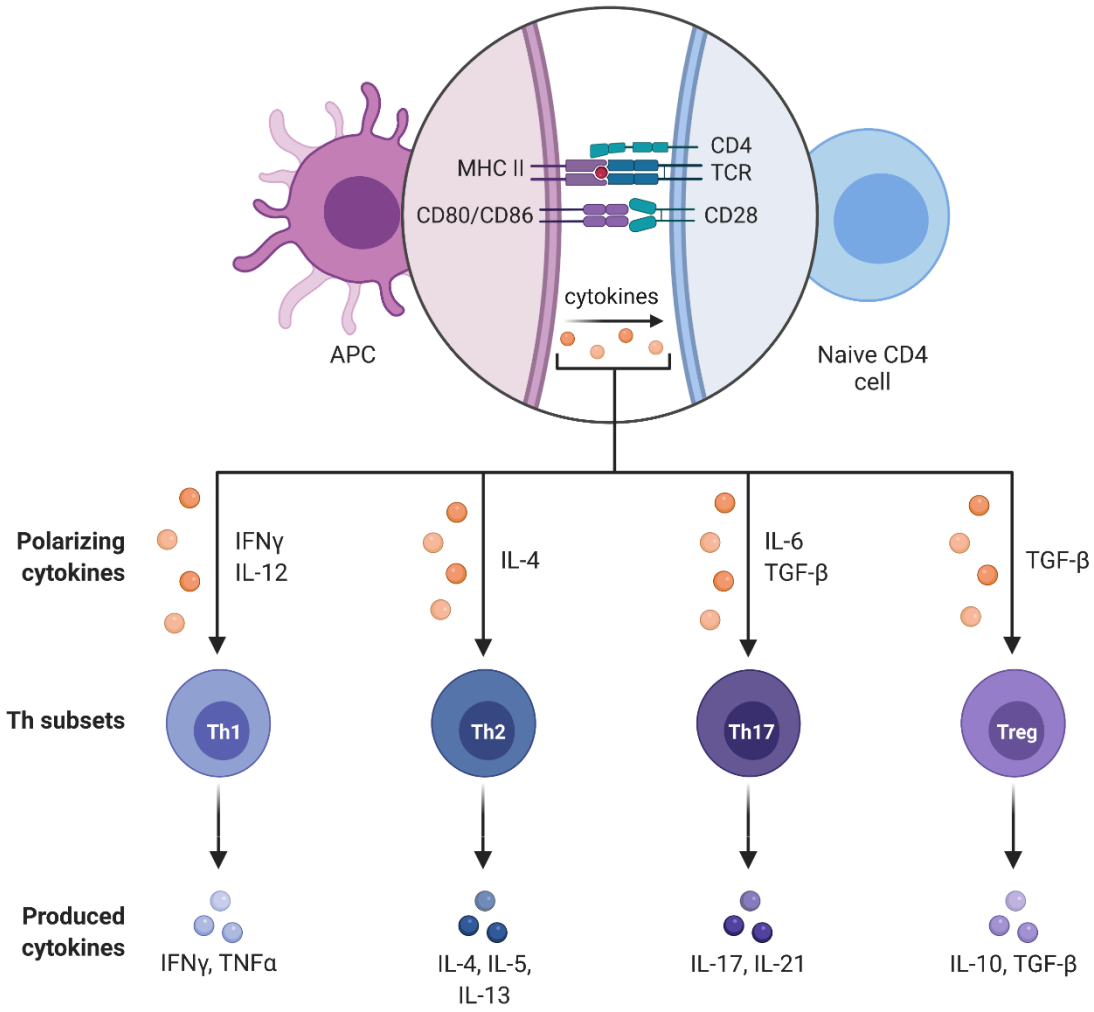

Illustration 1: CD4 T helper differentiation.

Upon antigen (red sphere) recognition via the TCR/MHC II interaction, an activated naïve CD4 T cell differentiates into distinct T helper subsets. Depending on the cytokines that are being released by the APCs, CD4 T cells differentiate into 4 main subsets: Th1, Th2, Th17 and Treg. Each subsets produces a distinct array of signature cytokines. This illustration has been adapted from a template from BioRender.com, made by Anna Lazaratos.

T cell receptor (TCR) signalling

T cells are activated by antigen-presenting cells and their engagement of the TCR with the MHC-Ag complex, as well as co-stimulatory receptors (CD80/CD86) (**Illustration 1 CD4 T helper differentiation**). TCR signalling induces substantial cellular changes in the T cells in order to induce activation, clonal expansion and differentiation. These changes range from the expression of transcriptional activators, reorganisation of the cytoskeleton and

conversion of the metabolic activity and rely on proximal TCR signalling and downstream signalling pathways (**Illustration 2: Proximal TCR signalling**).

The TCR is associated with different chains of the CD3 receptors, namely 2 chains of CD3ε, 1 chain of CD3γ, 1 of chain of CD3δ and 2 chains of CD3ζ. The intracellular tails of these receptors contain conserved motifs known as an immunoreceptor tyrosine-based activation motif (ITAM), which are essential for their proximal TCR signalling [15, 16]. Upon TCR activation Lck is recruited to the TCR complex and phosphorylates ITAM signalling motives, which creates binding sites for the Zap70 kinase. Zap70 binds to the phosphorylated ITAM motifs and becomes activated through phosphorylation by Lck. In turn, Zap70 propagates the signal by phosphorylating the linker for activation of T cells (LAT), creating binding sites for additional downstream signalling molecules. LAT contains 4 phosphorylation sites (Y132, Y171, Y191, Y226) that are able to recruit different molecules in order to induce downstream signalling. For instance, phospho Y132 recruits PLCγ1 to induce Calcium (Ca^{2+})/NFAT and MAPK pathways. On the other hand, the other phosphorylation sites recruit the adaptor proteins Grb2 and Gads, which in turn bind SOS and SLP-76, leading to Ras, Rac, and Rho GTPase activation. In addition to the LAT signalling hub downstream of the TCR, signalling downstream of the co-stimulatory receptor CD28 is required for the full activation of the T cells. PI3K, downstream of CD28, phosphorylates phosphatidylinositol 4, 5-bisphosphate (PIP_2) to phosphatidylinositol (3, 4, 5)-trisphosphate (PIP_3) on the inner side of the plasma membrane [17]. In turn, PIP_3 is now able to recruit and activate the ITK kinase and SLP-76 to further activate PLCγ1. Activated PLCγ1 hydrolyses PIP_2 into the secondary messenger inositol 1, 4, 5-trisphosphate (IP_3) and diacylglycerol (DAG). While IP_3 subsequently binds to its receptor IP_3R on the endoplasmic reticulum (ER) to release Ca^{2+} into the cytoplasm and induce NFAT signalling, membrane-bound DAG activates protein kinase C (PKC) and RasGRP. PKC and RasGRP, together with SOS, further activate the Ras/MAPK and NFκB pathways via ERK and IKK, respectively. In addition to recruiting ITK kinase and SLP-76, PIP_3, downstream of PI3K, also initiates the recruitment of PDK1. Consecutively, PDK1 activates its substrate AKT by phosphorylating threonine 308 (T308). Activated AKT then activates the mammalian target of rapamycin complex 1 (mTORC1), which has downstream functions in protein translation via S6 and activation of metabolic pathways via HIF-1α and c-Myc. For full activation, AKT also requires to be phosphorylated at serine 473 (S473) by mTORC2, which is, among other functions, involved in the reorganisation of the cytoskeleton.

Together, all these signalling pathways downstream of the TCR and co-stimulatory receptors (Ca^{2+}/NFAT, MAPK, NFκB, mTOR) contribute to the activation, metabolic switch, clonal expansion, differentiation and effector functions of T cells. Although those signals are

all necessary for proper T cell functions, a plethora of additional regulatory nodes fine tune the activity of the different pathways by integrating environmental signals into the equation to mount the ideal context-specific immune response.

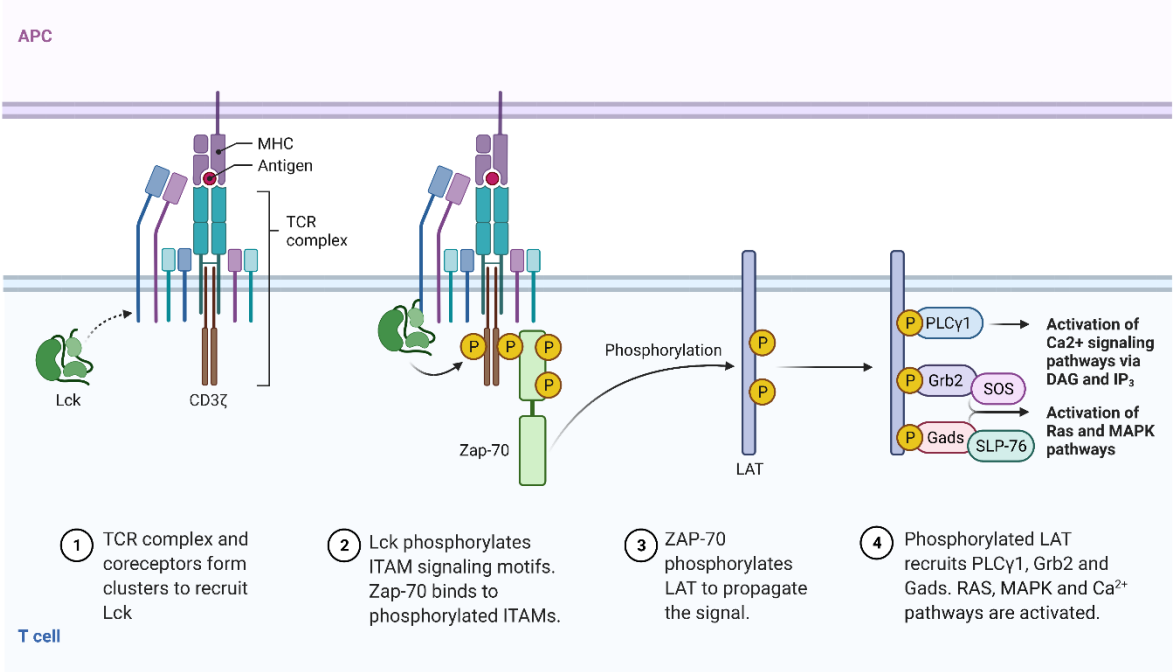

Illustration 2: Proximal T-cell receptor (TCR) signalling.

When the TCR complex recognizes a MHC-Ag-complex, it forms clusters with its co-receptors to recruit Lck. Lck phosphorylates ITAM motives, which allows Zap-70 to be recruited. In turn, Zap-70 phosphorylates LAT to propagate the signal. Phosphorylated LAT recruits PLCγ1, Grb2/SOS and Gads/SLP-76, which activate downstream signalling pathways, such as Ca^{2+}/NFAT signalling, NFκB and MAPK. This illustration has been adapted from a template from BioRender.com, made by Akiko Iwasaki and Ruslan Medzhitov.

Mechanisms of T cell regulation

It is out of the scope of this thesis to cover the entirety of factors that have been described to regulate CD4 and CD8 T cell responses. Therefore, only a few relevant examples of how environmental signals are integrated into the TCR pathways to fine-tune specific responses will be described here (**Illustration 3: Mechanisms of T cell regulation**).

As already mentioned above, cytokines secreted by surrounding immune cells or acting in an autocrine manner have a profound effect in guiding the differentiation of CD4 T helper cells into their different functionally distinct subsets. By binding to their respective receptors, cytokines activate the JAK/STAT signalling pathway leading the phosphorylation of different

STAT proteins, depending on the activated cytokine receptor [18]. In CD4 Th cells, STAT4 and STAT1 downstream of the IL-12 and IFNγ receptors, respectively, promote the expression of Tbet and Th1 differentiation. On the other hand, STAT6 downstream of IL-4 signalling is required for GATA3 expression and the Th2 subset. Th17 cell differentiation requires IL-6 and TGFβ signalling, which induce STAT3 phosphorylation and RORγT-dependent gene expression. In Treg, IL-2-induced STAT5 signalling is required for maintaining high levels of FOXP3 expression, which is required for Treg differentiation and suppressive functions [19]. Although the functions of STATs are quite well defined in CD4 Th cells, the knowledge on STATs in CD8 T cells is more limited. Nevertheless, evidence suggests that STAT3 is required for the maintenance and functions of memory CD8 T cells [20, 21], whereas STAT4 and STAT5 are crucial for CD8 effector differentiation [22, 23].

The mTOR signalling axis is an evolutionary conserved pathway that integrates different signals from the cellular environment into the TCR pathways [24]. Those signals include cytokines, co-stimulatory and inhibitory receptors, growth factor, as well as nutrients including amino acids and sugars. As previously indicated, mTOR exists in two distinct complexes, mTORC1 and mTORC2. mTORC1 mainly consists of three components: mTOR, Raptor (regulatory protein associated with mTOR), and mLST8 (mammalian lethal with Sec13 protein 8, also known as GβL). Instead of Raptor, mTORC2 contains Rictor (rapamycin insensitive companion of mTOR). Different activation signals and functions have been attributed to the two complexes. Of particular interest here, mTORC1 and mTORC2 signalling is required for the differentiation into different CD4 Th subsets [25, 26]. Although some controversy still remains about the contribution of each mTOR complex in the differentiation of CD4 T cells, due to the complex regulation of the system, a certain consensus has been obtained. mTORC1 is crucial for the differentiation into the Th1 and Th17 subsets, whereas mTORC2 drives Th2 differentiation. Similarly, mTOR also regulates the differentiation of CD8 T cells [27]. While mTORC1 signalling is essential for effector differentiation, mTORC2 enhances the generation of memory CD8 T cells. Overall, the recognition of a cognate antigen via the TCR induces several signalling pathways and activates T cells, but environmental stimuli, such as cytokines and nutrients that signal via mTOR, play a decisive role in the regulation of T cell differentiation and effector functions.

Beside major nutrients, such as amino acids and sugars, micronutrients, including vitamins A, C, D, E, B2, B6, B12 and folic acid, as well as trace elements such as iron, selenium, and zinc are essential for a competent immune response [28]. In the study presented in chapter 1 (Identification of VIMP as a gene inhibiting cytokine production in human CD4+ effector T cells), one micronutrient was of particular interest to us: Selenium (Se). Selenium is incorporated into the 21st amino acid selenocysteine and is thus required for the

expression of the 25 proteins that encode this amino acid [29]. Furthermore Selenium deficiency in humans has been linked to increased expression of inflammatory cytokines, whereas dietary selenium supplementation was described to alleviate inflammation [30]. VIMP, also referred to as Selenoprotein S (SELS), SELENOS, TANIS, or SEPS1, is one of the 25 genes encoding the 21st amino acid selenocysteine in humans [29]. In our study, we identified an anti-inflammatory role of VIMP and selenium in CD4 T cells via an intrinsic mechanism involving the Ca^{2+}/NFAT pathway. This shows a previously unrecognized mechanism in which micronutrients are involved in the regulation of CD4 T cell responses [31].

The mechanisms of T cell regulation operate in several different ways involving not only signals originating from immune cells, but also messages from other organ systems. In the recent past the role of the gut microbiome in physiology and pathophysiology has been increasingly appreciated and should be mentioned. Besides being important for organogenesis and tissue homeostasis [32, 33], metabolites originating from the microbiome can have a profound effect on the immune system [34-36]. In CD4 T cells, microbiome-derived short-chain fatty acids (SCFAs) promote the generation of Treg and immune tolerance [37]. On the other hand, SCFAs enhance the memory potential of Ag-specific CD8 T cells [38]. The ability of microbe-derived metabolites to regulate T cells, and the immune system in general, showcases how a seemingly unrelated system is able to regulate immune responses. Another organ that was always considered to be isolated from the immune system, but turned out highly connected, is the nervous system. This isolation of both systems partially arose from the misconception that the brain is an immune privileged organ with the blood-brain-barrier (BBB) avoiding the infiltration of immune cells. However, quite recently, the presence of a lymphatic system in the central nervous system has been discovered [39-41], generating many questions on the potential role of the immune system in neurodegenerative or psychiatric diseases [42, 43]. More than three decades prior this discovery, the field of neuroimmunology had appeared and already appreciated the deep regulatory interconnectivity of the immune system and the nervous system [44]. In the following sections we will discuss anatomical and functional connections between both systems and evidence some aspects of the regulation of CD4 T cells by the nervous system during a stress response.

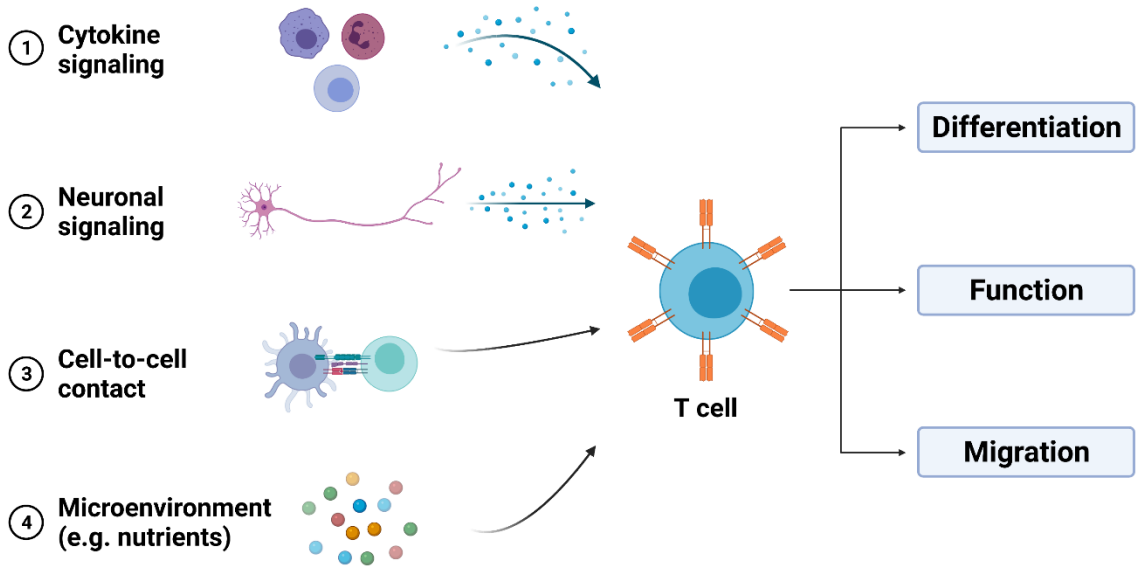

Illustration 3: Mechanisms of T cell regulation.

A myriad of different factors regulate the differentiation, function and migration of T cells. Some of the most important examples are highlighted in this thesis. 1) T cells are guided by the cytokines released into the microenvironment by other immune and non-immune cells. Distinct cellular programs are activated by specific cytokines and regulate T cell activities. 2) T cells have the ability to sense neuronal signals (e.g., stress hormones or neurotransmitters), which play an important role in maintaining homeostasis and guiding context-specific immune responses. 3) Cell-to-cell contact is another mode of T cells regulation. Although the receptor-based cell-to-cell contact is mainly required for the initial activation, co-stimulatory (e.g., CD28, ICOS) and-inhibitory receptors (e.g., PD-1, CTLA-4) fine tune the cell's activity. 4) Last but not least, the microenvironment, in which the cell resides, contains a plethora of different factors, hormones, nutrients and metabolites, which play an important role in the regulation of T cell responses. This illustration has been created with BioRender.com.

The nervous system in a nutshell

The nervous system can be broadly separated into the central nervous system (CNS) with the brain and the spinal cord and the peripheral nervous system spreading throughout our body. The peripheral nervous system can be further divided into the autonomic nervous system (ANS) and the sensory and motor nervous system. The latter functions in sensing environmental stimuli and sending the information to the brain, which reacts by sending an appropriate signal back to the periphery. The ANS can be sub-classified into three major

categories: the sympathetic nervous system (SNS), the parasympathetic nervous system (PaNS) and the enteric nervous system (ENS). Whereas the PaNS regulates involuntary responses in a resting state, the SNS is activated during the fight-or-flight response [45]. The ENS innervates the gastrointestinal tract to regulate gastro-intestinal behaviours independent of the CNS [46]. The ENS is the largest component of the ANS and, as it is isolated from the other nervous systems, is also termed “the second brain”. In addition to having their distinct functions in physiology, all those compartments of the nervous system interact with the immune system for mutual regulation [47]. This cross-talk only started to be appreciated in the last few decades [44] and will be outlined in more detail.

Anatomical and functional connection of the nervous system and the immune system

The connection between the nervous system and the immune system has long been ignored and both systems were studied in isolation until only a few decades ago. However, the neuro-immune axis is an evolutionary conserved pathway and exists in primitive animals, such as *Caenorhabditis elegans* [48]. This indicated that it must have a high importance in the regulation of our immune response. First, anatomical evidence set some cornerstones for the neuro-immune axis. Similar to every other organ, the primary (bone marrow and thymus) and secondary lymphoid organs (spleen and lymph nodes) are highly innervated, mainly by the SNS. Those nerve endings can release neurotransmitters into the vicinity of immune cells and regulate their responses [49, 50].The close proximity of both systems makes it evident that they interact with each other. In addition, the immune system and the nervous system also share many functional similarities [51, 52]. In short, the two systems are able to perceive, integrate and respond to environmental changes and develop a memory of that stimulus [53]. When it comes to the perception of the cellular environment the immune system and the nervous system both have their respective receptors and messenger molecules. The immune system senses foreign molecules or pathogens via PRR and reacts to signals of other immune cells via cytokine receptors. On the other hand, the nervous system signals through the secretion of neurotransmitters and their respective receptors. In addition, there is an overlap between the perception and production of messenger molecules between both systems. Indeed, nociceptors, a class of sensory neurons [54], also express PRR and have the ability to sense foreign antigens [55-57]. Furthermore neurons express cytokine receptors and are therefore able to react to immune signals [58-61]. At the same time, immune cells express receptors for neurotransmitters and other messenger molecules of the nervous system, making them capable of integrating

neurological signals into their immune pathways [62, 63]. Immune cells have also been reported to synthesize neurotransmitters intrinsically [64], giving them the ability to mediate neurological functions independent of the nervous system.

Another similarity between both systems is the ability to sense and produce local, as well as long range signals. Neurotransmitters and cytokines can travel via the bloodstream and act on cells distal from the location where the molecules were produced. In addition, immune cells and nerve endings are in close proximity and communicate through the local environment. Another ability displayed by both neurons and immune cells, is the communication via cell-to-cell contact. While electric signals “jump” from one neuron to the next via neurotransmitter signalling in the neurological synapse, the “immunological synapse” refers to the cell-to-cell contact during Ag-presentation [65-67]. Together, the anatomical proximity and functional similarities between the nervous system and the immune system create the basis for the extensive cross talk happening between both systems. In the following section, we will examine some examples where the immune system communicates with the nervous system and vice versa.

Immune-to-neuro communication

During an immune response, various immune cells release cytokines and other inflammatory molecules to control infections and clear the pathogen. These immune-derived signals not only regulate other immune cells, but also affect sensory neurons at the site of the immune response, modulating signalling in the CNS. An important class of sensory neurons with the ability to perceive immune signals, is the nociceptors, the “pain sensors” [54]. In the tissues, nociceptor nerve endings are located in the proximity of immune cells, including macrophages, neutrophils and mast cells, among others. The proximity of the nociceptors to the immune cells and the expression of cytokine receptors on nociceptors’ cell surface enable immune signals (cytokines) to modulate their function [68, 69]. Pain is one of the 5 cardinal signs of inflammation and is a good first example of a sensation that can be induced by cytokine signalling on nociceptive neurons [70]. Furthermore, the interaction between immune-derived cytokines and sensory neurons was described in itch, which is of particular importance in skin diseases, such as atopic dermatitis [71, 72]. Especially histamine, IL-31 and IL-33 were described to induce itch via their respective receptors on neurons. Also in allergy, infection or tissue damage, cytokines and immune-derived molecules activate nociceptors. In the context of allergic airway inflammation, the Th2 cytokine IL-5 activates nociceptors to produce vasoactive intestinal peptide (VIP). VIP further promotes Th2 responses of innate lymphoid cells (ILCs) and CD4

T cells to worsen the allergic reaction [73]. In a different context, the release of cytokines and in particular the so-called “pyrogens”, such as IL-1β, IL-6 and TNFα, also activate afferent vagus nerve signals to the brain to cause fever [74] and sickness behavior [75, 76]. Cytokine-induced sickness behavior was the first description for an immune-induced behavioural change, but in the meantime, the importance of inflammation and cytokine signalling has also found some ground in psychiatric diseases [77, 78], such as depression [79] and schizophrenia [80] or autism spectrum disorder (ASP) [81]. Aside from immune-derived signals regulating neuron activity in the context of peripheral inflammation, the immune-to-neuron communication is essential in neuronal development and brain homeostasis [82-84]. In particular microglia, the brain-residing macrophages, interact with most CNS-residing cells during embryonic and postnatal development to ensure proper brain functions [85-87]. More surprisingly, T cells, especially CD4 T cells, were also described to play an important role in neurogenesis, spatial learning and memory [85, 88, 89]. Although not exhaustive, the examples listed here, provide an overview of how immune-derived signals modulate neuronal cell functions that can lead to behavioural changes.

Neuro-to-immune communication

In the previous section, we discussed the regulation of the nervous system via messages from the immune system, such as cytokines. Vice-versa, the nervous system is also able to modulate immune responses via the secretion of neurotransmitters and hormones [47, 90]. The action potential signalling of neurons upon activation is several magnitudes faster than the release of cytokines by immune cells. This enables neurons to react to a sensed stimulus within milliseconds to start priming innate and adaptive immune responses with minimal delay after the first detection of the possible threat. This reactive regulation is similar to the definition of a reflex, which is characterized by 3 segments. First, a stimulus or change in the environment needs to be sensed by a specific receptor. The action potential generated by the stimulus is then transmitted from the periphery to the CNS via afferent nerves, to assess the signal and react adequately. Lastly, an action potential is sent back from the nervous system to the affected tissue, leading to a release of neurotransmitters that modulate the (micro)environment.

In a series of studies, Kevin Tracey and colleagues described for the first time such a reflex mechanism in the context of immunology and termed it the “inflammatory reflex” [91]. Efferent parasympathetic vagus nerves activate the sympathetic splenic nerve and the release of norepinephrine (NE) in the vicinity of T cells. In turn, a subset of T cells expressing

the choline acetyl transferase (ChAT) produce the neurotransmitter acetylcholine, which inhibits the expression of pro-inflammatory cytokines in macrophages and promotes anti-inflammatory, tissue protective macrophage cell programs via the nicotinic acetylcholine receptor subunit α7 (α7nAchR) [64, 92]. With this mechanism, the nervous system regulates inflammatory responses by utilizing the neuro-immune axis.

Masaaki Murakami and colleagues have identified a separate neuro-immune reflex regulating the infiltration of lymphocytes into the brain in the context of EAE (murine model for multiple sclerosis). This phenomenon was termed the “gateway reflex” and allows T cells to bypass the BBB and contribute to neuroinflammation [93-95]. They found that stimulation of nerves in a hind leg muscle (soleus muscle) by gravity triggers an IL-6 dependent expression of CCL20 in dorsal blood vessels of the 5th lumbar chord in the spine that leads to the local recruitment of pathogenic CD4 T cells. In this way, the 5th lumbar chord acts as a gateway for T cells to infiltrate the CNS. Similar gateway reflexes were later also suggested to be activated by additional stimuli, including electric stimulation, pain and stress [96, 97].

The intestines are highly innervated with extrinsic nerves from the SNS and PaNS (which has been described as the gut-brain axis), as well as with intrinsic enteric nerves that have been termed “the 2nd brain”. At the same time, the gut contains a large amount of lymphoid tissue which is home to different types of immune cells. Therefore, it comes with no surprise that the neuro-immune axis is also utilized to regulate immune functions and homeostasis in the gut [98-101]. Especially gastrointestinal macrophages are crucial in regulating homeostasis in the gut, depending on their location in the different intestinal tissue layers. Macrophages located in the “muscularis externa”, muscularis macrophages, have first been described to be involved in a bi-directional neuro-immune interaction to regulate gastrointestinal motility via a mechanism involving muscularis macrophages -derived BMP2 acting on enteric neurons to induce muscular contraction [102]. In turn, enteric neurons produce M-CSF to promote muscularis macrophage maintenance, which contributes to the tissue homeostasis. In the meantime, a myriad of examples have been discovered in which neuronal signals modulate the functions of immune cells residing in different tissues, such as the GI tract, the lung and the skin during tissue homeostasis or a disease context [103, 104]. This further showcases the control of the neuro-immune axis on tissue physiology.

The probably most-studied neuro-immune axis, is the action of the SNS-derived catecholamines (e.g. norepinephrine, epinephrine) and the glucocorticoids on immune cells during a stress response. The importance of stress hormone signalling in immune cells, and especially in T cells, will be described in more detail in the next section and is the focus of

the study described in chapter 2, entitled “Stress hormone signalling intrinsically inhibits Th1 polarization in naïve CD4 cells via the clock gene Period1 and mTORC1”.

Neuroimmunology during a stress response

Stress is a physiological reaction to a biological or psychological stimulus (stressor) that prepares the body to encounter a potential threat [105]. The human stress response involves two main communication axes based on either neural or endocrine signal transduction: the sympathetic-adrenal-medullary (SAM) axis and the hypothalamus-pituary-adrenal (HPA) axis. The immediate and short-term response to a stressor is the activation of the so-called fight-or-flight response and relies on the SAM axis [45]. Through direct innervation of most organs, sympathetic nerves initiate the physiological stress response by releasing norepinephrine (NE) directly into the organs. In addition, the SNS innervates the adrenal gland and triggers it to release of NE and epinephrine (EP) into the bloodstream. The SNS acts on the immune system during a stress response via the innervation of the primary and secondary lymphoid organs and the release of neurotransmitters into the vicinity of immune cells. Furthermore, the NE and EP released into the bloodstream can act on immune cells in the periphery. In addition to the quick response of the sympathetic nervous system that can act within seconds, the HPA axis relies on endocrine signalling that requires minute to hours. Upon perception of a stressor, neurons in the paraventricular nucleus (PVN) in the hypothalamus release corticotrophin-releasing factor (CRF) and arginine vasopressin (AVP), which in turn act on the pituary gland to secrete adrenocorticotropic hormone (ACTH) into the bloodstream. ACTH eventually reaches the adrenal gland to trigger the production of glucocorticoids (GC), such as cortisol in humans. Glucocorticoids in the bloodstream can travel to different organs, but also act on immune cells in the blood. Almost all immune cells express receptors for the stress hormones of the SAM and/or HPA axis and their signalling modulates specific immune functions [106, 107]. Stress hormones were long described as immunosuppressive molecules, but cell type-specific and context-dependant effects have emerged since then [108, 109]. In the study in chapter 2, we outline the effects of NE and GC on immune cells, in particular in the context of CD4 T cell polarization, and present a novel CD4 T-cell-intrinsic mechanism through which stress hormones inhibit Th1 polarization.

Clinical relevance of the neuro-immune axis

The discovery of neuro-immune circuits has provided potential targets for therapeutic intervention to treat different diseases, ranging from inflammatory and autoimmune disease, over cancer and allergy to psychiatric disorders [78, 110-115].

Adrenergic receptor or GC receptor agonists and antagonists have been used extensively to treat different diseases, such a cancer and inflammatory diseases and count as a prime example for utilizing a neuro-immune connection to treat pathologies [116-119]. More recently the inflammatory reflex was targeted for therapeutic intervention in rheumatoid arthritis (RA) [119-121]. In a clinical study, electrical vagus nerve stimulation by a small implanted device, reduced inflammation and attenuated disease severity in refractory RA patients [122, 123]. A similar approach was used in patients suffering from Crohn's disease, a type of inflammatory bowel disease (IBD) in which vagus tone is reduced. Stimulation of the vagus nerve for 6 months, increased the vagus tone, reduced inflammation and ameliorated disease severity in the patients of a small pilot study [124]. Furthermore, approaches blocking immune signals to treat psychiatric diseases have been utilized [125, 126]. As such, anti-cytokine treatment, like anti-TNFα antibodies (infliximab) showed promising results in treating inflammation-induced depression [127-129].

Ever since the misconception that the brain is an immune privileged organ was lifted, neurodegenerative diseases are on the map of immunologists [42]. This is not only because of the undeniable involvement of microglia, the brain-residing macrophages, in neurodegenerative diseases, such as Parkinson's disease (PD) and Alzheimer's disease [130], but also because of accumulating data suggesting that peripheral inflammation and autoimmune responses might play a role in the development and pathogenesis of those diseases [131-137]. Targeting the neuro-immune axis to modulate immune functions and restore homeostasis might be a promising therapeutic approach in various neurodegenerative diseases, including PD and AD [113, 138]. However, in order to design a mechanism-based therapy that aims at modulating immune responses in PD or AD, we first need to expand our understanding of the immune status of those patients. In chapter 3, we describe our study in which we systematically characterized the peripheral immune status of a highly selective cohort of PD patients and matched healthy controls (HC). We identified a distinct immunological fingerprint in the peripheral blood of early-to-mid stage PD patients, mainly in the CD8 T cell compartment. PD patients appear to have a peripheral immune status highly biased towards terminally-differentiated effector CD8 T cells (TEMRA). These active effector T cells, known to be highly cytotoxic [7, 8], in the blood of PD patients further indicate a potential role for the peripheral immune system in the pathogenesis of neurodegenerative diseases, i.e., PD. This underlines the potential of novel

immunomodulatory approaches to treat neurodegenerative diseases by targeting the easily-accessible peripheral immune system.

Scope and Aims

Scope and Aims

In this thesis, three separate studies are described with each one having their own objectives and outcomes in the studied setting, but they also share a common goal: they aim at deciphering unrecognized cellular and molecular pathways with the potential of providing new therapeutic targets in different immunological or clinical contexts. T cells are essential actors of the immune system and crucial for an adequate and robust immune response. At the same time, when dysregulated, T cells can cause or promote inflammatory and auto-immune diseases. We studied T cells in different experimental or clinical settings to better understand their biology and involvement in different diseases, with the aim to provide new ideas for therapeutic interventions (**Illustration 4: The overarching structure of the thesis**). To this end, we utilized the power of systems immunology to analyse transcriptomic or large-scale cytometry data sets [139-143]. In the light of recent ground-breaking research linking the immune system to neurodegenerative diseases, we especially focussed on the role of T cells in the context of neuroimmunology, such as during a stress response or Parkinson's disease.

In the first chapter, we aimed at predicting new genes regulating CD4 T-cell responses by using a previously published high-time-resolution time-series transcriptome data set [144]. This approach has a high potential to identify new genes and pathways that are involved in regulating immune cell functions. Indeed, we identified SELS/VIMP as a new anti-inflammatory gene of CD4 T effector cells and illustrate the molecular mechanisms through which VIMP mediates its function.

The second chapter focuses on the regulation of CD4 T cells during a stress response. Overall, stress hormone signalling is considered to inhibit cellular, type I immunity, while promoting humoral, type II immunity. This effect of stress on the immune system has profound consequences for a myriad of diseases and is believed to be executed through a T-cell extrinsic mechanism. In this study, we aimed at elucidating CD4 T cell-intrinsic mechanisms through which stress hormones regulate CD4 T cell differentiation. Identifying the molecular mechanisms of stress hormone signalling in human T cells, has the potential to identify new strategies to harness or counteract the effects of stress on immune cells in health and disease. We were able to pinpoint a novel molecular mechanism through which stress hormones hijack T cell differentiation pathways to specifically inhibit Th1 differentiation.

In the final chapter, we investigate the peripheral immune system in Parkinson's disease (PD) patients. Recently, a growing body of evidences shows that abnormalities in the peripheral immune system might be associated with pathogenesis of PD. However, the

status and composition of the peripheral immune system has not yet been systematically investigated. Therefore, we analysed peripheral immune cells of PD patients and healthy controls (HC) using a systems immunology approach to comprehensively assess the immune status of PD patients. By identifying a potential imbalance in the immune system of PD patients, this study could identify specific subsets of the peripheral immune system as a potential culprit in the progression of PD. Our analysis revealed a highly differentiated and effector-biased profile of CD8 T cells in PD patients, suggesting that CD8 T cells could contribute to the PD pathogenesis and providing a novel, easily-accessible therapeutic option to treat PD even at an earlier stage.

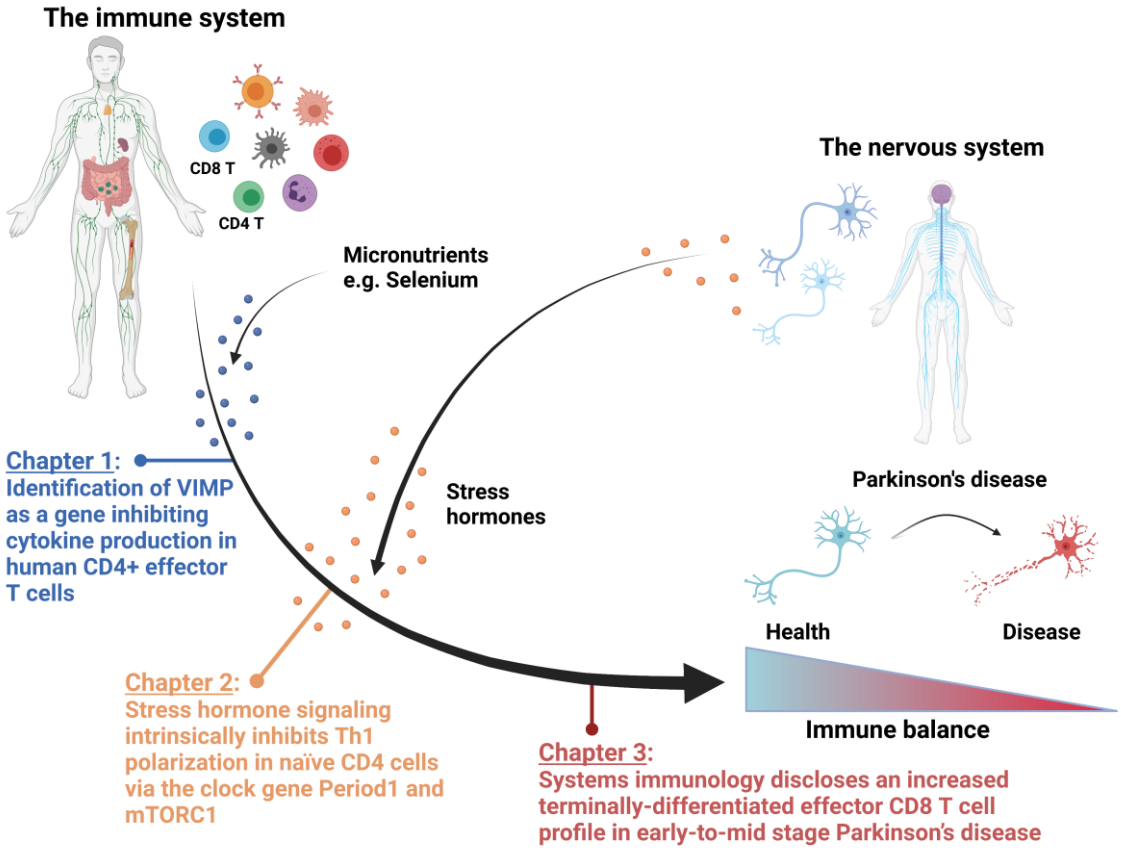

Illustration 4: The overarching structure of the thesis.

The immune system is regulated by various factors to ensure proper immune balance. Those factors are present in the cell microenvironment, including nutrients and metabolites, or are produced by other organs, such as the nervous system. In this thesis, we investigated regulatory mechanisms of T cells, especially in the context of neuroimmunology. In the first chapter, we described a novel role for the selenoprotein VIMP in inhibiting cytokine production of CD4 T cells. Selenoproteins require Selenium (Se) for their biosynthesis, making Se an important micronutrient to ensure an adequate immune response. In the

second chapter, we explored the effect of stress hormones on CD4 T cells and identified a previously unrecognized mechanism through which stress hormone signalling inhibits Th1 polarization in naïve CD4 T cells. Finally, in the third chapter, we investigated the role of the immune system in a neurodegenerative disease, with the example of PD, and revealed a potential role of terminally-differentiated CD8 T cells (TEMRA) in the pathogenesis of PD. This illustration has been created with BioRender.com.

Chapter 1

Identification of VIMP as a gene inhibiting cytokine production in human CD4+ effector T cells.

Chapter 1: Identification of VIMP as a gene inhibiting cytokine production in human CD4+ effector T cells.

Published in *iScience, 24, 4, 2021, 102289*, https://doi.org/10.1016/j.isci.2021.102289.

Christophe M. Capelle[1,2], Ni Zeng[1], Egle Danileviciute[1,3], Sabrina Freitas Rodrigues[3], Markus Ollert[1,4], Rudi Balling[3], Feng Q. He[1,3,5,6*]

[1] Department of Infection and Immunity, Luxembourg Institute of Health (LIH), 29, rue Henri Koch, L-4354, Esch-sur-Alzette, Luxembourg

[2] Faculty of Science, Technology and Medicine, University of Luxembourg, 2, avenue de Université, L-4365, Esch-sur-Alzette, Luxembourg

[3] Luxembourg Centre for Systems Biomedicine (LCSB), University of Luxembourg, 6, avenue du Swing, L-4367, Belvaux, Luxembourg

[4] Department of Dermatology and Allergy Center, Odense Research Center for Anaphylaxis (ORCA), University of Southern Denmark, Odense, 5000 C, Denmark

[5] Institute of Medical Microbiology, University Hospital Essen, University of Duisburg-Essen, D-45122, Essen, Germany

[6] Lead Contact

* Correspondence: feng.he@lih.lu

Abstract

Many players regulating the $CD4^+$ T cell-mediated inflammatory response have already been identified. However, the critical nodes that constitute the regulatory and signalling networks underlying CD4 T cell responses are still missing. Using a correlation-network-guided approach, here we identified *VIMP* (VCP-interacting membrane protein), one of the 25 genes encoding selenoproteins in humans, as a gene regulating the effector functions of human CD4 T cells, especially production of several cytokines including IL2 and CSF2. We identified VIMP as an endogenous inhibitor of cytokine production in CD4 effector T cells via both, the E2F5 transcription regulatory pathway and the Ca^{2+}/NFATC2 signalling pathway. Our work not only indicates that VIMP might be a promising therapeutic target for various inflammation-associated diseases, but also shows that our network-guided approach can significantly aid in predicting new functions of the genes of interest.

Graphical Abstract

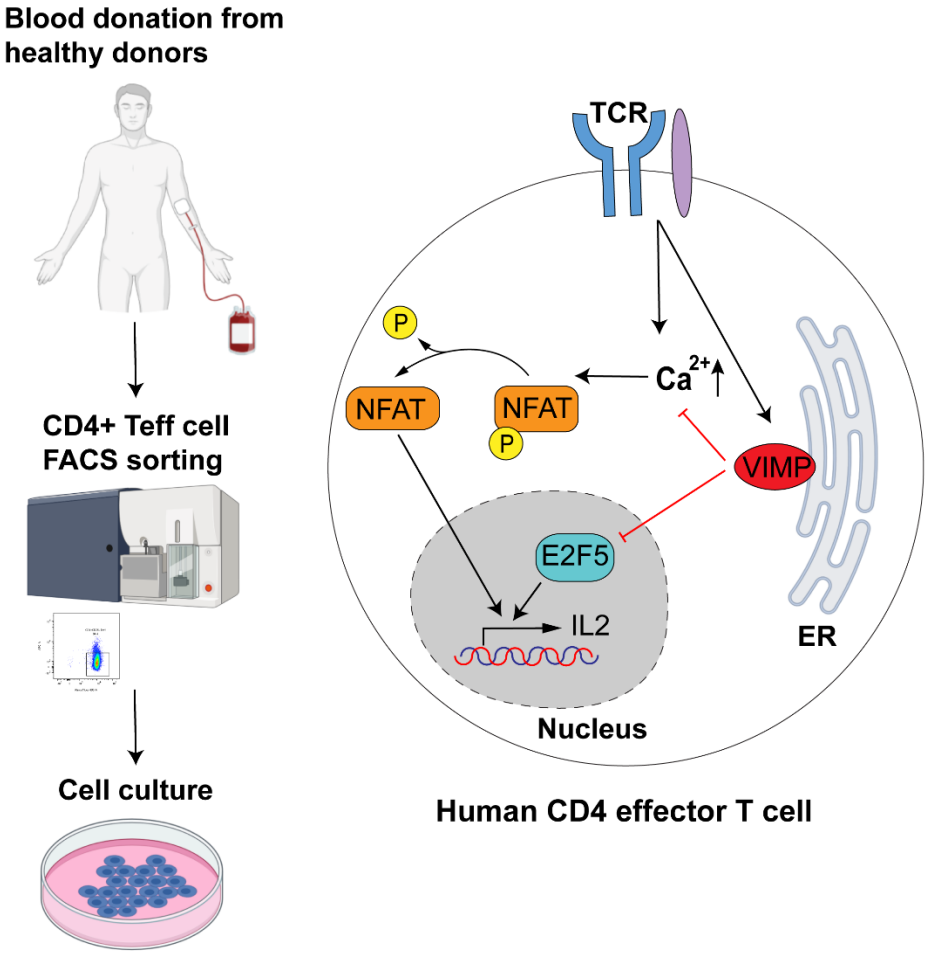

Keywords

Systems immunology; CD4 T cells; cytokine production; IL2; network-guided functional prediction; correlation network; VIMP/SELS/SEPS1; Selenoprotein; NFAT phosphorylation.

Introduction

$CD4^+$ T cells represent a major subset of immune cells that are crucial for mounting and regulating an adequate immune response. However, during many infectious and complex chronic diseases, those T cells are dysregulated, either having an impaired responsive capacity or causing adverse effects through self-recognition and/or overactivation. Therefore, rebalancing the $CD4^+$ T cell-mediated inflammatory response has been essential for the design of therapeutic options for those diseases [145]. Although, many players regulating the inflammatory response, cytokine production and differentiation of $CD4^+$ T cells have already been identified in the past [146-149], a thorough understanding of the regulatory and signalling networks governing inflammatory cytokine production in T cells is still missing. The gap is not only attributable to the long-standing nature of traditional trial-and-error experimental procedures, but also due to the lack of the reliable high-throughput computational prediction.

VIMP, also known as Selenoprotein S (SELS), SELENOS, TANIS or SEPS1, is one of the only 25 genes encoding the 21st amino acid selenocysteine in humans [150]. Located in the endoplasmic reticulum (ER) membrane, VIMP is mainly known as an important component of the ER-associated degradation (ERAD) complex [151, 152] and physically binds to several ER membrane proteins [153, 154]. VIMP plays a role in mediating retro-translocation of misfolded proteins from the ER lumen to the cytosol, where the ubiquitin-dependent proteasomal degradation takes place [155]. Genome-wide association studies have shown that polymorphisms in the promoter region of *VIMP* are linked to a wide spectrum of common complex diseases, including cardiovascular disease [156], diabetes [157, 158], cancer [159-161], sepsis [162] and autoimmune diseases [163, 164], in which activation of the immune system is believed to be dysregulated [165].

Meanwhile, dysfunction of the ER and the unfolded protein response causes intestinal inflammatory diseases in several murine models [166]. Additionally, a reduced expression of VIMP causes an increased expression of inflammatory cytokines, such as IL6, IL1β and TNFα in macrophages [167], as well as IL1β and IL6 expression in astrocytes [168]. However, other studies did not show significant association between *VIMP* and the examined human inflammatory diseases [169]. This controversy underlines the necessity for a better understanding of how *VIMP* contributes to the pathogenesis of some inflammatory diseases, i.e., through which cell types and which molecular pathways *VIMP* contributes to the observed dysregulated inflammatory responses. Therefore, we sought to investigate whether and how *VIMP* plays a role in relevant specific immune cells, e.g., $CD4^+$

T cells, a key subset of immune cells orchestrating different types of immune responses and being heavily involved in different complex diseases, as well as infectious diseases, such as COVID-19 [170, 171].

We have previously developed a correlation-network guided approach, based on the guilt-by-association theory [172-174], to predict novel key genes of a given biological process or function and have successfully applied it to human $CD4^+CD25^{high}CD127^{low}$ regulatory T cells (Tregs) [144, 175]. Here, we extended the strategy to human $CD4^+$ effector T cells (Teffs) that were derived and expanded from sorted $CD4^+CD25^-$ T cells by co-culturing with EBV-transformed B cells and were able to predict that VIMP might play an important role in regulating the effector responses of Teffs. Combining both the network analysis and experimental verification, we identify VIMP as a previously unreported vital endogenous inhibitor of cytokine production in human $CD4^+$ Teffs and reveal the molecular mechanisms through which VIMP regulates $CD4^+$ Teff responses.

Results

VIMP is temporally upregulated following TCR stimulation in Teffs

Using our previously reported high-time-resolution time-series (HTR) transcriptome data of Tregs and Teffs following TCR (T cell receptor) stimulation in the first six hours [144], we observed that in Teffs the transcript level of VIMP temporally peaked within 2-3 hours following stimulation, which was followed by a gradual decrease (**Fig. 1A**). In contrast, the *VIMP* mRNA level was kept almost constant in Tregs during the first six hours following TCR stimulation (**Fig. 1A**), indicating a possible specific role for VIMP in Teffs. Our quantitative real-time PCR (qPCR) results validated the transitionally elevated expression of the VIMP transcript in Teffs isolated from different healthy donors (**Fig. 1B**). We also observed a correlation over time between the transcription levels of *VIMP*, *IL2*, *IL13* and *CSF2 (*GM-CSF*)* following TCR stimulation, indicating a potential regulatory relationship between *VIMP* and some of the cytokines in Teffs (**Fig. 1B**). By flow cytometry (**Fig. 1C**), we confirmed the gradual upregulation of VIMP protein expression in the first 5 hours following TCR stimulation. In summary, both mRNA and protein expression of VIMP were upregulated following TCR stimulation, which was correlated with the expression of several examined cytokines, indicating a potential role of VIMP in regulating Teff responses.

VIMP inhibition upregulates cytokine expression in Teffs

The upregulation of VIMP and its correlation to cytokine expression encouraged us to further investigate VIMP's potential role in CD4 T cell responses. We and others have

previously shown that the enriched pathways or processes or functions among the genes surrounding a given hub gene in the correlation network might give valuable indications on potential new functions of the given hub gene [144, 175]. Therefore, we used our correlation network-guided approach to predict the potential functions of *VIMP* by identifying the enriched pathways among the genes that are linked to *VIMP* within the subnetwork of the Teff correlation network, which was extracted from our published HTR datasets and networks [144] (**Fig. 2A**).

Consistent with its known function and its localization in the ER membrane, the genes surrounding *VIMP* in the correlation network were significantly enriched for ER components (*P-value=1.7E-7*, cumulative Binomial distribution) (**Fig. 2A**). Furthermore, 3 out of the 10 experimentally-validated VIMP-binding partners found in the literature in other cellular types are directly linked to *VIMP* in the Teff correlation network [*P-value=2.0E-4*, http://string-db.org [176]], indicating the reliability of our method. Surprisingly, the pathway enrichment analysis shows that the genes linked to *VIMP* are significantly enriched for components involved in the TCR signalling pathway (*P-value=1.2E-3*, cumulative Binomial distribution) (**Fig. 2A**), suggesting a potential role of VIMP in the Teff response according to our network-based analysis strategy [144, 175]. However, the genes linked to the hub gene of interests in the correlation network could follow at least two scenarios [177-179]. First, those genes could be co-regulated by chance with the hub gene and perform independent functions. Second, those genes could be co-expressed with the hub gene and play related roles in the same pathways to coordinate cellular resources for a particular function or purpose under certain conditions. We will test these possibilities in this work.

In order to systematically assess whether and how *VIMP* controls the inflammatory response of Teffs, we performed a transcriptome analysis of CD4 Teffs isolated from peripheral blood mononuclear cells (PBMC) of three healthy donors that were subjected to a specific-siRNA knockdown of VIMP (si_VIMP) or a control unspecific scrambled siRNA (si_NS) followed by anti-CD3/-CD28 stimulation (**Fig. 2B**). As shown in **Fig. 2C,** the mRNA expression of *VIMP* was significantly downregulated in Teffs by using siRNA knockdown.

As VIMP has reported functions in ER stress, we first checked the ER-stress responsive genes in the transcriptomic data of the Teffs transfected with si_VIMP versus (vs.) that treated with control siRNA (si_NS). By perturbing the expression of *VIMP*, we expected a change in expression of some ER-stress responsive genes. Nonetheless, our transcriptome data of Teffs with VIMP partial knockdown did not show any significant change in mRNA expression of those genes (e.g., *CHOP (DDIT3), GRP78 (HSPA5), EDEM1, DNAJC3*

(P58IPK) and *DNAJB9 (ERdj4)* [180]) (**Fig. 2D**). Only the expression of the ER-stress regulator *XBP1* [181] was significantly but modestly decreased. Indeed, data from intestinal epithelial cells show that VIMP is only a marker, but not a regulator of ER stress [182]. This shows that the direct involvement of VIMP in ER stress might not be ubiquitous to all cell types. We therefore ruled out the possibility that VIMP directly regulates the expression of the ER-stress responsive genes, indicating other roles of VIMP in modulating the Teff responses.

Considering that the TCR signalling pathways were significantly enriched in the VIMP correlation network, we further analyzed the genes related to the TCR signalling pathway in Teffs after *VIMP* knockdown. Notably, we found 13 significantly upregulated genes involved in the TCR signalling, including several cytokines, namely *IL2*, *IL4*, *CSF2* and *IFNG* (refer to https://www.genome.jp/kegg-bin/show_pathway?hsa04660) in the microarray datasets of the Teffs, although subjected to only a partial knockdown of *VIMP* (**Fig. 2E**). Moreover, transcripts of the key TCR related signalling molecules, such as *GRAP2*, *ZAP70*, *RASGRP1* and *RAF1* were significantly affected (**Fig. 2E**). With the observation in mind that *VIMP* and the TCR signalling related genes were directly linked in our HTR correlation network (**Fig.2A**), this effect of the siRNA perturbation was not unexpected. Our results suggest that VIMP negatively regulates the expression of specific cytokines and influences the expression of important components of the TCR signalling pathway.

To further confirm whether *VIMP* regulates cytokine expression in Teffs, using PBMC of independent donors we measured the cytokine mRNA expression by qPCR and the secreted cytokines of Teffs that were exposed to a *VIMP* knockdown. Indeed, *IL2, IL21 and CSF2* mRNA were significantly upregulated in stimulated Teffs transfected with si_VIMP, compared with control Teffs (with si_NS) (**Fig. 2F**). This observation was further consolidated by increased IL2, IL21 and GM-CSF protein production in the culture media of stimulated Teffs transfected with si_VIMP, compared with that treated with control scrambled siRNA (**Fig. 2G**). Furthermore, the VIMP knockdown also significantly promoted T cell proliferation as indicated by both CFSE peak shifting and Teff cell number counting experiments (**Fig. 2I**). As IL2 concentration was already significantly higher at 3 hours following stimulation (**Fig. 2G**) and no cell division was already expected, the enhanced IL2 secretion following VIMP knockdown was not simply caused by more Teffs. All the analyses were done under the precondition that VIMP protein was successfully silenced (**Fig. 2H**). In short, VIMP negatively regulates the expression of several cytokines in Teffs following stimulation.

Considering that *VIMP* encodes Selenocysteine, thus requiring selenium (Se) for its protein synthesis and the fact that a relatively low concentration of Se was used in our T-cell media (IMDM, ~0.066 uM), we next supplemented sodium selenite in the T-cell culture media to the range of physiological concentrations (~1 uM) [183-185]. In line with the reported effect of Se supplementation on inflammatory cytokines in human serum and our knockdown results, increasing the concentration of Se in the media generated a dose-dependent suppressive effect on IL2 production of sorted CD4 Teffs following TCR stimulation (**Fig. S1A, B**). Meanwhile, increasing Se concentration to a physiological concentration upregulated the VIMP expression of stimulated CD4 Teffs among 3 out of 5 tested donors (**Fig. S1C, D**). These results again indicate that Se, at least partially, negatively regulates the expression of cytokines, e.g., IL2 in CD4 Teffs via VIMP.

VIMP controls cytokine expression via the transcription factor E2F5

Next, we aimed to identify any (co-)transcription factors (TFs), whose expression were significantly affected after silencing VIMP, as they often serve as the key components orchestrating the activity of the relevant pathways. Through a systematic analysis of all the known mammalian TFs or co-factors [186] in our microarray datasets, *E2F5* was found as the most significantly upregulated TF, following a partial VIMP knockdown (**Fig. 3A**). Conversely, *RNF14* (ring finger protein 14) was the most downregulated cofactor together with the downregulated TFs such as *CEBPG* (CCAAT Enhancer Binding Protein Gamma*)*, *ZBTB20* (zinc finger and BTB domain containing 20) and *IRX3* (Iroquois homeobox 3) (**Fig. 3A**). We further confirmed the expression change of these (co-)TFs by qPCR in independent healthy donors (**Fig. 3B**).

E2F5 has previously been reported to be a downstream target of IL-2 in an immortalized human T cell line [187]. But to our knowledge, there are no reports yet of *E2F5* sitting at the upstream pathways regulating inflammatory responses, especially cytokine production. Nevertheless, being the most significantly upregulated TF following a partial knockdown of *VIMP*, we assumed that *E2F5* might be an important component in the regulatory pathway through which *VIMP* regulates the Teff inflammatory response.

Therefore, we decided to investigate whether *VIMP* controls the cytokine expression by negatively regulating *E2F5* expression in stimulated Teffs. In order to examine this hypothesis, we silenced *VIMP* alone or in combination with *E2F5* and measured the expression of selected cytokines by qPCR. In addition to the reduced expression of *VIMP*, the upregulation of *E2F5* expression that was driven by *VIMP* knockdown was abolished in the *VIMP* and *E2F5* double knockdown Teffs (**Fig. 3C**). While silencing *VIMP* alone upregulated *IL2* expression in stimulated Teffs, a dual knockdown of *VIMP* and *E2F5*

suppressed the surge of *IL2* caused by VIMP knockdown alone (**Fig. 3C**). Even though *E2F5* is a general regulator of transcription, we did not observe any effect of *E2F5* knockdown on genes that are not directly involved in Teff inflammatory response, such as *CTLA4* (**Fig. 3C**). This excluded a generalized effect of *E2F5* on the transcriptional regulation in Teffs. In brief, our data support that *VIMP* regulates the expression of inflammatory cytokines, i.e., IL2, by restraining the expression of the TF *E2F5* in Teffs.

VIMP controls cytokine expression via the Ca^{2+}/NFATC2 signalling pathway

To further delineate VIMP's regulatory pathways beyond the altered expression of individual TFs determined by the differential-expression analysis of our microarray datasets, applying the Ingenuity Pathway Analysis (IPA), we mapped the up- or down-regulated cytokine and TCR related genes into the known regulatory network structures. We found that many of those differentially-expressed genes are controlled by the expression change of the so-called hub genes *IL2*, *RAF1*, *IL21*, *TNFSF11,* as well as nuclear factor of activated T cells (NFAT) activity (**Fig. 4A**). Although *NFAT* transcript expression was not significantly affected (**Fig. 4A**), its activity was predicted to be increased by the IPA computational analysis. Meanwhile, we investigated the *VIMP* subnetwork in the Teff correlation network in more depth (**Fig. 2A**). We found that genes for several components of NFκB, NFAT and MAPK signalling pathways were also directly linked to *VIMP*, indicating that those pathways might be involved in the regulation of the inflammatory response of Teffs by VIMP. In order to determine whether any of the relevant signalling pathways downstream of the TCR pathway that were suggested by the computational analysis are affected by VIMP expression, we quantitatively assessed the phosphorylation levels of up to 10 various signalling proteins by flow cytometry (**Fig. 4B**). Canonical (NFKB1 p105 and p65) and non-canonical (NFKB2 p100 and RELB) NFκB signalling pathways, as well as several MAP kinase sub-pathways (ERK1/2, p38, JNK1/2 and cJun) were not significantly affected in their phosphorylation levels (**Fig. S2A-E, S3**). The phosphorylation level in one of the NFAT family members, NFATC1, was also not significantly affected by VIMP knockdown in stimulated Teffs (**Fig. S2F, S3**). However, the phosphorylation level at the specific site Ser326 of another NFAT family member, NFATC2 (also known as NFAT1) was significantly reduced even following a partial VIMP knockdown, as quantified by both flow cytometry and western blotting in Teffs isolated from different donors (**Fig. 4C-E, Fig.S2G**). Total NFAT protein remained unaffected by the partial VIMP knockdown (**Fig. S2H**). In resting T cells, NFAT proteins are phosphorylated and reside in the cytoplasm [188, 189]. In order to be able to translocate to the nucleus and induce gene expression, NFAT is de-phosphorylated following the TCR signalling. As the NFAT activity is known to regulate IL2 expression in T cells [190], the observed downregulation of NFATC2 phosphorylation, following *VIMP*

knockdown, demonstrated that the upregulation of IL2 expression was, at least in part, due to an increase in NFAT activity.

The distinguishable feature of NFAT is that it relies on Ca^{2+} influx and subsequent Ca^{2+}/calmodulin-dependent phosphatase calcineurin to become dephosphorylated and being able to translocate to the nucleus to induce gene expression [191]. Although *VIMP* has not yet been linked to the calcium signalling, other selenoproteins have been described to regulate the calcium signalling and homeostasis [192]. We therefore further asked whether *VIMP* knockdown affects the calcium flux in Teffs and measured it by flow cytometry using the calcium indicator Indo-1. Indeed, the Teffs in which *VIMP* was silenced vs. the control Teffs, showed a significantly higher flux of Ca^{2+} ions (**Fig. 4F**), further illustrating the increased NFATC2 activity and IL2 expression.

In summary, our data strongly suggest that *VIMP* inhibition upregulates the expression of cytokines, such as IL2 by two mechanisms at different levels (**Fig. 4G**). On the transcription regulatory level, *VIMP* controls the expression of transcription factor E2F5 and multiple genes involved in the TCR signalling and the inflammatory response. On the signalling transduction level, *VIMP* knockdown modulates Teff responses by controlling the Ca^{2+} flux and the downstream NFATC2 de-phosphorylation.

Discussion

So far many important components in the regulatory or signalling networks modulating the inflammatory responses of Teffs still remain elusive. With the development of systems biomedicine, researchers have greater opportunities to use top-down approaches to objectively infer and identify novel key genes or proteins in the process of interest.

In this work, we have applied our previously published correlation network-guided strategy to predict new genes regulating the effector functions of $CD4^{+}CD25^{-}$ Teff cells, i.e., cytokine production. We identified VIMP, encoding an ER membrane associated selenoprotein, as a previously unrecognized negative regulatory gene of the Teff response. VIMP is most known for its critical functions in ER stress, which was demonstrated in some tested cell types. Our transcriptomic correlation network in Teffs also indicates that VIMP might be involved in ER-stress related functions. However, as shown here, inhibiting the VIMP expression in human primary Teffs did not support that VIMP is critical for the transcriptional regulation of ER-stress responsive genes in Teffs. Next, the correlation network navigated us to check the TCR signalling pathways in Teffs. As demonstrated in different layers, VIMP

indeed substantially regulated the expression of several inflammatory cytokines, especially IL2, in Teffs. We next investigated the VIMP regulatory mechanisms using primary human Teffs isolated from different healthy donors, the most clinically relevant available materials. Combining the analysis in both time-series correlation network and knockdown-based regulatory networks, we further predicted that VIMP might go through the NFAT signalling pathway, or MAP kinase or NFKB signalling pathways to mediate the effector functions of Teffs. After testing those signalling pathways one by one, we finally pinpointed that VIMP inhibition enhances cytokine production of Teffs via the NFATC2 signalling pathway. The involvement of the NFAT signalling pathway was further backed by the influence of VIMP inhibition on calcium (Ca2+) influx, which is vital to the activation of the NFAT signalling pathway. Coincidently, Joost and colleagues have recently reported the co-expression of *VIMP* and *NFATC2* transcripts within the murine interfollicular epidermis using single-cell RNA-seq analysis, indicating from another angle that our conclusion might hold true [193]. We have also shown that *E2F5* plays a significant role in the VIMP-mediated regulation of the Teff IL2 expression. However, whether the *E2F5* pathway and the Ca2+/NFATC2 signalling pathway controls VIMP-mediated IL2 expression in a sequential manner or in parallel requires further investigation. Although the previously published association studies have already shown that the VIMP expression levels and/or SNPs are correlated with the risk of several type of diseases, it remains unsolved whether VIMP deficiency can regulate the effector functions of Teffs in vivo.

In our transcription-factor (TF) focused analysis, we identified not only *E2F5*, as the most upregulated TF, but also several downregulated TF genes, following VIMP knockdown. Among those downregulated ones, *RNF14* (ring finger protein 14), a less characterized gene, represented the most significantly downregulated co-factor, attributable to VIMP knockdown in Teffs. Although very limited, a published report shows that *RNF14* modulates the expression of inflammatory and mitochondria-related genes in a murine myoblast cell line [194]. Another downregulated TF, *ZBTB20* has originally been studied in human dendritic cells [195], later in myeloid cells [196] and B cells [197], has been shown to regulate their effector functions and differentiation. The Iroquois homeobox 3 (*IRX3)* has been recently linked to human CD8 T cell survival and fate determination *in vitro* [198]. Although there is no direct evidence of *CEBPG* being involved in the regulation of cytokine expression in CD4 effector T cells, other C/EBP protein family members have been shown to act as negative regulators in the production of inflammatory cytokines [199, 200]. Therefore, those TFs might deserve a further investigation.

Selenoproteins fully rely on selenium for their biosynthesis and function. Dietary selenium supplementation in mice has been shown to increase the biosynthesis of several selenoproteins including SELS/VIMP [201, 202] and to reduce the expression of several inflammatory cytokines, such as tumor necrosis factor α (TNFα), monocyte chemoattractant protein 1 (MCP1) and IL2 [201, 203-205]. Dietary selenium supplementation has further been linked to alleviate several complex and multifactorial diseases [206-209]. On the other hand, selenium deficiency might affect the synthesis of multiple selenoproteins in mice, resulting in an increased pathology from influenza viral infections, due to an exaggerated inflammatory immune response [205]. In our media (the complete IMDM) for short-term T-cell culture, the Se concentration (0.066 μM) was around 15 times lower than in human sera (~1 μM) [183-185]. Although the Se concentration used in our media was low, our western blotting results (**Fig. 4C**) have demonstrated that the Se concentration was not a limiting factor yet for VIMP protein synthesis during the tested period of up to 24 hours following stimulation, as the protein expression of VIMP still increased following TCR stimulation. In the VIMP-knockdown T cells, where the VIMP protein synthesis was further reduced, the low concentration of Se in the media was thus not a concern. Therefore, our conclusion derived from IMDM media with a VIMP-knockdown approach is reliable. Last but not least, increasing Se concentration showed a dose-dependent suppressive effect on IL2 production (**Fig. S1A,B**). Following Se supplement, the majority of the tested donors exhibited enhanced expression of VIMP in CD4 Teffs (**Fig. S1D)**. For those donors, already having a high level of VIMP expression (**Fig. S1D)**, Se supplementation cannot further increase the expression of VIMP anymore, but still inhibited cytokine production possibly via enhancing the expression of the other selenoproteins. These observations indicate that at least for some patients with VIMP deficiency-causing mutations, Se supplementation would show beneficial values in suppressing pro-inflammatory cytokine responses of CD4 T cells.

Interestingly, the immune system presents a sexual dimorphism [210], where females appear to have a stronger humoral and cellular immune response in general, making them more resistant to infectious diseases [211], nevertheless, more susceptible to autoimmune diseases [212, 213]. CD4 T cells, the focus of this study and the central orchestrators of immune responses, also show a differential sex-specific regulation [210, 214, 215]. Multiple factors on the genetic [216-218], hormonal [219] or environmental level [220, 221] have been shown to regulate sex-specific effects in immune responses. It is worthy to note that selenium also displays intriguing sex-specific differences in regard to its metabolism [222], tissue distribution [223] and effects in several physiological and pathological conditions, including immune associated diseases [201, 224-228]. Excitingly, the expression of VIMP

increases following selenium supplementation in the liver of male mice, whereas in female mice VIMP expression only reaches a maximum after LPS challenge to induce an acute immune response [201]. In regard to our data, this leads us to hypothesize that selenium supplementation and its potential sex-specific effects on VIMP expression might also result in a gender-biased effect on CD4 T cells.

Overall, using both hypothesis-free top-down computational analyses and bottom-up experimental methods, we have shown a regulatory role for the selenoprotein VIMP in controlling cytokine expression in $CD4^+CD25^-$ Teffs via several signalling pathways and transcriptional regulatory pathways. The same strategy should be generally extendable to other cell types in assisting the prediction and discovery of novel functions of any other genes of importance. In summary, our data identified an unrecognized critical regulatory role of the selenoprotein S (SELS/VIMP) in the inflammatory responses of human $CD4^+$ Teffs. Our observation provides a viable insight into how dietary supplementation of selenium might mediate its effects on $CD4^+$ Teffs and underscores the potential in therapeutically targeting VIMP in the treatment of various inflammatory and inflammation-related diseases.

Limitations of the study

Although we have successfully demonstrated a novel role for *VIMP* in the regulation of CD4 T cytokine expression and the underlying mechanisms, our study still presents certain limitations. As aforementioned, selenium supplementation and immune cell responses display a sexual dimorphism. In this study, we are aware that the majority of healthy donors were male. However, due to ethic regulations, we could not specify the gender of each individual donor, making it impossible to determine a possible sex-specific effect of *VIMP* on the effector functions of CD4 T cells.

In addition, our data is based on primary human CD4 T cells expanded *in vitro* and do not take into account all the complex cellular regulatory mechanism directly and indirectly acting on CD4 T cells present *in vivo*. Our work has shown an intrinsic role of *VIMP* on human CD4 effector T cells, but to better elucidate the importance of our findings in a disease context, *Vimp*-deficient mice could have been used, which, however, were not availble in the lab. Even though the whole-body deficiency of some selenoproteins is embryonically lethal [229], *Vimp*-deficient mice have been recently reported and mainly used to study the role of *Vimp* in muscle functions [230-232]. Excitingly, in line with our notion in human CD4 T cells, the reduction of *Vimp* expression even in heterozygous mice has been shown to increase the expression of several inflammatory genes in fast-twitch skeletal muscles [232].

Resource availability

Lead Contact

Further information and requests for different resources should be directed to and will be fulfilled by the lead contact, Feng He (feng.he@lih.lu).

Materials Availability

The study did not generate any unique specific materials.

Data and Code Availability

The microarray data have been deposited into Gene expression Omnibus (GEO) repository with the access code GSE151266. To review, go to https://www.ncbi.nlm.nih.gov/geo/query/acc.cgi?&acc=GSE151266 enter the token **wpudcscuxnyjbcb** into the box. All other data and information needed to evaluate the conclusions of this work are presented in the Supplemental information and Figures.

Methods

Primary T cell isolation and culture

Buffy coats from healthy donors were provided by the Red Cross Luxembourg and the informed consent was obtained from each donor by the Red Cross Luxembourg. The T cell isolation and culture procedures have been described in our previous works [144, 175, 233]. For the requirement of the STAR methods, here we described briefly again. We added the RosetteSep™ Human CD4+ T cell Enrichment Cocktail (15062, Stemcell) to undiluted blood at a concentration of 50 µl/ml and incubated for 30 min at 4°C. The incubated samples were then diluted 2 times with FACS buffer (PBS + 2% FBS) and the CD4+ T cells were obtained following gradient centrifugation at 1200 g for 20 min, using Lympoprep (07801, StemCell) and SepMate™-50 tubes (85450, Stemcell). Before sorting, the CD4+ T cells were first stained with mouse monoclonal [RPA-T4] anti-human CD4 FITC (555346, BD Biosciences) (dilution 1:20), mouse monoclonal [M-A251] anti-human CD25 APC (555434, BD Biosciences) (dilution 1:20) and LIVE/DEAD® Fixable Near-IR Dead Cell Stain (L10119, ThermoFisher Scientific) (dilution 1:500). Primary CD4 T cells ($CD4^+CD25^-$) were then sorted on a BD FACSAria™ III cell sorter (BD Biosciences).

Target	Fluorochromes	Dilution	Company	Clone	Reference
CD4	FITC	1:20	BD Biosciences	RPA-T4	555346
CD25	APC	1:20	BD Biosciences	M-A251	555434

Live/Dead	Near Infra-Red	1:500	ThermoFisher Scientific	N.A.	L10119

Sorted human CD4+ T cells were cultured in IMDM (21980-032, ThermoFisher Scientific) complete medium, supplemented with 10% heat-inactivated (56°C, 45 min) fetal bovine serum (FBS) (10500-064, ThermoFisher Scientific), 1x Penicillin+Streptomycin (15070-063, ThermoFisher Scientific), 1x MEM non-essential amino acids (M7145, Sigma-Aldrich) and 1x β-mercaptoethanol (21985-023, ThermoFisher Scientific). Every seven days for a maximum of four weeks, Teffs were derived from isolated $CD4^{+}CD25^{-}$ T cells by restimulating them with irradiated Epstein–Barr virus (EBV) transformed B-cells (EBV-B cells) [234], at a 1:1 ratio to expand and maintain the culture. The EBV-B cells were irradiated in RS2000 X-Ray Biological Irradiator (Rad Source Technologies) for 30 min with a total of 90 Gy.

Teff siRNA knockdown and stimulation

Targeted gene's expression was knocked-down in up to 5 x 10^6 cells using the P3 Primary Cell 4D-Nucleofector X Kit L (V4XP-3024, Lonza) with 90 µl P3 Primary cell solution and 100 pmol of corresponding si_RNA (resuspended in 10 ul RNAse-free H2O): si_Non-Specific scrambled control siRNA (si_NS or si_CTRL) (SC-37007, Santa Cruz), si_VIMP/SELS (SI03053512, Qiagen), si_E2F5 (SI00030436, Qiagen). siRNA transfection electroporation was performed in the Amaxa 4D-Nucleofector™ X System (Lonza) according to the manufacturer's recommended program for primary human T cells (with the program code EO-115). Following transfection, the Teffs were first transferred into a 12-well plate with pre-warmed complete IMDM medium and incubated at 37 °C for 24 hours before being stimulated with 25 µl/ml of soluble antibodies (Immunocult™ Human CD3/CD28 T Cell Activator) (10971, StemCell), or 10ng/ml PMA (Phorbol 12-myristate 13-acetate, P8139, Sigma-Aldrich) and 100 ng/ml Ionomycin (I0634, Sigma-Aldrich) or Dynabeads® Human T-Activator CD3/CD28 for T Cell Expansion and Activation (11131D, ThermoFischer Scientific) (with 1:1 ratio between number of cells and beads) in a 24-well plate for different specified time periods.

RNA extraction

The RNeasy Mini Kit (74106, Qiagen) was employed for RNA extraction following the manufacturer's instructions and including the digestion of genomic DNA with DNAse I (79254, Qiagen). The cells were lysed in RLT buffer (79216, Qiagen), supplemented with 1% beta-Mercaptoethanol (63689, Sigma-Aldrich). NanoDrop 2000c Spectrophotometer

(ThermoFisher Scientific) was used to measure RNA concentration. For the microarray analysis, the quality of RNA was first checked by assessing the RNA integrity number (RIN) using the Agilent RNA 6000 Nano kit (5067-1511, Agilent) and the Agilent 2100 Bioanalyzer Automated Analysis System (Agilent), according to the manufacture's protocol. Only the samples with RIN of 8.5 or higher were used in the further analysis.

Microarray measurement and analysis

The transcriptomic analysis of human effector T cells expanded from CD4+CD25- T cells isolated from the PBMCs of healthy donors were performed on the Affymetrix human gene 2.0 ST array at EMBL Genomics core facilities (Heidelberg, led by Dr. Benes Vladimir). The facility used 500 ng of total RNA in the protocol with the Ambion® WT Expression Kit (cat. 4411974) in order to obtain 10 ug of cRNA, which was then converted to ssDNA. 5.5 ug of ssDNA was labeled and fragmented using the WT Terminal Labeling, polyA and hyb Controls Kit (Affymetrix, cat. 901524). 3.75 ug of fragmented/labeled ssDNA (with hybridization controls) was hybridized to Affymetrix HuGene 2.0 Genechip at 45 °C for 16 h with rotation (60rpm) and washed and stained on GeneChip Fluidics Stations 450 using GeneChip® Hybridization Wash and Stain Kit (Affymetrix, cat. 900720). Arrays were scanned using GeneChip Scanner 3000 7G with GeneChip Command Console software.

The expression signal at the exon level was summarized by the Affymetrix PLIER approach using the sketch approximation of quantile normalization with the option PM-GCBG (a GC content based background correction) using Affymetrix Expression Console v1.3.1.187. Before performing differential analysis, we first pre-processed the data with certain filtering steps. The filtering steps following the PLIER summary method included: 1) first removing any probeset whose cross-hyb type was not equal to 1; 2) removing any probeset corresponding to no identified gene or multiple genes according to the annotation (the file HuGene-2_0-st-v1.na33.2.hg19.transcript) and the library version r4 (May 23, 2012); 3), excluding the probesets with the average expression value in both groups (si_NS and si_VIMP) ≤ 2 times of the median value of the arrays (in our case, 2x the median was equal to the intensity value of 170); 4) if the mean intensity of the probesets in one group was higher, the number of absent calls among the three biological replicates should not be ≥ 1 in the group with higher mean intensity. To secure more robust analysis, we also analyzed the dataset using another model-based method [235, 236], i.e., RMA-sketch summary/normalization method (of note, the filtering steps mentioned above did not apply to the data resulted by the RMA-sketch summary method). We selected the probeset for further analysis only if the two-sided pair-wised T-test generated a P-value lower than 0.05

from the datasets summarized by both PLIER and RMA methods as demonstrated somewhere else [236]. To obtain a certain number of starting candidates, we lowered the threshold of the change fold to 1.2, which had to be recurrent in all the three donors, for our further analysis in consideration of both facts that VIMP is not a (co)transcription factor and the siRNA knockdown efficiency was not 100%. The database of mammalian transcription factors or cofactors, or chromatin remodeling factors was downloaded from the work of others [186].

In this way, around 800 genes were significantly upregulated and around 550 genes were downregulated following VIMP knockdown, which were used for further analysis.

Correlation network and IPA

The Teff correlation network based on high-resolution time series datasets of Teffs was already calculated and constructed in our previous work [144] and we extracted the VIMP subnetwork for a deeper analysis in this work. Ingenuity Pathway Analysis (IPA) was used to reconstruct the regulatory network from the Ingenuity database following the instruction of provider (QIAGEN).

cDNA synthesis

The SuperScript™ IV First Strand Synthesis System (18091050, ThermoFisher Scientific) was used for human cDNA synthesis using a maximum of 500ng of RNA following the manufacturer's protocol. The master mix for the first step per sample including: 0.5 µl of 50 µM Oligo(dT)20 primers (18418020, ThermoFisher Scientific), 0.5 µl of 0.09 U/µl Random Primers (48190011, ThermoFisher Scientific), 1 µl of 10 mM dNTP mix (18427013, ThermoFisher Scientific) and RNAse free water for a final volume of 13 µl in 0.2 ml PCR Tube Strips (732-0098, Eppendorf). The C1000 Touch Thermal Cycler (Bio-Rad) or UNO96 HPL Thermal Cycler (VVR) were employed with the following program: 5 min at 65 °C, followed by 2 min at 4 °C. For the second reaction step, the reaction mix was accompanied with 40 U RNaseOUT™ Recombinant Ribonuclease Inhibitor (10777019, ThermoFisher Scientific), 200 U SuperScript™ IV Reverse Transcriptase (18090050, ThermoFisher Scientific), a final concentration of 5mM Dithiothreitol (DTT) (70726, ThermoFisher Scientific) and 1x SuperScript™ IV buffer to reach a final reaction volume of 20 µl. We used the following thermocycler program for the second step: 10 min at 50 °C, then 10min at 80 °C and at 4 °C until further usage. The nuclease-free water was used to dilute the obtained cDNA 5 times with a final volume of 100 µl.

Quantitative real-time PCR

The quantitative real-rime PCR (qPCR) reaction mix per sample enclosed: 5 µl of the LightCycler 480 SYBR Green I Master Mix (04707516001, Roche), 2.5 µl cDNA and 2.5 µl primers in a total reaction volume of 10 ul. The PCR reaction was performed in a LightCycler 480 (384) RT-PCR platform (Roche), using the LightCycler 480 Multiwell 384-well plates (04729749 001, Roche) sealed with the LC 480 Sealing Foil (04729757001, Roche). The program for qPCR used was as follows: 5 min at 95 °C; 45 cycles of (10 sec at 55 °C, 20 sec at 72 °C, 10 sec at 95 °C); melting curve (65-97 °C). The results were analyzed using the LightCycler 480 SW 1.5 software. Primers used for qPCR: RPS9 (QT00233989, Qiagen) as a reference gene, VIMP/SELS (QT00008169, Qiagen), IL2 (QT00015435, Qiagen), CSF2 (QT00000896, Qiagen), IL21 (QT00038612, Qiagen), CEBPG (QT00224357, Qiagen), E2F5 (QT00062965, Qiagen), IRX3 (QT00227934, Qiagen), RNF14 (QT00088291, Qiagen), ZBTB20 (QT00069776, Qiagen) and CTLA4 (QT01670550, Qiagen).

Western blotting

Novex™ WedgeWell 4-20% Tris-Glycine pre-casted gels (XPO4202Box, Invitrogen) were used to run and separate proteins in the Novex™ Tris-Glycine SDS Running buffer (LC2675-4, Invitrogen). The proteins were then transferred (dry transfer) using an iBlot2™ Gel Transfer Device (IB21001, Invitrogen) and iBlot2™ PVDF stacks (IB24002, Invitrogen). Following the transfer, the membranes were blocked in 5% milk in PBS with 0.2% Tween20 (PBS-T) for 1 hour at room temperature with gentle shaking overnight at 4°C together with the primary antibodies, diluted in 5% BSA in PBS-T with 0.025% sodium azide. The membrane was then washed three times (10 min each time) before and after incubation with secondary goat anti-rabbit HRP-coupled antibodies at the next day. The Amersham ECL Prime Western Blotting Detection Reagent (RPN2232, GE Healthcare Life Sciences) was used to detect the proteins and the image of the membranes was visualized on the ECL Chemocam Imager (INTAS). If necessary, the contrast and brightness of the obtained whole gel pictures was adjusted using *ImageJ*. The signal intensity of the protein bands was quantified using *ImageJ* and normalized to that of the housekeeping gene GAPDH. For the quantification of phospho proteins, both the phospho and the pan protein were normalized to GAPDH, before normalizing the phospho protein to the total protein.

Target	Dilution	Company	Clone	Reference
pNFATC2 (Ser326)	1:100	Sigma-Aldrich		SAB4503945

NFAT1	1:1000	Cell Signalling	D43B1	5861S
VIMP	1:1000	Sigma-Aldrich	Polyclone	V6639
GAPDH	1:200	Santa Cruz Biotechnology	FL-335	SC-25778

Proliferation assay

The proliferation of the Teffs was assessed using the CellTrace™ CFSE cell proliferation kit (C34554, Invitrogen). The final concentration of 1 µM CFSE dye was used in our work. To label the cells, they were incubated for exactly 2 min and 45 seconds at RT in the dark. To stop the reaction, 10 ml FBS was added and the cells were centrifuged at 200 g for 10 min. After washing the cells in IMDM medium, the cells were subjected to the siRNA knockdown and counted. 10^5 Teff in a 96-well plate were used for each condition and stimulated for 2 days with a ratio of 1:1 of irradiated Epstein Barr Virus (EBV) B cells as previously described [144]. After the stimulation, the cells were stained for living cells using LIVE/DEAD® Fixable Near-IR Dead Cell Stain (L10119, ThermoFisher Scientific) (dilution 1:500) and acquired on a BD Fortessa™ analyzer. The data was analyzed in FlowJo 7.6.5.

Cytokine measurement by Mesoscale discovery (MSD) platform

The cell supernatant was collected after centrifugation of the cells (250 g, 10 min) and the selected list of secreted cytokines (CSF2, IL2, IL21) was measured in the undiluted cell culture medium using the MSD U-PLEX Human Biomarker group 1 kit (MSD, K15067L-1) and following the manufacturer's instructions. MESO QuickPlex SQ 120 instrument was used to read the plate and the data was analyzed with the MSD Workbench software.

Cytokine measurement by Cytometric Bead Array (CBA)

The cell supernatant was collected after centrifugation of the cells and the secreted IL2 in the diluted cell culture medium (1:4 dilution) was measured using the IL2 Flex set cytometric bead array (CBA) (BD, 558270) following the manufacturer's instructions. The acquisition was done on a BD Fortessa™ analyzer and the data was analyzed in FCAP Array™ v3.0.

PhosFlow cytometry analysis

Following stimulation, the cells were immediately fixed by adding the same volume of pre-warmed BD Cytofix Fixation Buffer (554655, BD) for 1h at 37 °C. After collecting the samples at all the different time points, they were then washed in FACS buffer and re-suspended in 200 µL of BD Phosflow Perm Buffer III (558050, BD) containing the antibodies for 30min at 4 °C. After washing the cells with FACS buffer, they were re-suspended in FACS buffer to be acquired on the BD Fortessa™.

The antibodies used are the following (Table below): VIMP/SELS (V6639, Sigma-Aldrich) (dilution 1:200) with Goat Anti-rabbit IgG H&L Alexa Fluor® 647 (A-21245, Invitrogen) (dilution 1:200), NFAT1 FITC (611060, BD) (dilution 1:50), phospho p38 MAPK (T180/Y182) Alexa Fluor 647 (562066, BD) (dilution 1:50), Anti-Human phospho NFATC1 (pS172) mAb (MAB5640, R&D Systems) (dilution 1:400), phospho NFATC2 (NFAT1) (S326) (SAB4503945, Sigma-Aldrich) (dilution 1:800), PE-Cy7 Mouse anti-ERK1/2 (pT202/pY204) (560116, BD) (dilution 1:50), phospho JNK1/2 (T182/Y185) (dilution 1:200) (558268, BD), phospho cJun (S63) (9261S, Cell Signalling) (dilution 1:200), phospho p105 NFκB1 (S933) (4806S, Cell Signalling) (dilution 1:400), phospho p100 NFκB2 (S866/870) (4810S, Cell Signalling) (dilution 1:400), phospho p65 (S529) (558422, BD) (dilution 1:50), phospho RelB (S552) (4999S, Cell Signalling) (dilution 1:400) , Anti-Rabbit IgG H&L Alexa Fluor 647 (ab 150079, Abcam) (dilution 1:1000), APC Goat Anti-mouse IgG (minimal X-reactivity) (405308, Biolegend) (dilution 1:200). For the acquisition a BD Fortessa™ was used and the data was analyzed in FlowJo 7.6.5.

Target	**Dilution**	**Company**	**Clone (if applicable)**	**Reference**
Anti-VIMP/SELS	1:200	Sigma-Aldrich	Polyclone	V6639
FITC anti-NFATC2 (NFAT1)	1:50	BD Biosciences	1/NFAT-1	611960
Mouse anti-human pNFATC1 (pS172) MAb	1:400	R&D Systems	679340	MAB5640
APC Goat Anti-mouse IgG (minimal X-reactivity) Antibody	1:200	Biolegend	N.A.	405308
Alexa Fluor 647 Mouse anti-NFκB p65 (pS529)	1:50	BD Biosciences	K10-895.12.50	558422
PE-Cy7 Mouse anti-ERK1/2 (pT202/pY204)	1:50	BD Biosciences	20A	560116
Alexa Fluor 647 Mouse Anti-p38 MAPK (pT180/pY182)	1:50	BD Biosciences	36/p38	562066
phospho NFAT1/NFATC2 (S326)	1:800	Sigma-Aldrich	Polyclone	SAB4503945
phospho c-Jun (S63)	1:200	Cell Signalling	Polyclone	9261S

phospho JNK1/2 (T183/Y185)	1:200	BD Biosciences	Polyclone	558268
phospho p105 NFκB1 (S933)	1:400	Cell Signalling	18E6	4806S
phospho p100 NFκB2 (S866/870)	1:400	Cell Signalling	Polyclone	4810S
phospho RelB (S552)	1:400	Cell Signalling	Polyclone	4999S
Goat Anti-rabbit IgG H&L (Alexa Fluor® 647)	1:200	Invitrogen	N.A.	A-21245

Calcium/Ca2+ flux

To measure the calcium flux in Teffs, the cells were stained with mouse monoclonal [RPA-T4] anti-human CD4 FITC (555346, BD Biosciences) (dilution 1:100), LIVE/DEAD® Fixable Near-IR Dead Cell Stain (L10119, ThermoFisher Scientific) (dilution 1:500) and the calcium dye Indo-1 (I1203, ThermoFisher Scientific) (5 uM) for 60 min at 37 °C in supplemented IMDM medium as for the culture of Teffs. Following 3 washes with medium the cells were re-suspended in 300ul of medium and incubated for another 15-30min at 37°C. The baseline of the calcium signal was measured for approximatively 30 seconds before adding the soluble CD3/CD28 antibodies (1:40) (10971, StemCell) or 100ng/ml Ionomycin (I0634, Sigma-Aldrich) to measure the activation-induced calcium flux. The cells were acquired on a BD Fortessa™ analyzer and the data was analyzed in FlowJo v10.5.

Ethics statement

The study procedures were approved by the ethic committee of the Red Cross Luxembourg. Informed consent was obtained from healthy blood donors through the Red Cross Luxembourg.

Statistical analysis

P values were calculated with paired two-tailed Student t test (Graphpad prism or Excel) as specified in Figure legend. If the other test was used, it has also been specified in the corresponding Figure legend. All error bars represent the standard deviation.

Acknowledgements

We thank Annegrät Daujeumont, Alexandre Baron and Olga Kondratyeva for their expert technical supports. We particularly appreciate Luxembourg Red Cross for providing buffy

coats to us. The Feng He group was supported by Luxembourg National Research Fund (FNR) through different programs including PRIDE (CRITICS DTU)/2015/10907093 to support C.C., individual Aide à la Formation Recherche (AFR) grants PHD-2014-1/7603621 and PHD-2015-1/9989160 to support E.D. and N.Z. respectively, and intramural funding within Luxembourg Institute of Health and Luxembourg Centre for Systems Biomedicine from Ministère de l'Enseignement supérieur et de la Recherche (MESR). M.O. was supported as coordinator by the Luxembourg National Research Fund (FNR) through the FNR PRIDE program for doctoral training unit (PRIDE/11012546/NEXTIMMUNE). Some icons in the graphic abstract were created with BioRender.com.

Author contributions

C.C., N.Z., E.D. designed and performed experiments. C.C. analyzed the data and wrote the manuscript. S.F.R. performed parts of the experiments. R.B., M.O. and F.H. supervised the project. F.H. designed the project, oversaw the whole project and revised the manuscript. All the authors read and edited the manuscript.

Declaration of Interests

The authors declare that they have no conflict of interest.

Figures

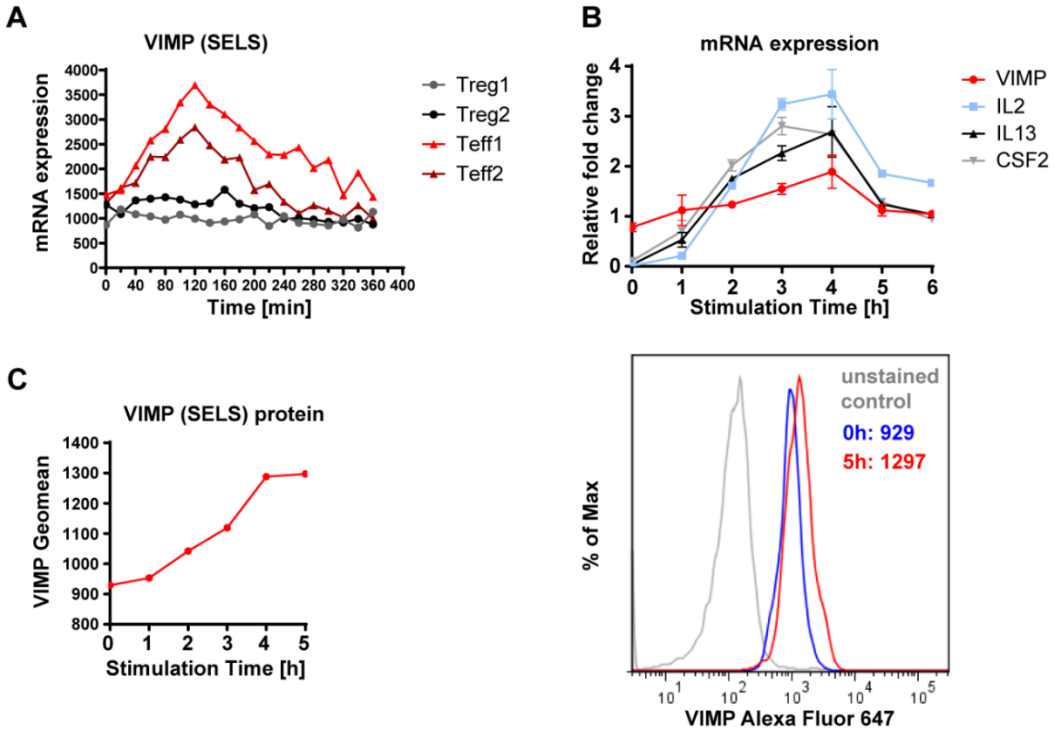

Figure 1. VIMP is temporally upregulated in Teffs following TCR stimulation.

(**A**) The kinetics of transcriptional expression of VIMP in the first 6 h following anti-CD3/-CD28 stimulation assessed by HTR time-series microarray data. Teff1 and Teff2 are the two independent repeated HTR time-series experiments from different donors. (**B**) Representative experiments, reproduced in 4 independent donors showing mRNA expression of *VIMP*, *IL2*, *IL13* and *CSF2* measured by qPCR in Teffs stimulated by anti-CD3/-CD28 beads. The data represents the gene expression normalized to *RPS9*. Data are mean± standard deviation (s.d.).. (**C)** Representative flow cytometry quantitative analysis showing elevation of VIMP protein expression in Teffs following TCR stimulation. Results represent four (**B**) and three (**C**) independent experiments of different donors.

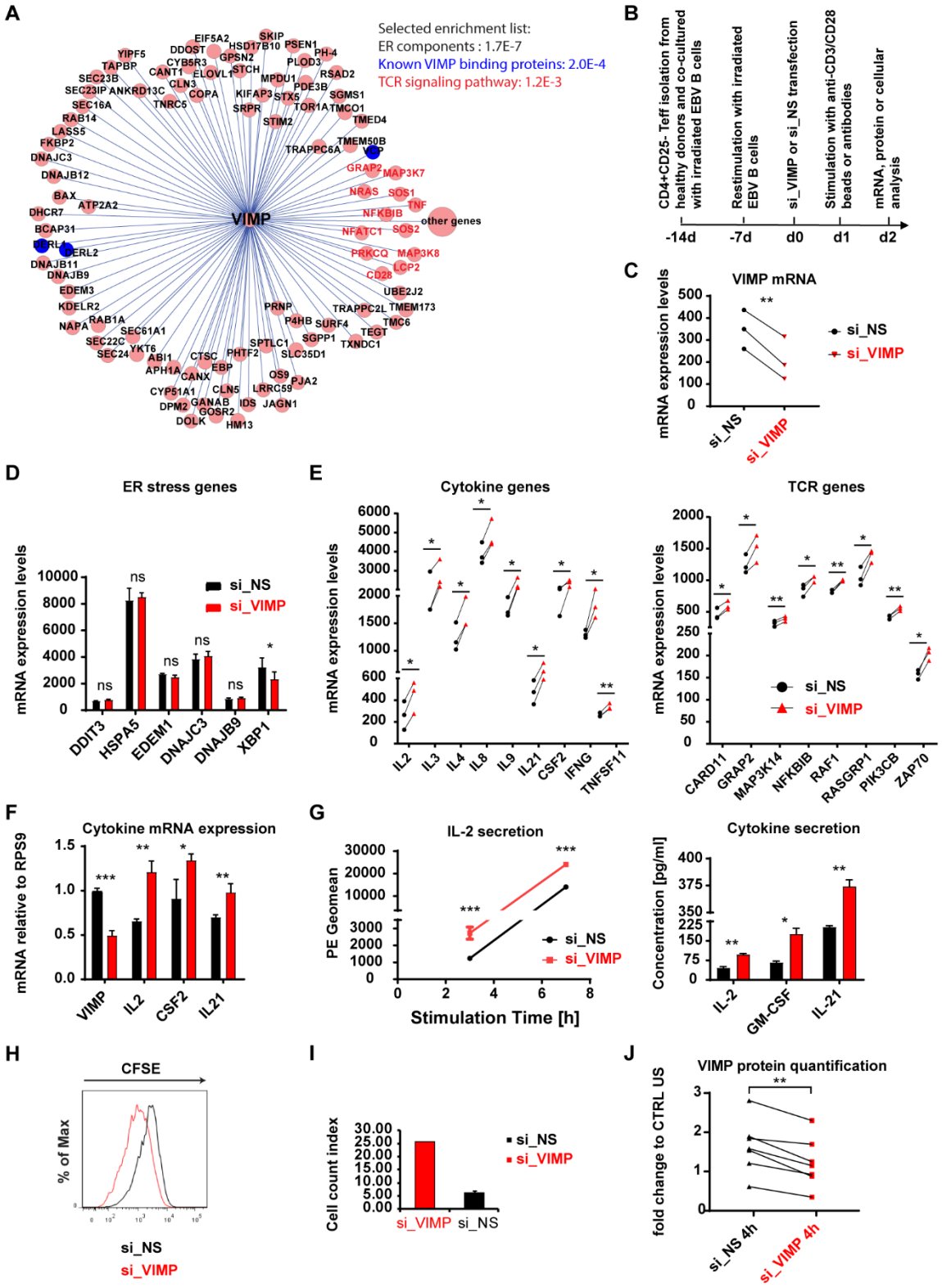

Figure 2. VIMP controls cytokine expression in Teffs and interferes with the TCR signalling pathway.

(**A**) The *VIMP* subnetwork extracted from the constructed Teff correlation network based on the HTR transcription microarray data. Each circle represents one gene. Each line between *VIMP* and the other genes represents a correlation link. The selected list of

significantly enriched pathways or components is displayed (the P-value resulted by cumulative Binomial distribution test was provided for each item). (**B**) Schematic of the experimental flow for the stimulation, gene silencing and analysis of Teffs. (**C)** mRNA expression showing the significant knockdown of VIMP in the microarray experiment. **(D, E**) Microarray data showing the fold change or expression values in the mRNA expression of ER-stress responsive genes (**D**), cytokine and TCR signalling genes (**E**). We only presented the transcripts with P-values lower than 0.05 by both PLIER and RMA methods and at least a 1.2 fold change in all 3 independent donors (for details, see Methods). (**F**) mRNA expression measured by qPCR of the genes *VIMP*, *IL2, CSF2* and *IL21* of Teffs following TCR stimulation and knockdown with either control non-specific scrambled siRNA (si_NS) or *VIMP*-specific siRNA (si_VIMP). Before stimulation, the cells were first transfected with siRNA for 1 day (for all the figures). (**G**) The concentration of the cytokines IL2, GM-CSF and IL21 detected in the cell culture medium following anti-CD3/-CD28 stimulation for different time points (left panel, IL2 alone by CBA measurement) or 8 hrs (right panel, multiplexing by MSD). PE geometric mean (Geomean) corresponds to the IL2 concentration signal in the media. (**H**, **I**) Proliferation of Teffs following TCR stimulation and VIMP knockdown, measured by CFSE proliferation assay (**H**) by counting the T cells following stimulation (**I**). Before Teffs were co-cultured with EBV-transformed B cells for 2 days, they were first transfected with siRNA for 1 day. (**J**) Quantification of the western blot protein bands and normalization of VIMP to the housekeeping gene GAPDH. Each dot represents one sample. CTRL US, unstimulated Teffs treated with si_NS. Data are mean± standard deviation (s.d.). The P-values are determined by a two-tailed paired Student's t test (except for **A** and **G**). The results in **G** was analyzed using non-paired t test. ns or unlabeled, non-significant; *P<=0.05, **P<=0.01 and ***P<=0.001. Results represent three (**C-E**) and six (**F-J**) independent experiments of different donors. See also Figure S1.

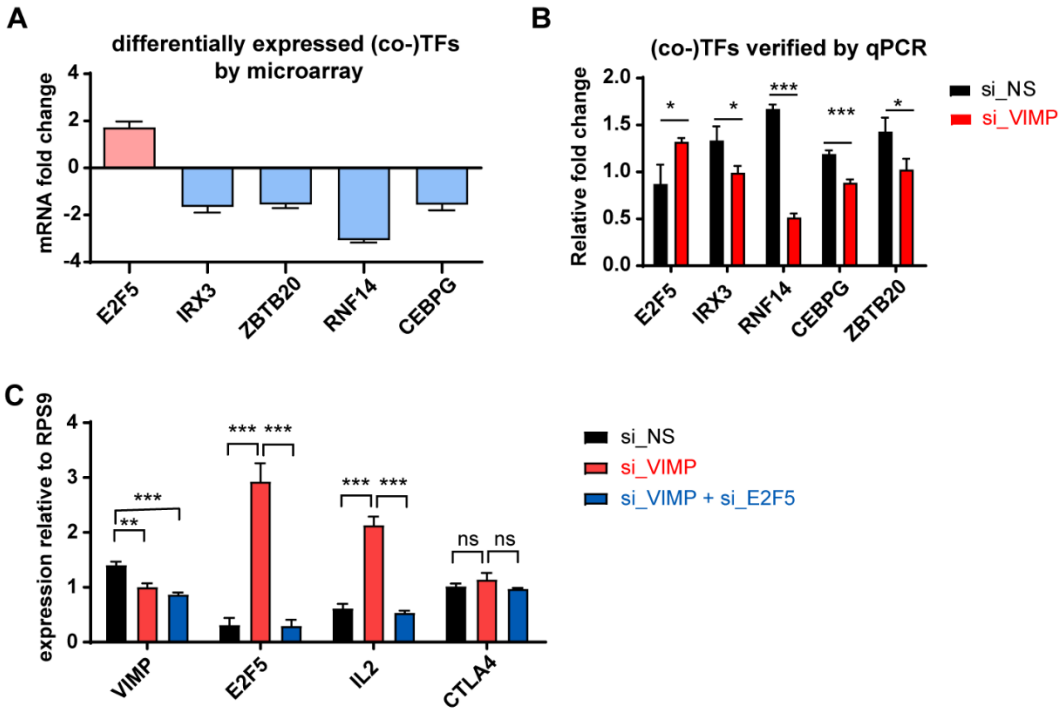

Figure 3. VIMP inhibits E2F5 to regulate IL2 expression.

(**A**) The most significantly affected (co-)transcription factors selected from our microarray analysis; the y-axis indicates the fold change between Teffs transfected with siRNA specific against VIMP(si_VIMP) or non-specific scrambled si_RNA (si_NS). (**B**) mRNA expression measured by qPCR from Teffs of independent healthy donors of the genes displayed in **A** to confirm the change in their expression levels following *VIMP* knockdown. (**C**) mRNA expression measured by qPCR of the genes *VIMP*, *E2F5, IL2* and *CTLA4* of Teffs transfected with si_NS, si_VIMP, or both si_VIMP and si_E2F5. Data are mean± standard deviation (s.d.). The P-values are determined by a two-tailed paired Student's t test. ns or unlabeled, non-significant; *P<=0.05, **P<=0.01 and ***P<=0.001. Results represent three (**A**) and four (**B-C**) independent experiments of different donors.

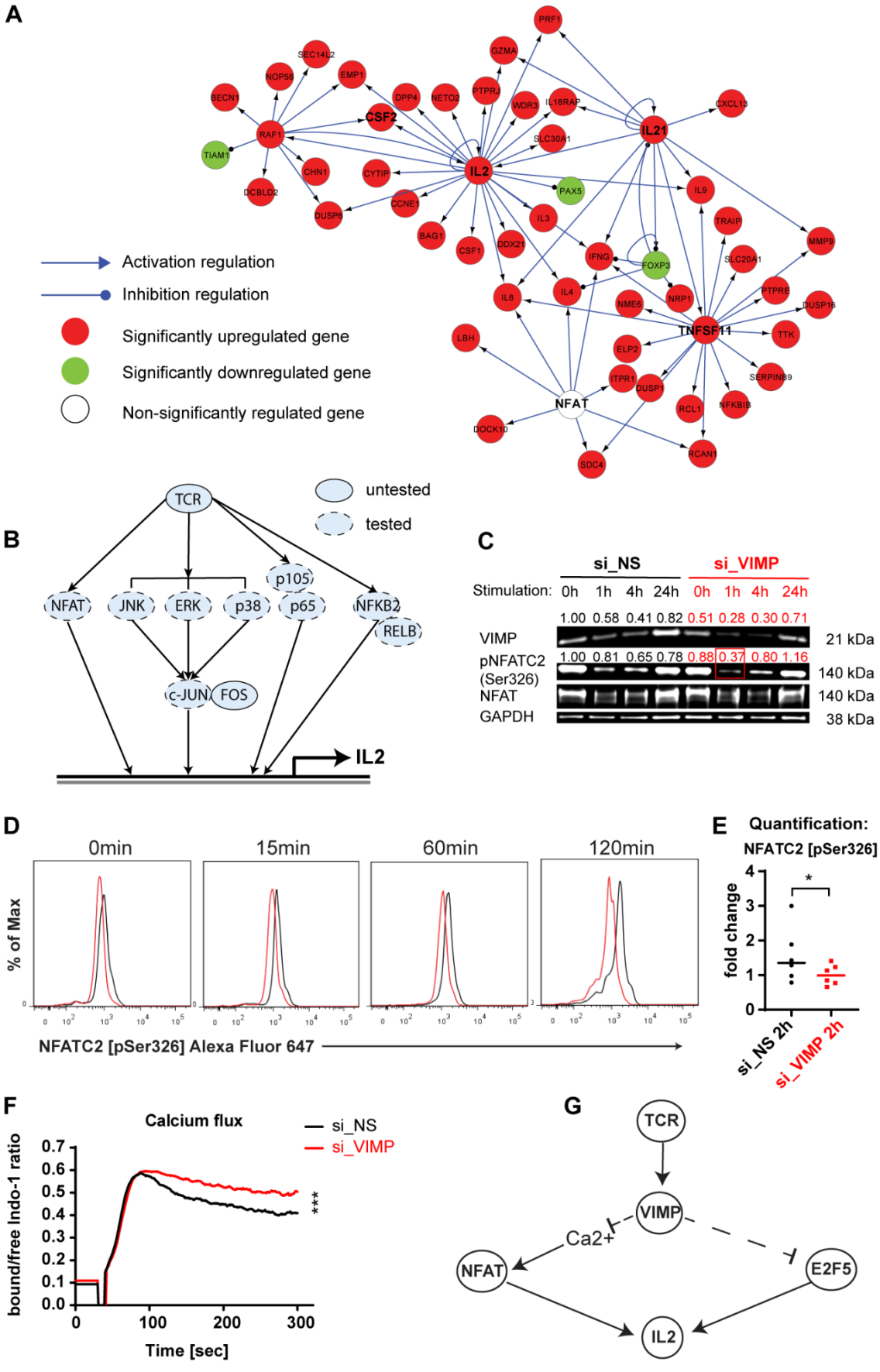
A
Activation regulation
Inhibition regulation
Significantly upregulated gene
Significantly downregulated gene
Non-significantly regulated gene
PRF1
GZMA
SEC14L2
NOP56
EMP1
BECN1
DPP4
NETO2
PTPRJ
WDR3
IL18RAP
CXCL13
CSF2
RAF1
IL21
SLC30A1
TIAM1
CHN1
CYTIP
IL2
PAX5
IL9
DCBLD2
CCNE1
DUSP6
IL3
TRAIP
MMP9
BAG1
CSF1
DDX21
IFNG
FOXP3
SLC20A1
IL8
IL4
NME6
NRP1
PTPRE
DUSP16
TNFSF11
TTK
LBH
ELP2
SERPINB9
ITPR1
DUSP1
NFAT
RCL1
NFKBIE
DOCK10
RCAN1
SDC4
B
untested
tested
TCR
p105
NFAT
JNK
ERK
p38
p65
NFKB2
RELB
c-JUN
FOS
IL2
C
si_NS
si_VIMP
Stimulation: 0h 1h 4h 24h 0h 1h 4h 24h
1.00 0.58 0.41 0.82 0.51 0.28 0.30 0.71
VIMP
21 kDa
1.00 0.81 0.65 0.78 0.88 0.37 0.80 1.16
pNFATC2 (Ser326)
140 kDa
NFAT
140 kDa
GAPDH
38 kDa
D
0min
15min
60min
120min
% of Max
NFATC2 [pSer326] Alexa Fluor 647
E
Quantification:
NFATC2 [pSer326]
fold change
*
si_NS 2h
si_VIMP 2h
F
Calcium flux
si_NS
si_VIMP
bound/free Indo-1 ratio
***
Time [sec]
G
TCR
VIMP
Ca2+
NFAT
E2F5
IL2

Figure 4. VIMP controls cytokine expression via the Ca2+/NFATC2 phosphorylation pathway.

(**A**) Network representation of the cytokine and TCR related genes affected by the knockdown of VIMP by Ingenuity Pathway Analysis (IPA). Red, significantly upregulated genes; green, significantly downregulated genes; white, non-significantly affected gene at the transcriptional level. The link with arrow indicates a known direct or indirect positive transcription regulation, the link with circle indicating a negative one from the IPA knowledge databases. (**B**) Graphical representation of the major signalling pathways downstream of the TCR signalling, (un)tested for their phosphorylation levels. (**C, D**) Phosphorylation of NFATC2 (NFAT1) in Teffs assessed by western blot (**C**) or flow cytometry (**D**) at different time points following anti-CD3/-CD28 stimulation (**C**) or PMA/Ionomycin stimulation (**D**). Before stimulation, Teffs were first transfected with specific siRNA against VIMP (si_VIMP) or non-specific siRNA (si_NS) for 24 hrs. (**D**) Representative flow-cytometry plots of pNFATC2 in Teffs. (**E**) Pooled pNFATC2 data from multiple donors at 120 min post stimulation. For **D** and **E**, only gated viable Teffs were displayed for all the phosphorylation results. The y-axis represents the percentage of maximum (scales each curve to mode=100%) (% Max). The fold change was calculated by normalizing the geometric mean (Geomean) of the fluorescence intensities of all the conditions to that of the unstimulated control siRNA knockdown condition. (**F**) Representative graph out of 3 independent experiments for the calcium flux in Teffs following stimulation. The one displayed here used Ionomycin stimulation after si_VIMP or si_NS transfection for 24h. The y-axis represents the ratio between calcium bound and free Indo-1 dye over time. (**G**) Graphical representation summarizing the two mechanisms through which VIMP regulates cytokine expression in CD4 Teffs. Data are mean± standard deviation (s.d.). The P-values are determined by a two-tailed paired Student's t test. ns or unlabeled, non-significant; *P<=0.05, **P<=0.01 and ***P<=0.001. Results represent three (**C, F**), six (**D, E**) independent experiments of different donors. See also Figure S2 and S3.

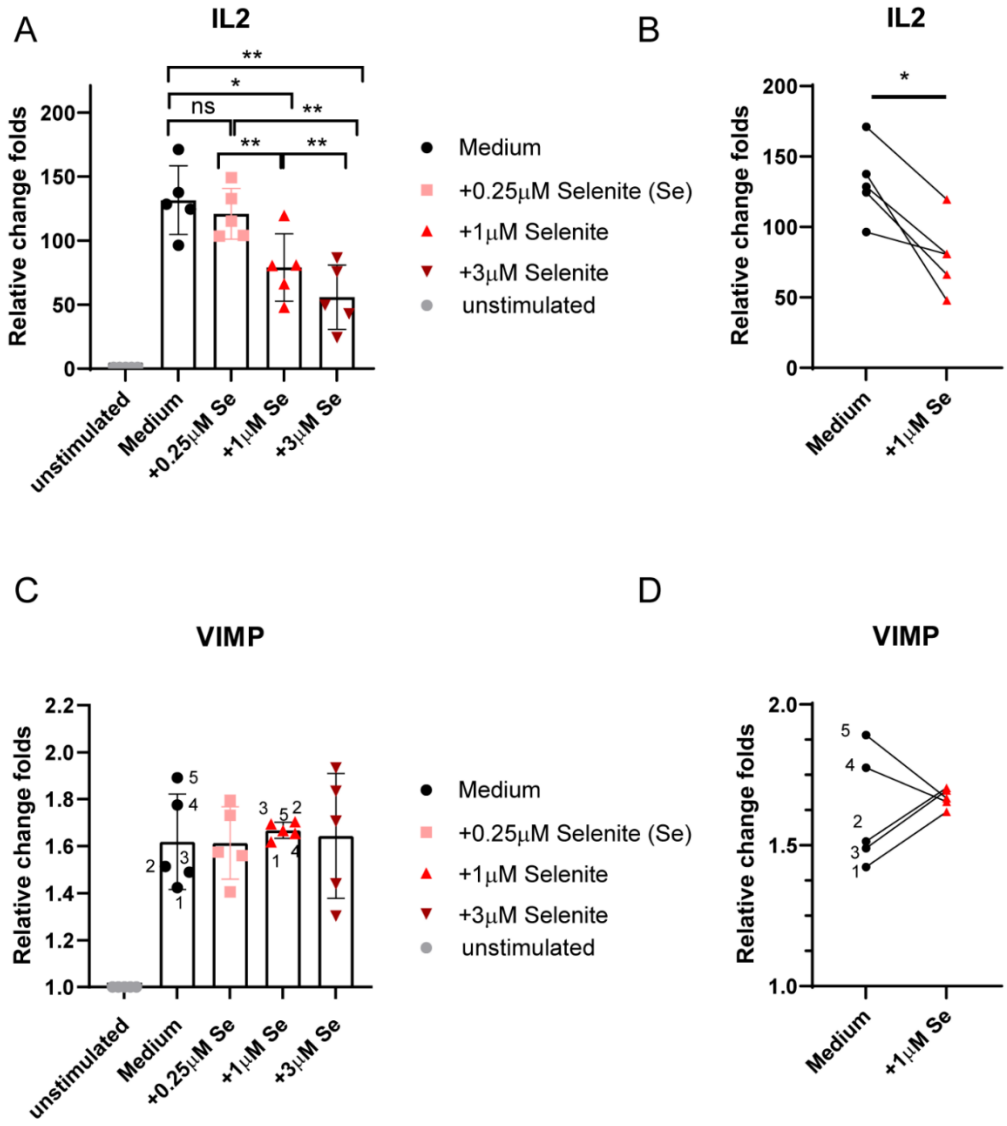

Supplemental Figure S1. Selenium supplementation suppresses IL2 production in CD4 Teffs.

Human CD4+CD25- T cells sorted from human healthy donors were unstimulated in normal IMDM complete media or stimulated for 24 hours by soluble anti-CD3/CD28 antibodies either in IMDM complete media alone or supplemented with different concentration of sodium selenite (Se, S5261, Sigma Aldrich). (**A, C**) The mRNA expression of IL2 and VIMP were quantified relative to the housekeeping gene RPS9 by qPCR. All the values were then normalized to that of the unstimulated samples of the given donor. (**B, D)** A "zoom-in" analysis of the two selected concentrations of Se for IL2 (**B**) and VIMP (**D**). Each dot represents one heathy donor. The donor ID was indicated for the concentration of interests. The P-values are determined by a two-tailed paired Student's t test. ns or unlabeled, non-significant; *P<=0.05, **P<=0.01 and ***P<=0.001.

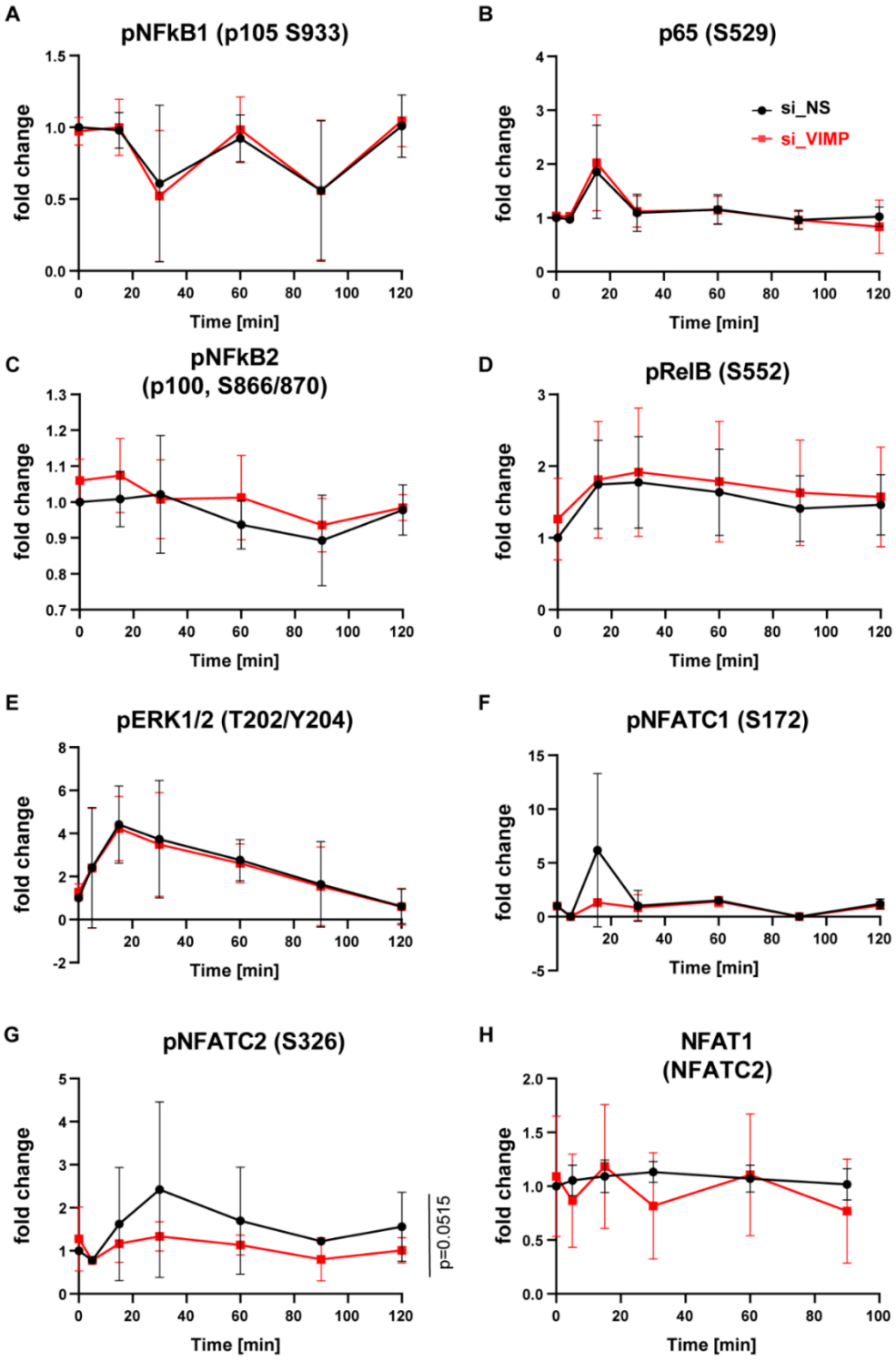

Supplemental Figure S2. VIMP knockdown only affects the phosphorylation of NFATC2, not the other major signalling pathways downstream of the TCR.

Phosphorylation of proteins involved in the major signalling pathways downstream of the TCR signalling in Teffs, assessed by flow cytometry at different time points following PMA/Ionomycin stimulation. Before stimulation, the cells were transfected with specific

siRNA against VIMP (si_VIMP) versus non-specific siRNA (si_NS) for 1 day. (**G**) Only pNFATC2 was significantly decrease by VIMP knockdown. The other measured targets remain no significant change (**A**-**F, H**). The fold change was calculated by normalizing the geometric mean (Geomean) of the fluorescence intensities of all the conditions to that of the unstimulated control knockdown condition. Data are mean± standard deviation (s.d.). The P-values are determined by a two-tailed paired Student's t test over time including the data at different time points. ns or unlabeled, non-significant; *P<=0.05, **P<=0.01 and ***P<=0.001. All the graphs represent the pooled flow cytometry data for the fold change from 2-7 independent donors.

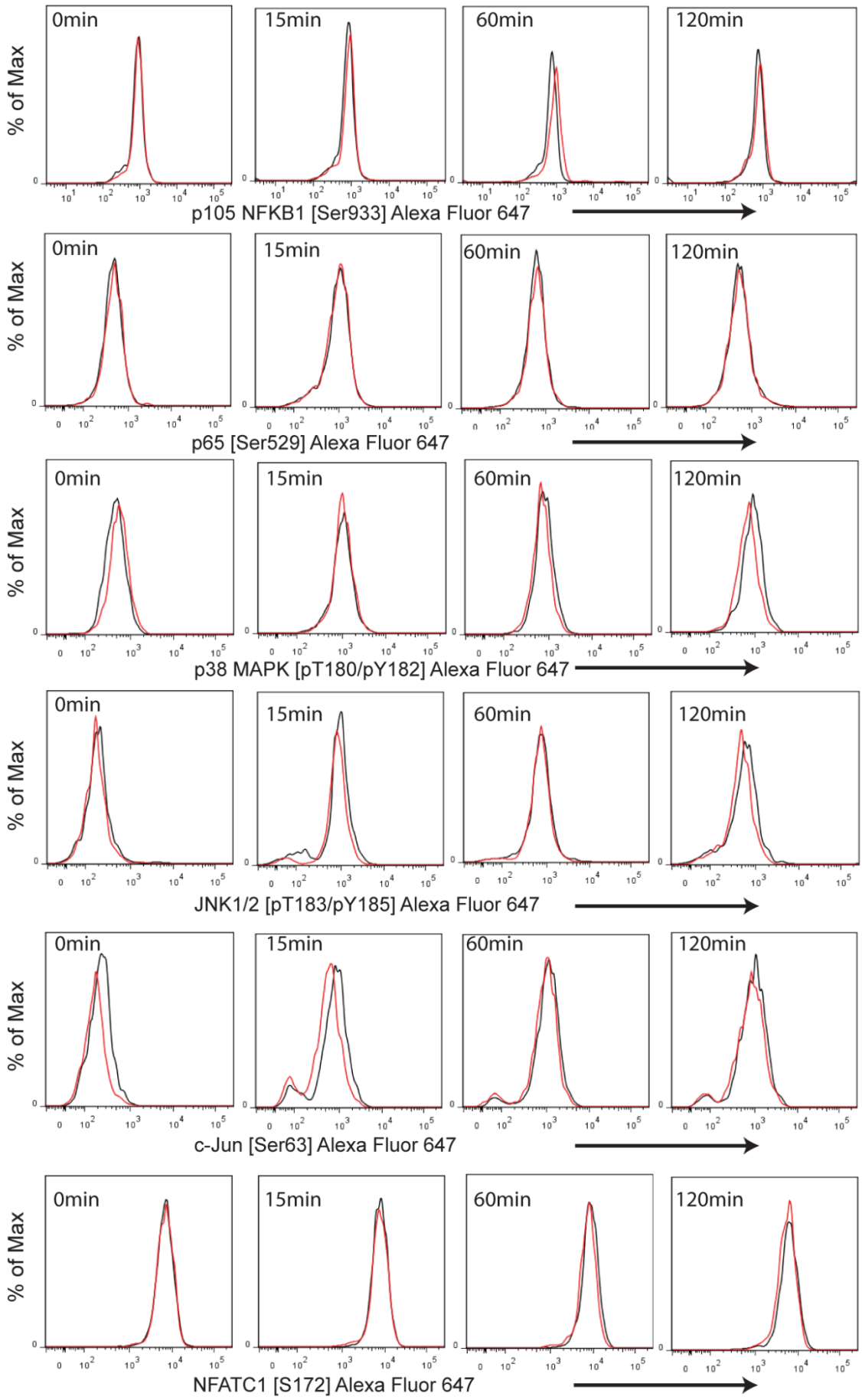
0min
15min
60min
120min
% of Max
p105 NFKB1 [Ser933] Alexa Fluor 647
p65 [Ser529] Alexa Fluor 647
p38 MAPK [pT180/pY182] Alexa Fluor 647
JNK1/2 [pT183/pY185] Alexa Fluor 647
c-Jun [Ser63] Alexa Fluor 647
NFATC1 [S172] Alexa Fluor 647

Supplemental Figure S3. VIMP knockdown does not affect other major signalling pathways downstream of the TCR.

Representative histogram overlay for the phosphorylation of major signalling transduction proteins downstream of the TCR signalling in Teffs, assessed by flow cytometry at different time points following PMA/Ionomycin stimulation. Before stimulation, the cells were first transfected with specific siRNA against VIMP (si_VIMP) versus non-specific siRNA (si_NS) for 1 day. No significant effects on the phosphorylation levels of MAPK (p38, ERK1/2, cJun, JNK1/2) pathways and canonical (p65, p105) or non-canonical (RELB, NFκB2) NFκB pathways during the first 120 min stimulation after siRNA knockdown in Teffs. The expression of total NFAT1 protein was also unaffected by VIMP knockdown. The numbers in x-axis indicate the geometric mean (Geomean) fluorescence intensity of the different proteins or phosphorylation sites. Data are mean± standard deviation (s.d.). The other measured targets remain no significant change (**A**-**G**). The P-values are determined by a two-tailed paired Student's t test. ns or unlabeled, non-significant; *P<=0.05, **P<=0.01 and ***P<=0.001. All the graphs represent data from 2-7 independent donors.

Chapter 2

Stress hormone signalling intrinsically inhibits Th1 polarization in naïve CD4 cells via the clock gene Period1 and mTORC1.

Chapter 2: Stress hormone signalling intrinsically inhibits Th1 polarization in naïve CD4 cells via the clock gene Period1 and mTORC1.

Published in *Immunology, 2022; 165: 428– 444*, https://doi.org/10.1111/imm.13448

Christophe M. Capelle[1,2], Anna Chen[1], Ni Zeng[1,2], Alexandre Baron[1], Kamil Grzyb[3], Thais Arns[3], Alexander Skupin[3], Markus Ollert[1,4], Feng Q. Hefeng[1,5,*]

1 Department of Infection and Immunity, Luxembourg Institute of Health (LIH), 29, rue Henri Koch, L-4354, Esch-sur-Alzette, Luxembourg

2 Faculty of Science, Technology and Communication, University of Luxembourg, 2, avenue de Université, L-4365, Esch-sur-Alzette, Luxembourg

3 Luxembourg Centre for Systems Biomedicine (LCSB), University of Luxembourg, 6, avenue du Swing, L-4367, Belvaux, Luxembourg

4 Department of Dermatology and Allergy Center, Odense Research Center for Anaphylaxis (ORCA), University of Southern Denmark, Odense, 5000 C, Denmark

5 Institute of Medical Microbiology, University Hospital Essen, University of Duisburg-Essen, D-45122, Essen, Germany

* Corresponding author. Direct correspondence to feng.he@lih.lu

Abstract

During a stress response an extensive crosstalk exists between the peripheral nervous system and the immune system. Stress is believed to guide the CD4 T-cell differentiation toward a Th2 response via a T cell-extrinsic mechanism. Here we show that both adrenergic- and glucocorticoid-mediated stress signalling pathways play a CD4 T cell-intrinsic role in regulating the Th1/Th2 balance, independent of the presence of exogenous cytokines and other types of immune cells. Both stress hormones inhibited Th1 polarization and cytokine production via mTORC1 and a mechanism involving the circadian clock gene Period1 (PER1). Both stress hormones induced the expression of PER1, which inhibited mTORC1 signalling, thus reducing Th1 cytokine production. This previously unrecognized mechanism connects stress hormone signalling with the circadian clock machinery and

specific CD4 T cell differentiation and advances our understanding of how stress hormones regulate the immune system during a stress response and along the circadian cycle.

Keywords: Neuroimmunlogy; Stress; Circadian rhythm; CD4 T cells; T cell differentiation; Neuroendocrine.

Introduction

During a stress response, the neuroimmune interaction is mediated by the sympathetic nervous system and the adrenal gland releasing particular stress hormones in the vicinity of immune cells expressing the corresponding receptors, such as the adrenergic receptors (e.g., β2 adrenergic receptor, β_2AR) and glucocorticoid receptor (GR). The stress hormones were initially considered purely immunosuppressive and generally harmful [109], especially in autoimmune or inflammatory diseases [237-240], cancer [241-244] and viral infections [245-247].

Following extensive studies, many cell type-specific effects of stress hormones, either promoting or reducing specific immune effector functions in different health and disease contexts have been revealed [108]. For instance, total CD4 T cells reduce the expression of cytokines, such as IFNγ and IL-2 [248-250] upon stress hormone signalling via a multitude of different pathways involving cAMP/PKA [251, 252], NFκB [253] and inhibiting early TCR singling [254-256], among others [257, 258]. Regulatory CD4 T cells (Treg) on the other hand seem to benefit from stress hormone signalling by increasing their suppressive capability [134, 259, 260]. In CD8 T cells stress hormones reduce IFNγ and TNFα production and cytotoxic capacity [261-263], by inhibiting the glycolytic switch and preventing the cells to properly activate [262]. B cells have been described to profit from beneficial stress-induced effects, increasing the production of different classes of immunoglobulins [264-267]. Dendritic cells (DCs), monocytes and macrophages have also been shown to reduce the expression of pro-inflammatory cytokines, such as TNFα and IL-12, but increase the expression of anti-inflammatory cytokines, such as IL-10 and IL-4 [268-273]. Furthermore, the effect of stress hormones has also been described to suppress NK cell responses, inhibiting cell cytotoxicity and cytokine production [274-277], at least partially by increasing the expression of the inhibitory receptor PD-1 [278]. Meanwhile, a beneficial intrinsic effect of β_2-AR signalling on NK cells has been reported [279]. In addition to the outlined effects of stress hormones on different major immune cell types, other cell-type specific effects have been reported in other immune cells, such as ILC2 [280], myeloid-derived suppressor cells [281], neutrophils [282-284] and basophils [285].

Connecting the dots between the various aforementioned cell-type specific/intrinsic effects on different immune cells, the stress hormones might more specifically inhibit cellular immunity and Th1 responses, while favoring a Th2 response and humoral immunity [107, 248, 250, 286-291]. This process was proposed to be dependent on the reduced expression of IL-12 by DCs [270]. This increase in Th2 responses, can explain stress-induced exacerbation of allergic diseases [238], a Th2-driven pathology. At the same time, the stress-induced decrease in Th1 immunity has the functional consequence of increasing susceptibility to viral infections [245, 246] and reducing anti-tumor immunity [241, 292]. Indeed, blocking the adrenergic or glucocorticoid signalling, increased anti-tumor immune responses and treatment efficacy [293-295]. In the light of all the evidence indicating a shifted Th1/Th2 balance and various cell-intrinsic mechanisms being described in several other immune subsets, we wondered whether stress hormones have a CD4 T cell-intrinsic mechanism to regulate T-cell differentiation. Discovering new pathways through which stress hormones mediate CD4 T cell responses will greatly help our understanding in how stress mediates its grip on the immune system in health and disease. Our work has the potential to identify novel targets for therapeutic interventions in a wide spectrum of diseases in which CD4 T cells are dysregulated.

The stress hormones not only play a role in the stress response, but also as peripheral regulators of the circadian clock governing the internal daily diurnal cycle of the body. Virtually every cell in the body is somehow regulated in a circadian manner by the molecular circadian machinery. Interestingly, stress hormones have been shown to induce the expression of several clock components [296, 297]. Recently, the circadian rhythm and clock genes have been described to play a profound role in immune cell trafficking [298-305] and other functions [306-310]. Considering those existing reports, we hypothesize a potential role of the molecular circadian pathways in the regulation of the CD4 T differentiation, downstream of stress hormone signalling.

Using sorted primary human CD4 naïve and memory T cells, we show that stress hormone signalling in naïve CD4 T cells intrinsically inhibited Th1 polarization via the circadian gene Period1 (*PER1*) and the mTORC1 signalling pathway.

Results

Stress hormones decrease the activity and proliferation of naive and memory CD4 T cells.

The immunosuppressive role of stress hormones has been established for several decades. Nevertheless, before investigating the potential effects of stress hormones on CD4 T helper cell polarization, we sought to investigate the well-known effect of stress hormones on general activation status of naïve and memory CD4 T cells following TCR stimulation. To this end, we sorted naïve and memory CD4 T cell subpopulations from peripheral blood mononuclear cells (PBMCs) of heathy human donors **(Suppl. Fig. 1A**). We exposed them for 1 h to isoproterenol (ISO) (β_2-AR agonist) or hydrocortisone (HC) (synthetic glucocorticoid) before a 48 h anti-CD3/-CD28 stimulation and assessed different activation and proliferation markers by flow cytometry (**Fig.1A**). Confirming the known immunosuppressive role of the stress hormones, we observed a decrease in the expression of the activation markers PD-1 and ICOS, and the proliferation marker Ki67 in naïve CD4 T cells (**Fig.1B-D**). In memory T cells, this effect was less pronounced and only significant for ICOS and Ki67 (**Fig. 1B-D**). In line with the reduced activation and proliferation, both naïve and memory CD4 T cells treated with a stress hormone analogue showed a decreased expression of cMyc and HiF1α (**Fig.1E-F**)). These results indicate a decreased metabolic activity, as both signalling molecules are crucial for the glycolytic switch upon T cell activation [311, 312]. Indeed, ISO and HC reduced expression of GLUT1 and ATP production in naïve and memory CD4 T cells (**Suppl. Fig 1B, C**), indicating a reduced level of glucose uptake and a lower metabolic output. These data are in line with a recent report that adrenergic signalling blocks the metabolic reprograming by inhibiting glucose uptake, although in CD8 T cells [262]. Adrenergic signalling, the downstream of the β_2-AR, activates the adenylate cyclase to produce cAMP, which then acts as a second-messenger on downstream targets. Forskolin (Forsk), an adenylate cyclase agonist leads to high levels of cAMP, independent of β_2AR signalling (**Suppl. Fig. 1D**). When exposed to Forsk, T cell activation (PD-1, ICOS), proliferation (Ki67) and metabolic activity was decreased in both naïve and memory CD4 T cells (**Fig. 1B-F; Suppl. Fig. 1B, C**). This indicates the involvement of a previously described cAMP-dependent mechanism of ISO (even in a dose-dependent manner, **Suppl. Fig. 1D**), downstream of β_2-AR signalling to suppress CD4 T cells [251, 313]. Here we show that both naïve and memory CD4 T cells displayed decreased activation, proliferation and metabolic activity when treated with a β_2AR agonist or a synthetic glucocorticoid, even though memory CD4 seemed to be less sensitive to these effects.

Stress hormones change the balance of the CD4 T helper differentiation in naive CD4

Many studies have suggested that during a stress response CD4 T cells favor a Th2 over a Th1 polarization [286-288] via a T-cell extrinsic manner, i.e., by inhibiting the expression of IL-12 in dendritic cells [270, 314]. However, we wondered whether CD4 T cells have an intrinsic mechanism, independent of exogenous cytokine to regulate Th cell polarization. To investigate this, we exposed sorted naïve and memory CD4 T cells to ISO, HC or Forsk and measured the expression of the lineage transcription factors (LTFs) of different T helper subsets 48 h after TCR stimulation. As we were interested in the T cell intrinsic mechanism, we did not add any Th1-, Th2- or Th17-polarizing cytokine mix to the cells. Indeed, both ISO and HC selectively decreased the expression of the Th1 and Th17 LTFs, Tbet and RORγT, respectively, whereas the Th2 LTF GATA3 remained unchanged in naïve CD4 T cells (**Fig.2A**). In contrast, memory CD4 T cells displayed a more universal decrease of the LTFs, even though GATA3 was most significantly decreased (**Fig. 2A**). In addition, we only observed a slight decrease of FOXP3 expression in naïve following ISO and in memory CD4 T cells following HC. Overall, this data indicates a cell type-specific effect of the stress hormone analogues on naïve or memory CD4 T cells, where Th1 and Th17 polarization was most reduced in naïve CD4, whereas memory CD4 showed a most significant decrease in the Th2 cell program. In fact, it is the balance between those LTFs that determines the functional outcome of the CD4 T cell differentiation. Therefore, we calculated the ratios between various LTFs to analyze which of the signals is dominating. We found that only the Tbet/GATA3 ratio, reflecting the Th1/Th2 balance was consistently reduced in naïve CD4 cells, but not in memory CD4 T cells (**Fig. 2B**), in an ISO dose-dependent manner (**Suppl. Fig. 2A**). When the cells were treated with HC, both naïve and memory CD4 had a decreased Th1/Th2 ratio, indicating that β_2-AR has a more differential effect than HC. Interestingly, Forsk treatment even increased GATA3 expression, while still decreasing the expression of Tbet and RORγT in naïve CD4 T cells (**Fig. 2A**), further pushing toward a Th2 polarization.

Another family of transcription factors regulating the fate of CD4 T cells during their differentiation are the signal transducers and activators of transcription (STATs). While STAT4 signalling is important for Th1 differentiation, STAT6 and STAT3 contribute to Th2 and Th17 differentiation, respectively. Therefore, we sought to assess the phosphorylation of the STAT proteins in naïve and memory CD4 T cells following ISO or HC treatment and TCR stimulation. In naïve CD4 T cells, ISO and HC reduced the phosphorylation of STAT4 and STAT6 (**Suppl. Fig. 3A**). Furthermore, Forsk only reduced pSTAT4 (**Suppl. Fig. 3A**), indicating that the effect of ISO on STAT6 is cAMP-independent. In memory CD4 T cells, ISO, HC and Forsk reduced the phosphorylation of STAT4, STAT6, STAT3 and STAT5

(**Suppl. Fig. 3A**). In line with the results from LTFs, only the ratio between pSTAT4 (Th1) and pSTAT6 (Th2) was reduced in naïve CD4 T cells after treatment with ISO, HC or Forsk, while no effect was observed in memory CD4 (**Suppl. Fig. 3B**). This further consolidates the notion that the stress hormones favor the Th2 polarization, by inhibiting the Th1 cell program, specifically in naïve CD4 T cells.

To confirm our observation of the classic Th1, Th2 and Th17 LTFs, we analyzed the Th1, Th2 and Th17 cytokines secreted into the cell culture media, using multiplex electro-chemoluminescence assays. In line with the LTF results, the Th1 cytokines, TNFα, IFNγ, GM-CSF (**Fig. 2C**) and to some extent IL-2 (**Suppl. Fig. 2B**) were reduced in naïve CD4 T cells, when treated with ISO or HC. On the other hand, ISO or HC reduced the secretion of Th2 cytokines, IL-4, IL-5 and IL-13 in memory CD4, but not in naïve CD4 (**Fig. 2C**), reflecting the significant decrease of GATA3 expression in memory, but not naïve CD4 (**Fig. 2A**). Concordantly, an intracellular cytokine staining of naïve CD4 T cells showed that ISO and/or HC significantly decreased the Th1 cytokines IFNγ, TNFα and IL-2, whereas the Th2 cytokine IL-4 remained unchanged and IL-5 only significantly decreased with HC (**Suppl. Fig. 2C**). Surprisingly, we did not observe any change in the expression of Th1 cytokines in memory CD4 (**Fig. 2C**), although Tbet was also significantly decreased in memory CD4. These results could be explained by the reported observation that the main function of Tbet in Th1 differentiation is to inhibit GATA3 instead of positively regulating IFNγ expression [315]. In this scenario, Th1 cytokine expression in memory CD4 could be maintained by other pathways even though Tbet expression was reduced. In the culture supernatants, IL-17 expression was slightly decreased in memory CD4 (**Suppl. Fig. 2B**), in line with the decreased expression of RORγT and decreased ratio of Th1/Th17 LTFs. Unexpectedly, the Th17 cytokines IL-17 and IL-21 remained unchanged in naïve CD4 (**Suppl. Fig. 2B**), although the Th17 master TF RORγT was decreased with ISO and HC. Interestingly, IL-21 secretion was significantly but only slightly increased in memory CD4 treated with HC. In naïve CD4 IL-10 was also slightly decreased by ISO (**Suppl. Fig. 2B**), in line with the decreased FOXP3 expression (**Fig. 2A**).

In summary, our data show that ISO and HC have a cell type-specific effect in naïve and memory CD4 T cells, inhibiting the Th1 cell program in naïve CD4 T cells to favor Th2 polarization. On the other hand, both hormones inhibit Th2 cytokine production in memory CD4 T cells. As no exogenous cytokines or co-culture with other cell types were employed, this unrecognized effect was regulated through a CD4-T-cell intrinsic mechanism.

Stress hormones alter mTOR signalling to inhibit Th1 polarization in naive CD4 T cells

The expression of the CD4 T cell LTFs is not the only pathway regulating the CD4 T cell differentiation and cytokine expression. Even though the whole extent of mTORC1 and mTORC2 regulation in CD4 T cells is still not fully understood, mTORC1 is considered to be crucial for Th1 and Th17 differentiation, while mTORC2 is determinant for Th2 differentiation [316] (reviewed here [317, 318]) (**Fig. 3A**). After observing that the stress hormones differentially affected cytokine production in naïve and memory CD4 Tells, we hypothesized that ISO and HC might interfere with the mTOR pathway in order to differentially affect Th1 and Th2 cytokine expression. To test this hypothesis, we analyzed the phosphorylation of S6 (Ser235/236) and Akt (Ser473) as a proxy for mTORC1 and mTORC2 activity, respectively. In line with the differential Th1/Th2 phenotype and cytokine expression in naïve and memory CD4, ISO reduced S6 phosphorylation in naïve CD4 T cells (**Fig. 3B, C**), while reducing Akt S473 phosphorylation in memory CD4 T cells (**Fig. 3B, 3D**). HC consistently reduced both pS6 S235/236 and pAkt S473 in naïve and memory CD4 T cells, displaying once again a more universal suppressive effect and suggesting that HC might regulate the Th1 polarization via other parallel pathways. Forsk also reduced pS6 (Ser235/236) in naïve CD4 and memory CD4, while only reducing pAkt (Ser473) in memory CD4, indicating the implication of cAMP signalling in the ISO-induced inhibition of mTORC in the respective subsets. Indeed, cAMP was previously described to inhibit mTOR in mouse embryonic fibroblasts (MEF) [319]. To further elucidate at which stage of the PI3K/Akt/mTOR pathway the stress analogues interfere with the mTORC1/2, we examined other proteins in the pathway, namely pAkt (Thr308) and pPDK1 (Ser241). In both naïve and memory CD4, pAkt (Thr308) and pPDK1 (Ser241) were decreased by ISO and HC (**Fig. 3E, F**), suggesting that the mode of action of both compounds acts upstream of PI3K. Forsk also reduced pAkt (Thr308) and pPDK1 (Ser241), indicating that ISO-induced cAMP might interfere with mTORC signalling upstream of PI3K (**Fig. 3E, F**). Here we showed that ISO inhibits mTORC1 selectively in naïve CD4 T cells, while inhibiting mTORC2 in memory CD4. This effect is, at least partially mediated via cAMP signalling acting upstream of PI3K, since Forsk, the positive control for cAMP induction, has a similar impact on mTOR signalling. On the other hand, HC has a more generally suppressive mode of action, inhibiting both mTORC1 and mTORC2 upstream of PI3K. In short, our data firmly shows that the stress hormones reduce Th1 cell programs by inhibiting mTORC1 signalling in naïve CD4 T cells, while mainly affecting mTORC2 in memory CD4.

Stress hormones induce the expression of Period1 to inhibit Th1 cytokine expression via mTORC1

Although the signalling modes of GC and β_2AR agonists differ substantially (reviewed here for GCs [257, 320]), the stress hormone analogues had similar effects on naïve CD4 T cell polarization and mTOR signalling. This indicates that there might be a common mode of action shared by both stress hormones in addition to the previously described differential pathways suppressing T cell activity. Among others, this reasoning guides us to circadian rhythm, since it is well known to be regulated by both stress hormones [321, 322]. The levels of norepinephrine, epinephrine and glucocorticoid are at their highest in the early morning, but decline throughout the day to reach their minimum in the night (**Suppl. Fig. 4A**). The sleep hormone melatonin follows an opposite rhythm. This diurnal cycle of the stress hormones is crucial to regulate different tissues and organs, including different functions of the immune cells [303, 305] via the molecular circadian clock [298, 301, 304, 307, 309]. As the circadian clock genes also display a cyclic pattern in T cells [323] and the circadian clock signalling is induced by norepinephrine and glucocorticoid [296, 297], we hypothesized that certain components of the circadian clock might play a role in the ISO/HC-induced inhibition of Th1 cell programs in naïve CD4. This hypothesis was further supported by our preliminary data, where the naïve CD4 T cells from 2 out of 3 donors, treated with melatonin, showed an increased expression of TBX21 (Tbet) and secretion of IFNγ and IL-2, 24 h after TCR stimulation. On the other hand, melatonin showed little or no effect on memory CD4 T cells of the 3 donors (**Suppl. Fig. 4B**). To further investigate the role of the specific circadian clock genes in naïve CD4 T cells, we measured the dynamic expression pattern of every major mammalian clock gene, following ISO or HC treatment and TCR stimulation.

The circadian clock machinery is a tightly regulated system controlled by the central regulators BMAL1 and CLOCK [307] and containing several positive and negative feedback mechanisms involving the Period genes (*PER1*, *PER2* and *PER3*), Cryptochromes (*CRY1* and *CRY2*) and the accessory clock genes *NR1D1/NR1D2* (Rev-Erbα/β), *RORA* (RORα) and *NFIL3* [324]. Nevertheless, the expression of some of the clock genes was altered upon TCR stimulation alone, without ISO or HC treatment (**Suppl. Fig. 4C, 4D; Fig. 4B**), already indicating a potential role of the molecular clock in T cell responses downstream of the TCR. Upon ISO or HC treatment, only a small number of clock genes showed a consistent expression pattern among most of the donors, namely *PER1*, *PER2* and *PER3*. *PER2* and *PER3* peaked 4 h following TCR stimulation and decreased over time (**Fig. 4A**). At the same time ISO and HC reduced the expression of *PER2* and *PER3*, even though *PER2* was only modestly affected. On the other hand, *PER1* expression was unaffected by TCR stimulation,

but was consistently induced after 4 h of ISO or HC treatment (**Fig. 4A**). Glucocorticoids have already been shown to directly induce *PER1* expression by binding to GR-binding sites near the transcription start site (TSS) of *PER1* [325].

mTOR exhibits circadian oscillations and has reciprocal regulatory interactions with the circadian proteins in other cell types [326-329]. To test whether there is an interaction between mTOR and the period genes in CD4 T cells, we treated naïve and memory CD4 T cells with the mTORC inhibitor rapamycin and analyzed the expression of the period genes at different time points. Intriguingly, rapamycin reduced the expression of *PER2* and *PER3* in naïve and memory CD4 T cells, whereas it had no effect on *PER1* expression (**Suppl. Fig. 5A, B**). This shows that the ISO- or HC-induced decrease of *PER2* and *PER3* is mediated through mTOR, while the induction of *PER1* is mTOR-independent.

Given that other clock proteins regulate specific functions in different immune cells, including T cells [306, 307], we wondered whether *PER1*, *PER2* and *PER3* have specific functions in the regulation of CD4 T cell polarization, through which ISO and HC would mediate their effects. To this end, we first knocked down (KD) *PER2* and *PER3* either alone or in combination by using specific siRNA and assessed the mRNA expression of the Th1 genes *TBX21* (Tbet), IFNG and IL2. This enabled us to examine if the reduced expression of either period gene individually or both genes together is sufficient to mimic the ISO/HC-induced inhibition of Th1 cell responses. The different siRNAs specifically decreased the expression of the targeted period gene without affecting the expression of the others (**Suppl. Fig. 5C**). However, neither *PER2* KD, nor *PER3* KD, nor the combination of both was sufficient to reduce the expression of Th1 genes (**Suppl. Fig. 5D**). This indicates that *PER2* and *PER3* only endure a bystander effect of ISO's and HC's capability to inhibit mTOR, but are not involved in the inhibition of Th1 responses. Regardless, the fact that *PER2* and *PER3* are upregulated downstream of mTOR following TCR stimulation, indicates that they might play a different function in CD4 T cell responses [306].

After ruling out that *PER2* and *PER3* are involved in T cell differentiation, we directed our attention towards *PER1*, the expression of which was induced by ISO and HC (**Fig. 4A**), although independent of mTOR (**Suppl. Fig. 5A**). To examine if the upregulation of *PER1* contributes to the inhibition of Th1 genes, we knocked down *PER1* in naïve and memory CD4 T cells before treating them with HC. HC was selected here over ISO, because HC was able to induce higher levels of *PER1* expression, compared to ISO (**Fig. 4A**). In this setting, *PER1* siRNA, relative to scrambled random siRNA (CTRL), blocks the upregulation of *PER1* following the HC treatment, hypothetically resulting in a rescue of Th1 gene expression. Indeed, successfully abolishing the upregulation of *PER1* (**Fig. 4B; Suppl. Fig. 6B**), partially rescued the HC-induced inhibition of the Th1 cytokines genes, IFNG and IL2

in naïve CD4 T cells, while having no impact on memory CD4 T cells (**Suppl. Fig. 6A**). Encouragingly, *PER1* KD without the presence of HC, also increased the mRNA expression of IFNG and IL2 (**Fig. 4B**), by further reducing the already low expression of *PER1* at baseline (**Fig. 4A, 4B**). In agreement with the RNA data, *PER1* KD increased the protein secretion of Th1 cytokines, such as IFNγ and IL-2 (**Fig. 4C**) in both HC-treated and -untreated scenarios. In addition, the secretion of the Th1 cytokine TNFα was partially rescued by *PER1* KD with HC treatment, whereas GM-CSF was unchanged. The Th17 cytokine IL-17A showed a trend to be increased by *PER1* KD (without HC: p=0.0627; with HC: p=0.0949, **Suppl. Fig. 7A**). Intriguingly, the expression of TBX21 (Tbet) did not consistently follow the same pattern, only showing an increase in 7/13 donors after *PER1* knockdown (**Fig. 4D**). These observations were independent of the multiple feedback mechanisms within the circadian clock signalling, as *PER1* KD did not affect the expression of other clock genes, in the naïve and memory CD4 T cells (**Suppl. Fig. 6B, 6C**). These data show that *PER1* has a function in regulating the expression of Th1 cytokines, although partially independent of Tbet expression. This independence of the expression of the total Tbet on the production of Th1 cytokines, such as IFNγ, comes less surprising in the light of the report showing that the main function of Tbet does not lie in the regulation of IFNγ expression [315]. Furthermore, Chornoguz et al. describe that Tbet requires to be phosphorylated by mTORC1 in order to induce the expression of its downstream target genes of the Th1 cell program [330].

Considering that ISO and HC inhibit mTORC1 in naïve CD4 T cells (**Fig. 3B, 3C**), while inducing the expression of *PER1* (**Fig. 4A**), we wondered whether *PER1* inhibits mTORC1 to mediate its capacity in regulating Th1 responses. To test this hypothesis, we knocked down *PER1* in naïve and memory CD4 T cells and assessed the mTORC1 and mTORC2 activity, by staining pS6 (S235/236) and pAkt (S473), respectively. Confirming our assumption, *PER1* KD partially rescued the HC-induced inhibition of mTORC1, shown by a significant increase of pS6 after *PER1* KD and under HC treatment (8/10 donors) (**Fig.4E**). Further reducing the already low basal levels of *PER1* with siRNA without HC treatment increased pS6 in 5 out of 10 tested donors. On the other hand, *PER1* KD did not alter the activity of mTORC2 (pAkt S473) in naïve CD4 T cells (**Fig. 4E**) and had no impact on either mTORC1 or mTORC2 in memory CD4 (**Suppl. Fig. 6D**). These results show that *PER1* is an inhibitor of mTORC1, thus regulating Th1 responses [316]. Considering that *PER1* KD only partially rescues the HC-induced effects, it is reasonable to believe that *PER1* only partially contributes to this regulation of Th1 cell programs. Taking into account that Forsk treatment reduced the PI3K/mTORC (**Fig. 3C-F**) pathway, cAMP-dependent signalling probably also contributes to the inhibition of mTORC1. However, this does not rule out the

possibility that other pathways known to be affected by β_2-AR [251, 252, 313, 331] or GR signalling [252, 254-256, 258, 332] in T cells are also involved in this process.

In summary, our data lays out a novel naïve CD4 T cell-restricted mechanism, though which stress hormones T cell-intrinsically modulate the T helper cell polarization in naïve CD4 T cells via inhibiting the mTORC1 pathway and inducing *PER1* expression (**Suppl. Fig. 7B**). This showcases the involvement of a circadian clock gene in the stress-response regulation of Th1 cell differentiation from naïve CD4 T cells and substantially contributes to a better understanding of the circadian regulation of immune responses.

Discussion

Stress hormones favor Th2 differentiation via inhibiting IL-12 production in DCs. Here we showed that both adrenergic- and glucocorticoid-mediated stress signalling regulate the Th1/Th2 balance in an intrinsic and cell type-specific manner in naïve CD4 T cells. Both stress hormones inhibit Th1 polarization and cytokine expression in naïve CD4 via the interplay between the circadian gene *PER1* and the mTORC1 signalling pathway. In line with our observation, previous studies have shown that *PER1* is able to inhibit Akt/mTOR signalling in squamous cell carcinoma [326] and plays a role in the regulation of cytokine expression, such as IFNG, in NK cells [333]. Here, we linked those separate observations in naive CD4 T cells. Upon stress hormone signalling, *PER1* was induced and inhibited mTORC1 signalling to regulate the expression of Th1 cytokines. We illustrated a novel CD4-T cell-intrinsic mechanism through which the stress hormones inhibit Th1 differentiation, thus consequentely shifting the balance towards Th2.

Our work adds a new layer of understanding to the current dogma that the shift in the Th1/Th2 balance is dependent on adrenergic receptor signalling in DCs to reduce the DC-derived IL-12 expression [270]. As a robust Th2 response is required for a high production of antibodies, the increased Th2 response during stress should lead to higher levels of secreted antibodies. Indeed, B cells exposed to a stress hormone have increased the production of different classes of immunoglobulins, depending on the experimental or disease context [264, 265, 334, 335]. Together, the effect on DCs, the effect on B cells and our observation on T-cell intrinsic effects converge to promote a type 2 immune response. Another example showing that the effect of stress hormones on T cells converges with the effect on other cells to mediate a type 2 immune response, was described previously [64, 266]. As described by Tracy and colleagues, norepinephrine released by the splenic nerves, induces choline acetyl transferase (ChAT)-expressing T cells to synthesize and release acetylcholine [64], which in turn promotes the production of plasma cells [266] and inhibits the expression of inflammatory cytokines in macrophages [64]. These studies, together with our work, showcase that during the immunological chain of events from Ag-uptake/presentation to antibody secretion in B cells, each cell type-specific/intrinsic effect induced by stress hormones, converges with each other to specifically boost one arm of the immune system. These overlapping mechanisms make it clear that the stress hormones act on different immune cells in parallel to meticulously regulate the context-specific immune responses.

Our findings in naïve CD4 T cells significantly complement the current understanding of how stress hormones are able to favour Th2 responses and suppress Th1 differentiation in naïve CD4 T cells, rather than only causing a universal immunosuppressive effect. On the

other hand, we showed that the stress hormones have an opposite effect in memory CD4, reducing the production of Th2 cytokines IL-4, IL-5 and IL-13, probably via an mTORC2-dependent mechanism. The related discrepancy between distinct immune subpopulations was first observed by Sanders and colleagues, describing that naïve and effector CD4 T cells respond in different ways to β_2-AR signalling. That effect was later also observed by others and attributed to differential β_2-AR expression levels, sensitivity to norepinephrine/cAMP or glucocorticoids and/or the stage of cell differentiation [248, 249, 336]. However, these studies did not investigate the intrinsic molecular pathways regulating these cell-type specific effects. More recently, norepinephrine has been shown to preferentially modulate the function of memory CD8 T cells, due to a higher sensitivity to norepinephrine, based on a higher expression of β_2-AR [337]. As a G protein-coupled receptor (GPCR), the β_2-AR signals through G proteins. However, depending on which specific G protein subunit is coupled to the receptor, a different downstream pathway might be induced. Foley et al. have shown that human T cells alter their G protein subunit repertoire during differentiation [338], which could at least partially account for the differential effect of norepinephrine on naïve/memory T-cell subpopulations.

As the stress hormones are a driving force not only in stress responses, but also in the regulation of the circadian rhythm, we and others believe that the circadian clock might play an important role in regulating the immune system. Norepinephrine and glucocorticoids have been shown to control lymphocyte trafficking during the 24h cycle via the molecular circadian clock machinery [298-305, 310]. Moreover, emerging evidence attributes specific functions to the clock genes in the context of distinct immune responses in different cell types (reviewed here [307, 309, 339]). In T cells, *NFIL3* has been found to inhibit Th17 differentiation [340], while positively controlling the expression Th2 cytokines [341]. In line with those reports, we have observed a trend for increased *NFIL3* expression following Forsk treatment in naïve and memory CD4 T cells, although not from all the donors, possibly because of the heterogeneity beween different individuals (**Suppl. Fig. 4C**). Further in line with the notion that *NFIL3* favors Th2 responses, the increase of *NFIL3* expression was accompanied by an increased protein expression of GATA3 in naïve CD4 treated with Forsk (**Fig. 2A**).

Together with a recent report showing that the central clock gene BMAL1 is dispensable for T cell functions [342], our study suggests that it is the specific circadian genes, instead of the central regulators, that regulate specific CD4 T-cell responses. We were able to show for the first time that the circadian clock gene Period1 (*PER1*) inhibits the expression of Th1 cytokines by reducing mTORC1 signalling. The cicadian machinary is dysregulated in many complex diseases, especially in various immune associated diseases [343-347] and

targeting the circadian machinery could be a potent, although challenging, new avenue to treat some of those diseases. Last but not least, the circadian clock also plays a role in an optimal vaccination response [348]. Due to the tight regulation of the molecular clock machinery, more research has to be performed to further characterize the role of the different circadian genes in specific immune responses. Our study contributes to this cause by identifying a novel pathway through which stress hormones inhibit Th1 responses via the specific circadian clock gene *PER1* and the mTORC1 pathway.

Materials and Methods

Primary naïve and memory CD4 T cell isolation

Buffy coats from more than 70 healthy donors were generously provided by the Red Cross Luxembourg, under strict ethical regulation, data protection and informed consent from each donor. Due to the sequential design of the project, the cells from different donors were used to perform different experiments, although always with a certain overlap. We isolated the total CD4 cells by adding the RosetteSep™ Human CD4+ T cell Enrichment Cocktail (15062, Stemcell) to undiluted blood at a concentration of 50 µl/ml and incubated the mix for 30 min at 4°C. Next, the same volume of FACS buffer (PBS + 2% FBS) was added to the blood and carefully transferred to a SepMate™ 50 tubes (85450, Stemcell), on top of the Lymphoprep solution (07801, StemCell) in order to isolate the total CD4+ T cells by gradient centrifugation at 1200 g for 20 min. The cells were washed 3 times in FACS buffer and stained for FACS sorting. Total CD4+ T cells were stained with mouse monoclonal [RPA-T4] anti-human CD4 FITC (555346, BD) (dilution 1:20), mouse monoclonal [M-A251] anti-human CD25 APC (555434, BD) (dilution 1:20), mouse anti-human CD45RA [HI100] PacificBlue (BioLegend, 304118), Mouse Anti-Human CD45RO [UCHL1] PE-CF594 (BD, 562299), and LIVE/DEAD® Fixable Near-IR Dead Cell Stain (L10119, ThermoFisher Scientific) (dilution 1:500). Primary naïve (CD4+CD25lowCD45RA+) and memory (CD4+CD25lowCD45RO+) CD4 T cells were sorted on a BD FACSAria^{TM} III cell sorter (BD Biosciences).

Target	Fluorochromes	Dilution	Company	Clone	Reference
CD4	FITC	1:20	BD Biosciences	RPA-T4	555346
CD25	APC	1:20	BD Biosciences	M-A251	555434
CD45RA	Pacific Blue	1:20	BioLegend	HI100	304118
CD45RO	PE-CF594	1:20	BD Biosciences	UCHL1	562299
Live/Dead	Near Infra-Red	1:500	ThermoFisher Scientific	N.A.	L10119

Alternatively, naïve/memory CD4 T cells were isolated with the EasySep™ Human Naïve CD4+ T Cell Isolation Kit(StemCell, #19555) or the EasySep™ Human Memory CD4+ T Cell Enrichment Kit (StemCell, #19157), following the manufacturer's instructions.

For some other donors PBMCs were first isolated by gradient centrifugation and naïve/memory CD4 T cells were isolated with the EasySep or Naive CD4+ T Cell Isolation

Kit II, human (Miltenyibiotec, 130-094-131) and Memory CD4+ T Cell Isolation Kit, human (Miltenyibiotec, 130-094-131), following the manufacturer's instructions.

The results were consistent no matter which isolation method was used, however the highest purity of cells was obtained through FACS sorting (>99%, **Supple. Fig. 1A**).

Cell culture conditions and treatment of primary T cells

Sorted naïve and memory CD4+ T cells were cultured in IMDM (21980-032, ThermoFisher Scientific) complete medium, supplemented with 10% heat-inactivated (56°C, 45 min) fetal bovine serum (FBS) (10500-064, ThermoFisher Scientific), 1x Penicillin+Streptomycin (15070-063, ThermoFisher Scientific), 1x MEM non-essential amino acids (M7145, Sigma-Aldrich) and 1x β-mercaptoethanol (21985-023, ThermoFisher Scientific) for 48-72 h before every experiment, to ensure that there are no more circadian fluctuations in the cells. The CD4 T cell-intrinsic fluctuations of the circadian genes were shown to be abolished after 48 h of cell culture [323].

Between 5 x10^5 and 1 x10^6 naïve or memory CD4 T cells were seeded in 1 ml culture media in 48-well plates in the presence or absence of different compounds: Isoproterenol hydrochloride, 50μM (Sigma-Aldrich, I6504), Forskolin (Forsk), 5 μM (Sigma-Aldrich, F3917), 0.5 μM Hydrocortisone (Sigma-Aldrich, H0396), Rapamycin (StemCell, 73362), L-(-)-Norepinephrine (+)-bitartrate salt monohydrate (Sigma-Aldrich, A9512).

The compounds were added 1 h prior to TCR stimulation by soluble anti-CD3/-CD28 antibodies (25 μl/ml Immunocult™ Human CD3/CD28 T Cell Activator) (10971, StemCell) and incubated for different durations depending on the experiment. For most of the flow cytometry staining following the treatment with different compounds, naïve and memory CD4 T cells were stimulated for 48 h.

siRNA knockdown

Targeted genes' expression (*PER1*, *PER2*, *PER3*) was knocked-down in up to 5 x 10^6 cells using the P3 Primary Cell 4D-Nucleofector X Kit L (V4XP-3024, Lonza) with 90 μl P3 Primary cell solution and 100 pmol of corresponding si_RNA (re-suspended in 10 ul RNAse-free H2O): si_Non-Specific scrambled control siRNA (si_NS or si_CTRL) (SC-37007, Santa Cruz), si_*PER1* (SI00040537, Qiagen), si_*PER2* (SI02632189, Qiagen), si_*PER3* (SI00117530, Qiagen). siRNA transfection was done by using the Amaxa 4D-Nucleofector™ X System (Lonza) following the manufacturer's recommended program for primary human T cells (with the program code EO-115). Following transfection, the naïve

or memory CD4 T cells were transferred into a 12-well plate with pre-warmed complete IMDM medium and incubated at 37 °C for 24 h. The next day the cells were stimulated with 25 µl/ml of soluble antibodies (Immunocult™ Human CD3/CD28 T Cell Activator) (10971, StemCell) for 24 h in 1 ml in a 48-well plate. The knockdown efficiency was assessed by qPCR to ensure siRNA-induced reduction of the targeted gene.

Flow cytometry

Naïve and memory CD4 T cells were harvested by centrifugation (250 x g, 10 min) at the end of the experiment, washed once in FACS buffer (PBS + 2% FBS) and re-suspended in the staining mastermix for the surface staining. Antibodies used are listed in the first half of the table below. Following the surface staining, the cells were washed 3 times in FACS buffer and fixed for 1h at room temperature (RT) using the fixation buffer of the True-Nuclear Transcription Factor Buffer Set (BioLegend, 424401). After fixation, the cells were washed once in permeabilization (Perm) buffer and re-suspended in Perm buffer, containing the antibodies for the intracellular staining (listed in 2nd half of the table below) and incubated for 30 min at RT. The cells were washed 3 times in Perm buffer and re-suspended in FACS buffer for the acquisition on the BD Fortessa.

Target	**Fluorochromes**	**Dilution**	**Company**	**Clone**	**Reference**
Surface markers					
CD4	BUV395	1:100	BD Biosciences	RPA-T4	564724
CD278 (ICOS)	BV605	1:50	BioLegend	C398.4A	313538
CD279 (PD-1)	BV605	1:50	BioLegend	EH12.2H7	329924
GLUT1	AF647	1:50	BD Biosciences	566580	202915
Live/Dead	Near Infra-Red	1:500	ThermoFisher Scientific	N.A.	L10119
Intracellular markers					

Ki-67	AF488	1:50	BD Biosciences	B56	561165
cMyc	AF488	1:50	Cell Signalling	D84C12	12855S
HIF-1α	AF647	1:50	BD Biosciences	54/HIF-1α	565924
Tbet	PE	1:50	BioLegend	4B10	644810
RORγT	BV650	1:20	BD Biosciences	Q21-559	563424
FOXP3	AF647	1:50	BioLegend	206D	320114
pS6 (S235/236)	AF488	1:50	Cell Signalling	D57.2.2E	4803S
pAkt (S473)	PE-CF594	1:20	BD Biosciences	M89-61	562465
pAkt (T308)	PE	1:20	BD Biosciences	J1-223.371	558275
pPDPK1 (S241)	AF647	1:20	BD Biosciences	J66-653.44.17	560091
pSTAT3 (Y705)	PE	1:50	BD Biosciences	4/P-STAT3	612569
pSTAT4 (Y693)	AF488	1:50	BD Biosciences	38/p-Stat4	558136
pSTAT5 (Y694)	PerCP-Cy5.5	1:50	BD Biosciences	47/Stat5 (pY694)	560118
pSTAT6 (Y641)	AF647	1:50	BD Biosciences	18/pStat6	612601

Intracellular cytokine staining

4 h before harvesting the cells, Golgistop (BD, 554724) was added to the cell cultures inhibit the secretion of the cytokines, leading to an accumulation inside the cells. Naïve and memory CD4 T cells were harvested by centrifugation (250 x g, 10 min) at the end of the experiment, washed once in FACS buffer (PBS + 2% FBS) and re-suspended in the staining mastermix for the surface staining (CD4 FITC and L/D APC-Cy7). Following the surface staining, the cells were washed 3 times in FACS buffer and fixed for 30 min at 4 °C using the Cytofix/Cytoperm buffer set (BD, 554714). After fixation, the cells were washed once in

Perm/Wash buffer and re-suspended in Perm/wash buffer, containing the antibodies for the intracellular staining (listed in the table below) and incubated for 30 min at RT. The cells were washed 3 times in Perm/Wash buffer and re-suspended in FACS buffer for the acquisition on the BD Fortessa.

Target	Fluorochromes	Dilution	Company	Clone	Reference
CD4	FITC	1:20	BD Biosciences	RPA-T4	555346
Live/Dead	Near Infra-Red	1:500	ThermoFisher Scientific	N.A.	L10119
IFNγ	PE-Cy7	1:50	BD Biosciences	4S.B3	560741
TNFα	BUV395	1:50	BD Biosciences	MAb11	563996
IL-2	BV650	1:50	BD Biosciences	5344.111	563947
IL-4	BUV737	1:50	BD Biosciences	MP4-25D2	612835
IL-5	PE	1:50	BD Biosciences	TRFK5	554395
IL-17	BV786	1:50	BD Biosciences	N49-653	563745

Cytokine measurement by MSD assay

The supernatant of the naïve and memory CD4 cell culture was collected after 24 h or 48 h following stimulation, depending on the experiment by centrifuging down the cells (250 x g, 10 min). The concentration of a selection of CD4 cytokines, especially Th1/Th2 cytokines (IFNγ, TNFα, GM-CSF, IL-2, IL-4, IL-5, IL-13, IL-17, IL-21, IL-9, IL-10) was measured in undiluted culture medium using the MSD U-PLEX Human Biomarker group 1 kit (MSD, K15067L-1) according to the manufacturer's instructions. The plates were read by the MESO QuickPlex SQ 120 instrument and the data was analysed with the provided MSD Workbench software.

RNA extraction, cDNA synthesis and qPCR

The RNeasy Mini Kit (74106, Qiagen) or RNeasy Micro Kit (74004, Qiagen) was used for RNA extraction according to the manufacturer's instructions and including a genomic DNA digestion step with DNAse I (79254, Qiagen). The cells were lysed in RLT buffer (79216, Qiagen), supplemented with 1% beta-Mercaptoethanol (63689, Sigma-Aldrich) and frozen at -20°C for several hours or days until the RNA extraction. The NanoDrop 2000c Spectrophotometer (ThermoFisher Scientific) was used to measure RNA concentration.

For the cDNA synthesis, the SuperScript™ IV First Strand Synthesis System (18091050, ThermoFisher Scientific) was used, with a maximum of 500ng of RNA. The master mix for the first step included per sample: 0.5 µl of 50 µM Oligo(dT)20 primers (18418020, ThermoFisher Scientific), 0.5 µl of 0.09 U/µl Random Primers (48190011, ThermoFisher Scientific), 1 µl of 10 mM dNTP mix (18427013, ThermoFisher Scientific) and RNAse-free water for a final volume of 13 µl. The C1000 Touch Thermal Cycler (Bio-Rad) or UNO96 HPL Thermal Cycler (VVR) were used for both steps. For the first step, the following program was used: 5 min at 65 °C, then 2 min at 4 °C. Before the second reaction step, the mix was supplemented with 40 U RNaseOUT™ Recombinant Ribonuclease Inhibitor (10777019, ThermoFisher Scientific), 200 U SuperScript™ IV Reverse Transcriptase (18090050, ThermoFisher Scientific), a final concentration of 5 mM Dithiothreitol (DTT) (70726, ThermoFisher Scientific) and 1x SuperScript™ IV buffer for a final reaction volume of 20 µl. The program for the second step: 10 min at 50 °C, 10 min at 80 °C and 4 °C until the samples are picked-up. The obtained cDNA was diluted 3 times with nuclease-free water to a final volume of 60 µl.

For the quantitative real-rime PCR (qPCR) a mastermix for following reaction mix was prepared per well: 5 µl of the LightCycler 480 SYBR Green I Master Mix (04707516001, Roche), 2.5 µl cDNA and 2.5 µl primers in a total reaction volume of 10 ul. The PCR was performed in a CFX384 Touch Real-Time PCR System (Bio-Rad), using LightCycler 480 Multiwell 384-well plates (04729749 001, Roche) sealed with the LC 480 Sealing Foil (04729757001, Roche). Following program was used: 5 min at 95 °C; 45 cycles of (10 sec at 55 °C, 20 sec at 72 °C, 10 sec at 95 °C); melting curve (65-97 °C). The results were analyzed using the $2^{-\Delta\Delta Ct}$ method. Primers used for qPCR: RPS9 (QT00233989, Qiagen) as a reference gene, *PER1* (QT00069265, Qiagen), *PER2* (QT00011207, Qiagen), *PER3* (QT00097713, Qiagen), *ARNTL1* (BMAL1) (QT00011844, Qiagen), *CLOCK* (QT00054481, Qiagen), *CRY1* (QT00025067, Qiagen), *CRY2* (QT00094920, Qiagen), *NFIL3* (QT00013944, Qiagen), *NR1D1* (RevErbα) (QT00000413, Qiagen), *IL2* (QT00015435, Qiagen), *IFNG* (QT00000525, Qiagen), *TBX21* (QT00042217, Qiagen).

ATP measurement

The CellTiter-Glo® Luminescent Cell Viability Assay (G7570, Promega) was used to measure the ATP concentration in the cells. 2 x 10^5 cells were lysed and prepared according to the manufacturer's recommendations.

cAMP assay

The intracellular cAMP concentration following the treatment with different compounds was analysed in undiluted samples with the cAMP 96-well kit (MSD, K150W5D), following the manufacturers protocol and measured by the MESO QuickPlex SQ 120 instrument.

Statisitical analysis

Statistics analysis was performed in Graphpad prism using either a one-way ANOVA with the Dunnett's multiple comparison correction, or a paired two-tailed t test, depending on the features of the corresponding experiment. The test used for the different figures is specified in the figure legends. The error bars in the related types of figures represent the standar deviation (s.d.).

Acknowledgements

We particularly appreciate Luxembourg Red Cross for providing buffy coats to us. The Feng He group was supported by Luxembourg National Research Fund (FNR) through different programs including AFR-RIKEN bilateral programme (TregBAR, 11228353), PRIDE/2015/10907093/CRITICS to support C.C., individual Aide à la Formation Recherche (AFR) grant PHD-2015-1/9989160 to support N.Z. and intramural funding within Luxembourg Institute of Health and Luxembourg Centre for Systems Biomedicine, from Ministère de l'Enseignement supérieur et de la Recherche (MESR). M.O. was supported as coordinator by the Luxembourg National Research Fund (FNR) through the FNR PRIDE program for doctoral training unit (PRIDE/11012546/NEXTIMMUNE). Some icons in the schematic Figures were obtained from BioRender.com.

Author contributions

C.M.C. designed and performed experiments. C.M.C. analyzed the data and wrote the manuscript. A.C. contributed to the project in the context of her master thesis. A.B., N.Z., K.G. and T.A. helped performing some experiments and gave technical advice. A.S., M.O. and F.Q.H. supervised the project. F.Q.H. oversaw the project and revised the manuscript. All the authors read and edited the manuscript.

Conflict of Interest

The authors declare no conflict of interest.

Figures

Figure 1: Stress hormones decrease the activity and proliferation of naive and memory CD4 T cells.

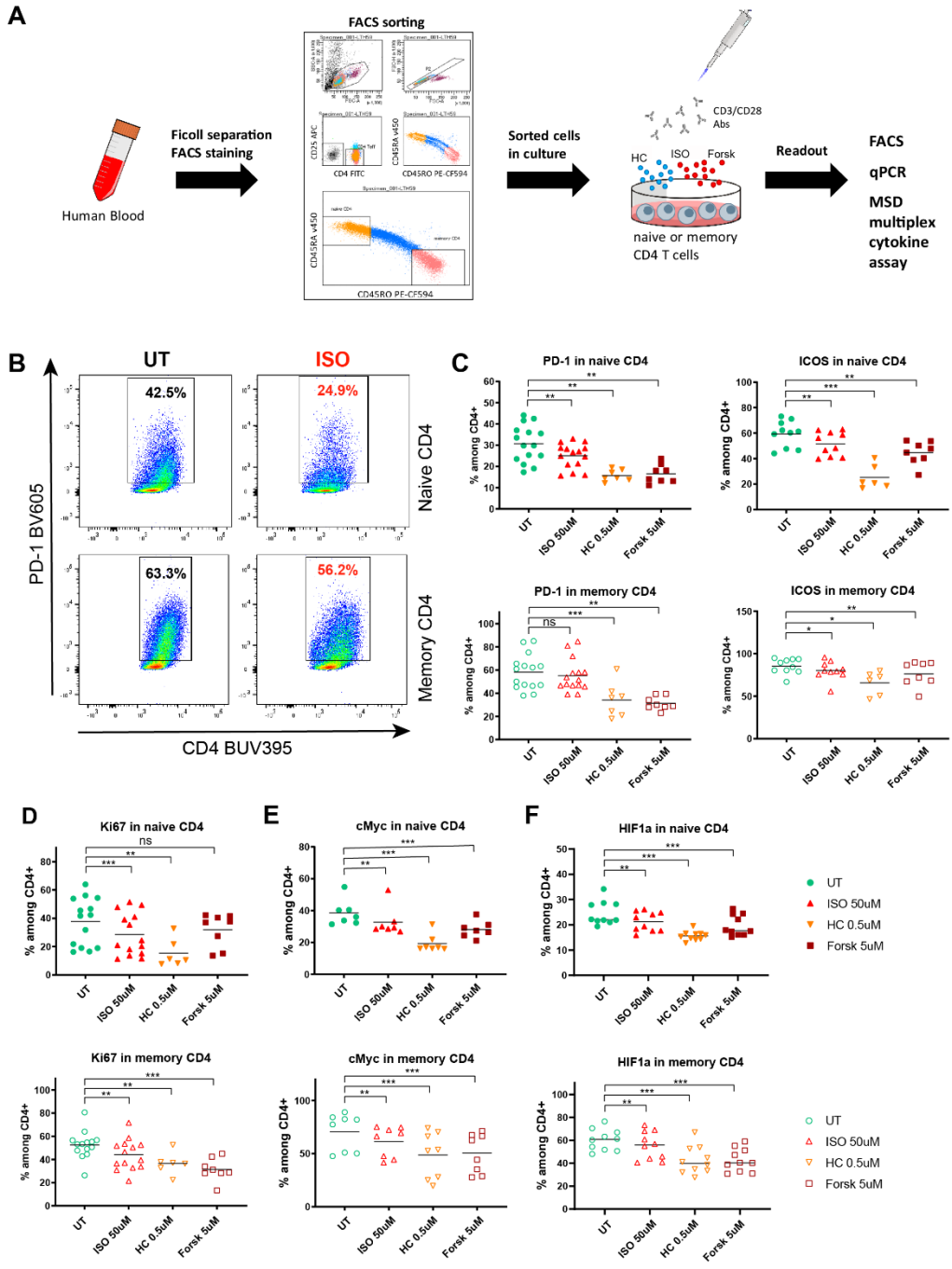

Figure 1: Stress hormones decrease the activity and proliferation of naive and memory CD4 T cells.

(**A**) Graphical representation of the experimental setup. Naïve (CD4+CD25lowCD45RA+) and memory (CD4+CD25lowCD45RO+) CD4 T cells are isolated by gradient centrifugation and FACS sorting. The isolated cells are exposed to stress hormones analogues Isoproterenol (ISO, β_2-AR agonist) and Hydrocortisone (HC, synthetic glucocorticoid) 1h

prior TCR stimulation and are harvested at different timepoint for different applications. (**B**) Representative FACS plots showing the decreased expression of PD-1 after ISO treatment, following 48h TCR stimulation. (**C**) Scatter dot plots showing the effect of ISO, HC and Forskolin (Forsk) on the expression of PD-1 (n=7-15) and ICOS (n=6-10) in naïve and memory CD4, measured by flow cytometry. (**D-F**) Scatter do plots showing the effect of ISO, HC and Forskolin (Forsk) on the expression of Ki67 (n=6-14) (D), cMyc (n=7) (E) and HIF1α (n=10) (F) in naïve and memory CD4, measured by flow cytometry. FACS, flow cytometry; qPCR, quantitative PCR; UT, untreated; US, unstimulated. Each individual value in the scatter dot plots was displayed with mean in each group. The results in (C-F) were analyzed using one-way ANOVA with multiple comparison correction. ns or unlabelled, non-significant; *p<=0.05, **p<=0.01, and ***p<=0.001. The horizontal bars in (C-F) represent the mean.

Figure 2: Stress hormones change the balance of the CD4 T helper programs in naive CD4

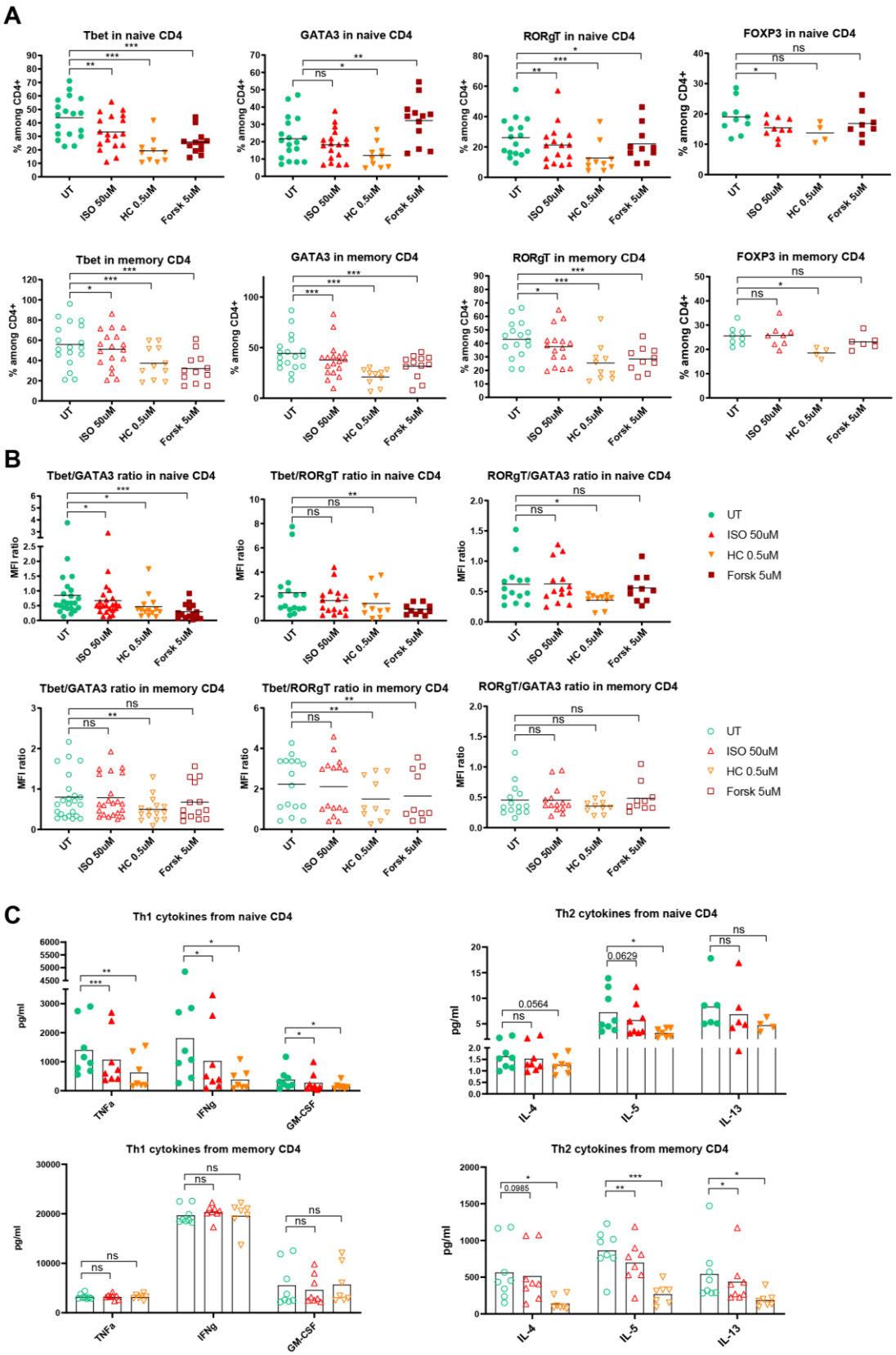

Figure 2: Stress hormones change the balance of the CD4 T helper programs in naive CD4.

(**A**) Expression of the CD4 master/lineage transcription factors for the Th1 (Tbet) (n=10-18), Th2 (GATA3) (n=01-18), Th17 (RORγT) (n=10-16) and Treg (FOXP3) (n=4-10) cells in naïve (top) and memory (bottom) CD4 T cells after 48h TCR stimulation in absence or presence of different stress hormone analogues, measured by flow cytometry. (**B**) Ratios between the geomean of different transcriptions factors in naïve (top) and memory (bottom) CD4 T cells. (**C**) Secreted cytokines, measured in the culture medium after 48h of TCR stimulation with the MSD multiplex assays. Cytokines secreted by naïve CD4 T cells are shown in the top row, and memory CD4 in the bottom row. Th1 cytokines (left) and Th2 cytokines (right) are grouped in different graphs (n=7-8). Isoproterenol (ISO) (β_2-AR agonist); hydrocortisone (HC) (synthetic glucocorticoid); UT, untreated; US, unstimulated. Each individual value was displayed with mean in each group. The results in (A-C) were analyzed using one-way ANOVA with multiple comparison correction. ns or unlabelled, non-significant; *p<=0.05, **p<=0.01, and ***p<=0.001. The horizontal bars in (A, B) and the boxes in (C) represent the mean.

Figure 3: Stress hormones alter mTOR signalling to inhibit Th1 polarization in naive CD4 T cells

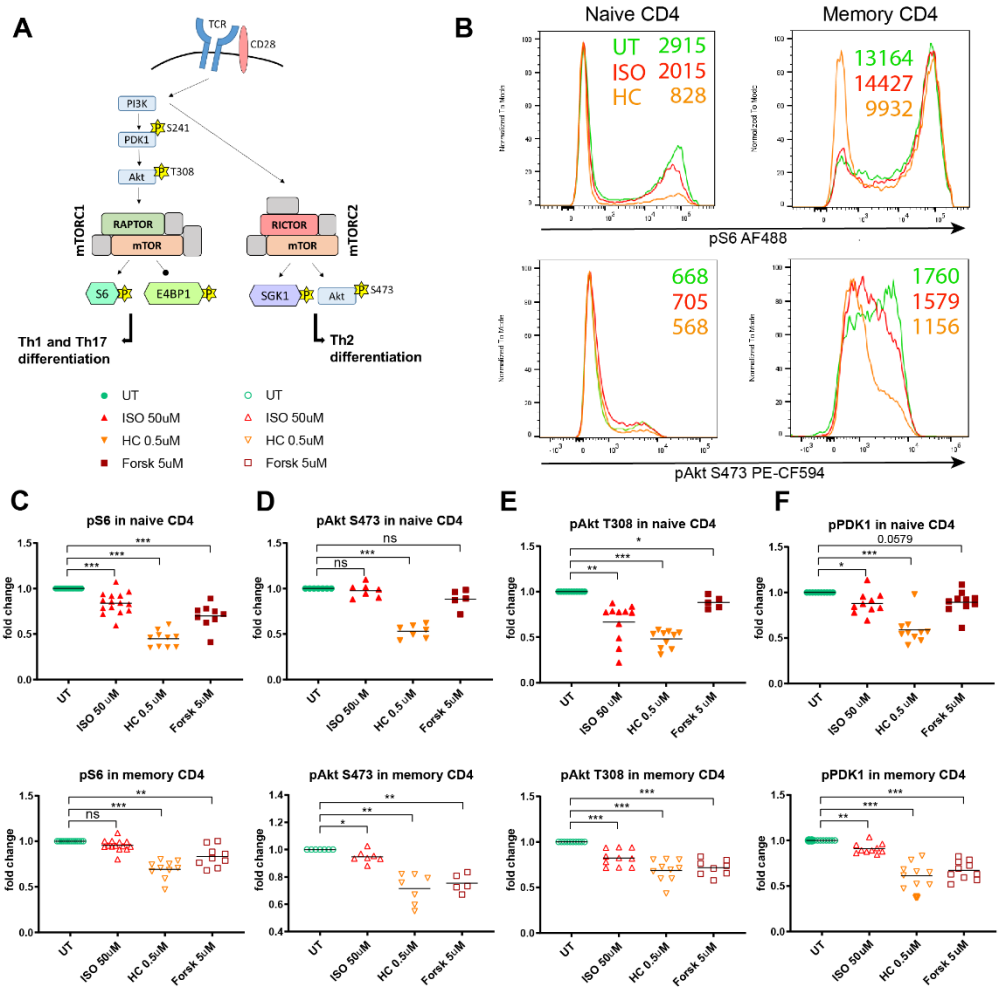

Figure 3: Stress hormones alter mTOR signalling to inhibit Th1 polarization in naive CD4 T cells.

(**A**) Graphical representation of a simplified view of the mTORC1 and mTORC2 involvement in the differentiation of CD4 T cells into different T helper subsets (adapted from [318]). (**B**) Histograms showing the geometric mean of pS6 (S235/236) and pAkt (S473) in naïve (left) and memory (right) CD4 T cells of a representative donor. (**C-F**) Statistic graphs showing the effect of ISO, HC and Forsk on the phosphorylation of proteins of the mTOR pathways: (C) pS6 (S235/236) (n=10-15), (D) pAkt (S473) (n=5-7), (E) pAkt (T308) (7-11), (F) pPDPK1 (S241) (n=10). The fold change was normalized to UT. Isoproterenol (ISO) (β_2-AR agonist); hydrocortisone (HC) (synthetic glucocorticoid); UT, untreated; US, unstimulated. Each individual value was displayed with mean in each group. The results in (C-F) were analyzed using one-way ANOVA with multiple comparison correction. ns or unlabelled, non-significant; *p<=0.05, **p<=0.01, and ***p<=0.001. The horizontal bars in (C-F) represent the mean.

Figure 4: Stress hormones induce the expression of Period 1 to inhibit Th1 cytokine expression via mTORC1

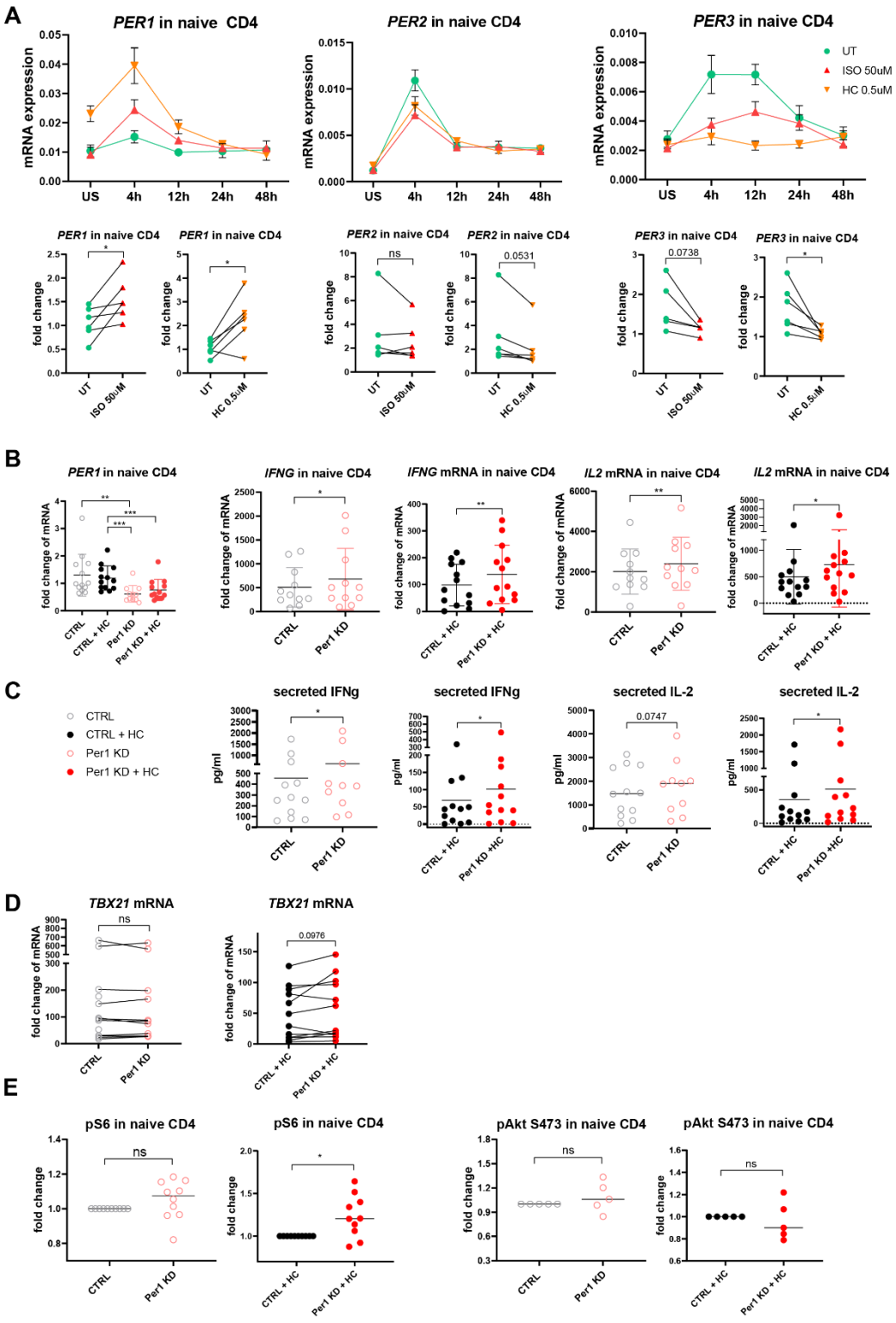

Figure 4: Stress hormones induce the expression of *PER1* to inhibit Th1 cytokine expression via mTORC1.

(**A**) mRNA expression of the clock genes *PER1*, *PER2* and *PER3* in naïve CD4 following ISO or HC treatment and TCR stimulation. Top row: time course over the first 48h of a

representative donor. Bottom row: Graphs showing the pooled results of several donors for the mRNA expression of *PER1*-3 after ISO (red) or HC (orange) treatment. (**B**) The mRNA expression of *PER1*, IFNG and IL2 following *PER1* specific siRNA (red) or scrambled control (CTRL) (grey/black) siRNA knockdown in the presence (full circles) or absence (empty circles) of HC in naïve CD4 (n=11-13). (**C**) Concentration of secreted IFNγ and IL-2 in the cell culture medium of naïve CD4 T cells following ISO or HC treatment and 48h TCR stimulation (n=10-12). (**D**) mRNA expression of TBX21 (Tbet) (n=11-13) following *PER1*-specific or CTRL siRNA knockdown in the presence or absence of HC in naïve CD4. (**E**) The fold change in the expression of pS6 (S235/236) (n=10) and pAkt (S473) (n=5) in naïve CD4 T cells following *PER1*-specific or CTRL siRNA knockdown and TCR stimulation in the presence or absence of HC. Isoproterenol (ISO) (β_2-AR agonist); hydrocortisone (HC) (synthetic glucocorticoid); UT, untreated; US, unstimulated. The results in (A-D) were analyzed using paired t test. ns or unlabelled, non-significant; *p<=0.05, **p<=0.01, and ***p<=0.001. The horizontal bars in (B, C, E) represent the mean.

Suppl. Figure 1: Sorting efficiency & additional measured markers for the activity phenotype

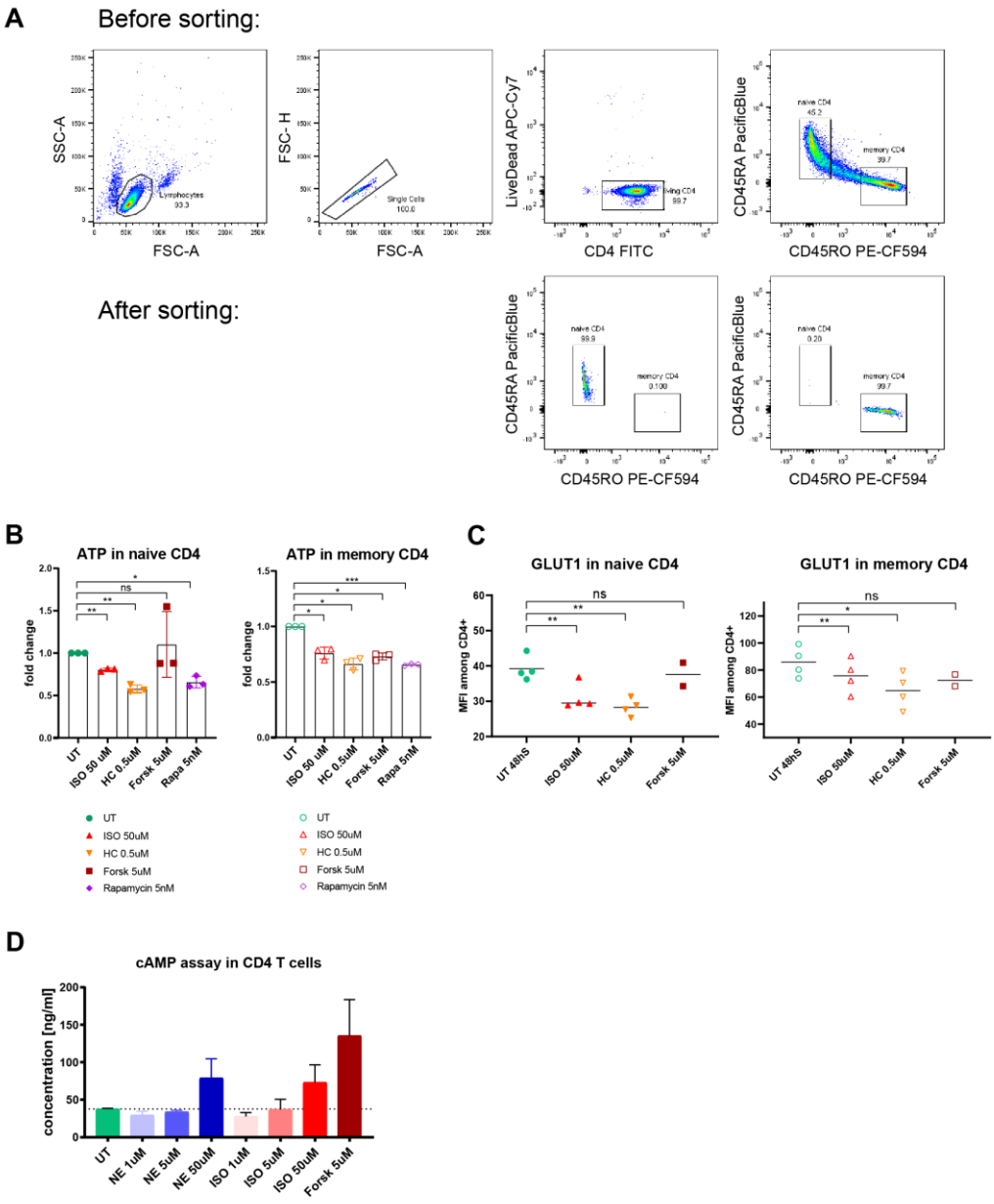

Supplementary Figure 1: Sorting efficiency & additional measured markers for the activity phenotype.

(**A**) FACS plots showing the sorting efficiency of naïve and memory CD4 T cells with a purity higher than 99%. (**B**) Fold change in intracellular ATP concentration following treatments with ISO, HC, Forsk and Rapamycin and 48h TCR stimulation in naïve (left) and memory (right) CD4 T cells. (**C**) Geomean of GLUT1 in naïve (left) and memory (right) CD4 following treatment with ISO, HC or Forsk and 48h TCR stimulation. (**D**) cAMP assay showing the induction of intracellular cAMP levels following treatments with Norepinephrine (NE), ISO or Forsk in different concentrations. Isoproterenol (ISO) (β_2-AR agonist); hydrocortisone (HC) (synthetic glucocorticoid); UT, untreated. The results in (B-D) were analyzed using

one-way ANOVA with multiple comparison correction. ns or unlabeled, non-significant; *p<=0.05, **p<=0.01, and ***p<=0.001. The horizontal bars or boxes in (B-D) represent the mean.

Suppl. Figure 2: Th17 and other cytokine secretion & intracellular cytokines in naive CD4

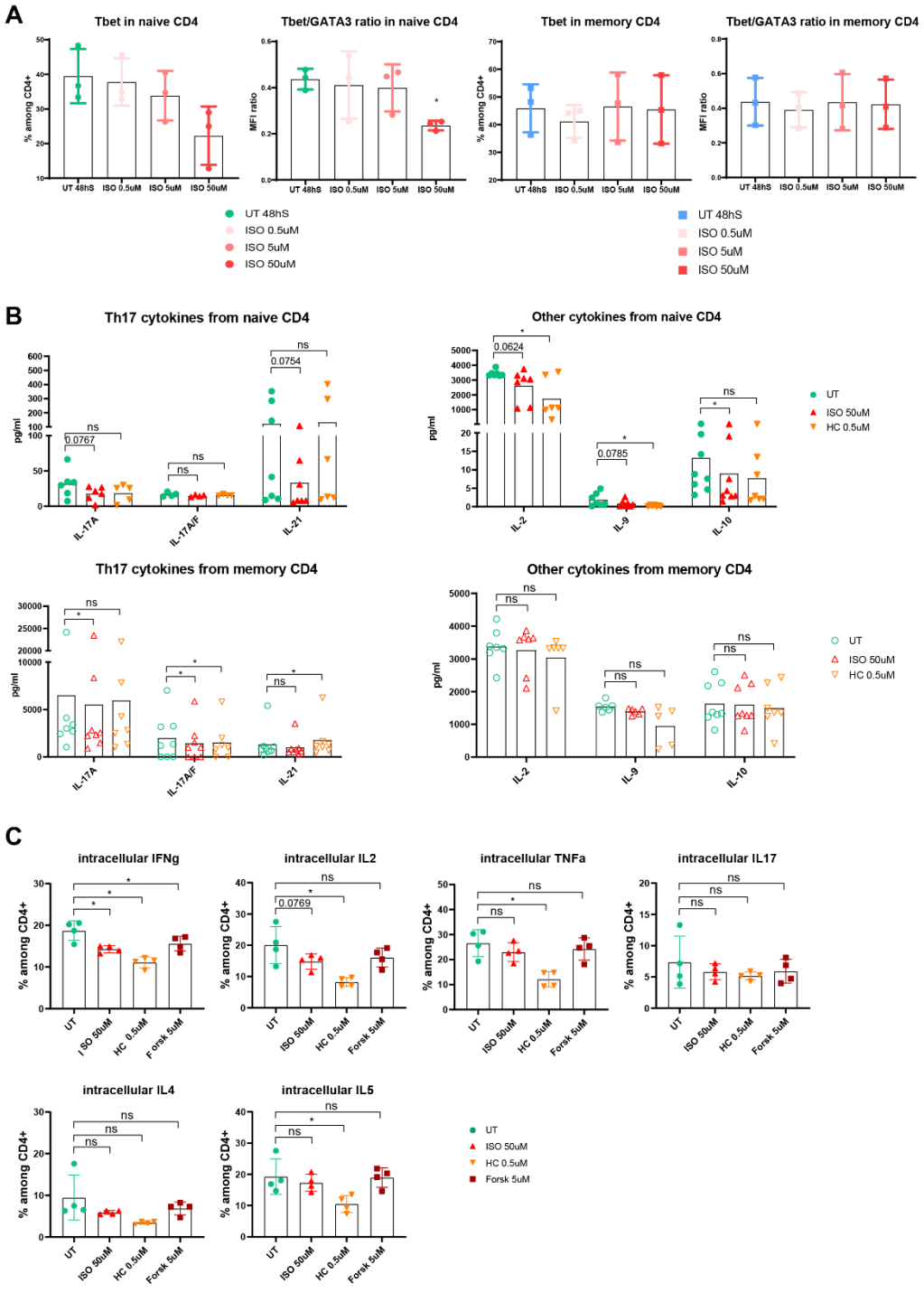

Supplementary Figure 2: Th17 and other cytokine secretion & intracellular cytokines in naive CD4.

(**A**) Secreted cytokines, measured in the culture medium after 48h of TCR stimulation with the MSD multiplex assays. Cytokines secreted by naïve CD4 T cells are shown in the top row, and memory CD4 in the bottom row. Th17 cytokines (left) and others (right) are grouped in different graphs (n=6-8). (**B**) Graphs showing the levels of intracellular cytokines

in naïve CD4 after ISO, HC or Forsk treatment and 48h TCR stimulations. (**C**) Expression of Tbet (left) and the Tbet/GATA3 ratio (right) in naïve (top row) and memory (bottom row) CD4 T cells treated with different concentrations of ISO followed by 48h TCR stimulation. Isoproterenol (ISO) (β_2-AR agonist); hydrocortisone (HC) (synthetic glucocorticoid); UT, untreated. The results in (A-C) were analyzed using one-way ANOVA with multiple comparison correction. ns or unlabelled, non-significant; *p<=0.05, **p<=0.01, and ***p<=0.001. The boxes in (A-C) represent the mean.

Suppl. Figure 3: STAT profile is slightly altered in favour of Th2 polarization in naive CD4

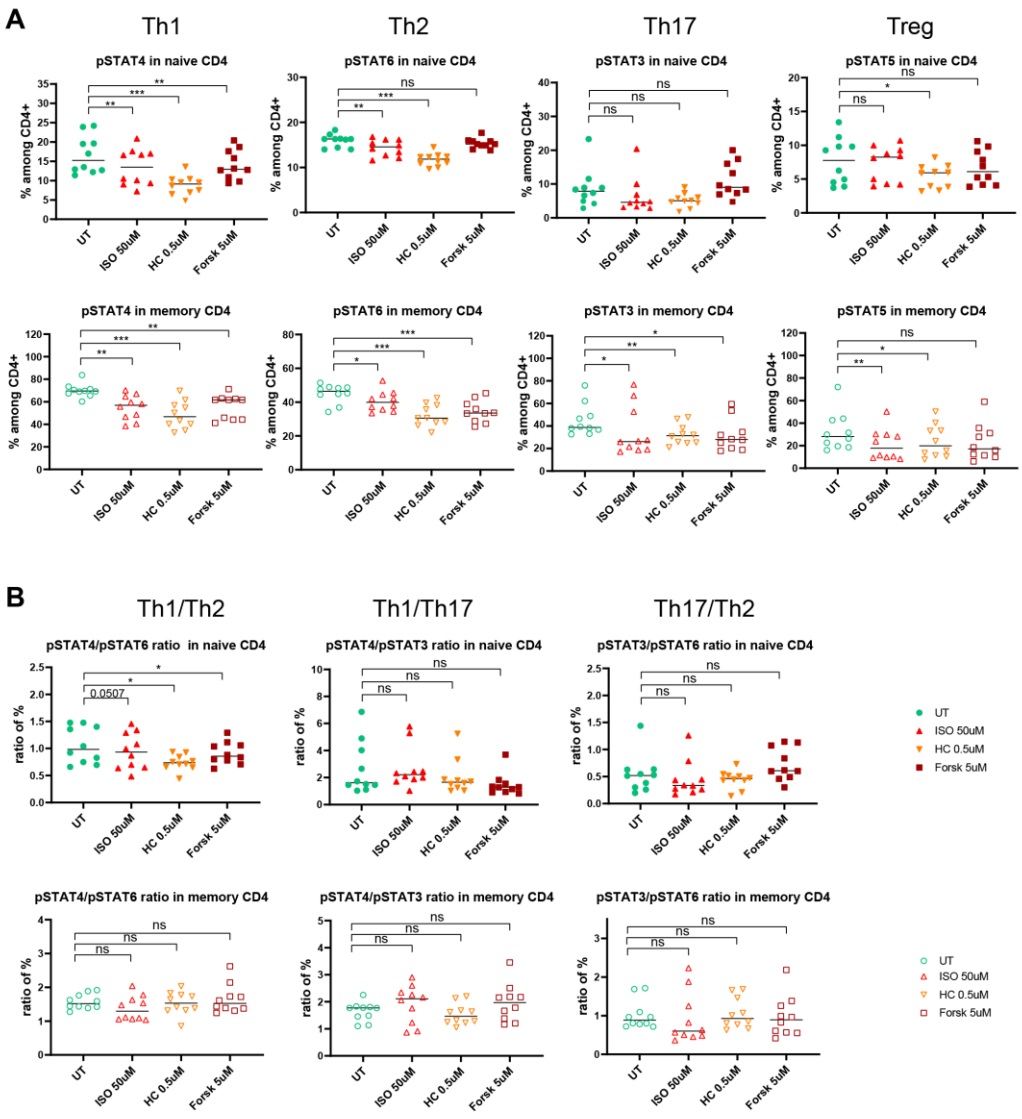

Supplementary Figure 3: STAT profile is altered in favour of Th2 polarization in naive CD4.

(**A**) Graphs showing the expression of various phosphorylated STAT proteins in naïve (top) and memory (bottom) CD4 T cells following ISO, HC or Forsk treatment and 48 h TCR stimulation. (**B**) Graphs showing the ratio between different STATs to assess the Th1/Th2/Th17 balance, based on STAT protein phosphorylation in naïve (top) and memory (bottom) CD4. Isoproterenol (ISO) (β_2-AR agonist); hydrocortisone (HC) (synthetic glucocorticoid); UT, untreated. The results in (A-B) were analyzed using one-way ANOVA with multiple comparison correction. ns or unlabelled, non-significant; *p<=0.05, **p<=0.01, and ***p<=0.001. The boxes in (A-C) represent the mean. The horizontal in (A, B) represent the mean.

Suppl. Figure 4: Effect of melatonin on CD4 T cells and clock gene expression following TCR stimulation and treatments

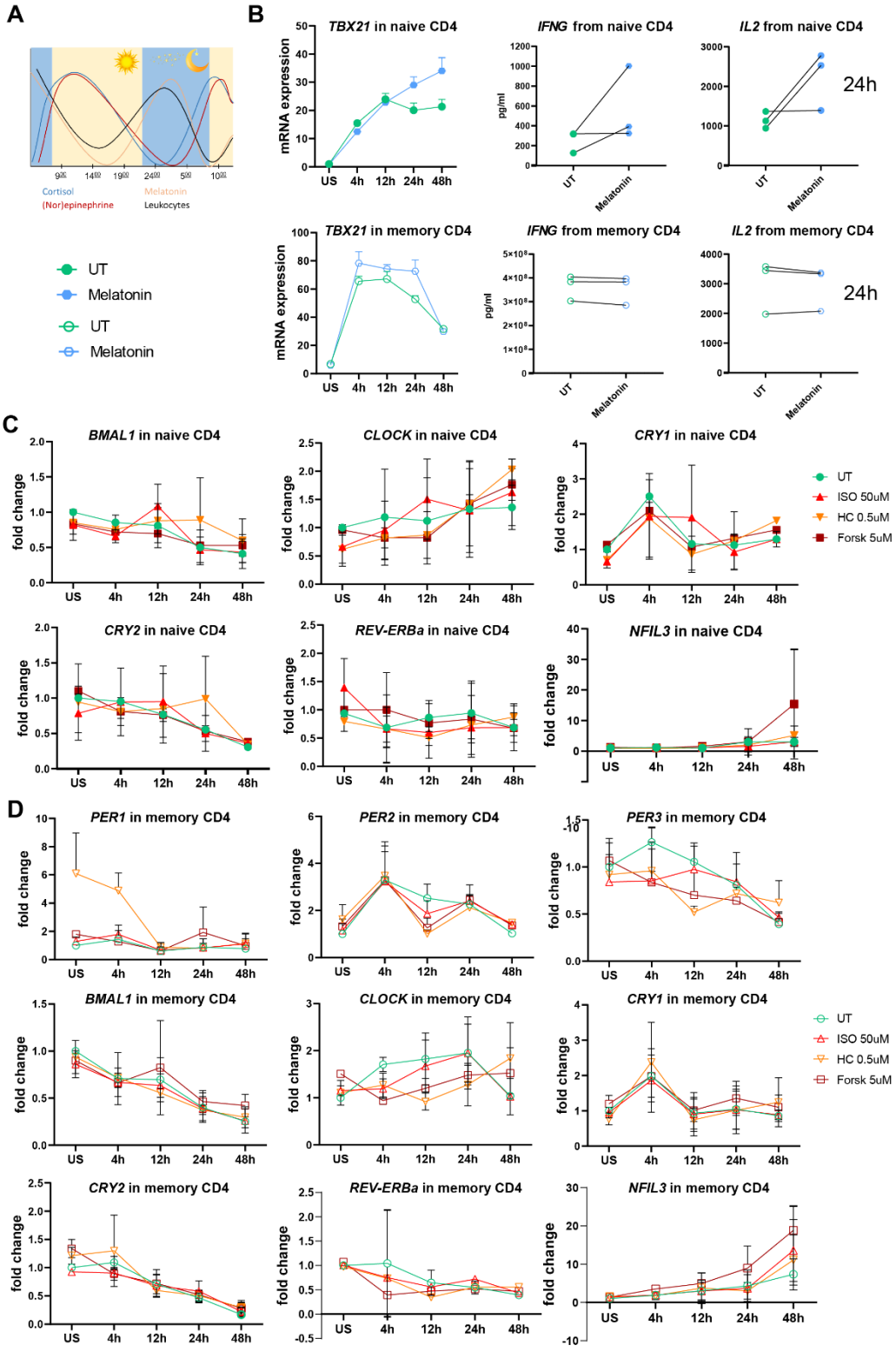

Supplementary Figure 4: Effect of melatonin on CD4 T cells and clock gene expression following TCR stimulation and treatments.

(**A**) Graphical representation of the diurnal patterns of (Nor) epinephrine, Glucocorticoids, Melatonin and Lymphocytes in the human blood. (**B**) Expression of Th1 genes in naïve (top)

and memory (bottom) CD4 T cells following up to 48 h of Melatonin treatment and TCR stimulation. Left: TBX21 mRNA time course. Secreted IFNγ (middle) and IL-2 (right) in naïve (top) and memory (bottom) CD4 following 24h melatonin treatment and TCR stimulation. (**C**) 48h-timecourse of mRNA expression of circadian clock genes in naïve CD4 following ISO or HC treatment and TCR stimulation. (**D**) 48h-timecourse of mRNA expression of circadian clock genes in memory CD4 following ISO or HC treatment and TCR stimulation. Isoproterenol (ISO) (β_2-AR agonist); hydrocortisone (HC) (synthetic glucocorticoid); UT, untreated; US, unstimulated.

Suppl. Figure 5: Period 2/3 depend on mTORC1 and have no impact on Th1 gene expression in naive CD4

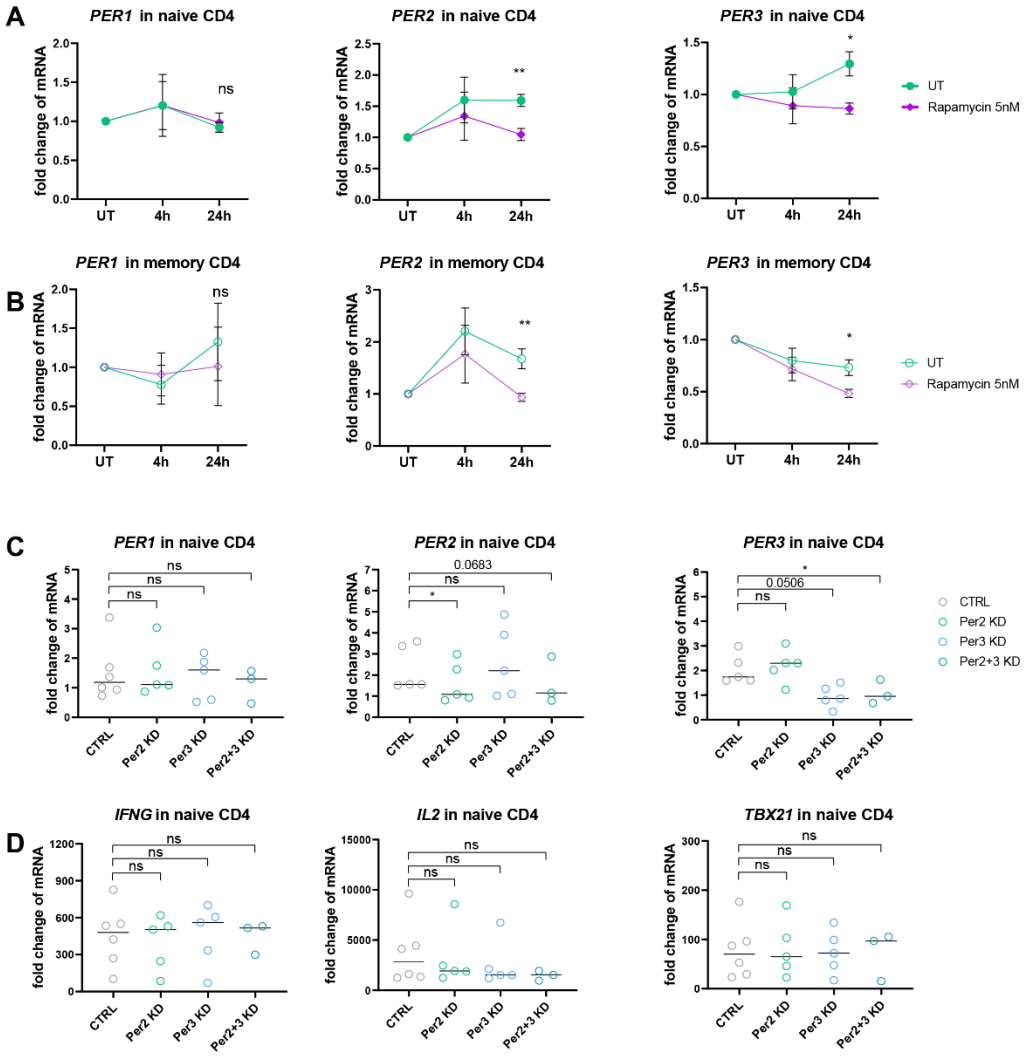

Supplementary Figure 5: Period2/3 depend on mTORC1 and have no impact on Th1 gene expression in naive CD4.

(**A**) mRNA expression of *PER1*, *PER2* and *PER3* in naïve CD4 T cells following 4 h and 24 h rapamycin treatment and TCR stimulation (n=5). (**B**) mRNA expression of *PER1*, *PER2* and *PER3* in memory CD4 T cells following 4 h and 24 h rapamycin treatment and TCR stimulation (n=5). (**C**) mRNA expression of Period genes in naïve CD4 T cells following *PER2* and/or *PER3* siRNA knockdown and 24h TCR stimulation (n=3-6) (**D**) mRNA expression of Th1 genes in naïve CD4 T cells following *PER2* and/or *PER3* siRNA knockdown and 24h TCR stimulation (n=3-6). UT, untreated. The results in (A-B) were analyzed using two-way ANOVA with multiple comparison correction. (C-D) were analyzed using one-way ANOVA with multiple comparison correction. ns or unlabelled, non-significant; *p<=0.05, **p<=0.01, and ***p<=0.001. The horizontal bars (C, D) represent the mean.

Suppl. Figure 6: Period 1 knockdown has no impact in memory CD4 and on other clock genes

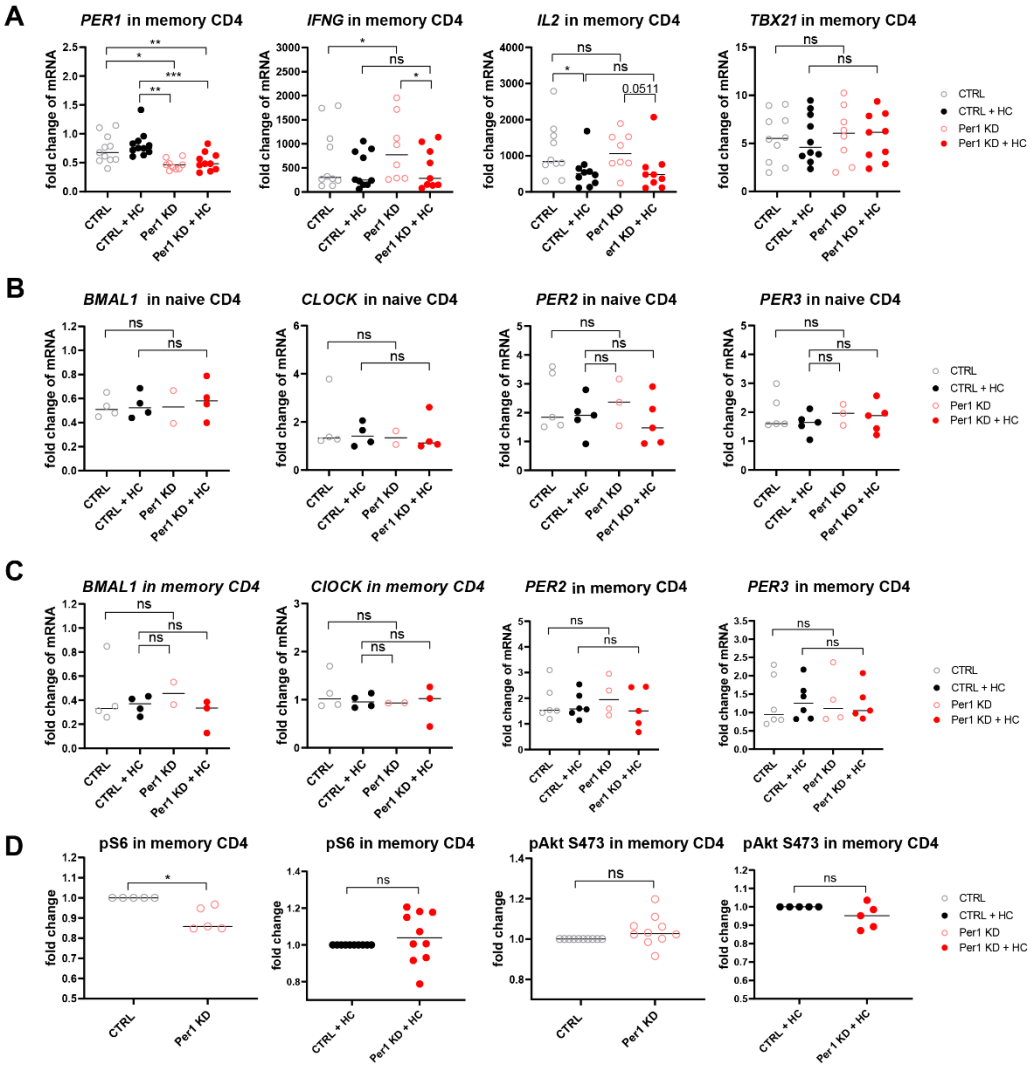

Supplementary Figure 6: Period1 knockdown has no impact in memory CD4 and on other clock genes.

(**A**) mRNA expression of clock genes in naïve CD4 following *PER1*-specific or scrambled control (CTRL) siRNA knockdown in the presence or absence of HC (n=2-4). (**B**) mRNA expression of *PER1* and Th1 genes in memory CD4 following *PER1*-specific or CTRL siRNA knockdown in the presence or absence of HC (n=2-4). (**C**) mRNA expression of clock genes in memory CD4 following *PER1* or CTRL siRNA knockdown in the presence or absence of HC (n=2-4). (**D**) The fold change in the expression of pS6 (S235/236) (n=10) and pAkt (S473) (n=5) in memory CD4 T cells following *PER1* or CTRL siRNA knockdown and TCR stimulation in the presence or absence of HC. Hydrocortisone (HC) (synthetic glucocorticoid). The fold change was normalized to CTRL. The results in (A-D) were analyzed using paired t test. ns or unlabelled, non-significant; *p<=0.05, **p<=0.01, and ***p<=0.001. The horizontal bars (A-D) represent the mean.

Suppl. Figure 7: Period 1 knockdown partially rescues the expression of other Th1 (and Th17) cytokines in naive CD4

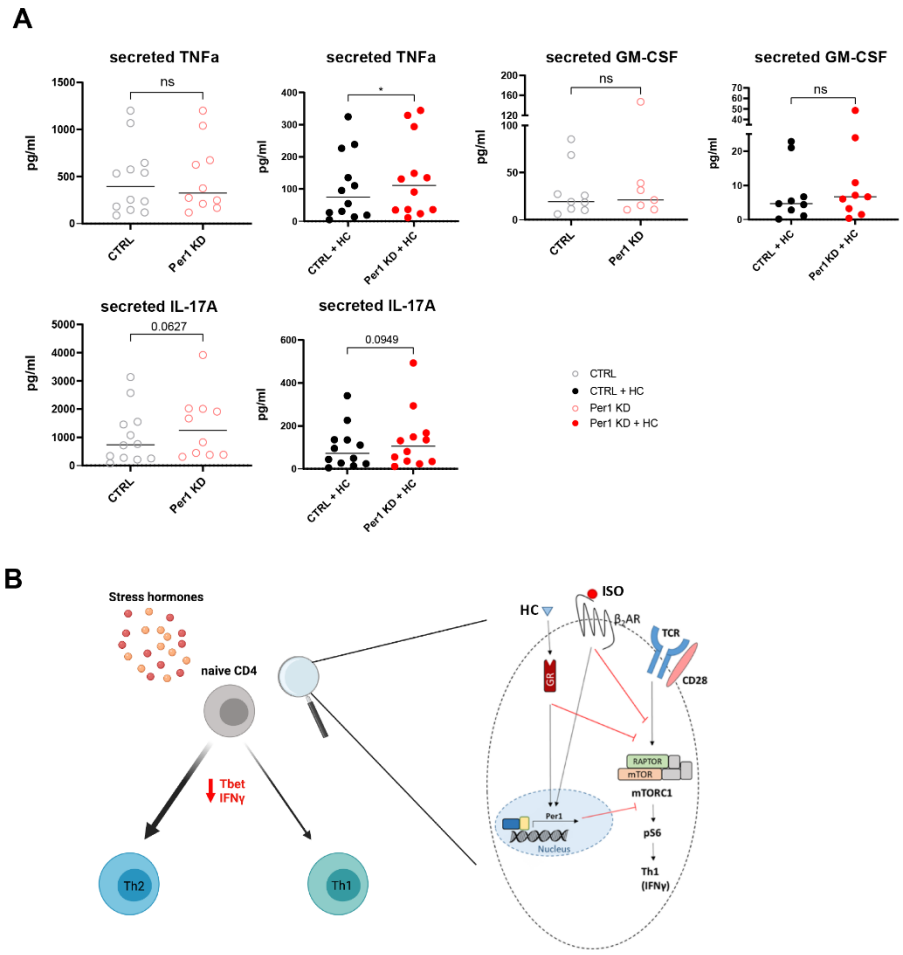

Supplementary Figure 7: Period1 knockdown partially rescues the expression of other Th1 (and Th17) cytokines in naive CD4 and graphical summary of our findings.

(**A**) Secreted Th1 cytokines from naïve CD4 T cells following *PER1*-specific or scrambled control (CTRL) siRNA knockdown in the presence or absence of HC. (**B**) Graphical representation of findings shown in this manuscript. Stress hormone signalling inhibits Tbet and IFNγ expression in naïve CD4 T cells via inducing the expression of *PER1* and inhibiting mTORC1 signalling, thus inhibiting Th1 differentiation. Red lines indicate an inhibitory effects, whereas the black lines represent the an inducing effects. Isoproterenol (ISO) (β_2-AR agonist); hydrocortisone (HC) (synthetic glucocorticoid); TCR, T cell receptor. The results in (**A**) were analyzed using paired t test. ns or unlabelled, non-significant; *p<=0.05, **p<=0.01, and ***p<=0.001. The horizontal bars **(A)** represent the mean.

Chapter 3

Systems immunology reveals a cytotoxic immune cell profile in Parkinson's disease patients.

Chapter 3: Systems immunology reveals a cytotoxic immune cell profile in Parkinson's disease patients.

Christophe M. Capelle1, 2, Séverine Ciré1, Maxime Hansen3, 4, Lukas Pavelka3, 4, Fanny Hedin5, Maria Konstantinou5, Dominique Revets5, Vera Tslaf1, 2, 6, Alexandre Baron1, Ni Zeng1 ,2, Patrick May3, Antonio Cosma5, Rudi Balling3, Rejko Krüger3, 4, 6, Markus Ollert1, 7, Feng Q. Hefeng1, 8, *

1 Department of Infection and Immunity, Luxembourg Institute of Health (LIH), 29, rue Henri Koch, L-4354, Esch-sur-Alzette, Luxembourg

2 Faculty of Science, Technology and Communication, University of Luxembourg, 2, avenue de Université, L-4365, Esch-sur-Alzette, Luxembourg

3 Luxembourg Centre for Systems Biomedicine (LCSB), University of Luxembourg, 6, avenue du Swing, L-4367, Belvaux, Luxembourg

4 Parkinson Research Clinic, Centre Hospitalier de Luxembourg (CHL), 4, Rue Nicolas Ernest Barblé, L-1210, Luxembourg, Luxembourg

5 National Cytometry Platform, Luxembourg Institute of Health, 29, rue Henri Koch, L-4354 Esch-sur-Alzette, Luxembourg

6 Transversal Translational Medicine, Luxembourg Institute of Health, 1A-B, rue Thomas Edison, L-1445, Strassen, Luxembourg

7 Department of Dermatology and Allergy Center, Odense Research Center for Anaphylaxis (ORCA), University of Southern Denmark, Odense, 5000 C, Denmark

8 Institute of Medical Microbiology, University Hospital Essen, University of Duisburg-Essen, D-45122, Essen, Germany

* Corresponding author. Direct correspondence to feng.he@lih.lu

Abstract

Parkinson's disease (PD) is the second most common neurodegenerative disease. Neuroinflammation in the brain plays a crucial role in PD pathogenesis, however the peripheral immune system has not yet been systematically investigated. With a systems immunology approach on a well-controlled cohort of 28 early-to-mid stage PD patients aged 60-70 years and 24 matched healthy controls (HC), we analyzed more than 700 combinatorial features of lineage and functional markers in fresh peripheral blood. We found an enhanced cytotoxic immune profile in PD patients, with a higher frequency of terminally-differentiated effector CD8 T (TEMRA), differentiated $CD8^+$ natural killer T (NKT) cells and neutrophils. The cytotoxic immune portrait was accompanied by a reduced frequency of regulatory cells, including CD8 regulatory T cells (Treg) and innate lymphoid cells (ILC2). The frequency of CD8 TEMRA was negatively correlated with disease duration, suggesting that CD8 T cell responses are of a high importance in PD pathogenesis. This study revealed an imbalance of the peripheral immune system, especially CD8 T cells, in PD patients, advancing our understanding on the early involvement of peripheral immunity in the pathogenesis of PD and providing a potential early biomarker for diagnosis.

Keywords: Systems immunology; Parkinson's disease; Peripheral immune system; effector CD8 T cells; CD8 TEMRA; CD8 regulatory T cells (Treg); Cytotoxic immune cells; Group 2 Innate lymphoid cells (ILC2).

Introduction

Parkinson's disease (PD) is the second most common neurodegenerative disease after Alzheimer's disease (AD), affecting around 10 million people worldwide [349]. The pathological hallmark of PD is the accumulation of α-synuclein (α-syn) aggregates (Lewy bodies) in dopaminergic neurons, leading to cell-autonomous neuronal death and progressive neurodegeneration [350]. Meanwhile, activated microglia and neuro-inflammation in the brain of PD patients are undeniably implicated in the pathogenesis of PD [138]. The infiltration of adaptive immune cells, namely T cells, into the brain of PD patients has also been described in patient post-mortem studies [351] and animal models of PD [352]. Furthermore, PD patients are characterized by the alteration in several circulating cytokines [131, 353]. Moreover, several studies have analyzed some selected immune cell populations in the peripheral blood and found a reduction of CD4 T cells in PD patients versus healthy controls [354]. Not only total CD4 T cells, but also the frequency of specific subsets of CD4 T cells, such as Treg, Th1 or Th17 [140, 355], have shown changes in PD patients. Nevertheless, the role of different CD4 subsets demonstrated in different cohorts is still controversial [356]. These inconsistent results underline the need to further clarify these questions.

Even though most studies have identified changes in CD4 T cells of PD patients, although not necessarily consistent, recently emerging evidence strongly suggests the involvement of peripheral CD8 T cells in other neurodegenerative diseases, e.g., in Alzheimer's disease [134]. In PD, cytotoxic CD8 T cells infiltration has been reported in post-mortem brain tissues even before the α-syn aggregation and neuronal death, suggesting a potential role of CD8 T cells in initiating PD pathology [357]. Recently, α-syn-specific T cells have been reported in the peripheral blood of PD patients [358] and associated with pre-clinical and early PD [359]. Meanwhile, the cytotoxic CD8 T-cell response against mitochondrial antigens caused PD-like motor symptoms, although in a genetic-PD mouse model [135]. Genome-wide association studies have related sporadic PD with human leukocyte antigen (HLA) haplotypes [360, 361]. Furthermore, dopaminergic neurons express major histocompatibility complex class-I (MHC I) molecules, which can activate CD8 T cells and result in cytotoxicity [362]. Together, the existence of antigen-specific T cells and the association of PD with specific HLA haplotypes suggests that the process of antigen presentation and subsequent T-cell responses might be involved in the development of PD. However, it still remains unknown whether and which specific subsets of peripheral T cells and/or antigen presenting cells contribute to the pathogenesis of PD.

Although the immune system is a complex multi-cellular system [143, 363], most studies so far have only focused on the analysis of a few selected immune subsets. Consequently, it still remains elusive whether the diverse reported dysregulations of various immune cells can occur simultaneously in the same individual PD patients. To address these challenging questions aforementioned, a systematic, unbiased investigation, rather than a hypothesis-driven or specific immune cell-focused analysis, is required to delineate the composition and functional status of the peripheral immune system in PD patients. To this end, we applied a systems-immunology approach to comprehensively analyze more than 700 immune features in the peripheral immune system of early-to-mid stage PD patients and matched healthy controls (HC). By focusing on early-to-mid stage patients, we aimed to identify the peripheral immune factors that drive the initiation of the pathogenesis of PD, rather than those secondarily responding to the PD pathological events.

Results

Whole-blood CyTOF analysis shows a cytotoxic and more differentiated immune profile in early-to-mid stage PD patients

In this study, we systematically analyzed various immune subsets and their functional status in 28 PD patients (25 idiopathic PD aged 60-70 years and three genetic PD patients with mutations in GBA or PINK1) and 24 matched healthy controls (HC) (refer to "cohort design" in **Materials and Methods**, **Suppl. Table 1** and **Table 2** for more details). This was realized by analyzing 37 different innate and adaptive immune subsets and more than 700 T-cell features, using a 35-marker mass cytometry panel and 33 lineage and functional T-cell markers in five multiple-color flow-cytometry panels, respectively (**Fig. 1 A**, **Suppl. Table 3** and **4**). We selected the participants from the ongoing nation-wide Luxembourg Parkinson's study with more than 800 PD patients and 800 controls [364] and controlled for several major confounding factors, medications and comorbidities, known to affect the immune system, to ensure that our observations are PD-specific (for details, refer to **Suppl. Fig 1**, **Fig. 1A** and **Suppl. Table 1**). Furthermore, we narrowed the patient selection to those with early-to-mid stage disease (H&Y staging: mean=2.3, ranging from 1.5 to 3.0; most of them were ≤2.5, except for five participants with a score of 3) and with a disease duration of less than 10 years (except for three patients with a duration of 12, 13 or 19 years). This increases the likelihood that the observed dysregulation of the immune system is a driving factor of the pathogenesis of PD, rather than a secondary pathological response.

To get an overview on the complete peripheral immune system, we performed a mass cytometry analysis, able to distinguish up to 37 immune subpopulations, on the whole blood of PD patients and HC (for gating strategy refer to **Suppl. Fig. 2**). A principle component analysis (PCA) showed that PD patients did not have a distinct immunological fingerprint based on the entire peripheral immune system (**Fig. 1B**). Nevertheless, several immune cell types were altered in PD patients compared to HC, in particular in the T-cell compartment (**Fig. 1C**). Total αβ classical T cells were modestly reduced in PD patients (**Suppl. Fig. 3A**), reflecting a decrease of total CD4 T cells (**Suppl. Fig. 3B**), whereas the γδ T cells were unchanged among living $CD45^+$ cells (**Suppl. Fig. 3C**). The frequency among living $CD45^+$ cells could well reflect the number of cells for the given subset as we loaded the same amount of whole blood from each participant and there was no difference in the number of total living $CD45^+$ cells between PD patients and HC (**Suppl. Table 5**). The decreased frequency of total CD4 T cells among living $CD45^+$ cells was mainly due to a decrease in $CD4^+CXCR5^+$ T follicular helper cells (Tfh) (**Suppl. Fig. 3D**), $CD45RA^+CCR7^+$ naïve (**Suppl. Fig. 3E**) and $CD45RA^-CCR7^+$ central memory (CM) $CD25^-$ conventional T cells (Tconv) among total living $CD45^+$ immune cells (**Suppl. Fig. 3F**), but not $CD45RA^-$

CCR7$^-$ effector memory (EM) Tconv (**Suppl. Fig. 3G**). Although the total CD8 T cells showed no difference in PD patients (**Fig. 1D**), the CD8 naïve/memory subset composition displayed significant alterations (**Fig. 1C**). More precisely, as demonstrated by an unbiased volcano plot analysis (**Fig. 1C**), the frequency of cytotoxic terminally-differentiated effector T cells (CD45RA$^+$CCR7$^-$, TEMRA) [365, 366], was increased among total CD8 T cells in PD patients (**Fig. 1C, E**), whereas the frequency of central memory (CM) cells was reduced among total CD8 T cells (**Fig. 1F**). The proportion of naïve and EM cells showed no difference among total CD8 T cells (**Suppl. Fig. 3H, I**). Furthermore, the expression of CD57, a marker of terminal differentiation, among CD8 TEMRA showed a trend to be increased (p=0.066) in PD patients (**Fig. 1G**), further indicating a more differentiated CD8 T-cell profile. Moreover, natural killer T (NKT) cells also exhibited a more differentiated state, as reflected by an increased frequency of CD8$^+$ NKT (**Fig. 1H**) among total NKT cells [367], while the frequency of less-differentiated CD4$^+$ (**Fig. 1I**) and CD4$^-$CD8$^-$ (**Fig. 1J**) NKT cells was either decreased or intact, respectively. Similar to CD8 T cells, CD8$^+$ NKT also expressed higher levels of CD57 (**Fig. 1K**). In line with the accelerated differentiation profile, the frequency of CD56^{high}CD57$^-$ immature NK cells was also decreased among total living CD45$^+$ cells (**Fig. 1L**). As the CD8 T-cell composition was considerably changed, while total CD8 T cells were intact, we performed an unsupervised analysis on gated CD8 T cells to substantiate our supervised analysis. Indeed, a viSNE plot analysis confirmed an enhanced frequency of CD8 TEMRA (CD45RA$^+$CCR7$^-$CD27$^-$) among total CD8 T cells in PD patients versus HC (**Fig. 1M**). Both supervised and unsupervised analyses demonstrated that the frequency of CD8 TEMRA cells was elevated in early-to-mid stage PD. To sum up, we observed an enhanced overall cytotoxic and more differentiated immune profile, as reflected by the altered frequency of several relevant cell types, such as CD8 TEMRA, differentiated NKT and immature NK cells.

With the 35-marker mass cytometry analysis, we were also able to assess various subsets of granulocytes (neutrophils, eosinophils and basophils), monocytes (classical, intermediate and non-classical), dendritic cells (myeloid DC and plasmacytoid DC, known as mDC and pDC respectively), NK (immature and late), B cells (naïve, memory, plasma cells) and innate lymphoid cells (ILCs; ILC1, ILC2 and ILC3) (**Suppl. Fig. 2** and **Suppl. Table 5**). Most of them did not show any significant change in PD patients versus matched HC in terms of the frequency among total CD45+ cells or the frequency among the relevant parent gates (**Suppl. Table 5**). In line with the increased cytotoxic profile in CD8 T cells, NKT and NK cells, we observed an increased frequency of neutrophils among living CD45$^+$ cells in PD patients (**Suppl. Fig. 3J**). The enhanced frequency of neutrophils was accompanied by a reduced fraction of eosinophils (**Suppl. Fig. 3K**), while basophils were unchanged in PD

patients (**Suppl. Fig. 3L**). The reduced frequency of eosinophils is in agreement with a negative association between eosinophils and the risk of PD in a study based on routine blood counts [368]. The finding of elevated neutrophil frequency is in line with that of a recent study, where the authors only focused on the analysis of neutrophils and other whole blood count parameters [369].

Notably, the frequency of ILC2 among total living $CD45^+$ immune cells was almost decreased to half in PD patients compared to HC (**Suppl. Fig. 3M, N**), while ILC1 and ILC3 showed no difference (**Suppl. Fig. 3O, P**). These data are aligned with the observed decrease in eosinophils, as ILC2 control eosinophil homeostasis in the context of Th2 immunopathology [370]. Finally, we found a slight decrease in the frequency of IgD^+CD27^- naïve B cells among total B cells (**Suppl. Fig. 3Q**).

In short, our comprehensive whole-blood immunophenotyping analysis revealed an enhanced cytotoxic immune cell profile, with an increased frequency of terminally-differentiated effector CD8 TEMRA cells, differentiated CD8 NKT cells and neutrophils, while the frequency of immature NK cells, eosinophils and ILC2 was significantly decreased in early-to-mid stage PD patients.

Flow cytometry analysis demonstrates an increased CD8 effector profile in PD patients

After our mass cytometry analysis showed substantial alterations at the T-cell level in peripheral blood of PD patients, we further analyzed the T-cell compartments in more depth using five flow-cytometry panels with a total of 33 relevant T-cell markers, the combinations of which gave rise to ~700 features. We assessed not only phenotypical markers and the proportions of different subpopulations, but also functional markers (**Suppl. Table S4**) in the same participants. The PCA based on ~700 different combinations (variables) of various T-cell lineage and functional markers determined a distinct immunological fingerprint in PD patients compared to HC (with the exception of one PD patient and one HC participant labelled as “PD9” and “HC17” in **Fig. 2A**). The three genetic PD patients were not identified as outliers compared to idiopathic PD patients in the PCA plot based on comprehensive T-cell analysis. Similar to the CyTOF data, no difference was observed in the frequency of total CD8 T cells among peripheral blood mononuclear cells (PBMC) in PD patients versus HC (**Suppl. Fig. 4A**). Different from the CyTOF data, we did not observe any significant difference in the frequency of total T cells and total CD4 T cells between the two groups (**Suppl. Fig. 4A**). The unchanged frequency of total T cells revealed by our flow cytometry analysis might be due to the exclusion of granulocytes from the PBMCs, which account for

the majority of immune cells in whole blood and were included in the CyTOF analysis. Although the overall frequency of major T-cell populations remained unchanged in the flow cytometry analysis (**Suppl. Fig. 4A**), a PCA analysis revealed a clear T-cell fingerprint in PD patients, reflecting changes in T-cell subsets (**Fig. 2A**).

Among the most significantly changed ($p<0.05$; fold change >1.4) immune subpopulations in PD patients, we found a strong increase in the frequency of terminally-differentiated effector memory CD8 (TEMRA) among total CD8 T cells (**Fig. 2B-D**), confirming the CyTOF results. CD8 TEMRA cells express CD45RA, but lose the expression of CD45RO, CCR7 and CD27. Accordingly, we observed a clear increase in the frequency of $CD45RA^{+}CD45RO^{-}$ CD8 T cells, whereas $CD45RA^{-}CD45RO^{+}$ CD8 T cells were reduced in PD patients compared to HCs (**Fig. 2C**). By analyzing the expression of CCR7 in combination with CD45RA and CD45RO, we were able to better differentiate the CD8 subpopulations and pinpointed that the increased $CD45RA^{+}$ T cell population in PD patients were CD8 $CD45RA^{+}CD45RO^{-}CCR7^{-}$ cells (the simplified gating strategy for CD8 TEMRA) (**Fig 2D**). To more precisely identify CD8 TEMRA cells, we also included CD27 to more strictly define different naïve/memory/effector subsets in the CD8 T-cell compartment (**Suppl. Fig. 4B**). In line with the previous gating strategy (**Fig. 2D**), the frequency of $CD45RO^{-}CCR7^{-}CD27^{-}$ CD8 T cells was also increased in PD patients (**Suppl. Fig. 4C**). Based on the small fraction of CD45RA/CD45RO double-negative (mean: ~5%) or double-positive (mean: ~5%) cells among CD8 T cells (**Suppl. Fig. 4B**), most of the $CD45RO^{-}CCR7^{-}CD27^{-}$ effector CD8 T cells should be $CD45RA^{+}$ CD8 TEMRA. This confirmed again the increased frequency of CD8 TEMRA cells regardless of the gating strategy (from different staining panels, refer to Materials and Methods) that was employed. Meanwhile, CM ($CD45RO^{+}CCR7^{+}CD27^{+}$) and transitional memory (TM) ($CD45RO^{+}CCR7^{-}CD27^{+}$) CD8 T cells were reduced (**Suppl. Fig. 4D, E**), while naïve ($CD45RO^{-}CCR7^{+}CD27^{+}$) CD8 T cells showed no difference between PD patients and HC (**Suppl. Fig. 4F**). The reduction in CD8 CM and TM cells was in line with a lower frequency of long-lived memory ($KLRG1^{-}CD127^{+}$) [371] CD8 T cells (**Suppl. Fig. 4G**) and consistent with the CyTOF results (**Fig. 1F**). In short, we found that CD8 TEMRA cells were increased among early-to-mid stage PD patients versus HC by utilizing various gating strategies and both state-of-the-art flow- mass cytometry approaches.

T-bet is an essential marker for effector CD8 T-cell functions [372, 373] and its expression is positively correlated with GZMB expression in humans infected with cytomegalovirus (CMV) [374]. In line with the notion of the increased effector profile, CD8 T cells from PD patients compared to HC also displayed a higher frequency of $T\text{-}bet^{high}$ and $CD45RO^{-}T\text{-}bet^{+}$ CD8 T cells (**Fig.2 E-F**). It is worthy to note that the $T\text{-}bet^{+}$ or $T\text{-}bet^{high}$ cells were mainly

CD45RO negative, but not CD45RO positive cells, indicating that those cells were mostly $CD45RA^+$ terminally-differentiated CD8 T cells, based on the largely mutually exclusive relationship between CD45RA and CD45RO expression (**Suppl. Fig. 4B**). The increased CD8 effector function was further consolidated by increased proliferation and activation levels among $CD45RO^-$ CD8 T cells, as assessed by the expression of Ki67 (**Fig. 2G**) and Helios [375] (**Fig. 2 H**), respectively. The increase of $CD45RO^-CD57^+$ (**Fig. 2I**) and $CD57^+$ (**Suppl. Fig. 4H**) among CD8 T cells further suggested the enhanced terminal differentiation state of CD8 T cells in PD patients, as the expression of CD57 increases during the CD8 differentiation stages [376]. Interestingly, the frequency of $CD45RO^-CCR7^-CD27^-$ CD8 TEMRA cells in PD patients showed a significantly-negative correlation with disease duration from the onset of initial symptoms (**Fig. 2J**) and also a trend to be negatively correlated with the disease duration after doctor's diagnosis (p=0.054, **Fig. 2K**). This suggests that CD8 TEMRA populations are a driver of PD, rather than a consequence of PD-associated neuropathology. In parallel, we performed the receiver operating characteristic (ROC) analysis to evaluate the potential of CD8 TEMRA cells as a cellular diagnosis biomarker of PD. Interestingly, early-to-mid stage PD patients could be distinguished from HC with an area under the curve (AUC) of 0.7731, based on CD8 TEMRA frequency alone (**Fig. 2L**). As the frequency of CD8 TEMRA cells negatively correlated with disease duration, we performed another ROC analysis focusing on patients diagnosed within 5 years. Notably, a much higher AUC of 0.8663 (sensitivity of 100% and specificity of 70.83% at the cut-off of 40.3% for CD8 TEMRA percentages among CD8) was obtained based on the CD8 TEMRA frequency of those diagnosed only within 5 years (**Fig. 2M**). These data indicate that CD8 TEMRA cells could be used as a valuable diagnostic cellular biomarker of PD, especially at an early stage of the disease.

Prolonged T cell activation and effector functions lead to T cell exhaustion, causing them to progressively become dysfunctional [377, 378]. Considering a more dominant effector CD8 T-cell profile in PD patients, we wondered whether those cells were exhausted by assessing the expression of established T-cell exhaustion markers. CD8 T cells from PD patients showed no sign of exhaustion, based on the expression of PD-1, CTLA4 and LAG3 (**Suppl. Fig. 4I-K**). During the aging process, both exhaustion- and senescence-related markers increase [379, 380]. Hence, we also analyzed immunosenescence markers. Similar to the exhaustion status, the CD8 T cell senescence marker KLRG1 was unchanged between PD patients and HCs (**Suppl. Fig. 4L**). Interestingly, ICOS was significantly decreased in CD8 T cells of PD patients (**Suppl. Fig. 4M**). However, this decline might only reflect the observed decrease in the frequency of CD8 CM cells (**Suppl. Fig. 4D**), as ICOS expression was only reduced in $CD45RO^+$, but not in $CD45RO^-$ CD8 T cells (**Suppl. Fig. 4N**). We also

observed a decreased expression of the amino acid transporter CD98 (**Suppl. Fig. 4O**), which was similarly expressed within $CD45RO^+$ and $CD45RO^-$ cells (**Suppl. Fig. 4P**). Together, these observations support the idea that CD8 T cells in early-to-mid stage PD patients exhibit a terminally-differentiated, but non-exhausted, effector profile.

Effector CD8 T cells tend to migrate to non-lymphoid tissues where an active immune response takes place [381, 382]. Therefore, we also assessed the expression of several relevant chemokine receptors, such as CXCR3, CCR4 and CCR6, to analyze the migratory potential of peripheral CD8 T cells in PD patients. In the blood of PD patients, we observed a lower frequency and expression levels (geometric mean, MFI) of CXCR3 and CCR4 among total CD8 T cells, whereas CCR6 showed no difference (**Suppl. Fig 5A, B**). The decrease in CXCR3 and CCR4 expression is most likely related to the observed decrease in the frequency of CM among total CD8 T cells (**Suppl. Fig. 4D**), since among all the four subsets, CD8 CM cells displayed the highest expression levels of these two chemokine receptors (**Suppl. Fig. 5C**). In addition to the decrease of individual chemokine receptors, the frequency of CCR4 and CCR6 co-expressing cells was also decreased (**Suppl. Fig 5D**), although the overall frequency expressing both receptors was sparse among total CD8 T cells (on average <1%). Accordingly, the frequency of cells lacking all three tested chemokine receptors (CXCR3, CCR4 and CCR6) was increased among total CD8 T cells in PD patients versus HCs (**Suppl. Fig 5D**). In short, the expression of the analyzed chemokine receptors did not show a clear alteration among CD8 TEMRA cells in PD patients.

We further asked whether the CD8 TEMRA cells express one of the major homing receptors to allow them to properly migrate to the central nervous system (CNS). Since integrin alpha 4 (also known as CD49d) is the major brain homing factor of peripheral CD8 T cells controlling trafficking of CD8 T cells into the CNS [383, 384], we particularly analyzed CD49d expression in CD8 T cells. However, we did not find any difference in CD49d expression between PD patients and HC among various subsets of CD8 T cells, including CD8 TEMRA (**Suppl. Fig. 5E**). In short, the unchanged expression levels of the analyzed chemokine receptors and brain homing factor among CD8 TEMRA cells indicate that CD8 TEMRA have an intact potential to migrate into the CNS.

In contrast to the CD8 T cells, the composition of various CD4 naïve/memory subsets displayed little change in PD patients compared to HCs (**Suppl. Fig. 6A**). While naïve CD4 cells displayed no difference in the flow cytometry data, CM CD4 T cells were slightly, but significantly decreased (**Suppl. Fig. 6B, C**). Moreover, intermediate CD4 ($CCR7^-$ $CD27^+CD45RO^-$) T cells were increased in PD patients (**Suppl. Fig. 6D**). Unlike CD8 T cells, the frequency of effector and TEMRA CD4 cells among total CD4 T cells remained

unchanged in PD patients (**Suppl. Fig. 6E, F**). In short, CD8, but not CD4 T cells in PD patients favored a terminally-differentiated effector cell program over the generation of a long-lived CD8 central memory T-cell profile.

The combination of the chemokine receptors, such as CXCR3, CCR4 and CCR6 can be also used to distinguish the CD4 T helper cell lineages Th1, Th2 and Th17 (refer to the gating strategy in **Suppl. Fig. 7A**). By applying this analysis and also assessing the expression of the CD4 Th master transcription factors T-bet, GATA3 and RORγT, we observed neither a significant change in the frequency of Th1, Th2 or Th17 cells nor in the ratios of Th subsets in PD patients versus HC (**Suppl. Fig. 7B-E**).

Together, our deep immunophenotyping analysis focusing on peripheral T cells firmly suggests that early-to-mid stage PD patients display a profile of functional, non-exhausted and terminally-differentiated effector CD8 T cells.

PD patients display a reduced CD8 Treg frequency

Regulatory T cells (Treg) play an important role in suppressing effector T-cell responses to avoid an overshooting immune response that could harm the surrounding host tissues [385-387]. Treg have been found to be dysfunctional or reduced in numbers in multiple autoimmune diseases. Furthermore, previous studies have found a reduced frequency of CD4 Treg and/or a reduced suppressive capability of Treg in PD and other neurodegenerative diseases [137, 355, 388]. In the light of these studies and having observed an increased frequency of functional CD8 TEMRA cells in our study, we speculated that CD4 and/or CD8 Treg might also be affected in terms of numbers or functional status in the PD patients of our cohort. Through our flow cytometry analysis based on fresh PBMCs, we did not observe any change in the frequency of $CD4^+FOXP3^+$ Treg (**Suppl. Fig. 4A**). However, we found that the frequency of $CD8^+FOXP3^+$ Treg was reduced in PD patients (**Fig. 4A, B**), which are also able suppress the responses of other immune cells, including CD8 cells [reviewed here [389-391]]. In line with our observation on reduced $FOXP3^+$CD8 Treg, we found that the expression of other markers related to CD8 Treg, such as CD25 (IL2RA) and CD122 (IL2RB) [392], was also reduced in CD8 T cells of PD patients compared to HC (**Fig. 3A**). Notably, the ratio between CD8 TEMRA and CD8 Treg was significantly increased in PD patients versus HC, with a mean of 68.58 in PD patients versus 30.37 in HC, further highlighting an effector-biased CD8 T-cell compartment (**Fig. 3C**). Although the frequency of $FOXP3^+$CD4 Treg was unchanged in our analysis between PD patients and HC, this data alone cannot exclude the possibility of a compromised suppressive function of CD4 Treg in PD patients. Therefore, we also analyzed the

expression of several functional markers, such as CD45RO and phospho S6 [reflecting mTORC1 activity [393]]. Interestingly, the expression levels of both CD45RO and pS6 were decreased among CD4 Treg in PD patients (**Fig. 3 D**). At the same time, the glucose transporter 1 (GLUT1), which has been shown to be dispensable for CD4 Treg suppressor function at least in mice [394], was also decreased among CD4 Treg in PD patients (**Fig. 3E**). Despite the reduction in those markers, the expression of FOXP3 and CTLA4, which are decisive for maintaining Treg suppressor function [387], remained unchanged among CD4 Treg (**Fig. 3F**). These data indicate that it is mainly CD8 Treg cellularity that was impaired in early-to-mid PD patients, whereas the CD4 Treg frequency and suppressive capacity was likely not changed in our cohort of PD patients.

Discussion

In this study, we were able to systematically characterize the peripheral immune system of a well-controlled cohort of PD patients and matched healthy controls. We revealed a cytotoxic and more differentiated immune profile, as reflected by a pronounced terminally-differentiated and functional effector CD8 T-cell profile, enhanced $CD8^+$ NKT cells and neutrophils in the blood of early-to-mid stage PD patients. This was accompanied by a reduced frequency of cells with a regulatory function, such as CD8 Treg and ILC2. Furthermore, the frequency of terminally-differentiated CD8 T cells was negatively correlated with disease duration, firmly suggesting a causative pathogenic role of CD8 T subsets in initiating PD.

In the early 2000's, it has been postulated that PD pathology might arise in the periphery and migrate to the central nervous system via the vagus nerve [395]. More recently, Kipnis and colleagues lifted the misconception around the immune privilege in the brain [42], making the peripheral immune system a potential candidate for the culprit of neurodegenerative diseases. Here we showed that early-to-mid stage PD patients displayed a highly-functional peripheral effector profile, with abundant terminally-differentiated effector memory CD8 T cells. By narrowing down our analysis to PD patients with an early-to-mid stage of the disease, our results indicate that abundant cytotoxic CD8 T cells are most likely a cause, rather than a consequence of PD pathology. Those cytotoxic CD8 T cells did not display any impairment in the expression of major chemokine receptors and brain homing factors in PD patients, indicating that they have a normal trafficking function to reach and cross the brain-blood barriers. This was further reinforced by a negative correlation of CD8 TEMRA frequency with the disease duration from the onset of initial symptoms or diagnosis. Such a negative correlation would suggest that possible immunotherapeutic approaches targeting CD8 TEMRA cells would only be feasible within an early window of opportunity. In support of our observations, CD8 T cells have been found to infiltrate into the CNS, prior to the onset of α-syn neuropathology and their density correlated with neuronal cell death, although in post-mortem brain tissues of PD patients [357]. Meanwhile, mitochondrial antigen-specific CD8 T cells with an autoimmune nature play a pivotal role in the degeneration of dopaminergic neurons in a genetic murine model [135]. Together with these reports, our data strongly supports the notion that the peripheral immune system, especially CD8 TEMRA cells, might contribute to PD pathogenesis and suggests that CD8 TERMA could serve as a potent easily-accessible target to treat or prevent the progression of PD. In addition, peripheral CD8 TEMRA alone might be a valuable early cellular biomarker for diagnosis, as indicated by an AUC value as high as 0.87 when only analyzing patients diagnosed within 5 years.

Our work suggests that abundant CD8 TEMRA cells contribute to the initiation of PD. In the meantime, the elevated effector profile of CD8 T cells and NKT cells in PD patients observed in our cohort might also explain why PD patients are better protected against some cancers [396]. Furthermore, an increased number of NK cells, another type of immune cells specialized in killing tumor cells, has been reported in PD patients through a meta-analysis [354], further indicating that the general immune status of PD patients is primed towards cellular immunity. In line with this and our observation regarding CD8 T cells and NKT cells, a reduced frequency of $CD56^{high}CD57^{-}$ immature NK cells among living $CD45^{+}$ cells was also observed, indicative of a more differentiated stage of NK cells in PD patients. The cytotoxic immune profile was further supported by our observation on the enhanced frequency of neutrophils.

While our PD patients displayed a generally cytotoxic immune profile, we also observed a reduced frequency of several cell types known to have regulatory functions. For instance, the CD8 Treg frequency in our PD patient cohort was substantially decreased. Previous studies have reported reduced CD4 Treg numbers or a decreased suppressive capability of CD4 Treg in PD patients [355, 388, 397]. However, this is the first evidence showing a reduced frequency of CD8 Treg in PD. Not only CD4 Treg are crucial mediators of immunity with the ability to suppress effector T cell responses to avoid an overshooting immune response and potential tissue damage [385], but also CD8 Treg play an essential role in suppressing CD8 responses and effector functions of other immune cells [392, 398, 399]. This suggests that a reduced frequency of CD8 Treg might fail to properly control the expansion or differentiation balance of terminally-differentiated CD8 T cells, leading to an increased cytotoxic effector CD8 profile, which might thus contribute to the pathogenesis of PD. It is also worthy to notice that the ILC2 frequency showed the strongest decrease in PD patients. Furthermore, IL-10-producing ILC2 play a critical regulatory role in the induction of immune tolerance [400], suggesting the reduced frequency of peripheral ILC2 in our cohort contribute to the over-shooting CD8 TEMRA responses in PD patients. ILC2 also produce type 2 cytokines such as IL-5 and IL-13 [401, 402], which in turn promote an anti-inflammatory M2-like polarization of brain-resident microglia. In line with this, infiltration of ILC2 into choroid plexus in an animal model of Alzheimer disease enhanced the cognitive function in aged mice [403]. Therefore, the reduced frequency of circulating ILC2, in synergy with the decreased frequency of CD8 Treg in early-to-mid stage PD might contribute to the pathogenesis of PD. Nonetheless, the relationship between peripheral and CNS-residing ILC2 in PD patients still requires further investigation, although ILC2 are the most prevalent ILC subset within the adult mouse CNS [404].

One recent single-cell RNA-seq and TCR repertoire analysis has reported enriched terminal effector CD8 T cells in PD patients, but only analyzed a small number of eight to nine patients [136]. That study has provided information neither on the disease stage nor on other relevant clinical metadata, making a direct comparison of those results with ours difficult. Opposite to our study and that single-cell RNA-seq work, another study showed a reduced frequency of $CD57^+$ CD8 T and CD8 TEMRA cells in the peripheral blood of PD patients, proposing a reduced phenotype of T-cell senescence in PD patients [405]. However, similar to ours, the authors did not observe any major changes within CD4 T cells. The differences between their observations and ours might be attributable to very different inclusion/exclusion criteria of the cohorts. In their study, they included patients aged between 55 and 80 years old, while we focused on a strictly-controlled and homogeneous group of patients and healthy controls, covering a more narrow age range (60-70 years old for idiopathic patients). One cannot underestimate the impact of a broader age range on the immunological observations, since aging has a substantial impact on the immune system [406, 407]. Furthermore, we controlled for the CMV-related immune status of all included participants in our analysis, as CMV is known to drive the immune ageing process [408]. Additionally, we excluded PD patients and HC with cancer as potential participants, which was not specified in that study, as local responses in the tumor microenvironments and peripheral immune disturbances are common in cancer patients [409]. These three important factors might already explain the seemingly-contradictory observations between our study and theirs.

Our work provides the first comprehensive resource on the compositions of the entire complexity of peripheral immune cell subsets and their functional status in early-to-mid stage PD patients. Although our immunological analysis was only applied to a homogenous group of 28 PD patients and 24 age-matched healthy controls, we started our selection from >800 PD patients and >800 controls from an ongoing nation-wide cohort. Furthermore, the final number of included participants for deep immunophenotyping is comparable to other high-standard resource studies in the immunological field [134]. Considering that a systematic immune profiling was even rarely performed in general healthy controls at such an advanced age, our data in healthy controls could also serve as immunological references for various age-related diseases. In short, our study discovers dominant circulating cytotoxic and differentiated immune subsets, accompanied with a reduction in regulatory or tolerance-inducing cell types in early-to-mid stage PD. This indicates that those altered peripheral immune cells we reported here could be prime candidates for novel easily-accessible immunotherapeutic options in order to control or halt the pathogenesis of PD.

Limitations of the study

Our data strongly suggests an imbalanced differentiation stage of several types of immune cells in early-to-mid stage PD. However, in this clinical study, we did not have opportunity to investigate the underlying cellular and molecular mechanism causing the cytotoxic and differentiated immune profile in PD patients. We have previously described that the deficiency of a key familial PD gene PARK7/DJ-1 reduced CD8 T-cell immunoaging in both mice and patients via regulating the immunometabolic process [410]. The accelerated differentiation in several immune subsets we observed here might also be attributable to an immunometabolic dysregulation. Supporting this notion, mitochondrial deficiency has been indeed widely reported in both sporadic and genetic PD patients [411-413].

In our study, we did not investigate the antigen-specificity or clonotypes of the T cells and are therefore unable to judge whether the effector CD8 T cells in PD patients are specific against PD-relevant antigens or developed unspecifically due to the lack of sufficient CD8 Treg to control the expansion or differentiation. Therefore, future studies are required to determine whether the enhanced peripheral CD8 TEMRA cells are antigen-specific for a PD-relevant antigen and if yes, to characterize those antigens. In support of our data, a very recent study revealed highly differentiated and expanded CD8 T cells sharing the same clonotypes in the periphery and cerebrospinal fluid (CSF) of a small number of PD patients, although the blood samples and CSF samples were taken from two different cohorts [136]. Despite the caveats of a preliminary study (e.g., a single-digit number of samples), that work still indicates that the peripheral terminally-differentiated effector CD8 T cells migrate to the CNS. A large-scale or multi-center cohort with the same stringent inclusion and exclusion criteria as we applied here, simultaneously assessing the peripheral blood and the CSF, is required to obtain more reliable conclusions.

Materials & Methods

Cohort design

We followed the ethic regulation of Luxembourg and obtained ethic approval from Luxembourg National Research Ethics Committee (CNER) [364]. Informed consent was obtained before each participant was recruited into the study by the clinical team. All study participants were recruited from the Luxembourg Parkinson's Study, a nation-wide, monocentric, observational longitudinal study with parallel healthy controls. The overall steps of selection are provided in **Suppl. Fig. 1**. As a first step, we screened for healthy controls (HC) and idiopathic PD patients aged 60-70 years (except the 3 genetic patients: one PD patient with two rare variants, one pathogenic homozygote variant N409S in GBA and another non-pathogenic heterozygote rare variant in PINK1 A383T, aged 48 years; one PD case with non-pathogenic heterozygote variant K13R in GBA, aged 55 years; one PD patient with the homozygote pathogenic variant L369P in PINK1, aged 45 years). We narrowed the selection to early-to-mid stage PD patients having a mean disease duration of 6.6 years after diagnosis. Since aging is the primary risk factor for PD [414] and aging dramatically affects the immune system [415], we focused on a relatively narrow age window (60-70 years) in the PD and the corresponding HC group. We also excluded potential participants if they were diagnosed with any immune-associated diseases, such as diabetes, cancer, chronic inflammatory disease, autoimmune disease and acute infection or if they were currently treated with immunosuppressive medication (see **Suppl. Table 1** for detailed overview of the exclusion criteria). After the first round of exclusion, 150 PD patients and 58 HC were further tested for their cytomegalovirus (CMV) serologic status. CMV has been well documented to facilitate the immunosenescence process [416]. In order to make the immunological analysis comparable at such an advanced age, we only invited HC subjects and PD patients as participants for deep immune phenotyping analysis if they were seropositive for anti-CMV IgG. As a result, a total of 28 PD and 24 HC CMV positive individuals agreed to be included in this study requiring additional blood sampling (see **Suppl. Table 2** for details on demographic and clinical information). To account for the circadian rhythm of immune cells trafficking throughout the body [298], all blood samples of the participants were collected in the mornings and processed within six hours.

Detection of αnti-CMV IgG

CMV infection is widely spread throughout the population and seropositivity correlates positively with age [417]. Previous reports have shown that CMV infection promotes immune ageing [416]. To exclude a potential bias in our analysis due to a differential CMV

status in PD patient and HCs, we measured the CMV serology of all the potential study participants (including HCs) fitting the inclusion and exclusion criteria and only selected participants who were seropositive for CMV. An ELISA was performed on plasma samples from previous visits that were preserved in the local biobank (Integrated Biobank of Luxembourg). We used the Human Anti-Cytomegalovirus IgG ELISA Kit (Abcam, ab108724) and followed the manufacturer's instructions.

CyTOF staining and analysis

Fresh whole blood was first incubated with Human TruStain FcX™ (FcX, CAT#:422302, Biolegend) for 10 min at RT. Surface staining was performed by transferring the blood into the Maxpar® Direct Immune Profiling Assay (MDIPA, CAT#:201325, Fluidigm) tube containing a dry antibody pellet. To the antibody-blood mixture, we added 4 in-house-conjugated and 2 pre-conjugated antibodies (**Suppl. Table 3**). The 4 in-house-conjugated antibodies were labeled with Maxpar® X8 Antibody Labeling Kit (201142A, 201159A, 201162A or 201169A, Fluidigm). Incubation lasted for 30 min at room temperature. Immediately after staining was completed, Cal-lyse solution (CAT#:GAS010, Thermo Fisher Scientific) was added to each tube for a 10 min incubation in the dark; then 3mL of deionized water were added for another 10 min incubation in the dark. Cells were washed twice with MaxPar Cell Staining Buffer (CSB, CAT#: 201068, Fluidigm) (400 x g, RT, 10 minutes). Cells were then fixed with 1.6% of formaldehyde solution (Pierce 16% Formaldehyde, CAT#:289006, Thermo Fisher Scientific). Centrifugation conditions after fixation were 800 x g, for 10 min at 4 ˚C. As a last step, samples were incubated with Ir-Intercalator (CAT#:201192A, Fluidigm), diluted (1:2000) in MaxPar Fix&Perm (CAT#:201067, Fluidigm), and rested at RT for 1 h. Then, the cells were stored at -80 ºC until the day of CyTOF acquisition. Prior to the acquisition, cells were washed 2 times with CSB and 2 times with Cell Acquisition Solution (CAS, CAT#: 201239, Fluidigm). Cells were resuspended at 5E5 per mL in 1:10 calibration beads (EQ Four Element Calibration Beads, CAT#: 201078, Fluidigm) diluted with CAS and the samples were analyzed with a Helios mass cytometer (Fluidigm) at a flow rate of 0.030 mL per min. Generated *.fcs files were normalized with the HELIOS acquisition software by using EQ beads as a standard. Of note, due to notable staining issues, we excluded CD25, CD16 and CD127 from the analysis. As a consequence, we were unable to analyze Tregs in our CyTOF panel (refer to **Suppl. Fig. 2**). Alternatively, for non-classic monocyte and ILC gating, we used CD38 instead of CD16 [418]. For NK subset gating, we used CD56 and CD57 to distinguish immature, mature and terminally-differentiated NK subset [419].

We first performed the supervised analysis based on manual gating (refer to **Suppl. Fig. 2**). The CD8+ T cells of 50 samples (23 HCs, 27 PDs; one HC sample was excluded due to a too low number of acquired cells; one PD sample was excluded due to the fact that a wrong CyTOF staining panel was used) were extracted using FlowJo v10 to perform the viSNE analysis on the CellEngine (https://cellengine.com/). The viSNE analysis was achieved using all the cells from each fcs file, with 1000 iterations and a perplexity of 80. The following markers were used to generate the viSNE: CD45RA/CCR7/CD27/CD57/CD38/HLADR. Of note, except for the results presented in **Fig. 1M**, all the other results were based on supervised analysis.

PBMC isolation

For detailed method description, please refer to our recent work [420]. In brief, 10-ml vacutainer K2EDTA blood collection tubes (367525, BD Biosciences) was used to sample blood from each participant in the morning. Peripheral blood mononuclear cells (PBMCs) were isolated from fresh whole blood by gradient centrifugation at 1200 x g for 20 min (room temperature, RT) using the SepMate™-50 tubes (85450, Stemcell) and Lymphoprep™ (07801, StemCell). The cells were washed three times with FCM (flow cytometry) buffer ($Ca2^+$ free PBS + 2% heat-inactivated FBS) and counted with a CASY cell counter.

Multi-color flow cytometry analysis

For each study participant, 1 million of fresh PBMCs were stained for each of the 5 staining panels. Prior to the cell staining, the PBMCs were incubated for 15 min at 4°C with 50 µL Brilliant Stain Buffer (BD, 563794), containing 2.5 µL Fc blocking antibodies (BD, 564765). 50 µL of 2x concentrated antibody master mixes diluted in Brilliant Stain Buffer were added to the cell suspension and incubated for 30 min at 4 °C to stain cell surface markers (**Suppl. Table 4**). Following three washing steps with FCM buffer (300 x g, 5 min, 4 °C), the stained PBMCs were fixed for 60 min at RT using the fixation reagent of the True-Nuclear Transcription Factor Buffer Set (Biolegend, 424401). After the fixation, the cells were centrifuged (400 x g, 5 min, 4 °C), re-suspended in 200 µL FCM buffer and left at 4°C overnight. The next day, the PBMCs were washed once in permeabilization buffer of the same kit and re-suspended in permeabilization buffer, containing 2.5 µL Fc blocking antibodies. After a 10 min incubation the cells were centrifuged and the cell pellet re-suspended in 100 µL permeabilization buffer containing the antibodies for the intracellular targets for a 30-40 min incubation at RT. Finally, the cells were washed three times in permeabilization buffer and re-suspended in 100 µL of FCM buffer for the acquisition on a BD LSRFortessa™. The data was analyzed using the *FlowJo* v10 software. Of note, with

our hypothesis-free approach, we could not foresee the CD8 TEMRA results. We never used CD45RA, CCR7 and CD27 in the same panel and this is why we had to demonstrate the CD8 TEMRA results combining different gating strategies from different panels.

Statistical analysis

Statistics analysis was performed in GraphPad prism 9.0 using an unpaired two-tailed Student *t* test. ROC analysis, volcano plot and PCA analysis were also performed using GraphPad Prism v9.0. The test used for the different figures is also specified in the corresponding figure legends. The error bars in the related types of figures represent the standard deviation (s.d.).

Acknowledgements

We would first like to show our gratitude to all the participants of the Luxembourg Parkinson's Study cohort for their participation in the study. We thank the recruitment team and study nurses of the Clinical and Epidemiological Investigation Centre of LIH for their excellent support, especially Daniela Valoura Esteves for the coordination of the recruitment of healthy controls. We also highly appreciate the expert support of the processing and biorepository teams at the Integrated Biobank of Luxembourg (IBBL). This study was mainly supported by the Luxembourg Personalized Medicine Consortium (PMC) (CoPImmunoPD, PMC/2018/01, F.Q.H.). F.Q.H. was partially supported by FNR CORE programme grant (CORE/14/BM/8231540/GeDES), FNR AFR-RIKEN bilateral programme (TregBAR, 11228353, F.Q.H. and M.O.) and PRIDE programme grants (PRIDE/11012546/NEXTIMMUNE and PRIDE/10907093/CRITICS). The Luxembourg Parkinson's study is funded within the National Centre of Excellence in Research on Parkinson's disease (NCER-PD) by the Luxembourg National Research Fund (FNR). The work of R.K. was supported by an Excellence Grant in Research within the PEARL programme of the FNR. Some icons in Fig. 1A were generated from BioRender.com.

Author contributions

C.C. contributed to the design of the study, performed the experiments, performed data analysis and drafted the manuscript. S.C., F.H., M.K., D.R., V.T., A.B. and N.Z. performed experiments. M.H., L.P. and R.K. participated in study design and coordinated the patient cohort recruitment and collection of the biological samples and clinical data. P.M. contributed to genetic PD confirmation and selection. A.C., R.B., R.K., and M.O. provided substantial insights and supervision to the project. M.O. and F.Q.H. conceived the project. F. Q. H. oversaw the whole project and revised the manuscript.

Conflict of Interest

The authors declare no conflict of interest.

Figures

Figure 1: CyTOF analysis shows a cytotoxic and late-differentiated immune profile in PD patients

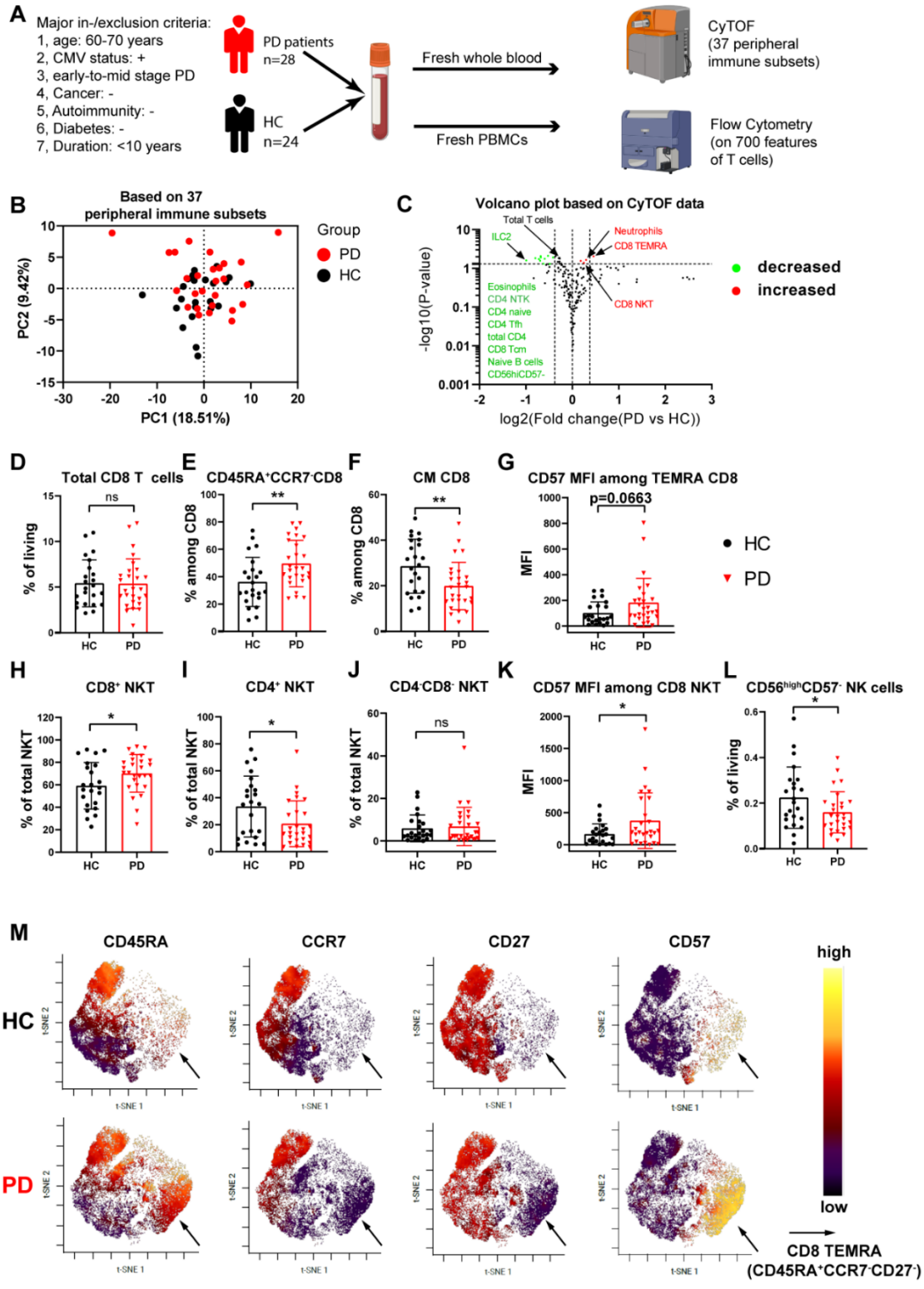

Figure 1: CyTOF analysis shows a cytotoxic and late-differentiated immune profile in PD patients.

(**A**) Graphical representation describing the cohort and the experimental setup. For more details about cohort design, please refer to **Suppl. Fig.1 and Suppl. Table 1**. (**B**) PCA plot showing no distinct immunological fingerprint based on the entire peripheral immune system analysed by CyTOF. (**C**) Volcano plot showing the most significantly ($p<0.05$, fold change >1.3) decreased (green) and increased (red) immune cell populations in PD patients compared to HC. The dashed line in the y axis corresponds to the value of 1.3 ($p=0.05$), while the two dashed lines in the x axis correspond to the value of -0.3785 or 0.3785 (a change fold of 1.3). (**D-G**) Scatter dot plots showing the frequency of total CD8 T cells among living $CD45^+$ singlets (**D**), CD8 $CD45RA^+CCR7^-$ (the simplified gating strategy for TEMRA) (**E**), CD8 central memory (**F**) and CD57 geometric mean (MFI, **G**) among CD8 TEMRA. (**H-L**) Scatter dot plots showing the frequency of $CD8^+$ NKT (**H**), $CD4^+$ NKT cells (**I**) and CD4/CD8 double negative (DN) NKT (**J**) and CD57 geometric mean (MFI) (**K**) among total NKT. (**L**), the frequency of $CD56^{high}CD57^-$ immature NK cells among living CD45+ cells. (**M**) Representative viSNE plot of one donor from either HC (upper panel) or PD (lower panel) highlighting the expression levels of CD45RA, CCR7, CD27 and CD57 in total CD8 T cells. The arrow indicates the CD8 $CD45RA^+CCR7^-CD27^-$ (TEMRA) cells. The results in (**D-L**) were analysed using an unpaired two-tailed Student *t* test. Data are presented as mean of the given group ± standard deviation (s.d.). Each symbol represents the measurement from one individual participant (**D-L**). As we explained in the text, the frequency among total living $CD45^+$ singlets reflect the number of cells for the given immune subset. ns or unlabelled, not significant; *p<=0.05, **p<=0.01, and ***p<=0.001. CyTOF, mass cytometry; CMV, cytomegalovirus; PBMC, peripheral blood mononuclear cells; HC, healthy controls; PD, Parkinson's disease.

Figure 2: Flow cytometry analysis demonstrates an increased effector CD8 T-cell profile in PD patients

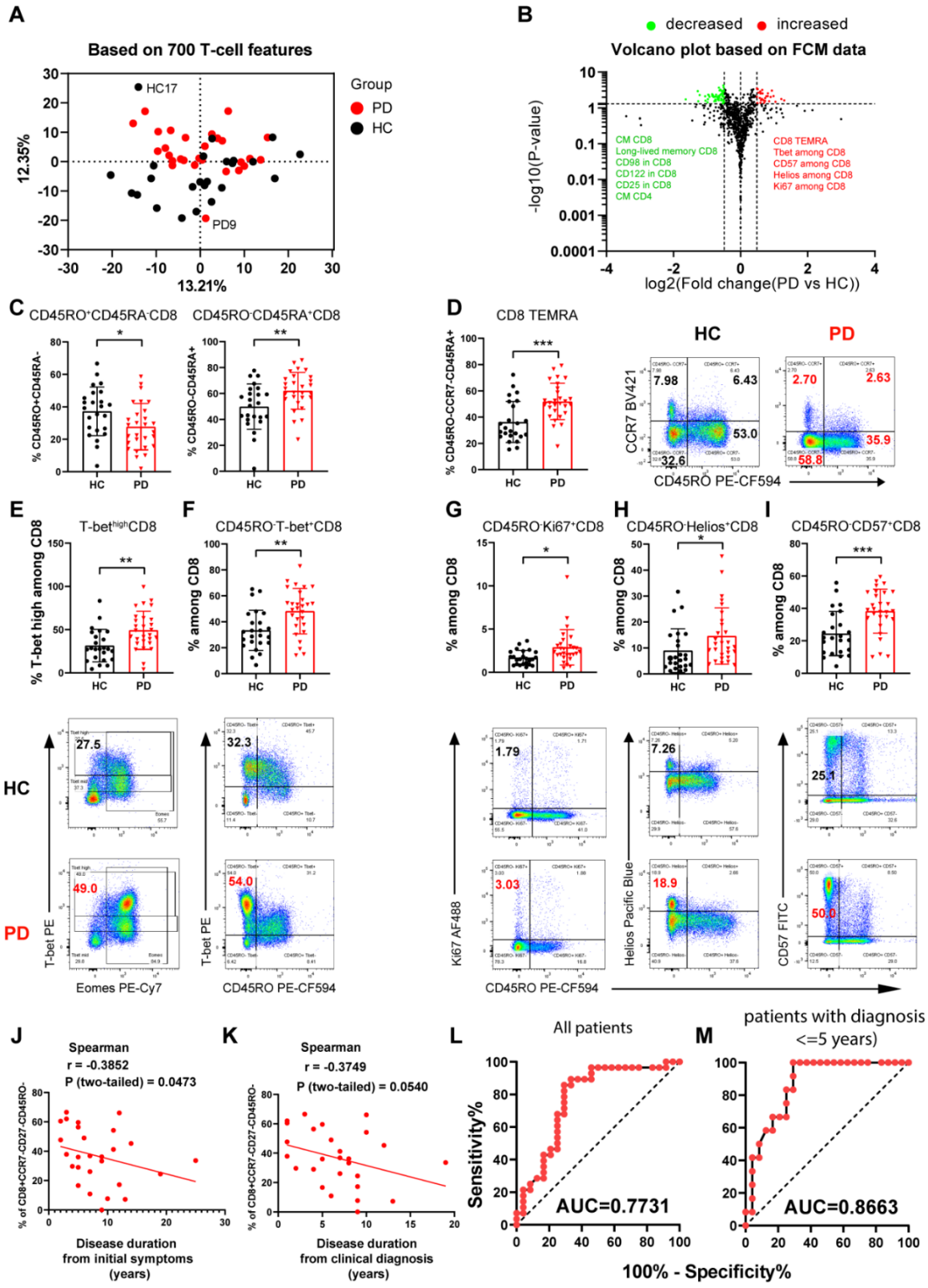

Figure 2: Flow cytometry analysis demonstrates an increased effector CD8 T-cell profile in PD patients

(**A**) PCA plot showing a distinct immunological fingerprint based on T-cell features. (**B**) Volcano plot showing the most significantly ($p<0.05$, fold change >1.4) decreased (green) and increased (red) - cell subpopulations in PD patients compared to HCs. CM, central memory. The dashed line in the y axis corresponds to the value of 1.3 ($p=0.05$), while the two dashed lines in x axis correspond to the value of -0.485 or 0.485 (a change fold of 1.4). (**C**) Scatter dot plots showing the frequency of $CD45RO^{+}CD45RA^{-}$ and $CD45RO^{-}CD45RA^{+}$ CD8 T cells in PD patients and HC. (**D**) Scatter dot plots (left) and representative flow cytometry plots (right) showing the increase in CD8 TEMRA ($CD45O^{-}CD45RA^{+}CCR7^{-}$, the simplified gating strategy for TEMRA without considering CD27) in PD patients. The combination of markers used to define TEMRA was described in the title of y axis. (**E-I**) Scatter dot plots (upper panel) and representative flow-cytometry plots (lower panel) showing the frequency of T-bet^{high} (**E**), $CD45RO^{-}$T-bet^{+} (**F**), $CD45RO^{-}Ki67^{+}$ (**G**), $CD45RO^{-}$ $Helios^{+}$ CD8 T cells (**H**) and CD45RO-CD57+ (**I**) in PD patients and HC. (**J, K**) Graphs showing the correlation between the frequency of CD8 TEMRA among total CD8 T cells and the disease duration from the onset of initial symptoms (**J**) or from the diagnosis (**K**). Correlation coefficient and P-value were calculated based on Spearman correlation. (**L, M**) ROC analysis based on the frequency of $CD45RA^{+}CD45RO^{-}CCR7^{-}$ among total CD8 T cells, yielding an AUC of 0.7731 and 0.8663 for all the early-to-mid stage PD patients (**L**) or patients diagnosed within 5 years, respectively (**M**). The results in (**C-I**) were analysed using an unpaired two-tailed Student *t* test. Data are presented as mean of the given group ± standard deviation (s.d.). Each symbol represents the measurement from one individual participant (**C-I**). ns or unlabelled, not significant; *p<=0.05, **p<=0.01, and ***p<=0.001. HC, healthy controls; PD, Parkinson's disease; FCM, flow cytometry.

Figure 3: PD patients display a reduced CD8 Treg frequency

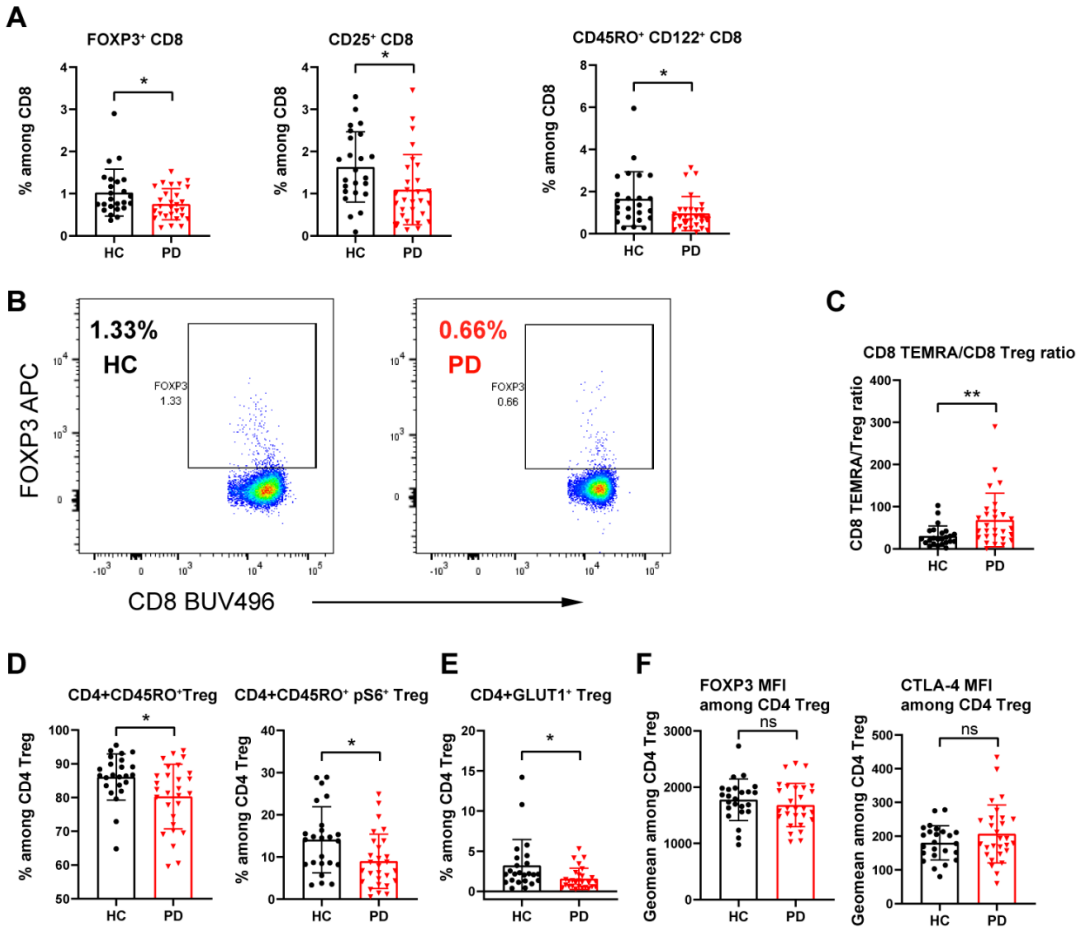

Figure 3: PD patients display a reduced CD8 Treg frequency

(**A**) Scatter dot plots showing the frequency of FOXP3+, CD25+ and CD122+ CD8 T cells in PD patients and HCs. (**B**) Representative flow-cytometry plots showing the reduced frequency of FOXP3+ CD8 T cells. (**C**) Scatter dot plots showing the ratio between CD8 TEMRA and CD8 Treg (**D, E**) Scatter dot plots showing the frequency of CD45RO+, CD45RO+pS6+ (**D**) and GLUT1+ (**E**) CD4 Treg in PD patients and HC. (**F**) Scatter dot plots showing the geometric mean (geomean, known as MFI) of FOXP3 and CTLA4 among total CD4+FOXP3+ Treg. The results were analysed using an unpaired two-tailed Student *t* test. Data are presented as mean of the given group ± standard deviation (s.d.). Each symbol represents the measurement from one individual participant (**A,C, D-F**). ns or unlabelled, not significant; *p<=0.05, **p<=0.01, and ***p<=0.001. HC, healthy controls; PD, Parkinson's disease.

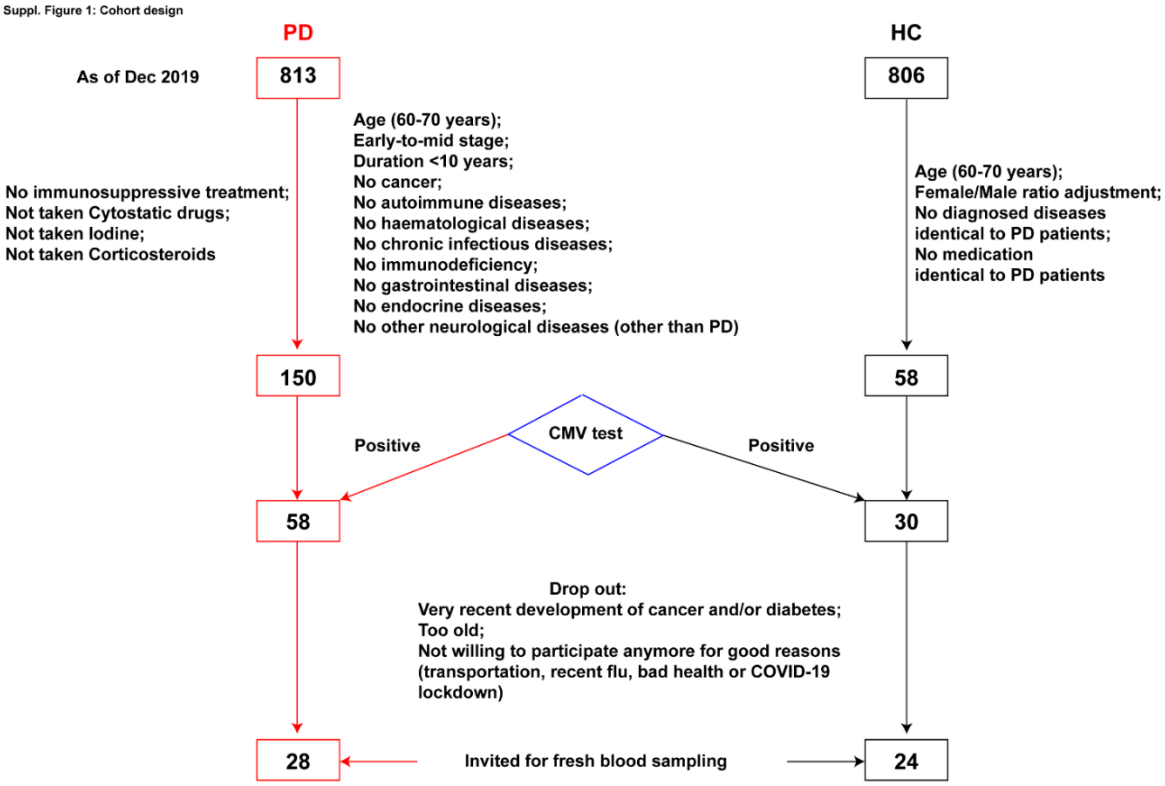

Suppl. Figure 1: Cohort design

Schematic representation showing the selection of the participants from the ongoing nation-wide Luxembourg Parkinson's Study in this work. The comorbidities indicate that PD patients or HC have never been diagnosed with any of those diseases. For the medications, it refers to the scenario that there were no record in receiving those treatments of the given participant. For the the limit of disease duration (<10 years), we exceptionally included three participants with longer duration (refer to text in **Material and Methods**). HC, healthy controls; PD, Parkinson's disease; CMV, cytomegalovirus.

Suppl. Figure 2: CyTOF gating strategy

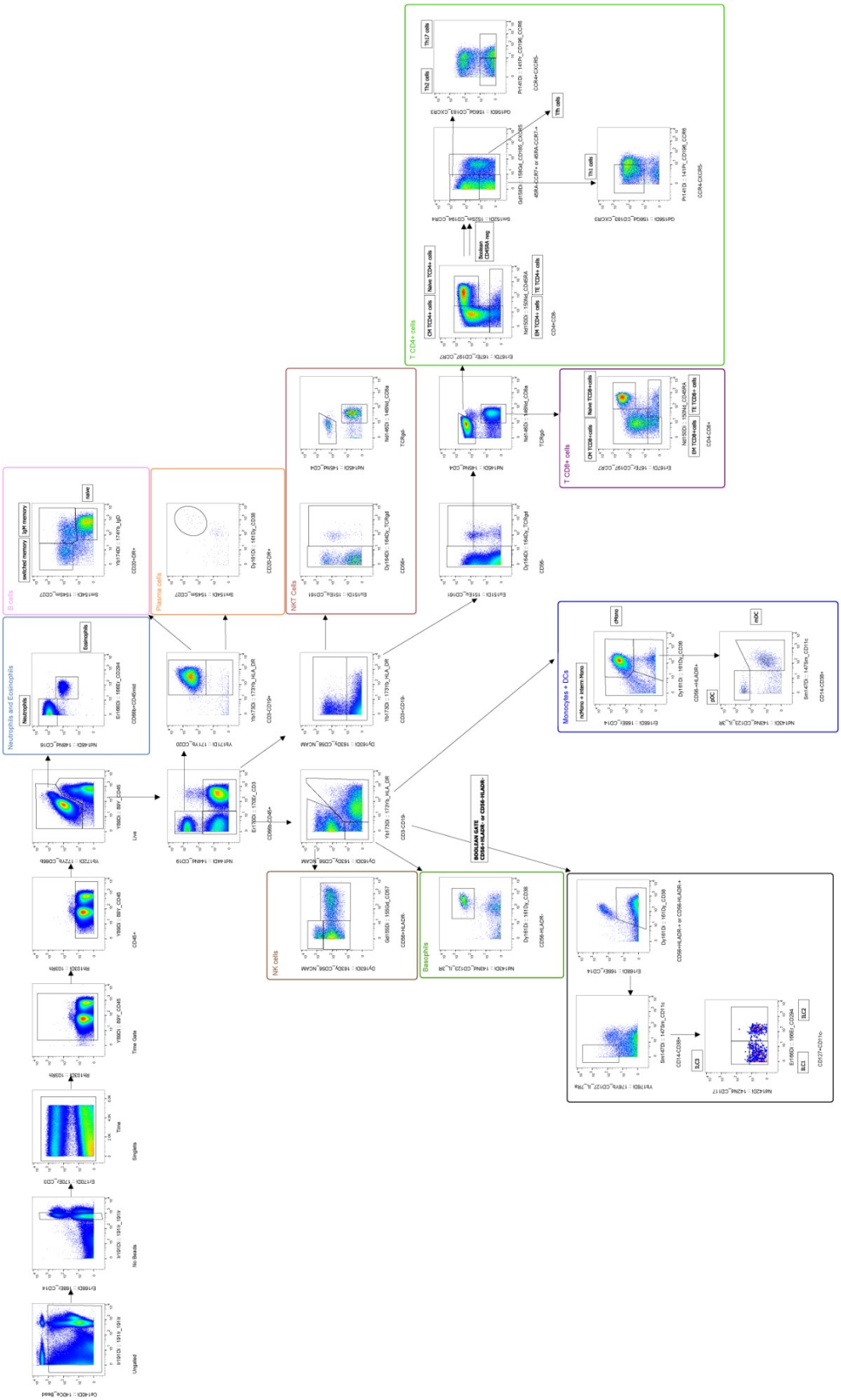

Suppl. Figure 2: CyTOF gating strategy

The gating stategy of the mass cytometry analysis for various peripheral immune cells we analyzed. The markers used in this study are provided in **Suppl. Table 3**.

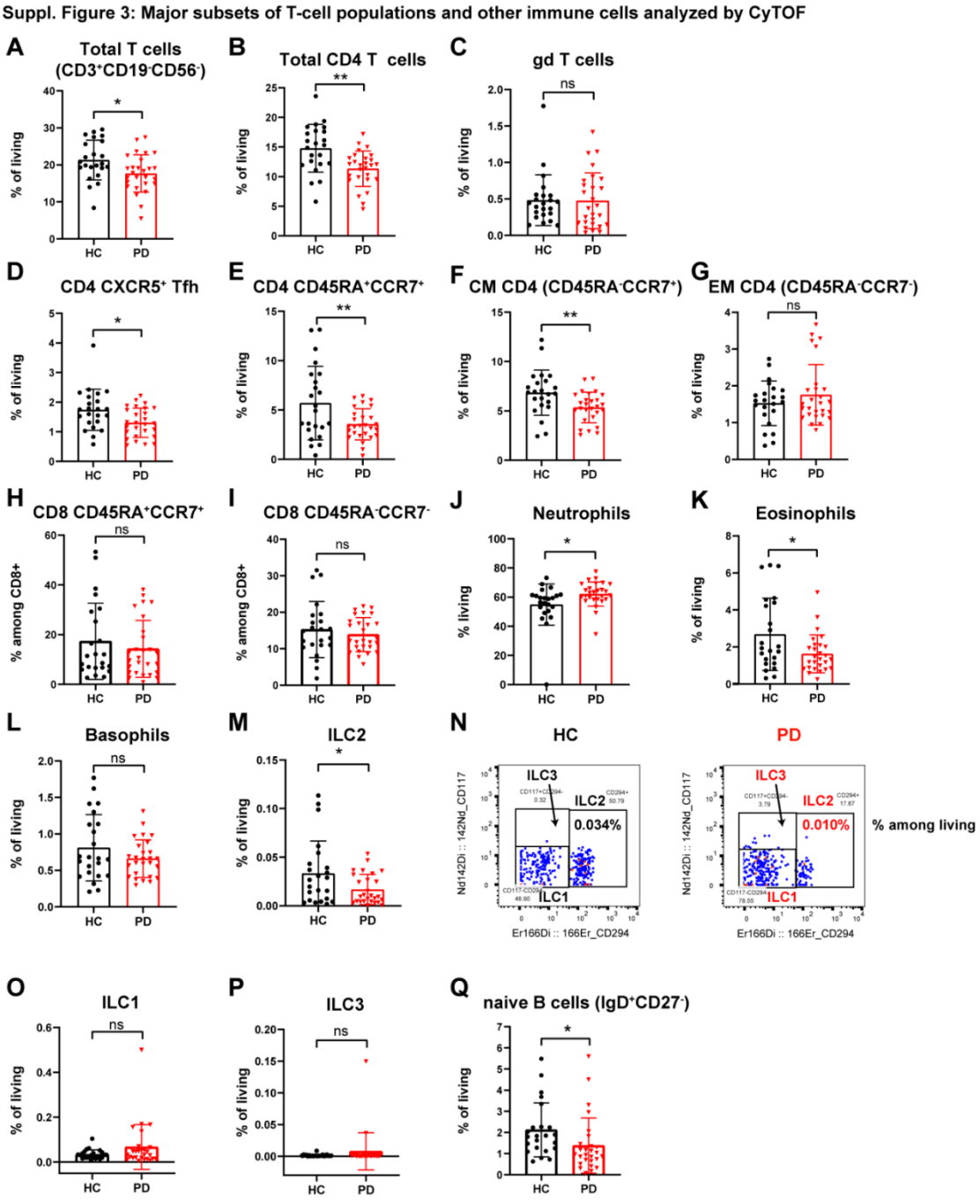

Suppl. Figure 3: Extended analysis on major subsets of T-cell populations and other immune cells analysed by CyTOF

Scatter dot plots showing the frequency of total CD3+ T cells ($CD3^+CD19^-CD56^-$) (**A**), total CD4 T cells (**B**) and γδ T cells (**C**) among living $CD45^+$ cells in PD and HC, as analysed by CyTOF. (**D-G**) Scatter dot plots showing the frequency of CD4 CXCR5+ Tfh (**D**), CD45RA+CCR7+ naïve (**E**), CD45RA-CCR7+ central memory (CM) (**F**) and CD45RA-CCR7- effector memory (EM) (**G**) CD4 T cells. (**H, I**) Scatter dot plots showing the frequency

of naïve (H) and effector memory (I) CD8 T cells. (**J-L**) Scatter dot plots showing the frequency of neutrophils (**J**), eosinophils (**K**) and basophils (**L**) among living $CD45^+$ immune cells. (**M**) Scatter dot plots showing the frequency Innate lymphoid cells 2 (ILC2) among living $CD45^+$ immune cells. (**N**) Representative flow-cytometry plots showing the reduced frequency of ILC2 in PD patients. The enlarged number showing the frequency among living $CD45^+$ cells. For detailed gating strategy, please refer to **Suppl. Fig 2**. (**O, P**) Scatter dot plots showing the frequency of ILC1 (**O**) and ILC3 (**P**) among living $CD45^+$ immune cells. (**Q**) Scatter dot plots showing the frequency of naïve B cells among living $CD45^+$ immune cells. All the results of major immune subsets were also provided in **Suppl. Table 5**. The results were analysed using an unpaired two-tailed Student *t* test. Data are presented as mean of the given group± standard deviation (s.d.). Each symbol represents the measurement from one individual participant (**A-M, O-Q**). ns or unlabelled, not significant; *p<=0.05, **p<=0.01, and ***p<=0.001. HC, healthy controls; PD, Parkinson's disease.

Suppl. Figure 4: PD patients show less memory CD8 and display no sign of accelerated exhaustion

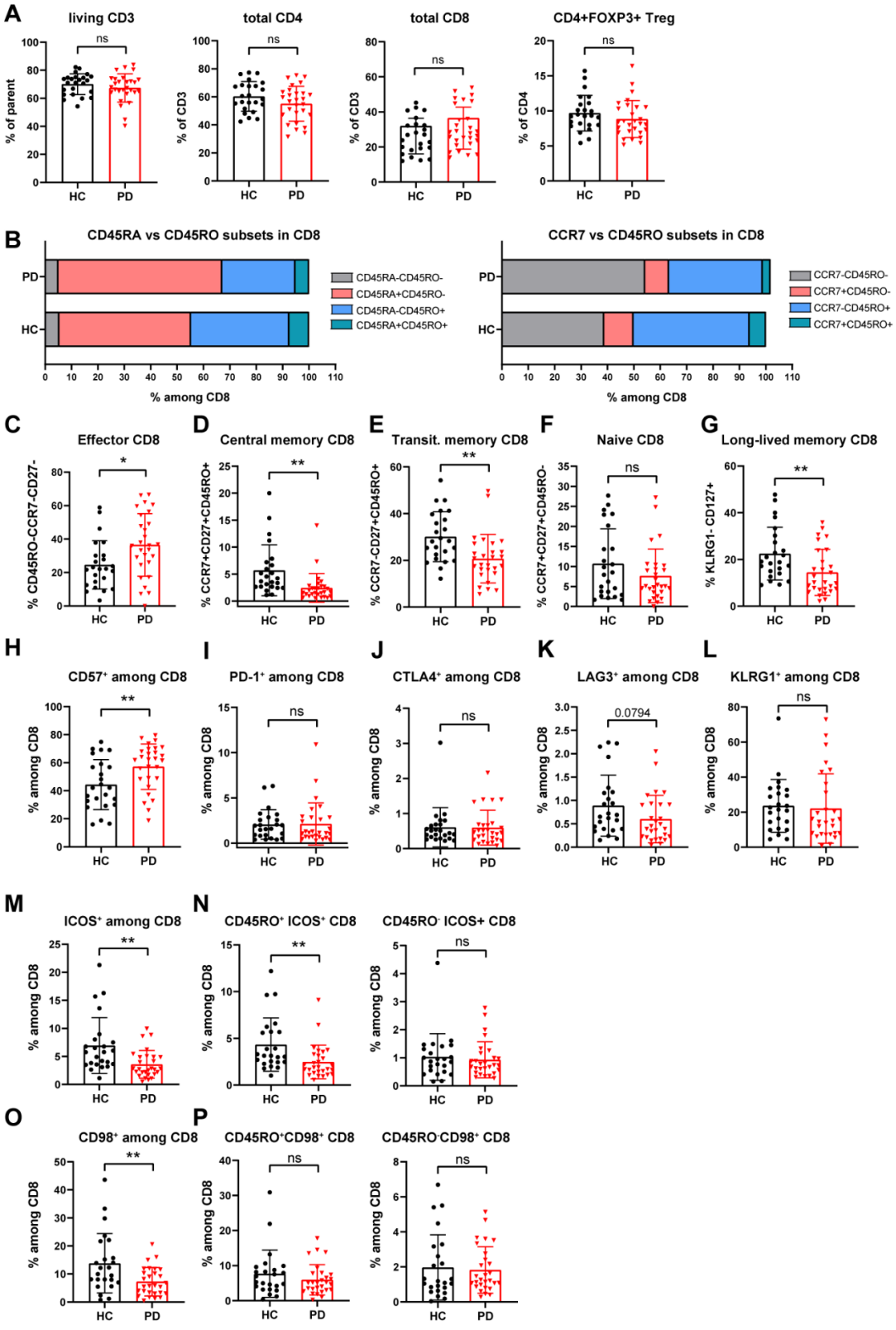

Suppl. Figure 4: PD patients show less memory CD8 T cells and display no sign of accelerated exhaustion

(**A**) Scatter dot plots showing the frequency of CD3+, CD4+, CD8+ T cells and FOXP3+ CD4 Treg in PD patients and HCs as analysed by flow cytometry. The parent gate of CD3+ cells is living lymphocyte singlets. (**B**) Graphs showing the relative proportions of CD45RA versus CD45RO (left) and CCR7 versus CD45RO subpopulations (right) of CD8 T cells. (**C-G**) Scatter dot plots showing the frequency of effector (**C**), central memory (**D**), transitional memory (**E**), naïve (**F**) and long-lived memory (**G**) CD8 T cells in PD patients and HCs. The combination of markers used to define the corresponding subset was described in the title of y axis of the corresponding panel. (**H-L**) Scatter dot plots showing the frequency of $CD57^+$ (**H**), $PD\text{-}1^+$ (**I**), $CTLA4^+$ (**J**), $LAG3^+$ (**K**) and $KLRG1^+$ (**L**) populations among CD8 T cells in PD patients and HC. (**M, N**) Scatter dot plots showing the frequency of $ICOS^+$ cells among total CD8 T cells (**M**), as well as in the $CD45RO^+$ or $CD45RO^-$ CD8 T cells in PD patients and HC (**N**). (**O, P**) Scatter dot plots showing the frequency of $CD98^+$ populations in total CD8 T cells (**O**), as well as in the $CD45RO^+$ or $CD45RO^-$ CD8 T cells in PD patients and HC (**P**). The results were analysed using an unpaired two-tailed Student *t* test. Data are presented as mean of the given group± standard deviation (s.d.). Each symbol represents the measurement from one individual participant (**A, C-P**). ns or unlabelled, not, significant; *p<=0.05, **p<=0.01, and ***p<=0.001. HC, healthy controls; PD, Parkinson's disease.

Suppl. Figure 5: CD8 TEMRA show normal expression of major chemokine receptors and CD49d among PD patients

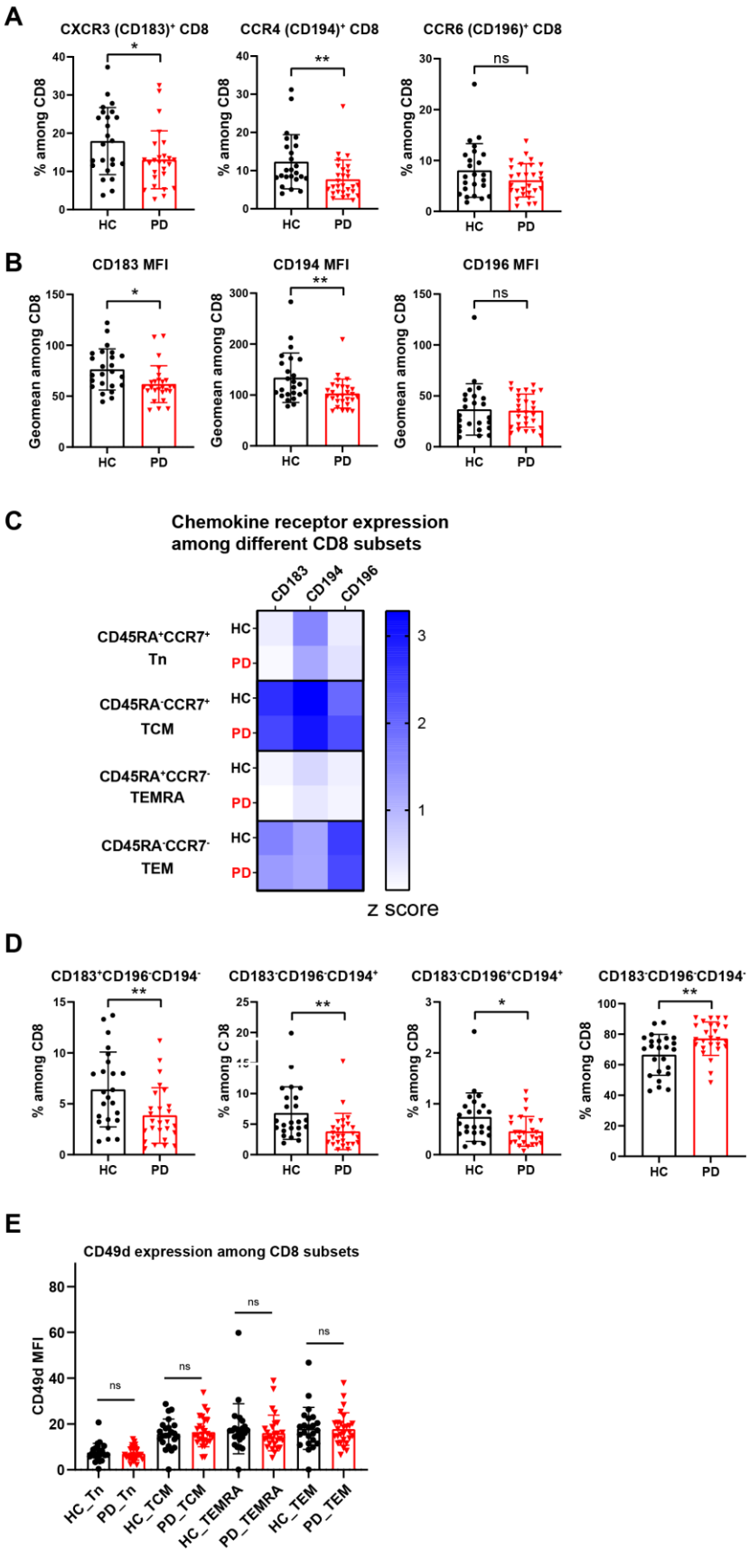

Suppl. Figure 5: CD8 TEMRA show normal expression of major chemokine receptors and CD49d among PD patients

(**A**) Scatter dot plots showing the frequency of CXCR3, CCR4 and CCR6 positive cells among total CD8 T cells. (**B**) Scatter dot plots showing the geometric mean (geomean, reflecting MFI) of CXCR3, CCR4 and CCR6 among total CD8 T cells. (**C**) Heatmap showing the averaged expression levels of the analysed chemokine receptors in different subpopulations of CD8 T cells for the given group. The frequency of cells expressing the given chemokine receptor was normalized along column. CCR7 expression was not shown because CCR7 was used to define CD8 memory/naïve T cell subsets. (**D**) Scatter dot plots showing the frequency of CD8 T cells expressing different combinations of the chemokine receptors CXCR3 (CD183), CCR4 (CD194) and CCR6 (PD196) in PD patients and HC. (**E**) Scatter dot plots showing the expression level (MFI) of the brain homing factor CD49d among different CD8 T-cell subsets in PD patients and HC. The results were analysed using an unpaired two-tailed Student *t* test. Data are presented as mean of the given group± standard deviation (s.d.). Each symbol represents the measurement from one individual participant (**A, B, D, E**). ns or unlabelled, not significant; *p<=0.05, **p<=0.01, and ***p<=0.001. HC, healthy controls; PD, Parkinson's disease. Of note, the CD49d expression was analysed by CyTOF while the expression of chemokine receptors was done in flow cytometry.

Suppl. Figure 6: CD4 T cells in PD patients also have a reduced CD4 central memory compartment

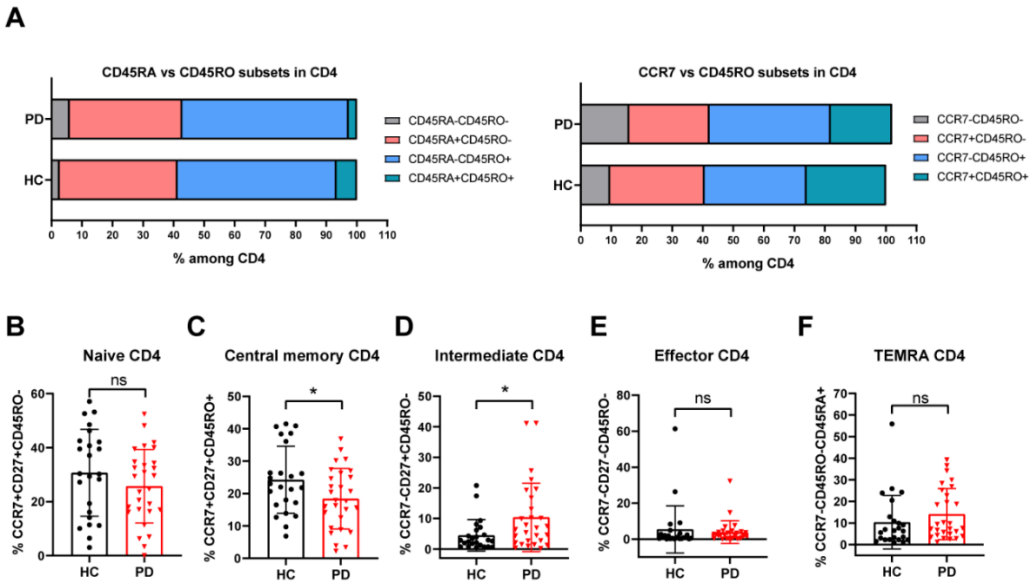

Suppl. Figure 6: CD4 T cells in PD patients also have a reduced central memory compartment

(**A**) Graphs showing the proportions of CD45RA versus CD45RO (left) and CCR7 versus CD45RO subpopulations (right) of CD4 T cells. (**B-F**) Scatter dot plots showing the frequency of naïve (**B**), central memory (**C**), intermediate (**D**), effector (**E**) and TEMRA (**F**) CD4 T cells in PD patients and HC. The combination of markers used to define the corresponding subset was described in the title of y axis of the corresponding panel. The results were analysed using an unpaired two-tailed Student *t* test. Data are presented as mean of the given group± standard deviation (s.d.). Each symbol represents the measurement from one individual participant (**B-F**). ns or unlabelled, not significant; *p<=0.05, **p<=0.01, and ***p<=0.001. HC, healthy controls; PD, Parkinson's disease.

Suppl. Figure 7: The CD4 T-helper balance is unaffected in PD patients

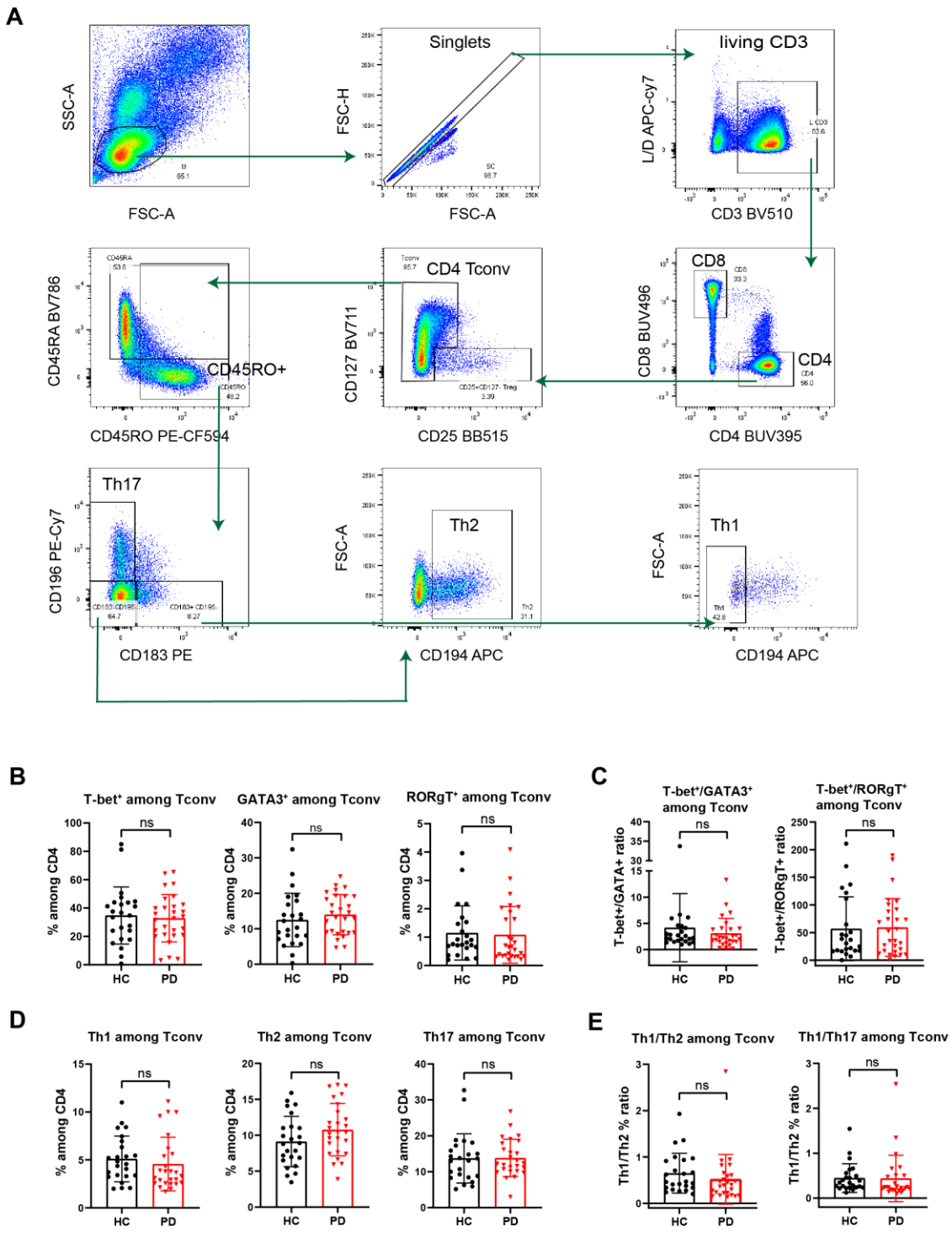

Suppl. Figure 7: The CD4 T-helper balance is unaffected in PD patients

(**A**) Gating strategy to define CD4 Th1, Th2 and Th17 subsets based on the combinations of the expression of the chemokine receptors CXCR3 (CD183), CCR4 (CD194), CCR6 (CD196) and CCR7 (CD197) in PD patients and HC using flow cytometry analysis. Arrows indicate the workflow. (**B**) Scatter dot plots showing the expression of the master CD4 T cell

transcriptions factors Tbet, GATA3 and RORγT in PD patients and HC. (**C**) Ratios between T-bet$^+$/GATA3$^+$ and T-bet$^+$/RORγT$^+$ CD4 T cells in PD patients and HC, reflecting the ratios of Th1/Th2 and Th1/Th17, respectively. (**D**) Scatter dot plots showing the frequency of Th1 (CXCR3$^+$CCR6$^-$CCR4$^-$), Th2 (CXCR3$^-$CCR6$^-$CCR4$^+$) and Th17 (CXCR3$^-$CCR6$^+$) cells based on the combinations of the expression of the chemokine receptors CXCR3, CCR4, CCR6 and CCR7. (**E**) Ratios of Th1/Th2 and Th1/Th17 cells in PD patients and HC. The ratios in **E** were calculated based on data of **D**. The results were analysed using an unpaired two-tailed Student *t* test. Data are presented as mean of the given group± standard deviation (s.d.). Each symbol represents the measurement from one individual participant (**B-E**). ns or unlabelled, not significant; *p<=0.05, **p<=0.01, and ***p<=0.001. HC, healthy controls; PD, Parkinson's disease.

Supplementary Tables

Supplementary Table 1: The exclusion criteria of the cohort.

Exclusion Criteria	
History or presence of medication taken	Corticosteroids Cytostatic drugs Immunosuppressive treatment Iodine*
Medical history	Autoimmune Disorders Chronic Infections Endocrine Diseases Gastrointestinal Diseases Haematological Diseases Immunodeficiency Malignancies Neurologic Diseases (other than Parkinson's disease)

* Iodine treatment could interfere with the mass cytometry (CyTOF) staining and was therefore excluded.

Supplementary Table 2. Basic demographics and clinical information of the participants in the cohort.

	Parkinson's cases (n=28)	Controls (n=24)	P-value
Male, % (n)	68 (19)	58 (14)	0.17 (Chi square test)
Age at basic assessment, mean (SD)[£]	64.9 (6.97)	63.92(3.75)	0.54 (two-tailed Student *t* test)
Age of Onset, mean (SD)	58.14 (9.42)	NA	NA
Disease duration from diagnosis (years), mean (SD)	6.64 (4.12)	NA	NA
Disease duration from initial symptom(s), mean (SD)	8.19 (5.37)	NA	NA
Family History of Parkinson's Disease, % (n)	43 (12)	NA	NA
Hoehn and Yahr Staging, mean (SD)	2.3 (0.42)	NA	NA
UPDRS-III*, mean (SD)	39.69 (13.15)	NA	NA
LEDD[¥], mean (SD)	610.58 (344.06)	NA	NA
MOCA[€], mean (SD)	25.21 (3.82)	NA	NA

[£], the descriptive statistics here includes information from both idiopathic and genetic PD patients.

*UPDRS-III: Motor Examination. The physician does a number of tests to rate the cardinal symptoms of PD such as rigidity, postural instability, facial expression etc.

[¥]LEDD: Levodopa Equivalent Daily Dose, so basically the sum of levodopa a patient is taking each day.

[€]MOCA: Montreal Cognitive Assessment. Provides an overall cognitive profile (0-30, with 30 meaning no cognitive deficits).

NA, no data available or not applicable; SD, standard deviation.

Supplementary Table 3: Mass Cytometry (CyTOF) antibodies used to stain the whole blood.

Metal Isotope	Antibody	Clone	Manufacturer	Catalogue#
89Y	CD45	HI30	Fluidigm	Part of MDIPA
103Rh	Live/Dead indicator		Fluidigm	Part of MDIPA
141Pr	CD196 (CCR6)	G034E3	Fluidigm	Part of MDIPA
142Nd	CD117 (c-kit)*	104D2	Biolegend	313223
143Nd	CD123	6H6	Fluidigm	Part of MDIPA
144Nd	CD19	HIB19	Fluidigm	Part of MDIPA
145Nd	CD4	RPA-T4	Fluidigm	Part of MDIPA
146Nd	CD8a	RPA-T8	Fluidigm	Part of MDIPA
147Sm	CD11c	Bu15	Fluidigm	Part of MDIPA
148Nd	CD16	3G8	Fluidigm	Part of MDIPA
149Sm	CD45RO	UCHL1	Fluidigm	Part of MDIPA
150Nd	CD45RA	HI100	Fluidigm	Part of MDIPA
151Eu	CD161	HP-3G10	Fluidigm	Part of MDIPA
152Sm	CD194 (CCR4)	L291H4	Fluidigm	Part of MDIPA
153Eu	CD25	BC96	Fluidigm	Part of MDIPA
154Sm	CD27	O323	Fluidigm	Part of MDIPA
155Gd	CD57	HCD57	Fluidigm	Part of MDIPA
156Gd	CD183 (CXCR3)	G025H7	Fluidigm	Part of MDIPA
158Gd	CD185 (CXCR5)	J252D4	Fluidigm	Part of MDIPA
159Tb	KLRG1*	SA231A2	Biolegend	367702
160Gd	CD28	CD28.2	Fluidigm	Part of MDIPA
161Dy	CD38	HB-7	Fluidigm	Part of MDIPA
162Dy	CD336 (NKp44)*	P44-8	Biolegend	325102
163Dy	CD56 (NCAM)	NCAM16.2	Fluidigm	Part of MDIPA
164Dy	TCRgd	B1	Fluidigm	Part of MDIPA
165Ho	CD223 (LAG3)	11C3C65	Fluidigm	3165037B
166Er	CD294	BM16	Fluidigm	Part of MDIPA
167Er	CD197 (CCR7)	G043H7	Fluidigm	Part of MDIPA
168Er	CD14	63D3	Fluidigm	Part of MDIPA
169Tm	CD49d*	9F10	Biolegend	304302
170Er	CD3	UCHT1	Fluidigm	Part of MDIPA
171Yb	CD20	2H7	Fluidigm	Part of MDIPA

172Yb	CD66b	G10F5	Fluidigm	Part of MDIPA
173Yb	HLA-DR	LN3	Fluidigm	Part of MDIPA
174Yb	IgD	IA6-2	Fluidigm	Part of MDIPA
175Lu	CD279 (PD1)	EH12.2H7	Fluidigm	3175008B
176Yb	CD127	A019D5	Fluidigm	Part of MDIPA

***** in house conjugation using Maxpar X8 Antibody Labeling Kits MDIPA (CAT#:201325, Fluidigm)

Supplementary Table 4: Flow cytometry antibodies used to stain the PBMCs of participants analysed in this study.

Ab Target	Fluorochrome	Dilution	Manufacturer	Reference	Clone
Fc Blocking Abs	/	1:50	BD	564765	/
CD3*	BUV737	1:100	BD	741822	HIT3a
CD3*	BV510	1:100	BD	564713	HIT3a
CD4	BUV395	1:100	BD	563550	SK3
CD8	BUV496	1:100	BD	564804	RPA-T8
CD25	BV786	1:50	BD	741035	2A3
CD25	BB515	1:50	BD	564467	2A3
CD27	BB700	1:50	BD	566450	M-T271
CD28	BUV785	1:50	BioLegend	302950	CD28.2
CD31	BV605	1:50	BD	562855	WM59
CD39	BV711	1:50	BioLegend	328228	A1
CD45RA	BV421	1:50	BioLegend	304130	HI100
CD45RA	BV785	1:50	BioLegend	304140	HI100
CD45RO	PE-CF594	1:50	BD	562299	UCHL1
CD57	FITC	1:50	BD	555619	NK-1
CD71	FITC	1:50	BioLegend	334104	CY1G4
CD98	BV786	1:50	BD	744507	UM7F8
CD122	PE	1:50	BioLegend	339006	TU27
CD127 (IL7R)	BV421	1:50	BD	562436	HIL-7R-M21
CD127 (IL7R)	BV711	1:50	BioLegend	351328	A019D5
CD183 (CXCR3)	PE	1:50	BD	560928	1C6/CXCR3

CD194 (CCR4)	APC	1:50	BioLegend	359408	L291H4
CD196 (CCR6)	PE-Cy7	1:50	BD	560620	11A9
CD197 (CCR7)	BV421	1:50	BioLegend	353208	G043H7
CD223 (LAG3)	BV711	1:50	BioLegend	369320	11C3C65
CD278 (ICOS)	BV605	1:50	BioLegend	313538	C398.4A
CD279 (PD-1)	BV605	1:50	BioLegend	329924	EH12.2H7
GLUT1	PE	1:500	Abcam	ab209449	EPR3915
KLRG1	PE-Cy7	1:50	BioLegend	368614	14C2A07
Intracellular markers					
CD152 (CTLA4)	PE-Cy5	1:20	BD	555854	BNI3
FOXP3	APC	1:20	BioLegend	320114	206D
Phospho S6	AF488	1:20	CST	4803S	D57.2.2E
Helios	Pacific Blue	1:20	BioLegend	137220	22F6
Ki-67	FITC	1:20	BD	561165	B56
GATA3	PE-Cy7	1:20	BD	560405	L50-823
RORγT	BV650	1:20	BD	563424	Q21-559
T-bet	PE	1:20	BioLegend	644810	4B10
Eomes	PE-Cy7	1:20	Thermo Fischer Scientific	25-4877-42	WD1928
Live/Dead	APC-Cy7	1:500	Thermo Fischer Scientific	L34976	/

*, different flurorochromes might be used in different staining panels as we employed five staining panels in parallel.

Supplementary Table 5. Mass cytometry analysis reveals the percentages of major immune subsets among living CD45+ singlets or among the parent gates (Suppl. Fig 2) in the peripheral blood of early-to-mid stage PD patients or healthy controls aged 60-70 years.

No.	Items	HC (n=24), mean (SD)	PD (n=28), Mean (SD)	P-value (two-tailed t test)
	Total number of living CD45+ singlets	627629 (136842)	679999 (155232)	0.22482
	Among living CD45+ singlets			
1	ncMono plus interm Mono among living cells	0.847 (0.518)	0.75 (0.422)	0.476922
2	mDC among living cells	0.253 (0.065)	0.215 (0.07)	0.062098
3	pDC among living cells	0.111 (0.04)	0.097 (0.04)	0.24072
4	cMono among living cells	5.964 (1.085)	5.913 (1.37)	0.887997
5	Basophils among living cells	0.81 (0.445)	0.662 (0.253)	0.154289
6	NK among living cells	3.658 (1.6)	3.53 (1.747)	0.794596
7	$CD56^{high}CD57^{-}$ immature NK among living cells	0.224 (0.131)	0.16 (0.088)	0.04992
8	$CD56^{mid}CD57^{-}$ NK among living cells	1.619 (0.78)	1.549 (0.989)	0.788334
9	$CD56^{mid}CD57^{+}$ late NK among living cells	1.815 (1.174)	1.823 (1.181)	0.982319
10	ILCs among living cells	0.069 (0.042)	0.091 (0.127)	0.419163
11	ILC1 among living cells	0.034 (0.021)	0.067 (0.098)	0.123848
12	ILC2 among living cells	0.033 (0.033)	0.017 (0.015)	0.025059
13	ILC3 among living cells	0.001 (0.002)	0.008 (0.029)	0.290684
14	B cells among living cells	3.24 (1.419)	3.453 (3.736)	0.801529
15	$CD27^{+}CD38^{+}$ plasma cells among living cells	0.02 (0.021)	0.015 (0.01)	0.313471
16	$CD20^{-}HLADR^{+}$ among living cells	0.12 (0.37)	0.62 (2.09)	0.270256
17	$CD20^{+}HLADR^{+}$ among living cells	3.082 (1.363)	2.731 (3.217)	0.635057
18	$CD27^{-}IgD^{+}$ naïve B cells among living cells	2.12 (1.25)	1.379 (1.282)	0.04885
19	$CD27^{+}IgD^{-}$ class-switched memory B among living cells	0.395 (0.226)	0.385 (0.368)	0.911043
20	$CD27^{+}IgD^{+}$ IgM memory among living cells	0.39 (0.253)	0.781 (2.146)	0.39954
21	Total T cells among living cells	21.318 (5.235)	17.673 (4.946)	0.016814
22	$TCRgd^{-}$ classic T cells among living cells	20.835 (5.119)	17.198 (4.728)	0.013785
23	CD8+ T among living cells	5.42 (2.514)	5.372 (2.671)	0.950139
24	$CD45RA^{-}CCR7^{-}$ CD8 TEM among living cells	0.795 (0.453)	0.748 (0.43)	0.712639
25	$CD45RA^{-}CCR7^{+}$ CD8 CM among living cells	1.528 (0.963)	0.955 (0.536)	0.012486
26	$CD45RA^{+}CCR7^{-}$ CD8 TEMRA among living cells	2.165 (1.829)	2.839 (2.109)	0.247063
27	$CD45RA^{+}CCR7^{+}$ CD8 naïve T among living cells	0.783 (0.567)	0.72 (0.613)	0.713217
28	CD4+ among living cells	14.776 (3.947)	11.321 (2.945)	0.001126
29	CD45RA- CD4 among living cells	8.371 (2.389)	7.099 (1.927)	0.046814

30	CD4 CXCR3+CCR6-CCR4-CXCR5- Th1 among living cells	1.829 (0.745)	1.636 (0.958)	0.443708
31	CD4 CXCR3-CCR6-CCR4+CXCR5- Th2 among living cells	1.246 (0.535)	1.01 (0.41)	0.090831
32	CD4 CXCR3-CCR6+CCR4+CXCR5-Th17 among living cells	0.519 (0.319)	0.549 (0.329)	0.749899
33	CD4 CXCR5+Tfh among living cells	1.741 (0.678)	1.304 (0.485)	0.012681
34	$CD45RA^{-}CCR7^{-}$ CD4 T among living cells	1.527 (0.594)	1.756 (0.81)	0.276958
35	$CD45RA^{-}CCR7^{+}$ CD4 T among living cells	6.848 (2.238)	5.345 (1.518)	0.008301
36	$CD45RA^{+}CCR7^{-}$ CD4 T among living cells	0.547 (0.598)	0.566 (0.647)	0.91715
37	$CD45RA^{+}CCR7^{+}$ CD4 T among living cells	5.699 (3.643)	3.55 (1.543)	0.00885
38	$TCRgd^{+}$ T among living cells	0.483 (0.341)	0.475 (0.376)	0.943847
39	NKT among living cells	2.407 (2.604)	2.431 (1.738)	0.969286
40	NKT $CD8^{+}$ among living cells	1.33 (1.146)	1.722 (1.345)	0.287332
41	NKT $CD4^{+}$ among living cells	0.973 (1.737)	0.546 (0.869)	0.27652
42	Eosinophils among living cells	2.682 (1.914)	1.628 (1.005)	0.018555
43	Neutrophils among living cells	54.853 (13.872)	62.153 (8.156)	0.028426
	Among parent gate			
44	ncMono plus interm Mono among CD3-CD19-CD56-+HLADR+	11.35 (5.243)	10.469 (4.895)	0.550335
45	cDC among $CD14^{-}CD38^{+}$	58.174 (5.712)	56.277 (9.996)	0.434193
46	pDC among $CD14^{-}CD38^{+}$	25.269 (6.242)	25.391 (8.386)	0.955228
47	cMono among $CD56^{-+}HLADR^{+}$	82.436 (5.429)	83.938 (5.407)	0.343294
48	Basophils among $CD56^{-}HLADR^{-}$	58.465 (18.293)	55.279 (15.374)	0.515111
49	NK among $CD3^{-}CD19^{-}$	28.807 (8.605)	28.745 (10.793)	0.982812
50	$CD56^{high}CD57^{-}$ immature NK among NK	7.04 (4.954)	6.009 (5.045)	0.47997
51	$CD56^{mid}CD57^{-}$ among NK	46.359 (13.894)	43.532 (15.477)	0.511909
52	$CD56^{mid}CD57^{+}$ late NK among NK	46.593 (16.195)	50.501 (16.552)	0.414395
53	ILCs among $CD14^{-}CD38^{+}$	1.831 (1.191)	2.776 (3.886)	0.276966
54	ILC1 among ILCs	56.917 (22.262)	67.578 (21.7)	0.100179
55	ILC2 among ILCs	40.648 (23.368)	28.852 (22.595)	0.082335
56	ILC3 among ILCs	2.447 (3.122)	3.641 (5.285)	0.356174
57	CD19 B cells among $CD66b^{-}CD45^{+}$	8.33 (3.671)	9.264 (8.883)	0.646487
58	$CD20^{-}HLADR^{+}$ among B cells	2.966 (7.355)	7.78 (20.574)	0.301677
59	$CD27^{+}CD38^{+}$ plasma cells among $CD20^{-}HLADR^{+}$ B cells	40.636 (23.249)	41.301 (22.297)	0.919915
60	$CD20^{+}HLADR^{+}$ among B cells	95.712 (7.352)	90.113 (22.339)	0.265394
61	$CD27^{-}IgD^{+}$ naïve among $CD20^{+}HLADR^{+}$	66.453 (14.11)	54.928 (20.903)	0.032729

62	$CD27^{+}IgD^{-}$ class-switched memory among $CD20^{+}HLADR^{+}$	13.723 (6.809)	17.912 (9.271)	0.085198
63	$CD27^{+}IgD^{+}$ IgM memory among $CD20^{+}HLADR^{+}$	13.893 (8.827)	17.886 (16.107)	0.303826
64	$CD56^{-}$ among $CD3^{+}CD19^{-}$	89.615 (7.828)	86.881 (6.587)	0.19508
65	$TCRgd^{-}$ among total T cells	97.757 (1.451)	97.493 (1.734)	0.574621
66	$CD4\text{-}CD8^{+}$ among classic T cells	25.705 (9.137)	30.118 (9.619)	0.1116
67	$CD45RA^{-}CCR7^{-}$ TEM among CD8	15.245 (7.516)	13.889 (4.561)	0.446601
68	$CD45RA^{-}CCR7^{+}$ CM among CD8	28.582 (11.591)	19.871 (10.181)	0.007914
69	$CD45RA^{+}CCR7^{-}$ TEMRA among CD8	36.179 (17.486)	49.607 (16.594)	0.008928
70	$CD45RA^{+}CCR7^{+}$ naïve among CD8	17.326 (14.998)	14.272 (11.24)	0.424869
71	$CD4^{+}CD8^{-}$ among classic T cells	71.145 (9.198)	66.911 (9.867)	0.132923
72	Th1 among CD4 $CCR4^{-}CXCR5^{-}$	61.282 (16.004)	54.486 (16.115)	0.150608
73	Th2 among CD4 $CCR4^{+}CXCR5^{-}$	35.101 (11.204)	34.506 (11.046)	0.854118
74	Th17 among CD4 $CCR4^{+}CXCR5^{-}$	14.757 (7.026)	18.987 (11.054)	0.127509
75	Tfh among CD4 $CD45RA^{-}$	20.455 (3.61)	18.299 (4.566)	0.079396
76	$CD45RA^{-}CCR7^{-}$ TEM among CD4	12.154 (8.916)	15.618 (5.296)	0.102741
77	$CD45RA^{-}CCR7^{+}$ CM among CD4	47.508 (12.756)	47.847 (9.05)	0.914884
78	$CD45RA^{+}CCR7^{-}$ TEMRA among CD4	4.052 (4.889)	4.934 (5.083)	0.545261
79	$CD45RA^{+}CCR7^{+}$ naïve among CD4	35.278 (16.482)	30.65 (10.146)	0.240098
80	$TCRgd^{+}$ T among $CD56^{-}$	2.24 (1.452)	2.506 (1.736)	0.570601
81	NKT among $CD56^{+}$	85.402 (12.74)	83.294 (15.719)	0.616183
82	NKT CD8 among NKT	59.129 (20.227)	70.188 (16.402)	0.041839
83	NKT CD4 among NKT	33.515 (22.057)	20.707 (16.692)	0.026705
84	Eosinophils among $CD66b^{+}CD45^{mid}$	4.529 (3.466)	2.604 (1.61)	0.014893
85	Neutrophils among $CD66b^{+}CD45^{mid}$	90.811 (19.671)	97.055 (1.653)	0.114084
86	$CD27^{+}CD38^{+}$ plasma cells among B cells	0.64 (0.58)	0.91 (1.11)	0.304309
87	$CD27^{-}IgD^{+}$ naive among B cells	64.28 (15.04)	51.7 (23.15)	0.033506
88	$CD27^{+}IgD^{-}$ class-switched among B cells	12.74 (4.82)	15.03 (8.13)	0.252162
89	$CD27^{+}IgD^{+}$ IgM memory among B cells	13.01 (7.8)	15.6 (15.92)	0.489398

General Discussion and Perspectives

General discussion and Perspectives

Each of the studies presented in this cumulative thesis investigate molecular and cellular mechanisms in a particular experimental or clinical context. First, we outlined the selenoprotein VIMP as a novel anti-inflammatory gene in CD4 T cells via E2F5 and the Ca^{2+}/NFAT pathway. We also investigated stress hormone signalling in CD4 T cells and described their role in T cell differentiation. We were able to reveal a CD4 T cell-intrinsic mechanism through which stress hormones regulate the Th1/Th2 balance via the circadian clock gene Period1 and the mTORC1 signalling pathway. Last but not least, we conducted a clinical study systematically examining the peripheral immune system in PD patients. We revealed a peripheral immune status highly biased towards terminally-differentiated effector CD8 T cells, thus contributing to better understanding the facets of autoimmunity in PD. Although all revolving around T cells, in particular in neuroimmunology, those studies are not directly connected on their own. We will discuss how the findings of the different studies relate to each other by connecting the dots based on existing literature.

In chapter one, we discussed the anti-inflammatory function of the selenoprotein SELS/VIMP in CD4 T cells and how these findings relates to the anti-inflammatory effect of Selenium (Se) supplementation on inflammatory and autoimmune diseases [30, 31, 421]. Se is an important micronutrient for brain homeostasis by regulating oxidative stress via selenoproteins [422]. Increased oxidative stress is considered to be a feature of PD [423]. Although it is currently unknown whether it is a cause or a consequence of the dopaminergic neuron cell loss, reducing oxidative stress was reported to be neuroprotective. Considering this, it was hypothesized that Se supplementation could have a neuroprotective effect by reducing oxidative stress [424, 425]. Indeed, Se supplementation was reported to reduce oxidative stress and neuronal loss, at least in a rat model of Parkinsonism [426], although the dose and chemical form of Se is still a matter of debate [427]. On the other hand, PD patients display higher levels of Se in the cerebrospinal fluid (CSF) [428, 429], potentially as a compensatory mechanisms to attempt to control the increased oxidative stress. PD is not only associated with oxidative stress, but is also increasingly considered to have features of autoimmunity, displaying peripheral inflammation and immune activity [131, 133]. Se supplementation could also be beneficial for this facet of PD. Although the causal role of the immune system in PD is not yet fully established, having anti-inflammatory properties, Se could reduce the inflammation in PD patients and potentially contribute to the improvement of PD pathogenesis. We showed that Se supplementation in the cell culture medium, reduced the cytokine expression of CD4 T cells [31]. Having generally very similar mechanisms of regulation, CD8 T cells might respond similarly to Se

supplementation and could potentially help to control the activated terminally-differentiated effector CD8 T cells that we and others have observed in PD and AD patients, respectively. Immune responses and inflammation lead to oxidative stress, which itself is an inducer of inflammation [430]. With that in mind, Se could disrupt this positive feedback and thus promote homeostasis by reducing oxidative stress directly and via reducing inflammation. The relationship between Parkinson's disease, the immune system and Selenium could potentially translate our findings of the role of Se and selenoproteins in CD4 T cells into an approach to reduce the immune activity, and thus controlling the potential autoimmune responses in PD patients.

Selenium also crosses paths with stress hormone signalling. Increased Selenium levels were measured in patients undergoing glucocorticoid treatment, although the reason for this remains unknown [431]. Considering this, together with the anti-inflammatory effect of Se, increased levels of Selenium could contribute to the known anti-inflammatory effect of the glucocorticoids. Meanwhile, Se was also shown to induce beta-adrenergic receptor activity in the thoracic aorta and the heart of rats [432, 433]. Considering the role of stress hormones signalling in regulating CD4 T cell differentiation, as described in chapter 2, the ability of Se to alter the responsiveness of beta-adrenergic receptors could also have implication in the regulation of the Th1/Th2 balance. Supporting this notion, a recent study has identified a role of Selenium and the selenoprotein GPX4 in the regulation of Tfh cells [434]. Se supplementation increased the numbers of Tfh cells and promoted an antibody response after influenza vaccination. On the other hand, supra-physiological levels of selenium skewed the CD4 Th balance towards Th1. Further studies are necessary to clarify the role of Se in CD4 T cells differentiation and the potential interplay with stress hormone signalling.

Stress has been shown to be detrimental for a wide range of diseases, including cancer, allergy, inflammatory and autoimmune diseases. Similarly, stress has also been hypothesized to contribute to the development of neurodegenerative diseases, including PD and AD [435-439]. Although there is an established link between stress and AD [440], the evidence linking stress and PD is scarcer and circumstantial. Nevertheless, stress accelerated dopaminergic neuron loss in a rat model of PD [441]. More recently, a survey performed in ~ 5.000 PD patient, suggested that stress worsens both motor and non-motor symptoms and that mindfulness could reduce stress and improve PD symptom severity [442]. Furthermore cortisol levels were reported to be increased in PD patients and its diurnal fluctuation was perturbed [443, 444]. On the other, the anti-inflammatory properties of GCs were shown to be beneficial and reduce microglial inflammation-induced neuronal cell death [445, 446]. Moreover, the synthetic GC, hydrocortisone, induces the expression

of the known PD-associated gene Parkin and prevented dopaminergic neuron loss in several PD animal models [447]. Similar to GCs, beta-adrenergic receptor agonist have anti-inflammatory properties and were shown to be beneficial in PD by suppressing pro-inflammatory microglial responses, thus reducing neural cytotoxicity in response to inflammation [448, 449]. Furthermore, β2AR was found to be a regulator of the α-synuclein gene (SNCA). While the β2AR agonist Salbutamol, was associated with a reduced risk of developing PD, the β2AR antagonists correlated with an increased disease risk [450, 451]. In chapter 2, we described how stress hormones inhibit cellular type I Immune responses in a T-cell-intrinsic manner, whereas promoting a humoral type II response. Meanwhile, we have observed increased CD8 T cell activity in PD patients. Although the implication of those CD8 T cells in PD are not yet fully understood, stress hormones signalling could inhibit the potentially harmful cytotoxic CD8 T cell responses, ameliorating peripheral inflammation in PD. Overall, the role of stress in the initiation or progression of PD is not fully understood and more studies are needed to address these questions.

Although this thesis has no direct link with the current global COVID-19 pandemic, some of the results outlined in the different chapters might have clinical implications in COVID-19. Although not included in this dissertation, it is worth mentioning that our group has made use of its immunological and clinical expertise and substantially contributed to deep immune profiling of COVID-19 patients and household controls in Luxembourg [452].

In chapter 1, we have shown that Selenium and the selenoprotein SELS/VIMP has anti-inflammatory properties in CD4 T cells, which has important implications for autoimmune diseases [453]. Considering these results and early reports of a cytokine storm in severely ill COVID-19 patients, one could hypothesize that Se supplementation would help reducing the excessive inflammation to avoid tissue damage. On the other hand, Se has been found to have immune-enhancing properties in the context of viral and bacterial infections by promoting a type I cellular immunity [454, 455]. Either way, Selenium deficiency has been associated with a higher mortality risk for different bacterial and viral infections, including COVID-19 [454, 456-458]. It is so far unclear whether the increased risk of mortality related with Se deficiency arises from the loss of the anti-inflammatory features of Se or the lack its immune enhancing properties. Others have put forward an additional hypothesis from a non-immune perspective. Redox active Selenite (Se^{4+}) is suggested to be able to react with the sulfhydryl groups in the active site of viral protein disulphide isomerase, rendering the hydrophobic viral spike protein to lose its ability to react with the cell membrane proteins and prevents the viral to enter the cell [459]. More research is required to determine the effect of Se on different immune cells and its potential in the context of COVID-19. A clinical trial investigating supranutritional doses of Selenium in hospitalized patients with moderate,

severe or critical COVID-19 is scheduled to give results before the end of 2021 (ClinicalTrials.gov Identifier : NCT04869579).

The anti-inflammatory and immune-suppressive effects of the stress hormones norepinephrine and cortisol have been used to reduce excessive inflammation in severe COVID-19 cases [460-462]. However, based on our results showing that the stress hormones induce a shift in the Th1/Th2 balance of CD4 T Cells, this therapy might result in unwanted effect that could be detrimental for a proper immune response and the clearance of the virus. A robust cellular type I immune response is well documented to be required for efficiently clearing viral pathogens. Stress hormones are considered to reduce the cellular immunity to promote humoral responses. Although, neutralizing antibodies represent an important component of the anti-viral immune response, promoting their production to the expense of cellular immunity might have an overall detrimental effect on the course of the immune response against SARS-CoV-2. This risk becomes even more apparent considering that a highly coordinated immune response is required to avoid a severe course of the disease, which we have recently demonstrated [452]. Supporting the ambiguity of using synthetic stress hormone analogues, high cortisol levels in COVID-19 patients have been associated with an increased mortality [463].

Last, but not least, implications of COVID-19 for Parkinson's disease patients have been suggested. It has been reported that following the Spanish flu pandemic, the risk of PD was dramatically increased [464]. This has also been discussed as a hypothetical scenario for COVID-19 [465]. During the current pandemic, reports of neurological problem arising after an infection with SARS-CoV-2 have also accumulated. Similarly, some small studies have reported a worsening of motor- and non-motor symptoms in PD patients that suffered from COVID-19 [466-468]. SARS-CoV-2 has been found to invade the central nervous system [469], where, at least in rodents, different type of neurons, including dopaminergic neurons, express the ACE2 receptor [470-473], which SARS-CoV-2 uses to infect cells. Reaching the brain, SARS-CoV-2 could infect and kill dopaminergic neurons and accelerate the progression of PD. In addition, the inflammation, and in extreme cases the cytokine storm, provoked by the infection could contribute to this cytotoxicity. Overall, there is reason to believe that COVID-19 could contribute to the pathogenesis of PD, although so far the evidence is scarce. Nevertheless, the scientific community has published several review or perspective articles trying to hypothesize about the possible relationship between COVID-19 and PD [474-478].

In summary, the studies outlined in this thesis provide novel mechanistic insights into T cell regulation in the context of neuroimmunology, as well as their possible contribution to the pathogenesis Parkinson's disease. The findings of the different chapters might have clinical

applications, not only in neurodegenerative diseases, but also in a wide range of infectious, inflammatory, and autoimmune diseases in which T cells are dysregulated.

Appendix

List of Abbreviations

ACE2	: Angiotensin-converting enzyme 2
ACTH	: Adrenocorticotropic hormone
AD	: Alzheimer's disease
Ag	: Antigen
AKT	: also known as Protein Kinase B (PKB)
ANS	: Autonomous nervous system
APC	: Antigen-presenting cell
AR	: Adrenergic receptor
ASP	: Autism spectrum disorder
ATP	: Adenosine triphosphate
AVP	: Arginine vasopressin
BBB	: Blood-brain-barrier
BCR	: B-cell receptor
BMAL1	: Brain and Muscle ARNT-Like 1
BMP2	: Bone Morphogenetic Protein 2
cAMP	: Cyclic Adenosine monophosphate
CBA	: Cytometric Bead Array
CCR	: CC chemokine receptor
CD	: Cluster of differentiation
CEBPG	: CCAAT Enhancer Binding Protein gamma
CFSE	: Carboxyfluorescein succinimidyl ester
ChAT	: Choline acetyl transferase
CHOP	: C/EBP Homologous Protein
cJun	: Jun proto-oncogene
CLOCK	: Clock Circadian Regulator
CM	: Central memory
CMV	: Cytomegalovirus
CNS	: Central nervous system
COVID19	: Coronavirus disease 2019 caused by SARS-CoV-2
CRF	: Corticotrophin-releasing factor
CRY1/2	: Cryptochrome 1 or 2
CSF	: Cerebrospinal fluid
CTLA4	: Cytotoxic T-lymphocyte-associated protein 4
Ctrl siRNA	: control scrambled random siRNA
CXCR	: CXC chemokine receptor

DAG	: Diacylglycerol
DCs	: Dendritic cells
DN	: Double negative
DNAJB9	: DnaJ Heat Shock Protein Family (Hsp40) Member B9
DNAJC3	: DnaJ Heat Shock Protein Family (Hsp40) Member C3
DP	: Double positive
E2F5	: E2F Transcription Factor 5
EAE	: Experimental autoimmune encephalitis
EDEM	: ER Degradation Enhancing Alpha-Mannosidase like Protein
EM	: Effector memory
ENS	: Enteric nervous system
EOMES	: Eomesodermin
EP	: Epinephrine
ER	: Endoplasmic reticulum
ERAD	: ER-associated degradation
ERK	: Extracellular signal-regulated kinase
Forsk	: Forskolin
FOXP3	: Forkhead box P3
Gads	: Grb2-related adaptor downstream of Shc
GAPDH	: Glyceraldehyde 3-phosphate dehydrogenase
GC	: Glucocorticoids
Geomean	: Geometric mean, also known as MFI
GI	: Gastro-intestinal
GLUT1	: Glucose Transporter 1
GM-CSF	: Granulocyte-macrophage colony-stimulating factor
GPX4	: Glutathione Peroxidase 4
GR	: Glucocorticoid receptor
GRAP2	: GRB2 Related Adaptor Protein 2
Grb2	: Growth Factor Receptor Bound Protein 2
GRP78	: Glucose regulated protein
GTP	: Guanosine triphosphate
GWAS	: Genome-wide association study
HC (in chapter 2)	: Hydrocortisone, synthetic glucocorticoid
HC (in chapter 3)	: Healthy control
HELIOS	: Zinc finger protein Helios
HIF-1α	: Hypoxia Inducible Factor 1 alpha
HLA	: Human leukocyte antigens

HPA : Hypothalamus-pituary-adrenal
HSC : Hematopoietic stem cell
HTR : high-time-resolution
IBD : Inflammatory bowel disease
ICOS : Inducible T-cell co-stimulator
IFNγ : Interferon gamma
Ig : Immunoglobulin
IKK : I kappa B Kinase
IL : Interleukin
ILC : Innate lymphoid cells
IMDM : Iscoves Modified Dulbecco's Medium
IP_3 : Inositol 1, 4, 5-trisphosphate
IR : Immune response
IRX3 : Iroquois homeobox 3
IS : Immune system
ISO : Isoproterenol, a β2AR agonist
ITAM : Immunoreceptor tyrosine-based activation motif
ITK : Interleukin-2-inducible T-cell kinase
JAK : Janus kinase
JNK : c-Jun N-terminal kinases
KLRG1 : Killer cell lectin-like receptor subfamily G member 1
LAG3 : Lymphocyte-activation gene 3
LAT : Linker for activation of T cells
Lck : Lymphocyte-specific protein tyrosine kinase
LN : Lymph nodes
LPS : Lipopolysaccharides
LTF : Lineage transcription factor
MAPK : mitogen-activated protein kinase
MCP1 : Monocyte chemo-attractant protein 1
M-CSF : Macrophage colony stimulating factor
MEF : Mouse embryonic fibroblast
MHC : Major histocompatibility complex
mLST8 : Mammalian lethal with Sec13 protein 8, also known as GβL
mRNA : Messenger RNA
MSD : Mesoscale discovery
mTORC : Mammalian target of rapamycin complex
NE : Norepinephrine

NFAT	: Nuclear factor of activated T-cells
NFIL3	: Nuclear Factor, Interleukin 3 Regulated
NFκB	: Nuclear factor kappa-light-chain-enhancer of activated B cells
NK	: Natural killer cells
NLR	: NOD-like receptor
NR1D1/2	: Nuclear receptor subfamily 1 group D member 1 or 2
NS	: non-significant
PAMP	: Pattern-associated molecular pattern
PaNS	: Parasympathetic nervous system
PBMCs	: Peripheral blood mononuclear cells
PD	: Parkinson's disease
PD-1	: Programmed cell death protein 1
PDK1	: 3-phosphoinositide-dependent protein kinase 1
PER1/2/3	: Period 1, 2, 3
PI3K	: Phosphoinositide 3-kinase
PIP_2	: Phosphatidylinositol 4, 5-bisphosphate
PIP_3	: Phosphatidylinositol 3, 4, 5-triphosphate
PKA	: Protein kinase A
PKC	: Protein kinase C
PLCγ	: Phospholipase C gamma
PRR	: Pattern recognition receptor
PVN	: Paraventricular nucleus
qPCR	: quantitative real-time PCR
RA	: Rheumatoid arthritis
Rac	: Rac (GTPase)
RAF1	: RAF proto-oncogene serine/threonine-protein kinase
Raptor	: Regulatory protein associated with mTOR
Ras	: Ras (GTPase), Rat sarcoma virus
RasGRP	: RAS guanyl-releasing protein 1
Rho	: Rho factor
Rictor	: Rapamycin insensitive companion of mTOR
RNF14	: Ring finger protein 14
RORα	: RAR related orphan receptor alpha
RORγT	: RAR-related orphan receptor gamma
S.D.	: Standard deviation
SAM	: Sympathetic-adrenal-medullary
SARS-CoV-2	: Severe acute respiratory syndrome coronavirus 2

SCFA	: Short-chain fatty acid
Se	: Selenium
SELS	: Selenoprotein S, also known as VIMP
Ser (or S)	: Serine
SLP76	: SH2 domain containing leukocyte protein of 76kDa
SNCA	: Synuclein alpha
SNP	: Single nucleotide polymorphism
SNS	: Sympathetic nervous system
SOS	: Son of Sevenless protein
SP	: Single positive
STAT	: Signal transducer and activator of transcription
TBX21 (Tbet)	: T-box transcription factor TBX21 (T-box expressed in T cells)
Tc	: Cytotoxic T cell
TCR	: T-cell receptor
Teff	: Effector T cells
TEMRA	: Terminally-differentiated effector cells
TF	: Transcription factor
TGFβ	: Transforming growth factor beta
Th	: T helper cell
Thr	: Threonine
TLR	: Toll-like receptor
TNFα	: Tumor necrosis factor alpha
Treg	: Regulatory T cells
Tyr	: Tyrosine
US	: Unstimulated
UT	: Untreated
VIP	: Vasoactive intestinal peptide
XBP1	: X-Box binding protein 1
Zap70	: Zeta Chain of T-cell Receptor Associated Protein Kinase 70
ZBTB20	: Zinc finger and BTB domain containing 20
α7nAchR	: Nicotinic acetylcholine receptor subunit alpha 7
β2AR	: Beta 2 adrenergic receptor

List of scientific outcomes

Christophe M. Capelle, Ni Zeng, Egle Danileviciute, Sabrina Freitas Rodrigues, Markus Ollert, Rudi Balling, Feng Q. He. Identification of VIMP as a gene inhibiting cytokine production in human CD4+ effector T cells. *Published in iScience, 24, 4, 2021, 102289*, https://doi.org/10.1016/j.isci.2021.102289.

Christophe M. Capelle, Anna Chen, Ni Zeng, Alexandre Baron, Kamil Grzyb, Alexander Skupin, Markus Ollert, Feng He, Stress hormone signalling intrinsically inhibits Th1 polarization in naïve CD4 cells via the clock gene Period1 and mTORC1. *Published in Immunology. 2022; 165: 428– 444.* https://doi.org/10.1111/imm.13448

Christophe M. Capelle, Séverine Ciré, Maxime Hansen, Lukas Pavelka, Fanny Hedin, Maria Konstantinou, Dominique Revets, Vera Tslaf, Alexandre Baron, Ni Zeng, Antonio Cosma, Rudi Balling, Rejko Krüger, Markus Ollert, Feng Q. Hefeng. Systems immunology discloses an increased terminally-differentiated effector CD8 T cell profile in early-to-mid stage Parkinson's disease. *Manuscript in Scriptum.*

Christophe M. Capelle, Séverine Ciré, Wim Ammerlaan, Maria Konstantinou, Rudi Balling, Fay Betsou, Antonio Cosma, Markus Ollert, Feng Q. Hefeng. Standard PBMC cryopreservation selectively decreases detection of nine clinically-relevant T-cell markers. *Published in ImmunoHorizons.* https://doi.org/10.4049/immunohorizons.2100049

Christophe M. Capelle[#], Séverine Cire[#], Olivia Domingues, Isabelle Ernens, Fanny Hedin, Aurélie Fischer, Chantal Snoeck, Wim Ammerlaan, Maria Konstantinou, Kamil Grzyb, Alex Skupin, Cara L. Carty, Christiane Hilger, Georges Gilson, Aljosa Celebic, Paul Wilmes, Antonio Del Sol, Ian M. Kaplan, Fay Betsou, Tamir Abdelrahman, Antonio Cosma, Michel Vaillant, Guy Fagherazzi, Markus Ollert*, Feng Q. Hefeng*. Combinatorial analysis reveals highly coordinatedearly-stage immune reactions that predict laterantiviral immunity in mild COVID-19 patients. *Published in Cell Reports Medicine 3, 100600 April 19, 2022.* https://doi.org/10.1016/j.xcrm.2022.100600

Egle Danileviciute*, Ni Zeng*, **Christophe M. Capelle**, Nicole Paczia, Mark A. Gillespie, Henry Kurniawan, Mohaned Benzarti, Myriam P. Merz, Djalil Coowar, Sabrina Fritah, Daniela Maria Vogt Weisenhorn, Gemma Gomez Giro, Melanie Grusdat, Alexandre Baron, Coralie Guerin, Davide G. Franchina, Cathy Léonard, Olivia Domingues, Sylvie Delhalle, Wolfgang Wurst, Jonathan D. Turner, Jens Christian Schwamborn, Johannes Meier, Rejko Krüger, Jeff Ranish, Dirk Brenner, Carole L. Linster, Rudi Balling, Markus Ollert, Feng Q. He. PARK7/DJ-1 promotes pyruvate dehydrogenase activity and maintains Treg homeostasis. *Published in Nature Metabolism **4**, 589–607 (2022).* https://doi.org/10.1038/s42255-022-00576-y

Ni Zeng*, **Christophe M. Capelle***, Alexandre Baron, Takumi Kobayashi, Séverine Cire, Vera Tslaf, Cathy Leonard, Djalil Coowar, Haruhiko Koseki, Astrid M. Westendorf, Jan Buer, Dirk Brenner, Rejko Krüger, Rudi Balling, Markus Ollert, Feng Q. Hefeng. DJ-1 depletion prevents immunoaging in T-cell compartments. *Published in EMBO reports (2022)23:e53302.* https://doi.org/10.15252/embr.202153302

Rucha Sawlekar[#], Stefano Magni[#], **Christophe M. Capelle**[#], Alexandre Baron, Ni Zeng, Laurent Mombaerts, Zuogong Yue, Ye Yuan, Feng Q. He* and Jorge Gonçalves*. Causal dynamical modelling predicts novel regulatory genes of FOXP3 in human regulatory T cells*. In revision in npj Systems Biology and Applications.*
https://doi.org/10.1101/2020.02.13.943688

Ni Zeng, Maud Theresine, **Christophe M. Capelle**, Neha Patil, Cécile Masquelier, Caroline Davril, Alexander Baron, Djalil Coowar, Xavier Dervillez, Aurélie Poli, Cathy Leonard, Rudi Balling, Markus Ollert, Jacques Zimmer, Feng Q. He. FAM13A regulates maturation and effector functions of natural killer cells. *Manuscript submitted to iScience.* https://doi.org/10.1101/2020.08.26.268490

Massimiliano Zanin, Bruno F. R. Santos, Paul M. A. Antony, Clara Berenguer-Escuder, Simone B. Larsen, Zoé Hanss,Peter A. Barbuti, Aidos S. Baumuratov, Dajana Grossmann **Christophe M. Capelle**, Joseph Weber, Rudi Balling, Markus Ollert, Rejko Krüger, Nico J. Diederich and Feng Q. He. Mitochondria interaction networks show altered topological patterns in Parkinson's disease. *Published in npj Systems Biology and Applications* **6,** 38 (2020). https://doi.org/10.1038/s41540-020-00156-4

References

1. Abul Abbas, A.L., Shiv Pillai, *Cellular and Molecular Immunology*. 8th ed. 2014. 544.
2. Fung-Leung, W.-P., et al., *CD8 is needed for development of cytotoxic T but not helper T cells.* Cell, 1991. **65**(3): p. 443-449.
3. Zhang, N. and M.J. Bevan, *CD8(+) T cells: foot soldiers of the immune system.* Immunity, 2011. **35**(2): p. 161-8.
4. Zhu, J. and W.E. Paul, *CD4 T cells: fates, functions, and faults.* Blood, 2008. **112**(5): p. 1557-69.
5. Germain, R.N., *T-cell development and the CD4-CD8 lineage decision.* Nat Rev Immunol, 2002. **2**(5): p. 309-22.
6. Mueller, S.N., et al., *Memory T cell subsets, migration patterns, and tissue residence.* Annu Rev Immunol, 2013. **31**: p. 137-61.
7. Golubovskaya, V. and L. Wu, *Different Subsets of T Cells, Memory, Effector Functions, and CAR-T Immunotherapy.* Cancers (Basel), 2016. **8**(3).
8. Willinger, T., et al., *Molecular signatures distinguish human central memory from effector memory CD8 T cell subsets.* J Immunol, 2005. **175**(9): p. 5895-903.
9. Mucida, D. and H. Cheroutre, *The many face-lifts of CD4 T helper cells.* Adv Immunol, 2010. **107**: p. 139-52.
10. Schmitt, E., M. Klein, and T. Bopp, *Th9 cells, new players in adaptive immunity.* Trends Immunol, 2014. **35**(2): p. 61-8.
11. Jia, L. and C. Wu, *The biology and functions of Th22 cells.* Adv Exp Med Biol, 2014. **841**: p. 209-30.
12. Beissert, S., A. Schwarz, and T. Schwarz, *Regulatory T cells.* J Invest Dermatol, 2006. **126**(1): p. 15-24.
13. Zhu, J., H. Yamane, and W.E. Paul, *Differentiation of effector CD4 T cell populations (*).* Annu Rev Immunol, 2010. **28**: p. 445-89.
14. Sawant, D.V. and D.A. Vignali, *Once a Treg, always a Treg?* Immunol Rev, 2014. **259**(1): p. 173-91.
15. Chakraborty, A.K. and A. Weiss, *Insights into the initiation of TCR signalling.* Nat Immunol, 2014. **15**(9): p. 798-807.
16. Courtney, A.H., W.L. Lo, and A. Weiss, *TCR Signalling: Mechanisms of Initiation and Propagation.* Trends Biochem Sci, 2018. **43**(2): p. 108-123.
17. Han, J.M., S.J. Patterson, and M.K. Levings, *The Role of the PI3K Signalling Pathway in CD4(+) T Cell Differentiation and Function.* Front Immunol, 2012. **3**: p. 245.
18. Seif, F., et al., *The role of JAK-STAT signalling pathway and its regulators in the fate of T helper cells.* Cell Commun Signal, 2017. **15**(1): p. 23.
19. Passerini, L., et al., *STAT5-signalling cytokines regulate the expression of FOXP3 in CD4+CD25+ regulatory T cells and CD4+CD25- effector T cells.* Int Immunol, 2008. **20**(3): p. 421-31.
20. Siegel, A.M., et al., *A critical role for STAT3 transcription factor signalling in the development and maintenance of human T cell memory.* Immunity, 2011. **35**(5): p. 806-18.
21. Cui, W., et al., *An interleukin-21-interleukin-10-STAT3 pathway is critical for functional maturation of memory CD8+ T cells.* Immunity, 2011. **35**(5): p. 792-805.
22. Li, Q., et al., *IL-12-programmed long-term CD8+ T cell responses require STAT4.* J Immunol, 2006. **177**(11): p. 7618-25.
23. Tripathi, P., et al., *STAT5 is critical to maintain effector CD8+ T cell responses.* J Immunol, 2010. **185**(4): p. 2116-24.

24. Wei, J., et al., *Nutrient and Metabolic Sensing in T Cell Responses.* Front Immunol, 2017. **8**: p. 247.

25. Chi, H., *Regulation and function of mTOR signalling in T cell fate decisions.* Nat Rev Immunol, 2012. **12**(5): p. 325-38.

26. Waickman, A.T. and J.D. Powell, *mTOR, metabolism, and the regulation of T-cell differentiation and function.* Immunol Rev, 2012. **249**(1): p. 43-58.

27. Pollizzi, K.N., et al., *mTORC1 and mTORC2 selectively regulate CD8(+) T cell differentiation.* J Clin Invest, 2015. **125**(5): p. 2090-108.

28. Maggini, S., A. Pierre, and P.C. Calder, *Immune Function and Micronutrient Requirements Change over the Life Course.* Nutrients, 2018. **10**(10).

29. Labunskyy, V.M., D.L. Hatfield, and V.N. Gladyshev, *Selenoproteins: molecular pathways and physiological roles.* Physiol Rev, 2014. **94**(3): p. 739-77.

30. Duntas, L.H., *Selenium and inflammation: underlying anti-inflammatory mechanisms.* Horm Metab Res, 2009. **41**(6): p. 443-7.

31. Capelle, C.M., et al., *Identification of VIMP as a gene inhibiting cytokine production in human CD4+ effector T cells.* iScience, 2021. **24**(4): p. 102289.

32. Donia, M.S. and M.A. Fischbach, *HUMAN MICROBIOTA. Small molecules from the human microbiota.* Science, 2015. **349**(6246): p. 1254766.

33. Lin, L. and J. Zhang, *Role of intestinal microbiota and metabolites on gut homeostasis and human diseases.* BMC Immunol, 2017. **18**(1): p. 2.

34. Garrett, W.S., *Immune recognition of microbial metabolites.* Nat Rev Immunol, 2020. **20**(2): p. 91-92.

35. Zheng, D., T. Liwinski, and E. Elinav, *Interaction between microbiota and immunity in health and disease.* Cell Res, 2020. **30**(6): p. 492-506.

36. Levy, M., C.A. Thaiss, and E. Elinav, *Metabolites: messengers between the microbiota and the immune system.* Genes Dev, 2016. **30**(14): p. 1589-97.

37. Arpaia, N., et al., *Metabolites produced by commensal bacteria promote peripheral regulatory T-cell generation.* Nature, 2013. **504**(7480): p. 451-5.

38. Bachem, A., et al., *Microbiota-Derived Short-Chain Fatty Acids Promote the Memory Potential of Antigen-Activated CD8(+) T Cells.* Immunity, 2019. **51**(2): p. 285-297 e5.

39. Louveau, A., et al., *CNS lymphatic drainage and neuroinflammation are regulated by meningeal lymphatic vasculature.* Nat Neurosci, 2018. **21**(10): p. 1380-1391.

40. Ahn, J.H., et al., *Meningeal lymphatic vessels at the skull base drain cerebrospinal fluid.* Nature, 2019. **572**(7767): p. 62-66.

41. Louveau, A., et al., *Structural and functional features of central nervous system lymphatic vessels.* Nature, 2015. **523**(7560): p. 337-41.

42. Louveau, A., T.H. Harris, and J. Kipnis, *Revisiting the Mechanisms of CNS Immune Privilege.* Trends Immunol, 2015. **36**(10): p. 569-577.

43. Kraneveld, A.D., et al., *The neuro-immune axis: prospect for novel treatments for mental disorders.* Basic Clin Pharmacol Toxicol, 2014. **114**(1): p. 128-36.

44. Nutma, E., et al., *Neuroimmunology - the past, present and future.* Clin Exp Immunol, 2019. **197**(3): p. 278-293.

45. Jansen, A.S., et al., *Central command neurons of the sympathetic nervous system: basis of the fight-or-flight response.* Science, 1995. **270**(5236): p. 644-6.

46. Goyal, R.K. and I. Hirano, *The enteric nervous system.* N Engl J Med, 1996. **334**(17): p. 1106-15.

47. Dantzer, R., *Neuroimmune Interactions: From the Brain to the Immune System and Vice Versa.* Physiol Rev, 2018. **98**(1): p. 477-504.

48. Zhang, X. and Y. Zhang, *Neural-immune communication in Caenorhabditis elegans.* Cell Host Microbe, 2009. **5**(5): p. 425-9.

49. Bellinger, D.L. and D. Lorton, *Autonomic regulation of cellular immune function.* Auton Neurosci, 2014. **182**: p. 15-41.

50. Godinho-Silva, C., F. Cardoso, and H. Veiga-Fernandes, *Neuro-Immune Cell Units: A New Paradigm in Physiology.* Annu Rev Immunol, 2019. **37**: p. 19-46.

51. Kioussis, D. and V. Pachnis, *Immune and nervous systems: more than just a superficial similarity?* Immunity, 2009. **31**(5): p. 705-10.

52. Sotelo, J., *The nervous and the immune systems: conspicuous physiological analogies.* J Comp Physiol A Neuroethol Sens Neural Behav Physiol, 2015. **201**(2): p. 185-94.

53. Habibi, L., M. Ebtekar, and S.B. Jameie, *Immune and nervous systems share molecular and functional similarities: memory storage mechanism.* Scand J Immunol, 2009. **69**(4): p. 291-301.

54. Dubin, A.E. and A. Patapoutian, *Nociceptors: the sensors of the pain pathway.* J Clin Invest, 2010. **120**(11): p. 3760-72.

55. Peltier, D.C., et al., *Human neuronal cells possess functional cytoplasmic and TLR-mediated innate immune pathways influenced by phosphatidylinositol-3 kinase signalling.* J Immunol, 2010. **184**(12): p. 7010-21.

56. Chen, C.Y., et al., *Beyond defense: regulation of neuronal morphogenesis and brain functions via Toll-like receptors.* J Biomed Sci, 2019. **26**(1): p. 90.

57. Kigerl, K.A., et al., *Pattern recognition receptors and central nervous system repair.* Exp Neurol, 2014. **258**: p. 5-16.

58. Steinberg, B.E., et al., *Cytokine-specific Neurograms in the Sensory Vagus Nerve.* Bioelectronic Medicine, 2016. **3**(1): p. 7-17.

59. Cook, A.D., et al., *Immune Cytokines and Their Receptors in Inflammatory Pain.* Trends Immunol, 2018. **39**(3): p. 240-255.

60. Becher, B., S. Spath, and J. Goverman, *Cytokine networks in neuroinflammation.* Nat Rev Immunol, 2017. **17**(1): p. 49-59.

61. Mousa, A. and M. Bakhiet, *Role of cytokine signalling during nervous system development.* Int J Mol Sci, 2013. **14**(7): p. 13931-57.

62. Kerage, D., et al., *Interaction of neurotransmitters and neurochemicals with lymphocytes.* J Neuroimmunol, 2019. **332**: p. 99-111.

63. Chen, C.-S., C. Barnoud, and C. Scheiermann, *Peripheral neurotransmitters in the immune system.* Current Opinion in Physiology, 2021. **19**: p. 73-79.

64. Rosas-Ballina, M., et al., *Acetylcholine-synthesizing T cells relay neural signals in a vagus nerve circuit.* Science, 2011. **334**(6052): p. 98-101.

65. Dustin, M.L., *Signalling at neuro/immune synapses.* J Clin Invest, 2012. **122**(4): p. 1149-55.

66. Tournier, J.-N. and A.Q. Hellmann, *Neuro-immune connections: evidence for a neuro-immunological synapse.* Trends in Immunology, 2003. **24**(3): p. 114-115.

67. Shaw, A.S. and P.M. Allen, *Kissing cousins: immunological and neurological synapses.* Nat Immunol, 2001. **2**(7): p. 575-6.

68. McMahon, S.B., F. La Russa, and D.L. Bennett, *Crosstalk between the nociceptive and immune systems in host defence and disease.* Nat Rev Neurosci, 2015. **16**(7): p. 389-402.

69. Ji, R.R., A. Chamessian, and Y.Q. Zhang, *Pain regulation by non-neuronal cells and inflammation.* Science, 2016. **354**(6312): p. 572-577.

70. Pinho-Ribeiro, F.A., W.A. Verri, Jr., and I.M. Chiu, *Nociceptor Sensory Neuron-Immune Interactions in Pain and Inflammation.* Trends Immunol, 2017. **38**(1): p. 5-19.

71. Storan, E.R., et al., *Role of cytokines and chemokines in itch.* Handb Exp Pharmacol, 2015. **226**: p. 163-76.

72. Datsi, A., et al., *Interleukin-31: The 'itchy' cytokine in inflammation and therapy.* Authorea, 2020.

73. Talbot, S., et al., *Silencing Nociceptor Neurons Reduces Allergic Airway Inflammation.* Neuron, 2015. **87**(2): p. 341-54.

74. Netea, M.G., B.J. Kullberg, and J.W. Van der Meer, *Circulating cytokines as mediators of fever.* Clin Infect Dis, 2000. **31 Suppl 5**: p. S178-84.

75. Dantzer, R. and K.W. Kelley, *Twenty years of research on cytokine-induced sickness behavior.* Brain Behav Immun, 2007. **21**(2): p. 153-60.

76. Dantzer, R., *Cytokine, sickness behavior, and depression.* Immunol Allergy Clin North Am, 2009. **29**(2): p. 247-64.

77. Miller, A.H., *Beyond depression: the expanding role of inflammation in psychiatric disorders.* World Psychiatry, 2020. **19**(1): p. 108-109.

78. Kipnis, J., et al., *T cell deficiency leads to cognitive dysfunction: implications for therapeutic vaccination for schizophrenia and other psychiatric conditions.* Proc Natl Acad Sci U S A, 2004. **101**(21): p. 8180-5.

79. Felger, J.C. and F.E. Lotrich, *Inflammatory cytokines in depression: neurobiological mechanisms and therapeutic implications.* Neuroscience, 2013. **246**: p. 199-229.

80. Rodrigues-Amorim, D., et al., *Cytokines dysregulation in schizophrenia: A systematic review of psychoneuroimmune relationship.* Schizophr Res, 2018. **197**: p. 19-33.

81. Masi, A., et al., *Cytokine aberrations in autism spectrum disorder: a systematic review and meta-analysis.* Mol Psychiatry, 2015. **20**(4): p. 440-6.

82. Morimoto, K. and K. Nakajima, *Role of the Immune System in the Development of the Central Nervous System.* Front Neurosci, 2019. **13**: p. 916.

83. Jakob, M.O., S. Murugan, and C.S.N. Klose, *Neuro-Immune Circuits Regulate Immune Responses in Tissues and Organ Homeostasis.* Front Immunol, 2020. **11**: p. 308.

84. Veiga-Fernandes, H. and D. Artis, *Neuronal-immune system cross-talk in homeostasis.* Science, 2018. **359**(6383): p. 1465-1466.

85. Ziv, Y., et al., *Immune cells contribute to the maintenance of neurogenesis and spatial learning abilities in adulthood.* Nat Neurosci, 2006. **9**(2): p. 268-75.

86. Wu, Y., et al., *Microglia: Dynamic Mediators of Synapse Development and Plasticity.* Trends Immunol, 2015. **36**(10): p. 605-613.

87. Li, Q. and B.A. Barres, *Microglia and macrophages in brain homeostasis and disease.* Nat Rev Immunol, 2018. **18**(4): p. 225-242.

88. Wolf, S.A., et al., *CD4-positive T lymphocytes provide a neuroimmunological link in the control of adult hippocampal neurogenesis.* J Immunol, 2009. **182**(7): p. 3979-84.

89. Radjavi, A., I. Smirnov, and J. Kipnis, *Brain antigen-reactive CD4+ T cells are sufficient to support learning behavior in mice with limited T cell repertoire.* Brain Behav Immun, 2014. **35**: p. 58-63.

90. Schiller, M., T.L. Ben-Shaanan, and A. Rolls, *Neuronal regulation of immunity: why, how and where?* Nat Rev Immunol, 2021. **21**(1): p. 20-36.

91. Tracey, K.J., *The inflammatory reflex.* Nature, 2002. **420**(6917): p. 853-9.

92. Olofsson, P.S., et al., *Rethinking inflammation: neural circuits in the regulation of immunity.* Immunol Rev, 2012. **248**(1): p. 188-204.

93. Arima, Y., et al., *Regional neural activation defines a gateway for autoreactive T cells to cross the blood-brain barrier.* Cell, 2012. **148**(3): p. 447-57.

94. Tanaka, Y., et al., *The Gateway Reflex, a Novel Neuro-Immune Interaction for the Regulation of Regional Vessels.* Front Immunol, 2017. **8**: p. 1321.

95. Tracey, K.J., *Immune cells exploit a neural circuit to enter the CNS.* Cell, 2012. **148**(3): p. 392-4.

96. Ohki, T., et al., *Gateway reflexes: A new paradigm of neuroimmune interactions.* Clinical and Experimental Neuroimmunology, 2017. **8**(1): p. 23-32.

97. Kamimura, D., et al., *Gateway reflex: Local neuroimmune interactions that regulate blood vessels.* Neurochem Int, 2019. **130**: p. 104303.

98. Jacobson, A., et al., *The intestinal neuro-immune axis: crosstalk between neurons, immune cells, and microbes.* Mucosal Immunology, 2021. **14**(3): p. 555-565.

99. Veiga-Fernandes, H. and V. Pachnis, *Neuroimmune regulation during intestinal development and homeostasis.* Nat Immunol, 2017. **18**(2): p. 116-122.

100. Huh, J.R. and H. Veiga-Fernandes, *Neuroimmune circuits in inter-organ communication.* Nat Rev Immunol, 2020. **20**(4): p. 217-228.

101. Rao, M. and M.D. Gershon, *The bowel and beyond: the enteric nervous system in neurological disorders.* Nat Rev Gastroenterol Hepatol, 2016. **13**(9): p. 517-28.

102. Muller, P.A., et al., *Crosstalk between muscularis macrophages and enteric neurons regulates gastrointestinal motility.* Cell, 2014. **158**(2): p. 300-313.

103. Chu, C., D. Artis, and I.M. Chiu, *Neuro-immune Interactions in the Tissues.* Immunity, 2020. **52**(3): p. 464-474.

104. Veiga-Fernandes, H. and D. Mucida, *Neuro-Immune Interactions at Barrier Surfaces.* Cell, 2016. **165**(4): p. 801-11.

105. McEwen, B.S., *Physiology and neurobiology of stress and adaptation: central role of the brain.* Physiol Rev, 2007. **87**(3): p. 873-904.

106. Padgett, D.A. and R. Glaser, *How stress influences the immune response.* Trends in Immunology, 2003. **24**(8): p. 444-448.

107. Segerstrom, S.C. and G.E. Miller, *Psychological stress and the human immune system: a meta-analytic study of 30 years of inquiry.* Psychol Bull, 2004. **130**(4): p. 601-30.

108. Quatrini, L. and S. Ugolini, *New insights into the cell- and tissue-specificity of glucocorticoid actions.* Cell Mol Immunol, 2021. **18**(2): p. 269-278.

109. Glaser, R. and J.K. Kiecolt-Glaser, *Stress-induced immune dysfunction: implications for health.* Nat Rev Immunol, 2005. **5**(3): p. 243-51.

110. Pavlov, V.A. and K.J. Tracey, *Neural regulation of immunity: molecular mechanisms and clinical translation.* Nat Neurosci, 2017. **20**(2): p. 156-166.

111. Bonaz, B., V. Sinniger, and S. Pellissier, *Therapeutic Potential of Vagus Nerve Stimulation for Inflammatory Bowel Diseases.* Front Neurosci, 2021. **15**: p. 650971.

112. Chavan, S.S., V.A. Pavlov, and K.J. Tracey, *Mechanisms and Therapeutic Relevance of Neuro-immune Communication.* Immunity, 2017. **46**(6): p. 927-942.

113. Deczkowska, A. and M. Schwartz, *Targeting neuro-immune communication in neurodegeneration: Challenges and opportunities.* J Exp Med, 2018. **215**(11): p. 2702-2704.

114. Ben-Eliyahu, S., *The promotion of tumor metastasis by surgery and stress: Immunological basis and implications for psychoneuroimmunology.* Brain, Behavior, and Immunity, 2003. **17**(1): p. 27-36.

115. Antoni, M.H. and F.S. Dhabhar, *The impact of psychosocial stress and stress management on immune responses in patients with cancer.* Cancer, 2019. **125**(9): p. 1417-1431.

116. van der Goes, M.C., J.W. Jacobs, and J.W. Bijlsma, *The value of glucocorticoid co-therapy in different rheumatic diseases--positive and adverse effects.* Arthritis Res Ther, 2014. **16 Suppl 2**: p. S2.

117. Porcelli, L., et al., *The beta-adrenergic receptor antagonist propranolol offsets resistance mechanisms to chemotherapeutics in diverse sarcoma subtypes: a pilot study.* Sci Rep, 2020. **10**(1): p. 10465.

118. Schuller, H.M., *Beta-adrenergic signalling, a novel target for cancer therapy?* Oncotarget, 2010. **1**(7): p. 466-469.

119. Tang, J., et al., *beta-Adrenergic system, a backstage manipulator regulating tumour progression and drug target in cancer therapy.* Semin Cancer Biol, 2013. **23**(6 Pt B): p. 533-42.

120. Koopman, F.A., et al., *Vagus nerve stimulation inhibits cytokine production and attenuates disease severity in rheumatoid arthritis.* Proc Natl Acad Sci U S A, 2016. **113**(29): p. 8284-9.

121. Tracey, K.J., *Hacking the inflammatory reflex.* The Lancet Rheumatology, 2021. **3**(4): p. e237-e239.

122. Genovese, M.C., et al., *Safety and efficacy of neurostimulation with a miniaturised vagus nerve stimulation device in patients with multidrug-refractory rheumatoid arthritis: a two-stage multicentre, randomised pilot study.* The Lancet Rheumatology, 2020. **2**(9): p. e527-e538.

123. Marsal, S., et al., *Non-invasive vagus nerve stimulation for rheumatoid arthritis: a proof-of-concept study.* The Lancet Rheumatology, 2021. **3**(4): p. e262-e269.

124. Bonaz, B., et al., *Chronic vagus nerve stimulation in Crohn's disease: a 6-month follow-up pilot study.* Neurogastroenterol Motil, 2016. **28**(6): p. 948-53.

125. Brymer, K.J., et al., *Exploring the Potential Antidepressant Mechanisms of TNFalpha Antagonists.* Front Neurosci, 2019. **13**: p. 98.

126. Uzzan, S. and A.N. Azab, *Anti-TNF-alpha Compounds as a Treatment for Depression.* Molecules, 2021. **26**(8).

127. Abbott, R., et al., *Tumour necrosis factor-alpha inhibitor therapy in chronic physical illness: A systematic review and meta-analysis of the effect on depression and anxiety.* J Psychosom Res, 2015. **79**(3): p. 175-84.

128. Kappelmann, N., et al., *Antidepressant activity of anti-cytokine treatment: a systematic review and meta-analysis of clinical trials of chronic inflammatory conditions.* Mol Psychiatry, 2018. **23**(2): p. 335-343.

129. Uguz, F., et al., *Anti-tumor necrosis factor-alpha therapy is associated with less frequent mood and anxiety disorders in patients with rheumatoid arthritis.* Psychiatry Clin Neurosci, 2009. **63**(1): p. 50-5.

130. Hickman, S., et al., *Microglia in neurodegeneration.* Nat Neurosci, 2018. **21**(10): p. 1359-1369.

131. Qin, X.Y., et al., *Aberrations in Peripheral Inflammatory Cytokine Levels in Parkinson Disease: A Systematic Review and Meta-analysis.* JAMA Neurol, 2016. **73**(11): p. 1316-1324.

132. Baird, J.K., et al., *The key role of T cells in Parkinson's disease pathogenesis and therapy.* Parkinsonism Relat Disord, 2019. **60**: p. 25-31.

133. Garretti, F., et al., *Autoimmunity in Parkinson's Disease: The Role of alpha-Synuclein-Specific T Cells.* Front Immunol, 2019. **10**: p. 303.

134. Gate, D., et al., *Clonally expanded CD8 T cells patrol the cerebrospinal fluid in Alzheimer's disease.* Nature, 2020. **577**(7790): p. 399-404.

135. Matheoud, D., et al., *Intestinal infection triggers Parkinson's disease-like symptoms in Pink1(-/-) mice.* Nature, 2019. **571**(7766): p. 565-569.

136. Wang, P., et al., *Single-cell transcriptome and TCR profiling reveal activated and expanded T cell populations in Parkinson's disease.* Cell Discov, 2021. **7**(1): p. 52.

137. He, F. and R. Balling, *The role of regulatory T cells in neurodegenerative diseases.* Wiley Interdiscip Rev Syst Biol Med, 2013. **5**(2): p. 153-80.

138. Wang, Q., Y. Liu, and J. Zhou, *Neuroinflammation in Parkinson's disease and its potential as therapeutic target.* Transl Neurodegener, 2015. **4**: p. 19.

139. Villani, A.C., S. Sarkizova, and N. Hacohen, *Systems Immunology: Learning the Rules of the Immune System.* Annu Rev Immunol, 2018. **36**: p. 813-842.

140. Sommer, A., et al., *Th17 Lymphocytes Induce Neuronal Cell Death in a Human iPSC-Based Model of Parkinson's Disease.* Cell Stem Cell, 2018. **23**(1): p. 123-131 e6.

141. Tomic, A., A.J. Pollard, and M.M. Davis, *Systems Immunology: Revealing Influenza Immunological Imprint.* Viruses, 2021. **13**(5).

142. Delhalle, S., et al., *A roadmap towards personalized immunology.* NPJ Syst Biol Appl, 2018. **4**: p. 9.

143. Davis, M.M., C.M. Tato, and D. Furman, *Systems immunology: just getting started.* Nat Immunol, 2017. **18**(7): p. 725-732.

144. He, F., et al., *PLAU inferred from a correlation network is critical for suppressor function of regulatory T cells.* Mol Syst Biol, 2012. **8**: p. 624.

145. Zhu, J. and W.E. Paul, *Heterogeneity and plasticity of T helper cells.* Cell Res, 2010. **20**(1): p. 4-12.

146. Zhu, J. and W.E. Paul, *Peripheral CD4+ T-cell differentiation regulated by networks of cytokines and transcription factors.* Immunol Rev, 2010. **238**(1): p. 247-62.

147. Rodriguez-Jorge, O., et al., *Cooperation between T cell receptor and Toll-like receptor 5 signalling for CD4(+) T cell activation.* Sci Signal, 2019. **12**(577).

148. Saez-Rodriguez, J., et al., *A logical model provides insights into T cell receptor signalling.* PLoS Comput Biol, 2007. **3**(8): p. e163.

149. Brownlie, R.J. and R. Zamoyska, *T cell receptor signalling networks: branched, diversified and bounded.* Nat Rev Immunol, 2013. **13**(4): p. 257-69.

150. Schomburg, L., *Selenium, selenoproteins and the thyroid gland: interactions in health and disease.* Nat Rev Endocrinol, 2011. **8**(3): p. 160-71.

151. Qin, H.S., et al., *Paclitaxel inhibits selenoprotein S expression and attenuates endoplasmic reticulum stress.* Mol Med Rep, 2016. **13**(6): p. 5118-24.

152. Kim, K.H., et al., *SEPS1 protects RAW264.7 cells from pharmacological ER stress agent-induced apoptosis.* Biochem Biophys Res Commun, 2007. **354**(1): p. 127-32.

153. Ye, Y., et al., *Recruitment of the p97 ATPase and ubiquitin ligases to the site of retrotranslocation at the endoplasmic reticulum membrane.* Proc Natl Acad Sci U S A, 2005. **102**(40): p. 14132-8.

154. Lee, J.H., et al., *Selenoprotein S-dependent Selenoprotein K Binding to p97(VCP) Protein Is Essential for Endoplasmic Reticulum-associated Degradation.* J Biol Chem, 2015. **290**(50): p. 29941-52.

155. Ye, Y., et al., *A membrane protein complex mediates retro-translocation from the ER lumen into the cytosol.* Nature, 2004. **429**(6994): p. 841-7.

156. Alanne, M., et al., *Variation in the selenoprotein S gene locus is associated with coronary heart disease and ischemic stroke in two independent Finnish cohorts.* Hum Genet, 2007. **122**(3-4): p. 355-65.

157. Olsson, M., et al., *Expression of the selenoprotein S (SELS) gene in subcutaneous adipose tissue and SELS genotype are associated with metabolic risk factors.* Metabolism, 2011. **60**(1): p. 114-20.

158. Karlsson H.K., T.H., Lake S., Koistinen H.A., and Krook A., *Relationship between serum amyloid A level and Tanis/SelS mRNA expression in skeletal muscle and adipose tissue from healthy and type 2 diabetic subjects.* Diabetes, 2004. **53(6)**: p. p. 1424-8.

159. Meplan, C., et al., *Genetic variants in selenoprotein genes increase risk of colorectal cancer.* Carcinogenesis, 2010. **31**(6): p. 1074-9.

160. Sutherland, A., et al., *Polymorphisms in the selenoprotein S and 15-kDa selenoprotein genes are associated with altered susceptibility to colorectal cancer.* Genes Nutr, 2010. **5**(3): p. 215-23.

161. Shibata, T., et al., *Selenoprotein S (SEPS1) gene -105G>A promoter polymorphism influences the susceptibility to gastric cancer in the Japanese population.* BMC Gastroenterol, 2009. **9**: p. 2.

162. He, L., et al., *Protective effects of the SEPS1 gene on lipopolysaccharide-induced sepsis.* Mol Med Rep, 2014. **9**(5): p. 1869-76.

163. Santos, L.R., et al., *A polymorphism in the promoter region of the selenoprotein S gene (SEPS1) contributes to Hashimoto's thyroiditis susceptibility.* J Clin Endocrinol Metab, 2014. **99**(4): p. E719-23.

164. Seiderer, J., et al., *The role of the selenoprotein S (SELS) gene -105G>A promoter polymorphism in inflammatory bowel disease and regulation of SELS gene expression in intestinal inflammation.* Tissue Antigens, 2007. **70**(3): p. 238-46.

165. Kuchroo, V.K., et al., *Dysregulation of immune homeostasis in autoimmune diseases.* Nat Med, 2012. **18**(1): p. 42-7.

166. McGuckin, M.A., et al., *ER stress and the unfolded protein response in intestinal inflammation.* Am J Physiol Gastrointest Liver Physiol, 2010. **298**(6): p. G820-32.

167. Curran, J.E., et al., *Genetic variation in selenoprotein S influences inflammatory response.* Nat Genet, 2005. **37**(11): p. 1234-41.

168. Fradejas, N., et al., *Selenoprotein S expression in reactive astrocytes following brain injury.* Glia, 2011. **59**(6): p. 959-72.

169. Martinez, A., et al., *Polymorphisms in the selenoprotein S gene: lack of association with autoimmune inflammatory diseases.* BMC Genomics, 2008. **9**: p. 329.

170. Mathew, D., et al., *Deep immune profiling of COVID-19 patients reveals distinct immunotypes with therapeutic implications.* Science, 2020. **369**(6508): p. eabc8511.

171. Braun, J., et al., *SARS-CoV-2-reactive T cells in healthy donors and patients with COVID-19.* Nature, 2020. **587**(7833): p. 270-274.

172. Beyer, A., S. Bandyopadhyay, and T. Ideker, *Integrating physical and genetic maps: from genomes to interaction networks.* Nat Rev Genet, 2007. **8**(9): p. 699-710.

173. Gillis, J. and P. Pavlidis, *The role of indirect connections in gene networks in predicting function.* Bioinformatics, 2011. **27**(13): p. 1860-6.

174. Oliver, S., *Guilt-by-association goes global.* Nature, 2000. **403**(6770): p. 601-3.

175. Danileviciute, E., et al., *PARK7/DJ-1 promotes pyruvate dehydrogenase activity and maintains Treg homeostasis.* 2019: p. https://doi.org/10.1101/2019.12.20.884809.

176. Szklarczyk, D., et al., *STRING v11: protein-protein association networks with increased coverage, supporting functional discovery in genome-wide experimental datasets.* Nucleic Acids Res, 2019. **47**(D1): p. D607-D613.

177. Langfelder, P. and S. Horvath, *WGCNA: an R package for weighted correlation network analysis.* BMC Bioinformatics, 2008. **9**: p. 559.

178. van Dam, S., et al., *Gene co-expression analysis for functional classification and gene-disease predictions.* Brief Bioinform, 2018. **19**(4): p. 575-592.

179. He, F.Q. and M. Ollert, *Network-Guided Key Gene Discovery for a Given Cellular Process.* Adv Biochem Eng Biotechnol, 2016.

180. Lee, A.H., N.N. Iwakoshi, and L.H. Glimcher, *XBP-1 regulates a subset of endoplasmic reticulum resident chaperone genes in the unfolded protein response.* Mol Cell Biol, 2003. **23**(21): p. 7448-59.

181. Yoshida, H., et al., *XBP1 mRNA is induced by ATF6 and spliced by IRE1 in response to ER stress to produce a highly active transcription factor.* Cell, 2001. **107**(7): p. 881-91.

182. Speckmann, B., et al., *Selenoprotein S is a marker but not a regulator of endoplasmic reticulum stress in intestinal epithelial cells.* Free Radic Biol Med, 2014. **67**: p. 265-77.

183. Rauhamaa, P., et al., *Selenium levels of Estonians.* Eur J Clin Nutr, 2008. **62**(9): p. 1075-8.

184. Safaralizadeh, R., et al., *Serum concentration of selenium in healthy individuals living in Tehran.* Nutr J, 2005. **4**: p. 32.

185. Stranges, S., et al., *Selenium status and blood lipids: the cardiovascular risk in Young Finns study.* J Intern Med, 2011. **270**(5): p. 469-77.

186. Zhang, H.M., et al., *AnimalTFDB: a comprehensive animal transcription factor database.* Nucleic Acids Res, 2012. **40**(Database issue): p. D144-9.

187. Brennan, P., et al., *Phosphatidylinositol 3-kinase couples the interleukin-2 receptor to the cell cycle regulator E2F.* Immunity, 1997. **7**(5): p. 679-89.

188. Sharma, S., et al., *Dephosphorylation of the nuclear factor of activated T cells (NFAT) transcription factor is regulated by an RNA-protein scaffold complex.* Proc Natl Acad Sci U S A, 2011. **108**(28): p. 11381-6.

189. Okamura, H., et al., *Concerted dephosphorylation of the transcription factor NFAT1 induces a conformational switch that regulates transcriptional activity.* Mol Cell, 2000. **6**(3): p. 539-50.

190. Chow, C.W., M. Rincon, and R.J. Davis, *Requirement for transcription factor NFAT in interleukin-2 expression.* Mol Cell Biol, 1999. **19**(3): p. 2300-7.

191. Hogan, P.G., et al., *Transcriptional regulation by calcium, calcineurin, and NFAT.* Genes Dev, 2003. **17**(18): p. 2205-32.

192. Pitts, M.W. and P.R. Hoffmann, *Endoplasmic reticulum-resident selenoproteins as regulators of calcium signalling and homeostasis.* Cell Calcium, 2018. **70**(70): p. 76-86.

193. Joost, S., et al., *Single-Cell Transcriptomics Reveals that Differentiation and Spatial Signatures Shape Epidermal and Hair Follicle Heterogeneity.* Cell Systems, 2016. **3**(3): p. 221-237.e9.

194. Ingham, A.B., et al., *RNF14 is a regulator of mitochondrial and immune function in muscle.* BMC Syst Biol, 2014. **8**: p. 10.

195. Zhang, W., et al., *Identification and characterization of DPZF, a novel human BTB/POZ zinc finger protein sharing homology to BCL-6.* Biochem Biophys Res Commun, 2001. **282**(4): p. 1067-73.

196. Liu, X., et al., *Zinc finger protein ZBTB20 promotes Toll-like receptor-triggered innate immune responses by repressing IkappaBalpha gene transcription.* Proc Natl Acad Sci U S A, 2013. **110**(27): p. 11097-102.

197. Zhu, C., et al., *Regulation of the Development and Function of B Cells by ZBTB Transcription Factors.* Front Immunol, 2018. **9**: p. 580.

198. Persengiev, S.P., *Identification of an Essential IL15-STAT1-IRX3 Prosurvival Pathway in T Lymphocytes with Therapeutic Implications.* bioRxiv, 2017: p. 178939.

199. Tanaka, S., et al., *CCAAT/enhancer-binding protein alpha negatively regulates IFN-gamma expression in T cells.* J Immunol, 2014. **193**(12): p. 6152-60.

200. Berberich-Siebelt, F., et al., *C/EBPβ enhances IL-4 but impairs IL-2 and IFN-γ induction in T cells.* European Journal of Immunology, 2000. **30**(9): p. 2576-2585.

201. Stoedter, M., et al., *Selenium controls the sex-specific immune response and selenoprotein expression during the acute-phase response in mice.* Biochem J, 2010. **429**(1): p. 43-51.

202. Tsuji, P.A., et al., *Dietary Selenium Levels Affect Selenoprotein Expression and Support the Interferon-gamma and IL-6 Immune Response Pathways in Mice.* Nutrients, 2015. **7**(8): p. 6529-49.

203. Hao, S., et al., *Selenium Alleviates Aflatoxin B(1)-Induced Immune Toxicity through Improving Glutathione Peroxidase 1 and Selenoprotein S Expression in Primary Porcine Splenocytes.* J Agric Food Chem, 2016. **64**(6): p. 1385-93.

204. Beck, M.A. and C.C. Matthews, *Micronutrients and host resistance to viral infection.* Proc Nutr Soc, 2000. **59**(4): p. 581-5.

205. Beck, M.A., et al., *Selenium deficiency increases the pathology of an influenza virus infection.* FASEB J, 2001. **15**(8): p. 1481-3.

206. Duffield-Lillico, A.J., et al., *Selenium supplementation, baseline plasma selenium status and incidence of prostate cancer: an analysis of the complete treatment period of the Nutritional Prevention of Cancer Trial.* BJU Int, 2003. **91**(7): p. 608-12.

207. Kim, H.-C., et al., *Protection of methamphetamine nigrostriatal toxicity by dietary selenium.* Brain Research, 1999. **851**(1-2): p. 76-86.

208. Kim, H.-C., et al., *Selenium deficiency potentiates methamphetamine-induced nigral neuronal loss; comparison with MPTP model.* Brain Research, 2000. **862**(1-2): p. 247-252.

209. Kudva, A.K., A.E. Shay, and K.S. Prabhu, *Selenium and inflammatory bowel disease.* Am J Physiol Gastrointest Liver Physiol, 2015. **309**(2): p. G71-7.

210. Klein, S.L. and K.L. Flanagan, *Sex differences in immune responses.* Nat Rev Immunol, 2016. **16**(10): p. 626-38.

211. vom Steeg, L.G. and S.L. Klein, *SeXX Matters in Infectious Disease Pathogenesis.* PLoS Pathog, 2016. **12**(2): p. e1005374.

212. Angum, F., et al., *The Prevalence of Autoimmune Disorders in Women: A Narrative Review.* Cureus, 2020. **12**(5): p. e8094.

213. Jacobson, D.L., et al., *Epidemiology and estimated population burden of selected autoimmune diseases in the United States.* Clin Immunol Immunopathol, 1997. **84**(3): p. 223-43.

214. Afshan, G., N. Afzal, and S. Qureshi, *CD4+CD25(hi) regulatory T cells in healthy males and females mediate gender difference in the prevalence of autoimmune diseases.* Clin Lab, 2012. **58**(5-6): p. 567-71.

215. Aldridge, J., et al., *Sex-based differences in association between circulating T cell subsets and disease activity in untreated early rheumatoid arthritis patients.* Arthritis Res Ther, 2018. **20**(1): p. 150.

216. Kocar, I.H., et al., *The effect of testosterone replacement treatment on immunological features of patients with Klinefelter's syndrome.* Clin Exp Immunol, 2000. **121**(3): p. 448-52.

217. Cacciari, E., et al., *Serum immunoglobulins and lymphocyte subpopulations derangement in Turner's syndrome.* J Immunogenet, 1981. **8**(5): p. 337-44.

218. Bianchi, I., et al., *The X chromosome and immune associated genes.* J Autoimmun, 2012. **38**(2-3): p. J187-92.

219. Straub, R.H., *The complex role of estrogens in inflammation.* Endocr Rev, 2007. **28**(5): p. 521-74.

220. Kawai, K., et al., *Sex differences in the effects of maternal vitamin supplements on mortality and morbidity among children born to HIV-infected women in Tanzania.* Br J Nutr, 2010. **103**(12): p. 1784-91.

221. Jensen, K.J., et al., *The effects of vitamin A supplementation with measles vaccine on leucocyte counts and in vitro cytokine production.* Br J Nutr, 2016. **115**(4): p. 619-28.

222. Seale, L.A., A.N. Ogawa-Wong, and M.J. Berry, *Sexual Dimorphism in Selenium Metabolism and Selenoproteins.* Free Radic Biol Med, 2018. **127**: p. 198-205.

223. Pitts, M.W., et al., *Competition between the Brain and Testes under Selenium-Compromised Conditions: Insight into Sex Differences in Selenium Metabolism and Risk of Neurodevelopmental Disease.* J Neurosci, 2015. **35**(46): p. 15326-38.

224. Li, J., et al., *Gender difference in the association of serum selenium with all-cause and cardiovascular mortality.* Postgrad Med, 2020. **132**(2): p. 148-155.

225. Lu, C.W., et al., *Gender Differences with Dose(-)Response Relationship between Serum Selenium Levels and Metabolic Syndrome-A Case-Control Study.* Nutrients, 2019. **11**(2).

226. Waters, D.J., et al., *Making sense of sex and supplements: differences in the anticarcinogenic effects of selenium in men and women.* Mutat Res, 2004. **551**(1-2): p. 91-107.

227. Riese, C., et al., *Selenium-dependent pre- and posttranscriptional mechanisms are responsible for sexual dimorphic expression of selenoproteins in murine tissues.* Endocrinology, 2006. **147**(12): p. 5883-92.

228. Schomburg, L. and U. Schweizer, *Hierarchical regulation of selenoprotein expression and sex-specific effects of selenium.* Biochim Biophys Acta, 2009. **1790**(11): p. 1453-62.

229. Santesmasses, D., M. Mariotti, and V.N. Gladyshev, *Tolerance to Selenoprotein Loss Differs between Human and Mouse.* Mol Biol Evol, 2020. **37**(2): p. 341-354.

230. Addinsall, A.B., et al., *Impaired exercise performance is independent of inflammation and cellular stress following genetic reduction or deletion of selenoprotein S.* Am J Physiol Regul Integr Comp Physiol, 2020. **318**(5): p. R981-R996.

231. Addinsall, A.B., et al., *Deficiency of selenoprotein S, an endoplasmic reticulum resident oxidoreductase, impairs the contractile function of fast-twitch hindlimb muscles.* Am J Physiol Regul Integr Comp Physiol, 2018. **315**(2): p. R380-R396.

232. Wright, C.R., et al., *A Reduction in Selenoprotein S Amplifies the Inflammatory Profile of Fast-Twitch Skeletal Muscle in the mdx Dystrophic Mouse.* Mediators Inflamm, 2017. **2017**: p. 7043429.

233. Sawlekar, R., et al., *Causal dynamical modelling predicts novel regulatory genes of FOXP3 in human regulatory T cells.* bioRxiv, 2020: p. 2020.02.13.943688.

234. Probst-Kepper, M., et al., *GARP: a key receptor controlling FOXP3 in human regulatory T cells.* J Cell Mol Med, 2009. **13**(9B): p. 3343-57.

235. Berchtold, N.C., et al., *Gene expression changes in the course of normal brain aging are sexually dimorphic.* Proc Natl Acad Sci U S A, 2008. **105**(40): p. 15605-10.

236. Weigand, J.E., et al., *Hypoxia-induced alternative splicing in endothelial cells.* PLoS One, 2012. **7**(8): p. e42697.

237. Cutolo, M. and R.H. Straub, *Stress as a risk factor in the pathogenesis of rheumatoid arthritis.* Neuroimmunomodulation, 2006. **13**(5-6): p. 277-82.

238. Dave, N.D., et al., *Stress and allergic diseases.* Immunol Allergy Clin North Am, 2011. **31**(1): p. 55-68.

239. Song, H., et al., *Association of Stress-Related Disorders With Subsequent Autoimmune Disease.* JAMA, 2018. **319**(23): p. 2388-2400.

240. Stojanovich, L. and D. Marisavljevich, *Stress as a trigger of autoimmune disease.* Autoimmun Rev, 2008. **7**(3): p. 209-13.

241. Dai, S., et al., *Chronic Stress Promotes Cancer Development.* Front Oncol, 2020. **10**: p. 1492.

242. Sephton, S. and D. Spiegel, *Circadian disruption in cancer: a neuroendocrine-immune pathway from stress to disease?* Brain Behav Immun, 2003. **17**(5): p. 321-8.

243. Ben-Eliyahu, S., *The promotion of tumor metastasis by surgery and stress: immunological basis and implications for psychoneuroimmunology.* Brain Behav Immun, 2003. **17 Suppl 1**: p. S27-36.

244. Shaashua, L., et al., *Perioperative COX-2 and beta-Adrenergic Blockade Improves Metastatic Biomarkers in Breast Cancer Patients in a Phase-II Randomized Trial.* Clin Cancer Res, 2017. **23**(16): p. 4651-4661.

245. Cohen, S., *Psychological stress and susceptibility to upper respiratory infections.* Am J Respir Crit Care Med, 1995. **152**(4 Pt 2): p. S53-8.

246. Biondi, M. and L.G. Zannino, *Psychological stress, neuroimmunomodulation, and susceptibility to infectious diseases in animals and man: a review.* Psychother Psychosom, 1997. **66**(1): p. 3-26.

247. Wieduwild, E., et al., *beta2-adrenergic signals downregulate the innate immune response and reduce host resistance to viral infection.* J Exp Med, 2020. **217**(4).

248. Brinkmann, V. and C. Kristofic, *Regulation by corticosteroids of Th1 and Th2 cytokine production in human CD4+ effector T cells generated from CD45RO- and CD45RO+ subsets.* J Immunol, 1995. **155**(7): p. 3322-8.

249. Ramer-Quinn, D.S., et al., *Cytokine production by naive and primary effector CD4+ T cells exposed to norepinephrine.* Brain Behav Immun, 2000. **14**(4): p. 239-55.

250. Sanders, V.M., et al., *Differential expression of the beta2-adrenergic receptor by Th1 and Th2 clones: implications for cytokine production and B cell help.* J Immunol, 1997. **158**(9): p. 4200-10.

251. Riether, C., et al., *Stimulation of beta(2)-adrenergic receptors inhibits calcineurin activity in CD4(+) T cells via PKA-AKAP interaction.* Brain Behav Immun, 2011. **25**(1): p. 59-66.

252. Arumugham, V.B. and C.T. Baldari, *cAMP: a multifaceted modulator of immune synapse assembly and T cell activation.* J Leukoc Biol, 2017. **101**(6): p. 1301-1316.

253. Ayroldi, E., et al., *Modulation of T-cell activation by the glucocorticoid-induced leucine zipper factor via inhibition of nuclear factor kappaB.* Blood, 2001. **98**(3): p. 743-53.

254. Lowenberg, M., et al., *Rapid immunosuppressive effects of glucocorticoids mediated through Lck and Fyn.* Blood, 2005. **106**(5): p. 1703-10.

255. Lowenberg, M., et al., *Glucocorticoids cause rapid dissociation of a T-cell-receptor-associated protein complex containing LCK and FYN.* EMBO Rep, 2006. **7**(10): p. 1023-9.

256. Lowenberg, M., et al., *Glucocorticoid signalling: a nongenomic mechanism for T-cell immunosuppression.* Trends Mol Med, 2007. **13**(4): p. 158-63.

257. Boldizsar, F., et al., *Emerging pathways of non-genomic glucocorticoid (GC) signalling in T cells.* Immunobiology, 2010. **215**(7): p. 521-6.

258. Cannarile, L., et al., *Implicating the Role of GILZ in Glucocorticoid Modulation of T-Cell Activation.* Front Immunol, 2019. **10**: p. 1823.

259. Engler, J.B., et al., *Glucocorticoid receptor in T cells mediates protection from autoimmunity in pregnancy.* Proc Natl Acad Sci U S A, 2017. **114**(2): p. E181-E190.

260. Ugor, E., et al., *Glucocorticoid hormone treatment enhances the cytokine production of regulatory T cells by upregulation of Foxp3 expression.* Immunobiology, 2018. **223**(4-5): p. 422-431.

261. Estrada, L.D., D. Agac, and J.D. Farrar, *Sympathetic neural signalling via the beta2-adrenergic receptor suppresses T-cell receptor-mediated human and mouse CD8(+) T-cell effector function.* Eur J Immunol, 2016. **46**(8): p. 1948-58.

262. Qiao, G., et al., *beta-Adrenergic signalling blocks murine CD8(+) T-cell metabolic reprogramming during activation: a mechanism for immunosuppression by adrenergic stress.* Cancer Immunol Immunother, 2019. **68**(1): p. 11-22.

263. Hong, J.Y., et al., *Long-Term Programming of CD8 T Cell Immunity by Perinatal Exposure to Glucocorticoids.* Cell, 2020. **180**(5): p. 847-861 e15.

264. Kasprowicz, D.J., et al., *Stimulation of the B cell receptor, CD86 (B7-2), and the beta 2-adrenergic receptor intrinsically modulates the level of IgG1 and IgE produced per B cell.* J Immunol, 2000. **165**(2): p. 680-90.

265. Podojil, J.R. and V.M. Sanders, *Selective regulation of mature IgG1 transcription by CD86 and beta 2-adrenergic receptor stimulation.* J Immunol, 2003. **170**(10): p. 5143-51.

266. Zhang, X., et al., *Brain control of humoral immune responses amenable to behavioural modulation.* Nature, 2020. **581**(7807): p. 204-208.

267. Pongratz, G., et al., *The level of IgE produced by a B cell is regulated by norepinephrine in a p38 MAPK- and CD23-dependent manner.* J Immunol, 2006. **177**(5): p. 2926-38.

268. Elenkov, I.J. and G.P. Chrousos, *Stress hormones, proinflammatory and antiinflammatory cytokines, and autoimmunity.* Ann N Y Acad Sci, 2002. **966**: p. 290-303.

269. Goyarts, E., et al., *Norepinephrine modulates human dendritic cell activation by altering cytokine release.* Exp Dermatol, 2008. **17**(3): p. 188-96.

270. Takenaka, M.C., et al., *Norepinephrine Controls Effector T Cell Differentiation through beta2-Adrenergic Receptor-Mediated Inhibition of NF-kappaB and AP-1 in Dendritic Cells.* J Immunol, 2016. **196**(2): p. 637-44.

271. Escoter-Torres, L., et al., *Fighting the Fire: Mechanisms of Inflammatory Gene Regulation by the Glucocorticoid Receptor.* Front Immunol, 2019. **10**: p. 1859.

272. Gabanyi, I., et al., *Neuro-immune Interactions Drive Tissue Programming in Intestinal Macrophages.* Cell, 2016. **164**(3): p. 378-91.

273. Ehrchen, J.M., J. Roth, and K. Barczyk-Kahlert, *More Than Suppression: Glucocorticoid Action on Monocytes and Macrophages.* Front Immunol, 2019. **10**: p. 2028.

274. Sun, Z., et al., *Norepinephrine inhibits the cytotoxicity of NK92MI cells via the beta2adrenoceptor/cAMP/PKA/pCREB signalling pathway.* Mol Med Rep, 2018. **17**(6): p. 8530-8535.

275. Holbrook, N.J., W.I. Cox, and H.C. Horner, *Direct suppression of natural killer activity in human peripheral blood leukocyte cultures by glucocorticoids and its modulation by interferon.* Cancer Res, 1983. **43**(9): p. 4019-25.

276. Nair, M.P. and S.A. Schwartz, *Immunomodulatory effects of corticosteroids on natural killer and antibody-dependent cellular cytotoxic activities of human lymphocytes.* J Immunol, 1984. **132**(6): p. 2876-82.

277. Capellino, S., M. Claus, and C. Watzl, *Regulation of natural killer cell activity by glucocorticoids, serotonin, dopamine, and epinephrine.* Cell Mol Immunol, 2020. **17**(7): p. 705-711.

278. Quatrini, L., et al., *Glucocorticoids and the cytokines IL-12, IL-15, and IL-18 present in the tumor microenvironment induce PD-1 expression on human natural killer cells.* J Allergy Clin Immunol, 2021. **147**(1): p. 349-360.

279. Diaz-Salazar, C., et al., *Cell-intrinsic adrenergic signalling controls the adaptive NK cell response to viral infection.* J Exp Med, 2020. **217**(4).

280. Moriyama, S., et al., *beta2-adrenergic receptor-mediated negative regulation of group 2 innate lymphoid cell responses.* Science, 2018. **359**(6379): p. 1056-1061.

281. Mohammadpour, H., et al., *beta2 adrenergic receptor-mediated signalling regulates the immunosuppressive potential of myeloid-derived suppressor cells.* J Clin Invest, 2019. **129**(12): p. 5537-5552.

282. Saffar, A.S., H. Ashdown, and A.S. Gounni, *The molecular mechanisms of glucocorticoids-mediated neutrophil survival.* Curr Drug Targets, 2011. **12**(4): p. 556-62.

283. Nicholls, A.J., et al., *Activation of the sympathetic nervous system modulates neutrophil function.* J Leukoc Biol, 2018. **103**(2): p. 295-309.

284. Wang, M., et al., *Impaired anti-inflammatory action of glucocorticoid in neutrophil from patients with steroid-resistant asthma.* Respir Res, 2016. **17**(1): p. 153.

285. Raap, U., et al., *The functional activity of basophil granulocytes is modulated by acute mental stress and sympathetic activation in vivo and in vitro.* J Allergy Clin Immunol, 2008. **122**(6): p. 1227-9.

286. Assaf, A.M., R. Al-Abbassi, and M. Al-Binni, *Academic stress-induced changes in Th1- and Th2-cytokine response.* Saudi Pharm J, 2017. **25**(8): p. 1237-1247.

287. Elenkov, I.J., *Glucocorticoids and the Th1/Th2 balance.* Ann N Y Acad Sci, 2004. **1024**: p. 138-46.

288. Iwakabe, K., et al., *The restraint stress drives a shift in Th1/Th2 balance toward Th2-dominant immunity in mice.* Immunology Letters, 1998. **62**(1): p. 39-43.

289. Glaser, R., et al., *Evidence for a shift in the Th-1 to Th-2 cytokine response associated with chronic stress and aging.* J Gerontol A Biol Sci Med Sci, 2001. **56**(8): p. M477-82.

290. Kin, N.W. and V.M. Sanders, *It takes nerve to tell T and B cells what to do.* J Leukoc Biol, 2006. **79**(6): p. 1093-104.

291. Paik, I.H., et al., *Psychological stress may induce increased humoral and decreased cellular immunity.* Behav Med, 2000. **26**(3): p. 139-41.

292. Yang, H., et al., *Stress-glucocorticoid-TSC22D3 axis compromises therapy-induced antitumor immunity.* Nat Med, 2019. **25**(9): p. 1428-1441.

293. Jean Wrobel, L., et al., *Propranolol induces a favourable shift of anti-tumor immunity in a murine spontaneous model of melanoma.* Oncotarget, 2016. **7**(47): p. 77825-77837.

294. Porcelli, L., et al., *The β-adrenergic receptor antagonist propranolol offsets resistance mechanisms to chemotherapeutics in diverse sarcoma subtypes: a pilot study.* Scientific Reports, 2020. **10**(1).

295. Kroon, J., et al., *Glucocorticoid receptor antagonism reverts docetaxel resistance in human prostate cancer.* Endocr Relat Cancer, 2016. **23**(1): p. 35-45.

296. So, A.Y., et al., *Glucocorticoid regulation of the circadian clock modulates glucose homeostasis.* Proc Natl Acad Sci U S A, 2009. **106**(41): p. 17582-7.

297. Terazono, H., et al., *Adrenergic regulation of clock gene expression in mouse liver.* Proc Natl Acad Sci U S A, 2003. **100**(11): p. 6795-800.

298. Druzd, D., et al., *Lymphocyte Circadian Clocks Control Lymph Node Trafficking and Adaptive Immune Responses.* Immunity, 2017. **46**(1): p. 120-132.

299. He, W., et al., *Circadian Expression of Migratory Factors Establishes Lineage-Specific Signatures that Guide the Homing of Leukocyte Subsets to Tissues.* Immunity, 2018. **49**(6): p. 1175-1190 e7.

300. Ince, L.M., J. Weber, and C. Scheiermann, *Control of Leukocyte Trafficking by Stress-Associated Hormones.* Front Immunol, 2018. **9**: p. 3143.

301. Nguyen, K.D., et al., *Circadian gene Bmal1 regulates diurnal oscillations of Ly6C(hi) inflammatory monocytes.* Science, 2013. **341**(6153): p. 1483-8.

302. Pick, R., et al., *Time-of-Day-Dependent Trafficking and Function of Leukocyte Subsets.* Trends Immunol, 2019. **40**(6): p. 524-537.

303. Suzuki, K., et al., *Adrenergic control of the adaptive immune response by diurnal lymphocyte recirculation through lymph nodes.* J Exp Med, 2016. **213**(12): p. 2567-2574.

304. Zhao, Y., et al., *Uncovering the mystery of opposite circadian rhythms between mouse and human leukocytes in humanized mice.* Blood, 2017. **130**(18): p. 1995-2005.

305. Shimba, A., et al., *Glucocorticoids Drive Diurnal Oscillations in T Cell Distribution and Responses by Inducing Interleukin-7 Receptor and CXCR4.* Immunity, 2018. **48**(2): p. 286-298 e6.

306. Carroll, R.G., et al., *Immunometabolism around the Clock.* Trends Mol Med, 2019. **25**(7): p. 612-625.

307. Curtis, A.M., et al., *Circadian clock proteins and immunity.* Immunity, 2014. **40**(2): p. 178-86.

308. Leach, S. and K. Suzuki, *Adrenergic Signalling in Circadian Control of Immunity.* Front Immunol, 2020. **11**: p. 1235.

309. Scheiermann, C., et al., *Clocking in to immunity.* Nat Rev Immunol, 2018. **18**(7): p. 423-437.

310. Shimba, A. and K. Ikuta, *Glucocorticoids Regulate Circadian Rhythm of Innate and Adaptive Immunity.* Front Immunol, 2020. **11**: p. 2143.

311. Gnanaprakasam, J.N.R., J.W. Sherman, and R. Wang, *MYC and HIF in shaping immune response and immune metabolism.* Cytokine Growth Factor Rev, 2017. **35**: p. 63-70.

312. Wang, R., et al., *The transcription factor Myc controls metabolic reprogramming upon T lymphocyte activation.* Immunity, 2011. **35**(6): p. 871-82.

313. Araujo, L.P., et al., *The Sympathetic Nervous System Mitigates CNS Autoimmunity via beta2-Adrenergic Receptor Signalling in Immune Cells.* Cell Rep, 2019. **28**(12): p. 3120-3130 e5.

314. Athie-Morales, V., et al., *Sustained IL-12 signalling is required for Th1 development.* J Immunol, 2004. **172**(1): p. 61-9.

315. Usui, T., et al., *T-bet regulates Th1 responses through essential effects on GATA-3 function rather than on IFNG gene acetylation and transcription.* J Exp Med, 2006. **203**(3): p. 755-66.

316. Delgoffe, G.M., et al., *The kinase mTOR regulates the differentiation of helper T cells through the selective activation of signalling by mTORC1 and mTORC2.* Nat Immunol, 2011. **12**(4): p. 295-303.

317. Zeng, H. and H. Chi, *mTOR signalling in the differentiation and function of regulatory and effector T cells.* Curr Opin Immunol, 2017. **46**: p. 103-111.

318. Pollizzi, K.N. and J.D. Powell, *Regulation of T cells by mTOR: the known knowns and the known unknowns.* Trends Immunol, 2015. **36**(1): p. 13-20.

319. Xie, J., et al., *cAMP inhibits mammalian target of rapamycin complex-1 and -2 (mTORC1 and 2) by promoting complex dissociation and inhibiting mTOR kinase activity.* Cell Signal, 2011. **23**(12): p. 1927-35.

320. Grzanka, A., et al., *Molecular mechanisms of glucocorticoids action: implications for treatment of rhinosinusitis and nasal polyposis.* Eur Arch Otorhinolaryngol, 2011. **268**(2): p. 247-53.

321. Linsell, C.R., et al., *Circadian rhythms of epinephrine and norepinephrine in man.* J Clin Endocrinol Metab, 1985. **60**(6): p. 1210-5.

322. Chung, S., G.H. Son, and K. Kim, *Circadian rhythm of adrenal glucocorticoid: its regulation and clinical implications.* Biochim Biophys Acta, 2011. **1812**(5): p. 581-91.

323. Bollinger, T., et al., *Circadian clocks in mouse and human CD4+ T cells.* PLoS One, 2011. **6**(12): p. e29801.

324. Cox, K.H. and J.S. Takahashi, *Circadian clock genes and the transcriptional architecture of the clock mechanism.* J Mol Endocrinol, 2019. **63**(4): p. R93-R102.

325. Reddy, T.E., et al., *The hypersensitive glucocorticoid response specifically regulates period 1 and expression of circadian genes.* Mol Cell Biol, 2012. **32**(18): p. 3756-67.

326. Yang, G., et al., *Loss of the clock gene Per1 promotes oral squamous cell carcinoma progression via the AKT/mTOR pathway.* Cancer Sci, 2020. **111**(5): p. 1542-1554.

327. Wu, R., et al., *The Circadian Protein Period2 Suppresses mTORC1 Activity via Recruiting Tsc1 to mTORC1 Complex.* Cell Metab, 2019. **29**(3): p. 653-667 e6.

328. Ramanathan, C., et al., *mTOR signalling regulates central and peripheral circadian clock function.* PLoS Genet, 2018. **14**(5): p. e1007369.

329. Lipton, J.O., et al., *The Circadian Protein BMAL1 Regulates Translation in Response to S6K1-Mediated Phosphorylation.* Cell, 2015. **161**(5): p. 1138-1151.

330. Chornoguz, O., et al., *mTORC1 Promotes T-bet Phosphorylation To Regulate Th1 Differentiation.* J Immunol, 2017. **198**(10): p. 3939-3948.

331. Wehbi, V.L. and K. Tasken, *Molecular Mechanisms for cAMP-Mediated Immunoregulation in T cells - Role of Anchored Protein Kinase A Signalling Units.* Front Immunol, 2016. **7**: p. 222.

332. Herold, M.J., K.G. McPherson, and H.M. Reichardt, *Glucocorticoids in T cell apoptosis and function.* Cell Mol Life Sci, 2006. **63**(1): p. 60-72.

333. Logan, R.W., et al., *Altered circadian expression of cytokines and cytolytic factors in splenic natural killer cells of Per1(-/-) mutant mice.* J Interferon Cytokine Res, 2013. **33**(3): p. 108-14.

334. Kennedy, S.L., et al., *Splenic norepinephrine depletion following acute stress suppresses in vivo antibody response.* J Neuroimmunol, 2005. **165**(1-2): p. 150-60.

335. Albor, A.R., et al., *Effect of acute stress on B cells and IgA production of large intestine.* Brain, Behavior, and Immunity, 2015. **49**.

336. Banuelos, J. and N.Z. Lu, *A gradient of glucocorticoid sensitivity among helper T cell cytokines.* Cytokine Growth Factor Rev, 2016. **31**: p. 27-35.

337. Slota, C., et al., *Norepinephrine preferentially modulates memory CD8 T cell function inducing inflammatory cytokine production and reducing proliferation in response to activation.* Brain Behav Immun, 2015. **46**: p. 168-79.

338. Foley, J.F., et al., *Differentiation of human T cells alters their repertoire of G protein alpha-subunits.* J Biol Chem, 2010. **285**(46): p. 35537-50.

339. Haspel, J.A., et al., *Perfect timing: circadian rhythms, sleep, and immunity - an NIH workshop summary.* JCI Insight, 2020. **5**(1).

340. Yu, X., et al., *TH17 cell differentiation is regulated by the circadian clock.* Science, 2013. **342**(6159): p. 727-30.

341. Kashiwada, M., et al., *NFIL3/E4BP4 controls type 2 T helper cell cytokine expression.* EMBO J, 2011. **30**(10): p. 2071-82.

342. Hemmers, S. and A.Y. Rudensky, *The Cell-Intrinsic Circadian Clock Is Dispensable for Lymphocyte Differentiation and Function.* Cell Rep, 2015. **11**(9): p. 1339-49.

343. Xiang, K., et al., *Circadian clock genes as promising therapeutic targets for autoimmune diseases.* Autoimmun Rev, 2021. **20**(8): p. 102866.

344. Zhang, Z., et al., *Circadian clock: a regulator of the immunity in cancer.* Cell Commun Signal, 2021. **19**(1): p. 37.

345. Paganelli, R., C. Petrarca, and M. Di Gioacchino, *Biological clocks: their relevance to immune-allergic diseases.* Clin Mol Allergy, 2018. **16**: p. 1.

346. Sutton, C.E., et al., *Loss of the molecular clock in myeloid cells exacerbates T cell-mediated CNS autoimmune disease.* Nat Commun, 2017. **8**(1): p. 1923.

347. Cutolo, M., et al., *Circadian rhythms in RA.* Ann Rheum Dis, 2003. **62**(7): p. 593-6.

348. Nobis, C.C., et al., *The circadian clock of CD8 T cells modulates their early response to vaccination and the rhythmicity of related signalling pathways.* Proc Natl Acad Sci U S A, 2019. **116**(40): p. 20077-20086.

349. Dorsey, E.R., et al., *Projected number of people with Parkinson disease in the most populous nations, 2005 through 2030.* Neurology, 2007. **68**(5): p. 384-6.

350. Poewe, W., et al., *Parkinson disease.* Nat Rev Dis Primers, 2017. **3**: p. 17013.

351. McGeer, P.L., et al., *Rate of cell death in parkinsonism indicates active neuropathological process.* Ann Neurol, 1988. **24**(4): p. 574-6.

352. Brochard, V., et al., *Infiltration of CD4+ lymphocytes into the brain contributes to neurodegeneration in a mouse model of Parkinson disease.* J Clin Invest, 2009. **119**(1): p. 182-92.

353. Reale, M., et al., *Peripheral cytokines profile in Parkinson's disease.* Brain Behav Immun, 2009. **23**(1): p. 55-63.

354. Jiang, S., et al., *The correlation of lymphocyte subsets, natural killer cell, and Parkinson's disease: a meta-analysis.* Neurol Sci, 2017. **38**(8): p. 1373-1380.

355. Kustrimovic, N., et al., *Parkinson's disease patients have a complex phenotypic and functional Th1 bias: cross-sectional studies of CD4+ Th1/Th2/T17 and Treg in drug-naive and drug-treated patients.* J Neuroinflammation, 2018. **15**(1): p. 205.

356. Storelli, E., et al., *Do Th17 Lymphocytes and IL-17 Contribute to Parkinson's Disease? A Systematic Review of Available Evidence.* Front Neurol, 2019. **10**: p. 13.

357. Galiano-Landeira, J., et al., *CD8 T cell nigral infiltration precedes synucleinopathy in early stages of Parkinson's disease.* Brain, 2020. **143**(12): p. 3717-3733.

358. Sulzer, D., et al., *T cells from patients with Parkinson's disease recognize alpha-synuclein peptides.* Nature, 2017. **546**(7660): p. 656-661.

359. Lindestam Arlehamn, C.S., et al., *alpha-Synuclein-specific T cell reactivity is associated with preclinical and early Parkinson's disease.* Nat Commun, 2020. **11**(1): p. 1875.

360. Hamza, T.H., et al., *Common genetic variation in the HLA region is associated with late-onset sporadic Parkinson's disease.* Nat Genet, 2010. **42**(9): p. 781-5.

361. Kannarkat, G.T., et al., *Common Genetic Variant Association with Altered HLA Expression, Synergy with Pyrethroid Exposure, and Risk for Parkinson's Disease: An Observational and Case-Control Study.* NPJ Parkinsons Dis, 2015. **1**.

362. Cebrian, C., et al., *MHC-I expression renders catecholaminergic neurons susceptible to T-cell-mediated degeneration.* Nat Commun, 2014. **5**: p. 3633.

363. Delhalle, S., et al., *A roadmap towards personalized immunology.* npj Systems Biology and Applications, 2018. **4**(1): p. 9.

364. Hipp, G., et al., *The Luxembourg Parkinson's Study: A Comprehensive Approach for Stratification and Early Diagnosis.* Front Aging Neurosci, 2018. **10**: p. 326.

365. Pereira, B.I. and A.N. Akbar, *Convergence of Innate and Adaptive Immunity during Human Aging.* Frontiers in Immunology, 2016. **7**(445).

366. Goronzy, J.J. and C.M. Weyand, *Successful and Maladaptive T Cell Aging.* Immunity, 2017. **46**(3): p. 364-378.

367. Liu, J., et al., *The peripheral differentiation of human natural killer T cells.* Immunol Cell Biol, 2019. **97**(6): p. 586-596.

368. Wang, Y., et al., *Principal component analysis of routine blood test results with Parkinson's disease: A case-control study.* Exp Gerontol, 2021. **144**: p. 111188.

369. Munoz-Delgado, L., et al., *Peripheral Immune Profile and Neutrophil-to-Lymphocyte Ratio in Parkinson's Disease.* Mov Disord, 2021.

370. Nussbaum, J.C., et al., *Type 2 innate lymphoid cells control eosinophil homeostasis.* Nature, 2013. **502**(7470): p. 245-8.

371. Kaech, S.M., et al., *Selective expression of the interleukin 7 receptor identifies effector CD8 T cells that give rise to long-lived memory cells.* Nature Immunology, 2003. **4**(12): p. 1191-1198.

372. Sullivan, B.M., et al., *Antigen-driven effector CD8 T cell function regulated by T-bet.* Proc Natl Acad Sci U S A, 2003. **100**(26): p. 15818-23.

373. Intlekofer, A.M., et al., *Effector and memory CD8+ T cell fate coupled by T-bet and eomesodermin.* Nat Immunol, 2005. **6**(12): p. 1236-44.

374. Popescu, I., et al., *T-bet:Eomes balance, effector function, and proliferation of cytomegalovirus-specific CD8+ T cells during primary infection differentiates the capacity for durable immune control.* J Immunol, 2014. **193**(11): p. 5709-5722.

375. Akimova, T., et al., *Helios expression is a marker of T cell activation and proliferation.* PLoS One, 2011. **6**(8): p. e24226.

376. Strioga, M., V. Pasukoniene, and D. Characiejus, *CD8+ CD28- and CD8+ CD57+ T cells and their role in health and disease.* Immunology, 2011. **134**(1): p. 17-32.

377. Yi, J.S., M.A. Cox, and A.J. Zajac, *T-cell exhaustion: characteristics, causes and conversion.* Immunology, 2010. **129**(4): p. 474-81.

378. Wherry, E.J., *T cell exhaustion.* Nat Immunol, 2011. **12**(6): p. 492-9.

379. Chou, J.P. and R.B. Effros, *T cell replicative senescence in human aging.* Curr Pharm Des, 2013. **19**(9): p. 1680-98.

380. Lee, K.A., et al., *Characterization of age-associated exhausted CD8(+) T cells defined by increased expression of Tim-3 and PD-1.* Aging Cell, 2016. **15**(2): p. 291-300.

381. Woodland, D.L. and J.E. Kohlmeier, *Migration, maintenance and recall of memory T cells in peripheral tissues.* Nat Rev Immunol, 2009. **9**(3): p. 153-61.

382. Galkina, E., et al., *Preferential migration of effector CD8+ T cells into the interstitium of the normal lung.* J Clin Invest, 2005. **115**(12): p. 3473-83.

383. Yednock, T.A., et al., *Prevention of experimental autoimmune encephalomyelitis by antibodies against α4βl integrin.* Nature, 1992. **356**(6364): p. 63-66.

384. Sasaki, K., et al., *Preferential Expression of Very Late Antigen-4 on Type 1 CTL Cells Plays a Critical Role in Trafficking into Central Nervous System Tumors.* Cancer Research, 2007. **67**(13): p. 6451-6458.

385. Sakaguchi, S., et al., *Regulatory T cells and immune tolerance.* Cell, 2008. **133**(5): p. 775-87.

386. Josefowicz, S.Z., L.-F. Lu, and A.Y. Rudensky, *Regulatory T Cells: Mechanisms of Differentiation and Function.* Annual Review of Immunology, 2012. **30**(1): p. 531-564.

387. Schmidt, A., N. Oberle, and P. Krammer, *Molecular Mechanisms of Treg-Mediated T Cell Suppression.* Frontiers in Immunology, 2012. **3**(51).

388. Thome, A.D., et al., *Ex vivo expansion of dysfunctional regulatory T lymphocytes restores suppressive function in Parkinson's disease.* NPJ Parkinsons Dis, 2021. **7**(1): p. 41.

389. Kiniwa, Y., et al., *CD8⁺ Foxp3⁺ Regulatory T Cells Mediate Immunosuppression in Prostate Cancer.* Clinical Cancer Research, 2007. **13**(23): p. 6947-6958.

390. Churlaud, G., et al., *Human and Mouse CD8+CD25+FOXP3+ Regulatory T Cells at Steady State and during Interleukin-2 Therapy.* Frontiers in Immunology, 2015. **6**(171).

391. Zhang, S., M. Wu, and F. Wang, *Immune regulation by CD8(+) Treg cells: novel possibilities for anticancer immunotherapy.* Cell Mol Immunol, 2018. **15**(9): p. 805-807.

392. Li, S., et al., *A naturally occurring CD8+CD122+ T-cell subset as a memory-like Treg family.* Cellular & Molecular Immunology, 2014. **11**(4): p. 326-331.

393. Zeng, H., et al., *mTORC1 couples immune signals and metabolic programming to establish T(reg)-cell function.* Nature, 2013. **499**(7459): p. 485-90.

394. Macintyre, A.N., et al., *The glucose transporter Glut1 is selectively essential for CD4 T cell activation and effector function.* Cell Metab, 2014. **20**(1): p. 61-72.

395. Braak, H., et al., *Idiopathic Parkinson's disease: possible routes by which vulnerable neuronal types may be subject to neuroinvasion by an unknown pathogen.* J Neural Transm (Vienna), 2003. **110**(5): p. 517-36.

396. Inzelberg, R. and J. Jankovic, *Are Parkinson disease patients protected from some but not all cancers?* Neurology, 2007. **69**(15): p. 1542-50.

397. Saunders, J.A., et al., *CD4+ regulatory and effector/memory T cell subsets profile motor dysfunction in Parkinson's disease.* J Neuroimmune Pharmacol, 2012. **7**(4): p. 927-38.

398. Correale, J. and A. Villa, *Role of CD8+ CD25+ Foxp3+ regulatory T cells in multiple sclerosis.* Annals of Neurology, 2010. **67**(5): p. 625-638.

399. Flippe, L., et al., *Future prospects for CD8(+) regulatory T cells in immune tolerance.* Immunol Rev, 2019. **292**(1): p. 209-224.

400. Golebski, K., et al., *Induction of IL-10-producing type 2 innate lymphoid cells by allergen immunotherapy is associated with clinical response.* Immunity, 2021. **54**(2): p. 291-307.e7.

401. Hoyler, T., et al., *The transcription factor GATA-3 controls cell fate and maintenance of type 2 innate lymphoid cells.* Immunity, 2012. **37**(4): p. 634-48.

402. Spits, H. and J.P. Di Santo, *The expanding family of innate lymphoid cells: regulators and effectors of immunity and tissue remodeling.* Nat Immunol, 2011. **12**(1): p. 21-7.

403. Fung, I.T.H., et al., *Activation of group 2 innate lymphoid cells alleviates aging-associated cognitive decline.* J Exp Med, 2020. **217**(4).

404. Russi, A.E., et al., *Cutting edge: c-Kit signalling differentially regulates type 2 innate lymphoid cell accumulation and susceptibility to central nervous system demyelination in male and female SJL mice.* J Immunol, 2015. **194**(12): p. 5609-13.

405. Williams-Gray, C.H., et al., *Abnormalities of age-related T cell senescence in Parkinson's disease.* J Neuroinflammation, 2018. **15**(1): p. 166.

406. Weng, N.P., *Aging of the immune system: how much can the adaptive immune system adapt?* Immunity, 2006. **24**(5): p. 495-9.

407. Goronzy, J.J. and C.M. Weyand, *Understanding immunosenescence to improve responses to vaccines.* Nature Immunology, 2013. **14**(5): p. 428-436.

408. Koch, S., et al., *Cytomegalovirus Infection.* Annals of the New York Academy of Sciences, 2007. **1114**(1): p. 23-35.

409. Hiam-Galvez, K.J., B.M. Allen, and M.H. Spitzer, *Systemic immunity in cancer.* Nature Reviews Cancer, 2021. **21**(6): p. 345-359.

410. Zeng, N., et al., *DJ-1 depletion slows down immunoaging in T-cell compartments.* bioRxiv, 2021: p. 2021.05.21.445139.

411. Park, J.S., R.L. Davis, and C.M. Sue, *Mitochondrial Dysfunction in Parkinson's Disease: New Mechanistic Insights and Therapeutic Perspectives.* Curr Neurol Neurosci Rep, 2018. **18**(5): p. 21.

412. Bose, A. and M.F. Beal, *Mitochondrial dysfunction in Parkinson's disease.* J Neurochem, 2016. **139 Suppl 1**: p. 216-231.

413. Abou-Sleiman, P.M., M.M. Muqit, and N.W. Wood, *Expanding insights of mitochondrial dysfunction in Parkinson's disease.* Nat Rev Neurosci, 2006. **7**(3): p. 207-19.

414. Reeve, A., E. Simcox, and D. Turnbull, *Ageing and Parkinson's disease: why is advancing age the biggest risk factor?* Ageing Res Rev, 2014. **14**: p. 19-30.

415. Nikolich-Zugich, J., *The twilight of immunity: emerging concepts in aging of the immune system.* Nat Immunol, 2018. **19**(1): p. 10-19.

416. Jergovic, M., N.A. Contreras, and J. Nikolich-Zugich, *Impact of CMV upon immune aging: facts and fiction.* Med Microbiol Immunol, 2019. **208**(3-4): p. 263-269.

417. Lachmann, R., et al., *Cytomegalovirus (CMV) seroprevalence in the adult population of Germany.* PLoS One, 2018. **13**(7): p. e0200267.

418. Picozza, M., L. Battistini, and G. Borsellino, *Mononuclear phagocytes and marker modulation: when CD16 disappears, CD38 takes the stage.* Blood, 2013. **122**(3): p. 456-7.

419. Lopez-Vergès, S., et al., *CD57 defines a functionally distinct population of mature NK cells in the human CD56dimCD16+ NK-cell subset.* Blood, 2010. **116**(19): p. 3865-3874.

420. Capelle, C.M., et al., *Standard Peripheral Blood Mononuclear Cell Cryopreservation Selectively Decreases Detection of Nine Clinically Relevant T Cell Markers.* Immunohorizons, 2021. **5**(8): p. 711-720.

421. Gartner, R., et al., *Selenium supplementation in patients with autoimmune thyroiditis decreases thyroid peroxidase antibodies concentrations.* J Clin Endocrinol Metab, 2002. **87**(4): p. 1687-91.

422. Cardoso, B.R., et al., *Selenium, selenoproteins and neurodegenerative diseases.* Metallomics, 2015. **7**(8): p. 1213-28.

423. Dias, V., E. Junn, and M.M. Mouradian, *The role of oxidative stress in Parkinson's disease.* J Parkinsons Dis, 2013. **3**(4): p. 461-91.

424. Ellwanger, J.H., et al., *Biological functions of selenium and its potential influence on Parkinson's disease.* An Acad Bras Cienc, 2016. **88**(3 Suppl): p. 1655-1674.

425. Zhang, X., et al., *Prioritized brain selenium retention and selenoprotein expression: Nutritional insights into Parkinson's disease.* Mech Ageing Dev, 2019. **180**: p. 89-96.

426. Zafar, K.S., et al., *Dose-dependent protective effect of selenium in rat model of Parkinson's disease: neurobehavioral and neurochemical evidences.* J Neurochem, 2003. **84**(3): p. 438-46.

427. Dominiak, A., et al., *Selenium in the Therapy of Neurological Diseases. Where is it Going?* Curr Neuropharmacol, 2016. **14**(3): p. 282-99.

428. Adani, G., et al., *Selenium and Other Trace Elements in the Etiology of Parkinson's Disease: A Systematic Review and Meta-Analysis of Case-Control Studies.* Neuroepidemiology, 2020. **54**(1): p. 1-23.

429. Zhang, Y.J., et al., *Selenium level does not differ in blood but increased in cerebrospinal fluid in Parkinson's disease: a meta-analysis.* Int J Neurosci, 2021. **131**(1): p. 95-101.

430. Chatterjee, S., *Oxidative Stress, Inflammation, and Disease*, in *Oxidative Stress and Biomaterials*, D.A.B. Thomas Dziubla, Editor. 2016. p. 35-58.

431. Marano, G., et al., *Increased serum selenium levels in patients under corticosteroid treatment.* Pharmacol Toxicol, 1990. **67**(2): p. 120-2.

432. Zeydanli, E.N., et al., *Selenium restores defective beta-adrenergic receptor response of thoracic aorta in diabetic rats.* Mol Cell Biochem, 2010. **338**(1-2): p. 191-201.

433. Sayar, K., et al., *Dietary selenium and vitamin E intakes alter beta-adrenergic response of L-type Ca-current and beta-adrenoceptor-adenylate cyclase coupling in rat heart.* J Nutr, 2000. **130**(4): p. 733-40.

434. Yao, Y., et al., *Selenium-GPX4 axis protects follicular helper T cells from ferroptosis.* Nat Immunol, 2021.

435. Djamshidian, A. and A.J. Lees, *Can stress trigger Parkinson's disease?* J Neurol Neurosurg Psychiatry, 2014. **85**(8): p. 878-81.

436. Dalle, E. and M.V. Mabandla, *Early Life Stress, Depression And Parkinson's Disease: A New Approach.* Mol Brain, 2018. **11**(1): p. 18.

437. Kibel, A. and I. Drenjancevic-Peric, *Impact of glucocorticoids and chronic stress on progression of Parkinson's disease.* Med Hypotheses, 2008. **71**(6): p. 952-6.

438. Smith, A., S. Castro, and M. Zigmond, *Stress-induced Parkinson's disease: a working hypothesis.* Physiology & Behavior, 2002. **77**(4-5): p. 527-531.

439. Zou, K., et al., *A Case of early onset Parkinson's disease after major stress.* Neuropsychiatr Dis Treat, 2013. **9**: p. 1067-9.

440. Rothman, S.M. and M.P. Mattson, *Adverse stress, hippocampal networks, and Alzheimer's disease.* Neuromolecular Med, 2010. **12**(1): p. 56-70.

441. Smith, L.K., et al., *Stress accelerates neural degeneration and exaggerates motor symptoms in a rat model of Parkinson's disease.* Eur J Neurosci, 2008. **27**(8): p. 2133-46.

442. van der Heide, A., et al., *Stress and mindfulness in Parkinson's disease - a survey in 5000 patients.* NPJ Parkinsons Dis, 2021. **7**(1): p. 7.

443. Charlett, A., et al., *Cortisol is higher in parkinsonism and associated with gait deficit.* Acta Neurol Scand, 1998. **97**(2): p. 77-85.

444. Hartmann, A., *Twenty-Four Hour Cortisol Release Profiles in Patients With Alzheimer's and Parkinson's Disease Compared to Normal Controls: Ultradian Secretory Pulsatility and Diurnal Variation.* Neurobiology of Aging, 1997. **18**(3): p. 285-289.

445. Ros-Bernal, F., et al., *Microglial glucocorticoid receptors play a pivotal role in regulating dopaminergic neurodegeneration in parkinsonism.* Proc Natl Acad Sci U S A, 2011. **108**(16): p. 6632-7.

446. Herrero, M.T., et al., *Inflammation in Parkinson's disease: role of glucocorticoids.* Front Neuroanat, 2015. **9**: p. 32.

447. Ham, S., et al., *Hydrocortisone-induced parkin prevents dopaminergic cell death via CREB pathway in Parkinson's disease model.* Sci Rep, 2017. **7**(1): p. 525.

448. Jiang, L., et al., *A novel role of microglial NADPH oxidase in mediating extra-synaptic function of norepinephrine in regulating brain immune homeostasis.* Glia, 2015. **63**(6): p. 1057-72.

449. O'Neill, E. and A. Harkin, *Targeting the noradrenergic system for anti-inflammatory and neuroprotective effects: implications for Parkinson's disease.* Neural Regen Res, 2018. **13**(8): p. 1332-1337.

450. Mittal, S., et al., *beta2-Adrenoreceptor is a regulator of the alpha-synuclein gene driving risk of Parkinson's disease.* Science, 2017. **357**(6354): p. 891-898.

451. Magistrelli, L. and C. Comi, *Beta2-Adrenoceptor Agonists in Parkinson's Disease and Other Synucleinopathies.* J Neuroimmune Pharmacol, 2020. **15**(1): p. 74-81.

452. Capelle, C.M., et al., *Deep immune profiling reveals early-stage and highly coordinated immune responses in mild COVID-19 patients.* 2021: p. 2021.08.31.21262713.

453. Schomburg, L., *Selenium Deficiency Due to Diet, Pregnancy, Severe Illness, or COVID-19—A Preventable Trigger for Autoimmune Disease.* International Journal of Molecular Sciences, 2021. **22**(16).

454. Steinbrenner, H., et al., *Dietary selenium in adjuvant therapy of viral and bacterial infections.* Adv Nutr, 2015. **6**(1): p. 73-82.

455. Hoffmann, F.W., et al., *Dietary selenium modulates activation and differentiation of CD4+ T cells in mice through a mechanism involving cellular free thiols.* J Nutr, 2010. **140**(6): p. 1155-61.

456. Majeed, M., et al., *An exploratory study of selenium status in healthy individuals and in patients with COVID-19 in a south Indian population: The case for adequate selenium status.* Nutrition, 2021. **82**: p. 111053.

457. Moghaddam, A., et al., *Selenium Deficiency Is Associated with Mortality Risk from COVID-19.* Nutrients, 2020. **12**(7).

458. Zhang, H.Y., et al., *Association between fatality rate of COVID-19 and selenium deficiency in China.* BMC Infect Dis, 2021. **21**(1): p. 452.

459. Kieliszek, M. and B. Lipinski, *Selenium supplementation in the prevention of coronavirus infections (COVID-19).* Med Hypotheses, 2020. **143**: p. 109878.

460. Poston, J.T., B.K. Patel, and A.M. Davis, *Management of Critically Ill Adults With COVID-19.* JAMA, 2020. **323**(18): p. 1839-1841.

461. Konig, M.F., et al., *Preventing cytokine storm syndrome in COVID-19 using alpha-1 adrenergic receptor antagonists.* J Clin Invest, 2020. **130**(7): p. 3345-3347.

462. Yang, L., et al., *The signal pathways and treatment of cytokine storm in COVID-19.* Signal Transduct Target Ther, 2021. **6**(1): p. 255.

463. Tan, T., et al., *Association between high serum total cortisol concentrations and mortality from COVID-19.* The Lancet Diabetes & Endocrinology, 2020. **8**(8): p. 659-660.

464. Jang, H., et al., *Viral parkinsonism.* Biochim Biophys Acta, 2009. **1792**(7): p. 714-21.

465. Eldeeb, M.A., F.S. Hussain, and Z.A. Siddiqi, *COVID-19 infection may increase the risk of parkinsonism - Remember the Spanish flu?* Cytokine Growth Factor Rev, 2020. **54**: p. 6-7.

466. Antonini, A., et al., *Outcome of Parkinson's Disease Patients Affected by COVID-19.* Mov Disord, 2020. **35**(6): p. 905-908.

467. Hainque, E. and D. Grabli, *Rapid worsening in Parkinson's disease may hide COVID-19 infection.* Parkinsonism Relat Disord, 2020. **75**: p. 126-127.

468. Cilia, R., et al., *Effects of COVID-19 on Parkinson's Disease Clinical Features: A Community-Based Case-Control Study.* Mov Disord, 2020. **35**(8): p. 1287-1292.

469. Song, E., et al., *Neuroinvasion of SARS-CoV-2 in human and mouse brain.* J Exp Med, 2021. **218**(3).

470. Doobay, M.F., et al., *Differential expression of neuronal ACE2 in transgenic mice with overexpression of the brain renin-angiotensin system.* Am J Physiol Regul Integr Comp Physiol, 2007. **292**(1): p. R373-81.

471. Lin, Z., et al., *RNA interference shows interactions between mouse brainstem angiotensin AT1 receptors and angiotensin-converting enzyme 2.* Exp Physiol, 2008. **93**(5): p. 676-84.

472. Xia, H. and E. Lazartigues, *Angiotensin-converting enzyme 2 in the brain: properties and future directions.* J Neurochem, 2008. **107**(6): p. 1482-94.

473. Hernández, V.S., et al., *ACE2 expression in rat brain: implications for COVID-19 associated neurological manifestations.* Preprint, 2021.

474. Papa, S.M., et al., *Impact of the COVID-19 Pandemic on Parkinson's Disease and Movement Disorders.* Mov Disord, 2020. **35**(5): p. 711-715.

475. Stoessl, A.J., K.P. Bhatia, and M. Merello, *Movement Disorders in the World of COVID-19.* Mov Disord Clin Pract, 2020. **7**(4): p. 355-356.

476. Bhidayasiri, R., et al., *COVID-19: An Early Review of Its Global Impact and Considerations for Parkinson's Disease Patient Care.* J Mov Disord, 2020. **13**(2): p. 105-114.

477. Tipton, P.W. and Z.K. Wszolek, *What can Parkinson's disease teach us about COVID-19?* Neurol Neurochir Pol, 2020. **54**(2): p. 204-206.

478. Sulzer, D., et al., *COVID-19 and possible links with Parkinson's disease and parkinsonism: from bench to bedside.* NPJ Parkinsons Dis, 2020. **6**: p. 18.